CONTROL SYSTEMS THEORY APPLIED TO METABOLIC HOMEOSTATIC SYSTEMS AND THE DERIVATION AND IDENTIFICATION OF MATHEMATICAL MODELS

Thesis by

Wilfred P. Charette

In Partial Fulfillment of the Requirements

For the Degree of

Doctor of Philosophy

California Institute of Technology

Pasadena, California

1969

(Submitted July 17, 1968)

ACKNOWLEDGMENT

Throughout the course of these investigations the author held a North American Rockwell Corporation Fellowship for which he is sincerely thankful. The author benefited significantly from contact with many individuals during this study, but he is particularly grateful to Dr. Arnold H. Kadish for many beneficial discussions and experimental data, to Gerald H. Schlosser for an orientation to the pertinent life science literature, to Dr. J. Stuart Soeldner for experimental data and helpful suggestions, to Dr. Lynn E. Wolaver for some illuminating insights, and to Dr. Robert V. Langmuir for a generous contribution of computer time. The author gratefully acknowledges the steadfast and enthusiastic support of this work by his research advisor, Dr. R. Sridhar, which was an indispensable ingredient for its successful culmination. A sincere thank you is extended to Paula Samazan for her expert librarian assistance and to Doris Schlicht for her rapid and accurate typing.

ABSTRACT

The relations among organs and processes resulting in the hormonal control of human metabolism are interpreted mathematically for the derivation and analysis of models using control systems theory and systems engineering techniques. A dynamic nonlinear model for glucose homeostasis including four controlling hormones is derived from the current biological knowledge of the normal system and simulated for comparison with experimental data. Mathematical algorithms are developed and demonstrated for the identification of the parameters of the proposed model and a series of experiments is proposed to yield the minimal requisite data for the application of the method. Control systems analyses are undertaken on the proposed model to demonstrate a consistent methodology for investigations of complex metabolic control systems in the intact animal.

TABLE OF CONTENTS

LIST OF ILLUSTRATIONS

I. INTRODUCTION

In many respects the field of biological and medical systems is a challenging new frontier for systems engineers. For our purposes a system may be thought of as an interacting group of components and processes reacting to various inputs to produce various outputs considered as an entity. Only recently have the tools and methods become available for a systematic study of high dimensional nonlinear biological processes. The area of physiological control systems related to metabolism is one which seems to be particularly amenable to the methods of investigation familiar to control systems engineers.

All animals are equipped with numerous intercoupled control systems which serve to maintain the animal's internal equilibrium regardless of outside influences; this condition is known as homeostasis. In the case of metabolism -- the processes involved in the animal's utilization of energy -- control is effected by specific hormones which are released by the endocrine system in direct response to deviations from the equilibrium state. Hence metabolic homeostasis is a consequence of interactions among the activity requirements of the organism, protein, lipid, and carbohydrate metabolism, and the control effected by hormones.

Although homeostatic systems in humans exhibit gross features familiar to control systems engineers, they also have some unique characteristics. Any specific control system being considered in the intact animal inevitably is coupled to many other control systems. In the few instances where quantitative information has been obtained about the behavior of a subsystem, surgery was performed on the animal, inevitably changing the dynamic characteristics of the very processes under

study in a manner impossible to ascertain. Hormonal controls are always nonnegative and at least two different controls are required to move a controlled variable in opposite directions. Many of the important processes of metabolism are inherently nonlinear and few of the system variables are directly observable.

Consequently, the study of human metabolic control requires a methodology that makes use of experiments performed only on the intact system. The theory of control systems possibly can furnish such a methodology, but it has not been applied effectively in the area of metabolic control. Before such applications can be made the metabolic control system must be characterized mathematically. Although there is a growing awareness among some life scientists that an understanding of the dynamic operation of the metabolic control system will only result from a systems approach, most of what is known about the system is unsuitable for use in a systems context. Most of the physiological experiments which have been performed on the system were designed to study local properties and not to elucidate subsystem behavior within the context of a complex multiloop coupled system, hence these results are difficult to interpret from a systems viewpoint.

It is the purpose of this investigation first to systematize the current physiological knowledge of metabolic control in order to establish the scope of the overall system, to derive and substantiate by system experiments a mathematical model for portions of the overall plant and controller, to develop and apply mathematical algorithms for the identification of parameters in the proposed model, and to motivate a logical sequence of human physiological experiments to sub-

stantiate the model.

It should be emphasized that the primary aim is to establish a methodology for the investigation of the human metabolic control system. It is expected that the proposed model will be only one of an evolutionary series of mathematical representations of the system eventually resulting in a comprehensive dynamic model of metabolism. However, these immediate results should accelerate bio-medical research on other homeostatic systems, they may promote the eventual development of better characterizations of metabolic abnormalities leading to improved diagnostic techniques, they are a necessary prerequisite for the development of auxiliary controllers for conditions such as diabetes, and they may promote new developments in the theory of automatic control systems.

II. THE METABOLIC CONTROL SYSTEM

2.1. Introduction.[1,2,3,4]

All vital processes require energy, which is obtained from chemical reactions occurring in the living cell. The oxidation of various substances is the principal mechanism for the liberation of energy. The total energy available from the breakdown of a molecule of a particular food to CO_2 and H_2O is inherent in the bonds linking the atoms together. It follows from thermodynamics that no more than the total bond energy can be derived from the complete breakdown of a substance regardless of the number of intermediate steps in the process. The energy obtained from chemical bonds is used in the organism for the production of heat, muscular contraction, and electrical activity. The phosphorylations from carbohydrate are the means by which the energy liberated from oxidations is prevented from being dissipated as heat and is temporarily held in the high energy bonds of adenosine triphosphate (ATP) for subsequent use by reactions requiring energy.

Metabolism involves numerous coupled pathways composed of enzyme controlled chemical reactions (Appendix A). The rates of these reactions are not constant but vary as a function of physiologic requirements. The metabolic system changes in response to food inputs, during the subsequent postabsorptive phase, and in response to external factors such as exercise and exposure to cold. Since animals require a continuous but variable output of energy, and replenishment by the ingestion of food occurs periodically, a means must be provided for controlled energy storage and release.

Ingested food accumulates in the stomach which releases partially digested food to the intestine from which absorption occurs. The duration of the following postabsorptive phase is determined by eating habits. During these two periods, metabolic energy is alternately undergoing net storage or release.

In the absorptive phase, glucose provides the major energy source, being oxidized to CO_2 and H_2O in tissues. In addition, a small amount of fat is oxidized, but most is stored in adipose tissue as triglyceride (lipogenesis). Excess carbohydrate is stored as glycogen (glycogenesis), but most of it is converted to fatty acid and subsequently stored as triglyceride in adipose tissue; the latter process results in more energy stored per unit volume.

As the postabsorptive phase progresses the oxidation of fatty acid becomes the predominant energy source rather than glucose. The fats so utilized are derived from adipose tissue. The brain and central nervous system depend mainly on glucose for fuel and oxidize it at a steady rate in both phases. In contrast to most tissues, the brain does not require the presence of insulin to utilize glucose. This constant sink on glucose supplies would rapidly deplete the extracellular fluid of glucose if the liver did not increase its rate of conversion of protein and amino acids to glucose (gluconeogenesis) during the postabsorptive phase. During the postabsorptive phase insulin levels decrease and muscle and adipose tissues oxidize less glucose but more fatty acids, conserving available glucose supplies for the brain. Under postabsorptive conditions, the mixture of fuels being consumed is estimated to be about 20% carbohydrate, 70% fat, and 10% protein. Since the brain is

the primary consumer of glucose most of the tissues are oxidizing fat almost exclusively during this phase.

The endocrine glands, through the production and release of hormones, control the exchange between stored fuels, viz. protein, triglyceride, and glycogen, and their mobilized equivalents, viz. amino acids, triglyceride derivatives, and glucose respectively, so as to maintain the homeostasis of the organism under varying environmental conditions. Hormones are substances secreted by endocrine glands into the general circulation which carries them to specific sites of action elsewhere in the organism. Here they affect the rates of action of specific processes without contributing significant amounts of energy to the surrounding tissues. The following hormones exert dominant control on the processes of carbohydrate, lipid, and protein metabolism: insulin, glucagon, epinephrine, corticosteroids, growth hormone, and thyroid hormone.

2.2. Carbohydrate Metabolism.[4,5,6,7]

The principal product of carbohydrate digestion and the dominant circulating sugar is glucose. The normal fasting level of glucose in plasma is 80-100 mg/100 mℓ or 80-100 mg%. From plasma, glucose diffuses to interstitial fluid and then enters the cells of tissues. In the cells it is phosphorylated to glucose-6-phosphate and then either converted to glycogen or catabolized. Glycogen formation from glucose is called glycogenesis and the reverse process is called glycogenolysis. Glycogen, the stored form of glucose, is present in most tissues, but the major supplies are in liver, kidney, and skeletal muscle. Glucose

catabolism can occur by oxidation and decarboxylation to pentoses, the "direct oxidative" circuit, and by cleavage to trioses to pyruvic acid, the "Embden-Meyerhof" circuit. Under conditions of relative oxygen lack, glycolysis, the breakdown of carbohydrate to pyruvic and lactic acids, is more dominant than glycogenolysis in muscle; the lactic acid released to the circulation can be converted back to glucose by the liver (gluconeogenesis). Other precursors can be converted to glucose by the liver, viz. glycerol from fat and some amino acids from protein. Conversely, glucose is converted through pyruvic acid to the amino acid alanine then to protein by the liver. Glucose can be converted to fat through pyruvic acid to acetyl - Co A, but this circuit is not reversible. The "citric acid cycle" or Krebs cycle, is a sequence of reactions in which acetyl - Co A is oxidized to CO_2 and H atoms. This cycle is the common oxidative circuit to CO_2 and H_2O of carbohydrate, fat, and some amino acids.

In contrast to other tissues, liver and kidney contain the enzyme glucose-6-phosphatase, hence glucose-6-phosphate can be converted in the liver to glucose from which it can be discharged into the circulation. The uptake and release of glucose by the liver is under the control of various hormones. In the kidney, glucose is freely filtered, but at normal glucose levels essentially all of it is reabsorbed. However, when the plasma glucose concentration exceeds approximately 180 mg%, reabsorption saturates and glucose is excreted into the urine.

A normal 70 kg. man with a liver mass of approximately 1.8 kg. and muscle mass of approximately 35 kg., would have 75-125 g. liver glycogen, 180-250 g. muscle glycogen, and assuming a glucose distribution

space (plasma and interstitial fluid volume) of 14 ℓ. and a glucose concentration of 100 mg%, 14 g. of glucose in circulation. Assuming a caloric requirement of 120 cal/hr., the maximum available carbohydrate, approximately 390 g., would supply the body's needs for only about 13 hours, ie. (390)(4.1)/120 = 13.3.

2.3. Fat Metabolism.[4,5,6,7]

The supply of neutral fat (triglyceride), within adipose tissue, is the major source of chemical energy for the living organism. These fat reserves are constantly being broken down and resynthesized. The stored form of fat, triglyceride, is converted within the adipose tissue cell to free fatty acid and glycerol (lipolysis) which in turn are released into the general circulation. Fatty acids are the form in which lipid is transported from storage depots to the tissues for oxidation, which occurs by the breakdown of fatty acids to acetyl-CoA which then enters the Krebs cycle. The glycerol fraction yielded during lipolysis is not metabolized to an appreciable extent by adipose tissue, but is transported to the liver where it is converted to glucose (gluconeogenesis) through conversion to phosphoglyceraldehyde.

Apparently all tissues of the mammalian organism so far examined can oxidize free fatty acids completely to CO_2 and H_2O. Glucose is converted to fat through the synthesis of fatty acids from acetyl-CoA and the subsequent conversion to triglyceride (lipogenesis), which occurs in adipose tissue and to a lesser extent in other tissues, including the liver. This circuit through fat as an intermediate is the dominant pathway for carbohydrate utilization. The partial

oxidation of fats in the liver leads to the formation of ketones which in turn can be oxidized by other tissues. Most amino acids can lead to glucose formation (gluconeogenesis), and in this manner eventually contribute to fat formation (lipogenesis). In addition, some amino acids increase ketone formation and thereby can be converted directly to fat. The size of the fat depot obviously varies, but in the normal individual may amount to 10% of body weight, or for a 70 kg man, 7 kg.

The fate of free fatty acids in the adipose tissue cell is a function of the amount of carbohydrate available. When the intake of carbohydrate exceeds the immediate energy requirements of the organism, the adipose tissue cell converts glucose to fatty acids and consequently to triglyceride (lipogenesis) for fat deposition. Since α-glycerophosphate, formed from glucose, is essential for the esterification of fatty acids to triglycerides, fat deposition can occur readily only in the absorptive phase. Only during this phase, when blood sugar and insulin levels are high, the latter promoting entry of glucose into the adipose tissue cell, will glucose be converted at a significant rate to α-glycerophosphate. Adipose tissue contains active lipases that continuously hydrolyze triglyceride to free fatty acid and glycerol (lipolysis). In the absorptive phase most of this fatty acid is recycled back to triglyceride. However, in the postabsorptive phase, when blood sugar and insulin levels are low, α-glycerophosphate is not abundant and free fatty acid leaves the cell for transport to other tissues to be oxidized.

2.4. Protein Metabolism.[4,5,6,7]

Ingested protein is broken down to amino acids which are absorbed from the gastrointestinal tract. Amino acids are not stored in tissues, but are converted back to protein or catabolized by deamination and further oxidation. Reserves of protein accumulate in the liver and possibly in the muscle. The body's own proteins are being continuously hydrolyzed to amino acids and resynthesized. Interconversions between amino acids and the products of carbohydrate and fat catabolism at the level of the common metabolic pool and the Krebs cycle involve transfer, removal, or formation of amino groups.

Deamination, the first step in the metabolic breakdown of amino acids, occurs in the liver. The deaminated residues of amino acids fall into two groups, those which are glycogenic, i.e. capable of being converted to glycogen and glucose, and those which are ketogenic, i.e. capable of being converted to keto acids. The keto acid formed can be reconverted to an amino acid by reamination, directly catabolized to CO_2 and H_2O, or converted to carbohydrate (gluconeogenesis) and fat. The conversion of keto acids to carbohydrate is the major source of glycogen obtained by gluconeogenesis.

2.5. The Endocrine System.[1,4,7,8,9]

The operation and effects produced by the endocrine system (ductless glands which discharge their products into the general circulation), are closely coupled to events occurring in the nervous system. Common to the two systems is their ability to synthesize and release specific chemicals that are capable of being transported over finite

distances to their sites of action. Many endocrine glands through their hormones act on the nervous system, and endocrine glands can be stimulated or inhibited by products of the nervous system. The functional interdependence of these two systems is so pervasive that they are often referred to as a unit, the neuroendocrine system.

The hormones act upon target tissues and organs by affecting the enzymes determining the rates of specific metabolic processes without contributing significant quantities of matter or energy to the constituent cells. Each endocrine organ probably has a nominal rate of secretion which changes as a function of other humoral changes, neural mechanisms, or physiological needs, in such a manner that the effect of the hormone is to induce changes tending to counteract the original secretion stimulus. In contrast to the rapid coordinations of the body controlled by the nervous system, hormones which are transported in the general circulation and must be carried through interstitial fluid in order to reach their target tissues, regulate processes such as those of metabolism in which events take place over longer periods of time. The sequence of evolutionary development of these regulatory mechanisms seems to have been: nerve cells producing neurohumors, neurosecretory cells producing neurohormones, and finally endocrine glands producing hormones. Control in humans, consisting as it does of all three mechanisms, is highly coupled and interdependent and to some extent redundant.

The isolation and identification of the active principle of a hormone is often extremely difficult, requiring the combined efforts of many specialists. The nature of the various known hormones differs but

most of them are unstable and many are proteins difficult to separate from other cellular substances. Finally, hormones are present in the body in minute concentrations; in many cases the only measure of their presence is their physiological activity.[10,11,12]

In the sequel, attention will be focused upon six hormones which are believed to exert the dominant effects upon the processes of metabolism in humans. The pancreas produces two hormones which affect metabolism: insulin from the beta cells and glucagon from the alpha cells. Insulin is a protein (molecular weight about 6000) which is produced by the beta cells of the islets of Langerhans in response to the concentration and rate of change of the concentration[13] of glucose in blood. It is the only known hormone whose effects result in a lowering of the circulating levels of blood glucose. Insulin is usually measured in terms of "units", one unit being equal to 1/23 mg. The basic peripheral action of insulin is to facilitate the transport of glucose across the tissue cell membrane.[14] (See Appendix B for a description of transport processes.) However, evidence also exists that insulin decreases liver glucose output (glycogenolysis), increases liver glucose uptake (glycogenesis), decreases liver glucose formation from other precursors (gluconeogenesis), and inhibits the release of free fatty acid from adipose tissue. Some studies have shown that insulin virtually stops liver release of glucose and increases its uptake by a factor of about three,[15] and increases glucose transport into the adipose tissue cell while curtailing fatty acid release.[16]

A typical plasma insulin concentration in the postabsorptive phase is 10 - 20 $\mu U/m\ell$. Measured by the radioimmunoassay method, typical peak

levels after an oral glucose input are 100 - 140 μU/mℓ.[17] Direct measurements of plasma insulin indicate that the normal human secretes only about 50 U/day. After intravenous infusions of 2 g/min glucose and 20 μg/min glucagon for 60 minutes, the level of endogenously generated plasma insulin measured by immunoassay, declined with a half-life of 7 - 15 minutes in normal humans.[18]

Although the remaining five hormones pertinent to this investigation all tend to be hyperglycemic, i.e. their effect is to increase the level of circulating glucose, the opposite effect is believed to have been observed with glucagon, viz. that glucagon, in addition to its hyperglycemic property, can stimulate insulin release in normal subjects by a different mechanism than does glucose.[19,20,21,22] This effect is opposite to the well demonstrated hyperglycemic effect of glucagon, but this is at present a controversial subject. In this investigation, glucagon is treated simply as a hyperglycemic agent. It has also been observed that insulin response following an intravenous injection of glucose differs from that following an orally administered dose, having a less rapid but more pronounced dynamic response in the latter case.[23] The existence of a "gastrointestinal factor" has been postulated to account for this seemingly anomalous observation.[24,25] In this investigation, only responses to intravenous inputs are considered. See Appendix C for a description of "glucose tolerance tests".

Glucagon, a polypeptide with a molecular weight of about 3450, is produced by the alpha cells of the islets of Langerhans within the pancreas. It is secreted in response to a below normal plasma glucose concentration and acts on the liver to stimulate glycogenolysis and

also gluconeogenesis from protein.[26] It reactivates liver phosphorylase which increases the conversion rate of liver glycogen to glucose-1-phosphate and ultimately to glucose-6-phosphate and to free glucose. There is no readily demonstrable effect on glycogen breakdown in muscle. The fact that blood pyruvate and lactate levels do not increase after a glucagon input indicates that it has no effect on muscle phosphorylase. A typical postabsorptive plasma concentration of glucagon in humans is 1 mμg/mℓ.

The adrenal glands, located superior to the kidneys, consist of an inner part, the medulla, and an outer part, the cortex, which have different endocrine functions. The adrenal medulla secretes epinephrine (adrenaline) whose effects are similar to stimulation by the sympathetic nervous system, the nerve endings of which secrete norepinephrine. Norepinephrine is also produced by the adrenal medulla, in fact it is a precursor for epinephrine. Both of these substances have the same effect on metabolism, but that of norepinephrine is about one fourth as effective. In this investigation both are treated as one quantity.

Epinephrine is a catecholamine of molecular weight 183.2. It has been estimated that the blood of normal resting man contains about 1 mμg/mℓ of total catecholamine (epinephrine and norepinephrine). Small amounts of catecholamines are released into circulation continuously, but secretion increases in response to sympathetic nervous impulses, hypoglycemia, and physiologic stress. Most investigators agree that hypoglycemia stimulates the secretion of epinephrine almost exclusively while anxiety and related emotional states stimulate mainly

norepinephrine secretion.

A basal rate of epinephrine production is thought to be established by signals from the hypothalamus (that portion of the brain which is attached to the pituitary gland by vascular and neural pathways) through the splanchnic sympathetic nerves. Production rates above nominal are stimulated by a glucose concentration that is below nominal and by a rapidly falling glucose concentration. When glucose is above nominal, but rapidly falling due to the insulin effect, it is believed that insulin release is attenuated. Experiments show that epinephrine inhibits insulin secretion directly at the beta cell level.[27,28]

Epinephrine[29] has two pronounced metabolic effects: it reactivates liver phosphorylase promoting glycogenolysis as much as three times above the unstimulated rate,[30] and increases lipolysis in adipose tissue liberating fatty acids.[31] The concentration of epinephrine observed during the reaction to insulin induced hypoglycemia is about 2 - 3 mμg/mℓ.[32] Epinephrine may also act on muscle glycogen breakdown with a resulting increase in plasma lactic acid.

The adrenal cortex produces several steroid hormones affecting metabolism. The most pronounced effect on carbohydrate, protein, and fat metabolism probably is exerted by hydrocortisone with a molecular weight of about 285. Henceforth we will use the term corticosteroid to refer to the hormones of the adrenal cortex affecting carbohydrate, fat, and protein metabolism. The adrenal cortex is stimulated by ACTH (adrenocorticotropic hormone) from the adenohypophysis (anterior pituitary). The adrenal cortex secretes its hormones continuously for

normal metabolism and increases its secretion in response to almost any change in the internal or external environment as mediated by ACTH secretion.

The total concentration of corticosteroids undergoes a cyclic variation with a period of 24 hours; in man the peak occurs around 8 A.M. (16 ± 10 μg/100 mℓ) and at 4 P.M. is about one half this value (8 ± 6 μg/100 mℓ).[33] In metabolism, corticosteroids are hyperglycemic, tending to increase plasma glucose both by reducing peripheral uptake by inhibiting glucose phosphorylation in muscle and adipose tissue,[34] and by increasing the availability of protein and fat for conversion to glucose by hepatic gluconeogenesis.[35,36]

Growth hormone, (somatotropin) is a protein produced by the anterior pituitary with a molecular weight of about 21,500.[37] The anterior pituitary is stimulated to release growth hormone by "growth hormone releasing factor" from the hypothalamus when plasma glucose is below nominal[38] or when plasma glucose is falling rapidly but not necessarily below nominal.[17,39] This effect appears to be independent of insulin, glucagon, and epinephrine. However, it has been found that insulin induced hypoglycemia stimulates growth hormone secretion and that the simultaneous administration of corticosteroids attenuates it.[40] Growth hormone increases lipolysis and decreases lipogenesis in adipose tissue, thereby increasing the level of circulating free fatty acids.[37] As a consequence of more fatty acid in circulation there is a decrease in phosphorylation of glucose in muscle hence a decrease in glucose uptake by these tissues.[34] A single injection of 1 mg of growth hormone in normal subjects has led to a threefold

increase of free fatty acid in plasma after a delay of about one hour. This effect is the result of increased release of free fatty acid from adipose tissue depots.[41] Growth hormone also selectively accelerates the transport of specific amino acids into cells promoting protein synthesis.[37]

The plasma concentration of growth hormone fluctuates widely in response to physiologic stimuli such as eating,[42] exercise, and psychological stress. Normal persons, after an overnight fast and before arising, have a growth hormone concentration less than 3 mμg/mℓ, but under a suitable stimulus concentrations as high as 70 mμg/mℓ have been observed.[40] The normal rate of excretion of growth hormone has been found to be 10 - 125 μg/day.[43] In normal subjects, after an insulin input, a drop in plasma glucose to less than half its initial value is followed by a five-fold increase in plasma growth hormone from an initial value below 5 mμg/mℓ.[39] However, a rapidly falling plasma glucose has stimulated growth hormone release to concentrations as high as 50 mμg/mℓ.[44] Calculation of the turnover of endogenously secreted growth hormone indicates that it leaves the circulation with a half-time of 20 - 30 minutes if simple first-order removal kinetics are assumed.[41] In an experiment in which the mean fasting blood glucose level among several subjects was 63 mg% and plasma growth hormone was 8.3 mμg/mℓ, and in which insulin was infused at a rate .01 units/kg weight/hr. for one hour, growth hormone secretion was stimulated when blood glucose decreased approximately 10 mg%.[38]

The principal function of thyroid hormone is that of a catalyst for the oxidative reactions of the body's cells, it thus maintains a

level of metabolism in the tissues that is optimal for their normal function. Thyroid function is controlled by TSH (thyroid stimulating hormone) of the anterior pituitary. The principal hormone secreted by the thyroid is thyroxin, an amino acid of molecular weight 776.9. However, another active form of the hormone on peripheral tissues may be triiodothyronine, which has one less iodine.

Approximately 100 μg of thyroid hormones are secreted per day. In addition to their overall metabolic effect they accelerate the rate of absorption of monosaccarides from the gastrointestinal tract. Thyroxin is normally degraded at a rate 51 μg/day. The half life of thyroxin is about 6 days and that of triiodothyronine about 2.5 days.

In the derivation of a mathematical model which is to follow in Chapter III, the specific effects of only insulin, glucagon, epinephrine and growth hormone upon carbohydrate metabolic processes will be included.

2.6. Hormonal Control of Metabolism.

In the previous sections we have tried to be consistent in summarizing what may be a consensus on at least the first-order effects of the hormones affecting carbohydrate, protein, and fat metabolism. However, the picture one obtains from the increasing mass of physiological investigation on this subject is neither clear nor consistent. The fact that the metabolic plant is comprised of several intercoupled loops with at least six and possibly more controls, is making itself abundantly clear as more conflicting results on the operation of various portions of the system are obtained. Until a

consistent investigative framework for the overall process is established, and a methodology derived to design physiological experiments in a systems context, the classical methods of investigation applied to this problem are likely to lead to even a more confused state of affairs.

A diagrammatic summary of the previous sections dealing with the metabolic plant is presented in Figure 1. This diagram represents what may be the minimal desired complexity for meaningful results with a dynamic description of metabolic control. The boxes represent "state variables", and the arrows connecting the boxes represent processes. The control signals, hormones produced by the endocrine glands, affect the dynamics of the processes connecting state variables. This type of description of a system, although common among life scientists, is the exact dual of an engineering representation.

As shown in Figure 1, the metabolic plant consists of three major intercoupled controlled loops. There is now a fairly general consensus that plasma glucose is a regulated variable in the classical control system sense. It is also possible that certain variables in the protein and lipid loops are regulated,[9] but these effects are not as well substantiated. The regulation of plasma glucose appears to be effected by two essentially distinct pathways. One is mediated through the pancreas which releases insulin when plasma glucose is above nominal and glucagon when plasma glucose is below nominal. The other is mediated through the hypothalamus and remaining endocrine glands, i.e. anterior pituitary, adrenal, and thyroid, responding to a low or decreasing plasma glucose concentration. The nominal concentra-

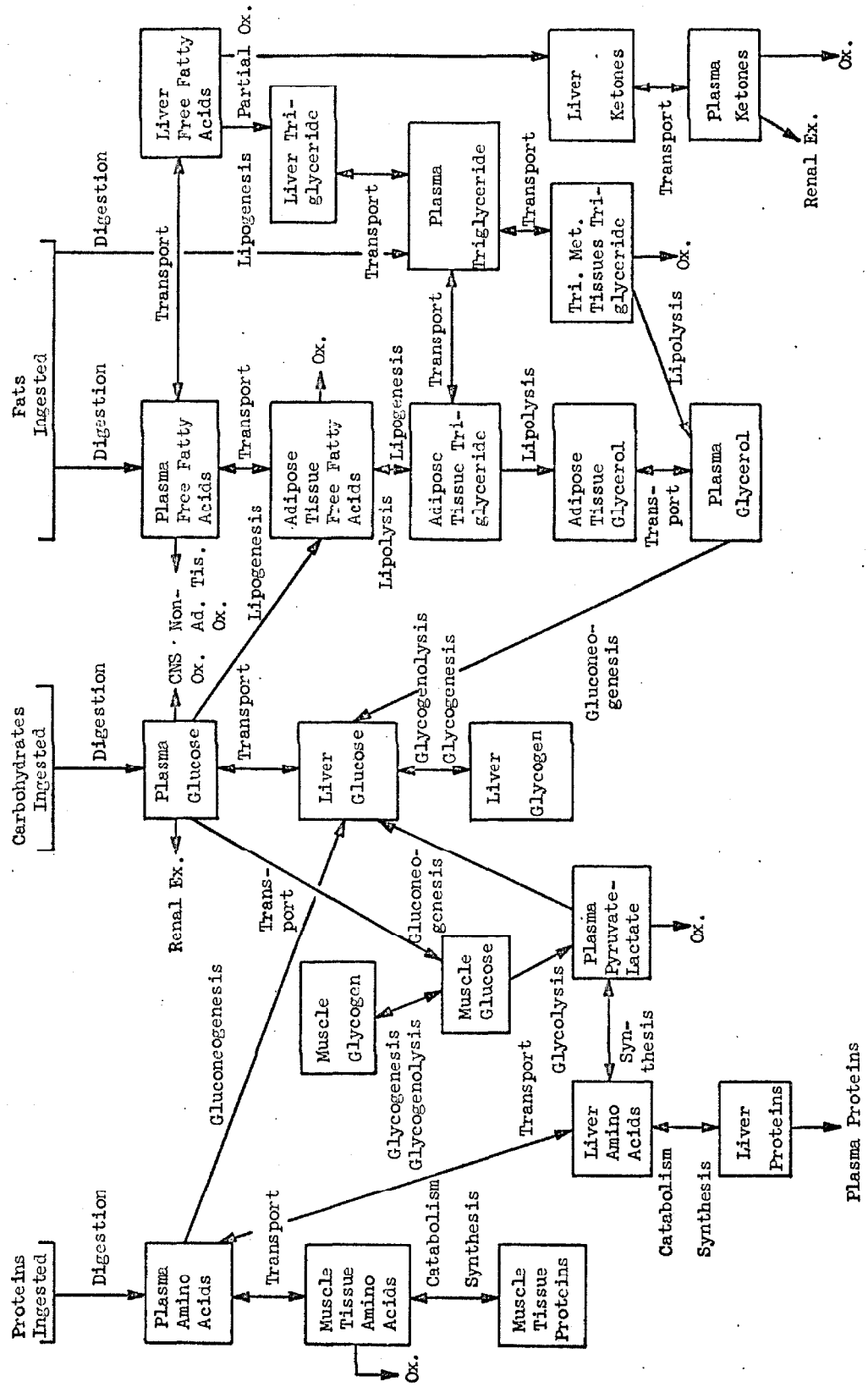

Figure 1. Metabolic Plant.

tion is believed to be determined by the higher cortical centers of the central nervous system and the hypothalamus is capable of sensing deviations in plasma glucose from the desired level.[45]

When the plasma concentration rises to some point between 100 and 150 mg% - normally as a result of the ingestion of food - the liver stops releasing glucose into plasma and begins to store the excess glucose as glycogen.[46,47] Simultaneously the tissue utilization of glucose increases under the influence of insulin; adipose tissue stores glucose as triglyceride[16,48] and muscle stores glucose as glycogen.[49] When the plasma concentration of glucose falls below nominal by approximately 5 - 10 mg%, growth hormone of the anterior pituitary is released at an increased rate, promoting gluconeogenesis. The pancreas responds by releasing glucagon and the adrenal medulla by releasing epinephrine, both of which promote glycogenolysis and gluconeogenesis.[50,51] Hydrocortisone from the adrenal cortex and triiodothyronine from the thyroid also are released under the stimulus of hypoglycemia. The evidence suggests that the pancreas and adrenal medulla perform comparator action directly, releasing their respective hormones as some function of glucose actuating error, whereas the hypothalamus functions as a comparator for the remaining hormones. The hormone controller appears to respond as proportional, derivative, and integral functions of the actuating error between the nominal and the actual plasma glucose concentration.

By classical indirect calorimetry it has been determined that a normal 70 kg. man under basal conditions requires about 1800 calories of fuel in one day. In this 24 hour period the liver output of

glucose is approximately 180 g., of which 144 g. are oxidized by the brain and nervous system, and 36 g. are metabolized by red cells and white cells to pyruvate and lactate. The resulting 36 g. of pyruvate and lactate are recycled to liver to fuel gluconeogenesis. The fuel source mix consists of 75 g. of protein converted to amino acids to fuel gluconeogenesis in liver and 160 g. of adipose tissue triglyceride which converts to 160 g. of fatty acids and 16 g. of glycerol, the latter going to liver for gluconeogenesis. Of the 160 g. of fatty acids, 40 g. are removed by the liver which partially oxidizes them to ketones, providing the necessary energy for liver function. The remainder of the body uses these ketones, and the remaining 120 g. of fatty acids. The precursors for hepatic gluconeogenesis, 16 g. of glycerol, 36 g. of lactate and pyruvate, and 75 g. of amino acids are inadequate to provide 180 g. of glucose, however the difference is made up by hepatic glycogenolysis.[52]

In our view then the overall metabolic control system is comprised of a "plant" consisting of processes relating the three storage forms of metabolic fuels (protein, triglyceride, and glycogen) to six metabolic fuels (amino acids, fatty acids, glucose, pyruvate, lactate, and ketones),[53] three inputs (protein, fat, and carbohydrate), at least one regulated output (plasma glucose), and a "controller" producing six control signals (insulin, glucagon, epinephrine, growth hormone, corticosteroids, and thyroid hormones). The metabolic control system is nonlinear and multidimensional with normal and parametric feedback. The parametric feedback arises from the changes induced by hormones in specific enzyme-catalyzed reactions and membrane transport

mechanisms thereby resulting in parametric changes to the dynamics associated with these processes or subsystems. In addition, many metabolic processes exhibit saturation and threshold properties.

The interpretation of these statements in terms of differential equations required for a dynamic description of system behavior will involve nonlinear mathematics. Hence the first step in systematizing the physiologic knowledge of the metabolic system has led to the conclusion that the system is inherently nonlinear and multidimensional. Any meaningful attempt to describe the system mathematically cannot ignore these facts.

A meaningful dynamic description of the metabolic system at the level of detail depicted in Figure 1 is predicated upon finding suitable mathematical representations for all of the processes linking each pair of state variables. Although we by no means have the required experimental data to carry out this task at the present time, it is nevertheless worthwhile to express the relations indicated in Figure 1 at least in functional mathematical form. Only in this way will the areas in which more physiological information is required be specifically identified allowing suitable experiments to be designed to yield these data.

There are twenty-two state variables indicated in Figure 1, hence twenty-two coupled nonlinear differential equations comprise the dynamic model of the metabolic plant. The controls, acting at the site of the processes connecting state variables, will require six or twelve differential equations depending upon whether one or two-compartment distribution dynamics are assumed.

Let: $x \triangleq$ state variable vector (22 x 1)

$u \triangleq$ control variable vector (6 x 1)

$v \triangleq$ input variable vector (3 x 1)

then functionally, the overall plant may be written:

$$\dot{x} = f(x,u,v) \tag{1-1}$$

where f is (22 x 1) and the hormonal controller may be written:

$$\dot{u} = g(x,\dot{x},u) \tag{1-2}$$

where g is (6 x 1). For a more detailed specification of the system we make the following definitions.

Let the inputs be designated:

$v_1 \triangleq$ Ingested carbohydrate

$v_2 \triangleq$ Ingested fat

$v_3 \triangleq$ Ingested protein

Let the states be designated:

$x_1 \triangleq$ Plasma glucose concentration

$x_2 \triangleq$ Plasma free fatty acid concentration

$x_3 \triangleq$ Plasma triglyceride concentration

$x_4 \triangleq$ Plasma ketones concentration

$x_5 \triangleq$ Plasma glycerol concentration

$x_6 \triangleq$ Plasma pyruvate and lactate concentration

$x_7 \triangleq$ Plasma amino acid concentration

$x_8 \triangleq$ Liver and kidney glucose concentration

$x_9 \triangleq$ Liver and kidney glycogen mass

$x_{10} \triangleq$ Muscle glucose concentration

$x_{11} \triangleq$ Muscle glycogen mass

$x_{12} \triangleq$ Liver amino acid concentration

$x_{13} \triangleq$ Liver protein mass

$x_{14} \triangleq$ Muscle tissue amino acid concentration

$x_{15} \triangleq$ Muscle tissue protein mass

$x_{16} \triangleq$ Adipose tissue free fatty acid concentration

$x_{17} \triangleq$ Adipose tissue triglyceride mass

$x_{18} \triangleq$ Adipose tissue glycerol concentration

$x_{19} \triangleq$ Triglyceride metabolizing tissues triglyceride mass

$x_{20} \triangleq$ Liver triglyceride concentration

$x_{21} \triangleq$ Liver free fatty acid concentration

$x_{22} \triangleq$ Liver ketones concentration

Let the controls be designated:

$u_1 \triangleq$ Plasma insulin concentration

$u_2 \triangleq$ Plasma glucagon concentration

$u_3 \triangleq$ Plasma epinephrine concentration

$u_4 \triangleq$ Plasma growth hormone concentration

$u_5 \triangleq$ Plasma corticosteroid concentration

$u_6 \triangleq$ Plasma thyroid hormone concentration

For purposes of illustration, processes will be depicted functionally except that all transport processes will be expressed in terms of linear diffusion kinetics. The processes represented by each function are in one to one correspondence with the arrows linking state variables

in Figure 1 and are written on the right hand side of the following equations taking the arrows clockwise for each variable starting at the top of each box.

$$V_1\dot{x}_1 = f_1^1(x_1, v_1, u_6) - f_1^2(x_1, u_6) - f_1^3(x_1, x_{16}, u_1, u_4) - \gamma_1(x_1 - x_8) - \gamma_2(u_1)[x_1 - x_{10}] - f_1^4(x_1) \tag{1-3}$$

$$V_2\dot{x}_2 = f_2^1(x_2, v_2) - \gamma_3(x_2 - x_{21}) - \gamma_4(x_2 - x_{16}) - f_2^2(x_2, u_6) \tag{1-4}$$

$$V_3\dot{x}_3 = f_3^1(x_3, v_2) - \gamma_5(x_3 - x_{20}) - f_3^2(x_3, x_{19}) - f_3^3(x_3, x_{17}) \tag{1-5}$$

$$V_4\dot{x}_4 = - \gamma_6(x_4 - x_{22}) - f_4^1(x_4, u_6) - f_4^2(x_4) \tag{1-6}$$

$$V_5\dot{x}_5 = - \gamma_7(x_5 - x_{18}) + f_5^1(x_5, x_{19}, u_3, u_4, u_5, u_6) - f_5^2(x_5, x_8, u_1) \tag{1-7}$$

$$V_6\dot{x}_6 = - f_6^1(x_6, x_8, u_1, u_2) - f_6^2(x_6, u_6) - f_6^3(x_6, x_{12}, u_4) + f_6^4(x_6, x_{10}, u_3, u_5) \tag{1-8}$$

$$V_7\dot{x}_7 = f_7^1(x_7, v_3) - f_7^2(x_7, x_8, u_2, u_4, u_5) - \gamma_8(x_7 - x_{12}) - \gamma_9(u_4)[x_7 - x_{14}] \tag{1-9}$$

$$V_8\dot{x}_8 = - \gamma_1(x_8 - x_1) + f_8^1(x_8, x_5, u_1) + f_8^2(x_8, x_9, u_1, u_2, u_3) + f_8^3(x_8, x_6, u_1, u_2) + f_8^4(x_8, x_7, u_2, u_4, u_5) \tag{1-10}$$

$$\dot{x}_1 = f_9^1(x_9, x_8, u_1, u_2, u_3) \tag{1-11}$$

$$V_{10}\dot{x}_{10} = -\gamma_2(u_1)[x_{10}-x_1] - f_{10}^1(x_{10}, x_6, u_3, u_5) - f_{10}^2(x_{10}, x_{11}, u_3, u_4, u_5) \tag{1-12}$$

$$\dot{x}_{11} = f_{11}^1(x_{11}, x_{10}, u_3, u_4, u_5) \tag{1-13}$$

$$V_{12}\dot{x}_{12} = -\gamma_8(x_{12}-x_7) + f_{12}^1(x_{12}, x_6, u_4) - f_{12}^2(x_{12}, x_{13}, u_1, u_2, u_4, u_5) \tag{1-14}$$

$$\dot{x}_{13} = f_{13}^1(x_{13}, x_{12}, u_1, u_2, u_4, u_5) - f_{13}^2(x_{13}) \tag{1-15}$$

$$V_{14}\dot{x}_{14} = -\gamma_9(u_4)[x_{14}-x_7] - f_{14}^1(x_{14}, x_{15}, u_1, u_2, u_4, u_5) - f_{14}^2(x_{14}, u_6) \tag{1-16}$$

$$\dot{x}_{15} = f_{15}^1(x_{15}, x_{14}, u_1, u_2, u_4, u_5) \tag{1-17}$$

$$V_{16}\dot{x}_{16} = -\gamma_4(x_{16}-x_2) - f_{16}^1(x_{16}, u_6) - f_{16}^2(x_{16}, x_{17}, u_1, u_3, u_4, u_5) + f_{16}^3(x_{16}, x_1, u_1, u_4) \tag{1-18}$$

$$\dot{x}_{17} = f_{17}^1(x_{17}, x_{16}, u_1, u_2, u_4, u_5) + f_{17}^2(x_{17}, x_3) - f_{17}^3(x_{17}, x_{18}, u_1, u_2, u_4, u_5) \tag{1-19}$$

$$V_{18}\dot{x}_{18} = f_{18}^1(x_{18}, x_{17}, u_1, u_2, u_4, u_5) - \gamma_7(x_{18}-x_5) \tag{1-20}$$

$$\dot{x}_{19} = f_{19}^1(x_{19}, x_3) - f_{19}^2(x_{19}, u_6) - f_{19}^3(x_{19}, x_5, u_3, u_4, u_5, u_6) \tag{1-21}$$

$$V_{20}\dot{x}_{20} = f^1_{20}(x_{20}, x_{21}, u_4) - \gamma_5(x_{20}-x_3) \tag{1-22}$$

$$V_{21}\dot{x}_{21} = -\gamma_3(x_{21}-x_2) - f^1_{21}(x_{21}, x_{22}, u_1) - f^2_{21}(x_{21}, x_{20}, u_4) \tag{1-23}$$

$$V_{22}\dot{x}_{22} = f^1_{22}(x_{22}, x_{21}, u_1) - \gamma_6(x_{22}-x_4) \tag{1-24}$$

The detailed mathematical representation of this model for the metabolic plant requires the specification of 48 functions representing processes (f^i_j), 2 variable permeability functions $(\gamma_j(u_i))$, 7 permeability constants (γ_j), and 16 distribution spaces (V_j).

If we define the exogenous input of hormones by $w_1, \cdots, w_6$, then the controller can be functionally written as follows if one-compartment distribution for each hormone is assumed.

$$U_1\dot{u}_1 = g^1_1(w_1) + g^2_1(u_1, u_3, x_1, \dot{x}_1) \tag{1-25}$$

$$U_2\dot{u}_2 = g^1_2(w_2) + g^2_2(u_2, x_1) \tag{1-26}$$

$$U_3\dot{u}_3 = g^1_3(w_3) + g^2_3(u_3, x_1, \dot{x}_1) \tag{1-27}$$

$$U_4\dot{u}_4 = g^1_4(w_4) + g^1_4(u_4, x_1, \dot{x}_1) \tag{1-28}$$

$$U_5\dot{u}_5 = g^1_5(w_5) + g^2_5(u_5, x_1) \tag{1-29}$$

$$U_6\dot{u}_6 = g^1_6(w_6) + g^2_6(u_6, x_1) \tag{1-30}$$

where it has been assumed that all six hormonal controls are generated as functions of the plasma glucose concentration.

Solving the inverse problem, i.e. identifying system model parameters based on noisy observations on the variables x_1 through x_7, for the complete system is a formidable task even if we assume the requisite experimental data to exist. The only possible approach at this time is to focus on specific portions of the system while lumping in an appropriate manner the neglected portions. In the sequel a detailed derivation and analysis of a model for glucose metabolic control will be presented.

III. MATHEMATICAL MODELS OF THE GLUCOSE CONTROL SYSTEM

3.1. Introduction.

Owing to the complexity of the system depicted in Figure 1 and the paucity of experimental data that can suggest reasonably valid analytical models for the relevant subsystems, we have tried to construct models using as small a set of basic analytical building blocks as possible with parameter values chosen for any specific process within a given class to accommodate the behavior of that process. The real objective in this work is to demonstrate by means of examples what control systems techniques can contribute to our investigative techniques and understanding of these biological regulation systems. Although a great amount of physiology has yet to be learned about the relevant subsystems involved before a definitive model can be established, it is our belief that the systems analyst can contribute to this effort now by systematizing our knowledge about the metabolic system in a consistent mathematical framework, by suggesting to the biological scientist specific experiments suggested by model building, simulation, and analysis, and by determining analytically the dynamical consequences of conflicting theories concerning the operation of specific portions of the system.

Beginning with the recognition that the system contains inherent nonlinearities such as saturation effects and threshold phenomena, the models are constructed from first order nonlinear differential equations. All the models are simulated by digital computer and compared to data obtained from controlled experiments, performed on young normal adult male subjects.

Our current understanding of the interrelated processes and physical organs constituting the metabolic system and its endocrine control is depicted in the generic diagram shown in Figure 2. This diagram represents an attempt to systematize the physiologic facts summarized in Chapter II as a first step in the eventual derivation of a detailed metabolic control model consistent with established engineering control systems concepts, theories, and techniques.

3.2. Mathematical Models of Metabolic Processes.

A mathematical model of a physical process or group of processes, i.e. a system, is a concise representation of the major characteristics of the system in a form which historically has proven to be of major significance in understanding physical phenomena. Entire fields of applied mathematics have been developed in response to the challenges to our understanding presented by various groups of physical phenomena. Common to most of these efforts has been the use of differential equations to represent the behavior of physical processes, making possible descriptions of the "dynamic" behavior, i.e. as a function of time, of systems. These mathematical methods have been most refined for linear systems, i.e. these for which the principle of superposition is valid.

Mathematically, a model of a system is a "transformation" of the inputs or stimuli to the outputs or responses both of which are defined intuitively or subjectively based on our understanding of the system. A differential or differential-difference equation representation of stimuli-response transformations usually involves intermediate variables called "state variables". From a mathematical viewpoint

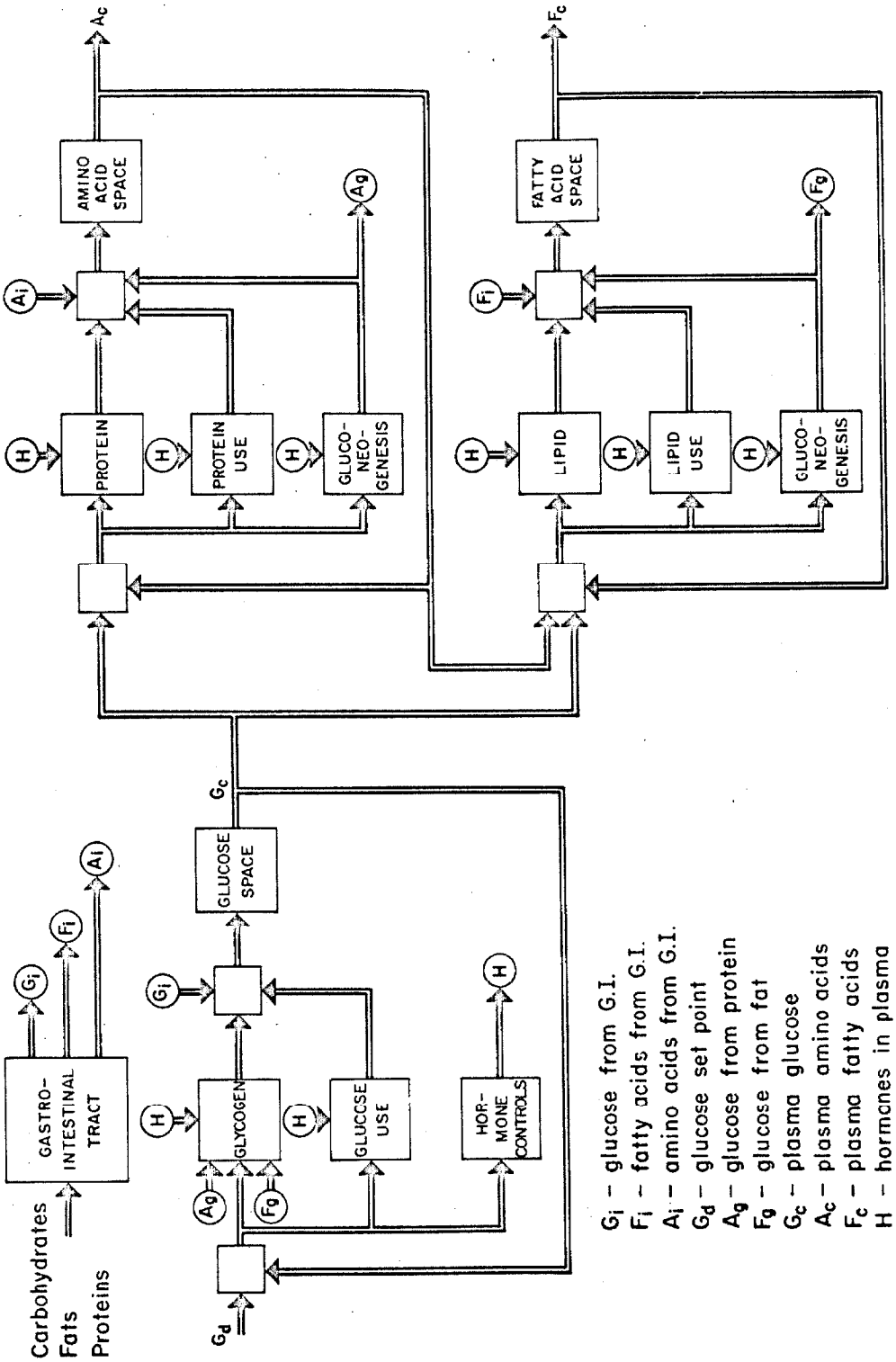

Figure 2. Metabolic Control System.

the choice of states is not unique, but this does not make the representation of the system ambiguous since the states are unique within a similarity transformation. In biological systems a reasonable choice of unique states results by insisting that the state variables represent biologically meaningful entities, for example see Figure 1. Obviously, the very choice of differential equations for representing a physical system involves subjective judgment.

The first matter for consideration in the construction of a model is to decide whether a deterministic or stochastic form is appropriate for the phenomenon of interest. The appropriateness of a deterministic model is influenced by the "repeatability" of each of the experiments. If it is not possible to conduct an experiment on the same subject under identical environmental conditions several times and observe identical responses then either a deterministic model is meaningless or all the causes which influence the model have not been considered.

Given a hypothesized model, the next step to consider is the so-called "inverse problem". This is the problem of determining the numerical values of the parameters in a model by suitably processing the data available on the stimulus and the associated response. This problem is far from trivial even from the strictly theoretical point of view. The inverse problem is often complicated by questions of "observability". Usually we are not sure whether the stimuli-response data contain enough information about the parameters, and typically we are unsure whether the response to the given stimulus is reasonably sensitive to changes in the values of the parameters.

Assuming that the inverse problem is meaningfully defined and algorithms are available for its solution, the model should next satisfy certain predictability requirements. The model with parameters numerically determined based on the necessary stimulus-response data should yield predicted responses which can be corroborated experimentally for different stimuli.

One of the major difficulties in constructing accurate models of metabolic systems is the limited reliable data that is available which is in a form useful for solving inverse problems. The solution of the inverse problem requires that data be obtained for different stimuli on the same individual with extraneous factors reduced to a minimum. It does not make sense from the modeling point of view to use glucose tolerance data from one individual and insulin tolerance data from another. Moreover, it is extremely important that the responses of interest be sampled at a rate that is consistent with the model. For example, a large number of models can be constructed which will agree very well with the response to an oral glucose load if only four data points spaced every half hour are taken. It is also very important to know precisely the exact times at which various stimuli were applied and the various responses were sampled. Model parameters are often extremely sensitive to the instants of time at which certain events occur.

The metabolic control system modeling problem is to find mathematical representations for the detailed processes depicted in Figure 2 and to relate them in a consistent manner resulting in an overall analytic representation of the metabolic system. The previous observa-

tions imply that a meaningful system model for metabolism will involve nonlinear mathematics, hence the analytic difficulties implicit in these efforts will necessitate the use of extensive computation facilities for simulation purposes. As will be seen in the sequel, a brief survey of efforts to model the glucose homeostatic system, most of the reported work on this problem avoids the above mathematical difficulties by introducing assumptions which ignore either or both the multidimensional and nonlinear aspects of the problem. Also characteristic of all the reported attempts at modeling the glucose control system is the use of in vitro data on subsystems taken from animal experiments, somehow extrapolating such numbers to that of a 70 kg. human, and finally simulating the system by trial and error to match qualitatively a human subject's response to an intravenous glucose input. There have been no reported attempts to establish a methodology whereby a proposed model of human metabolic control can be obtained by experiments performed directly on the human subject.

3.3. Reported Efforts at Modeling Glucose Regulation.

The first reported attempt to illustrate how the concepts of control systems engineering can be applied to the study of glucose homeostasis was supplied by Goldman in 1960.[54] He summarized qualitatively the major metabolic subsystems and controlling hormones relevant to glucose regulation and represented their interconnection in a block diagram suggestive of a multi-loop feedback control system (see Figure 3). Goldman did not attempt to develop his model in any more detail, but discussed the eventual application of modeling efforts

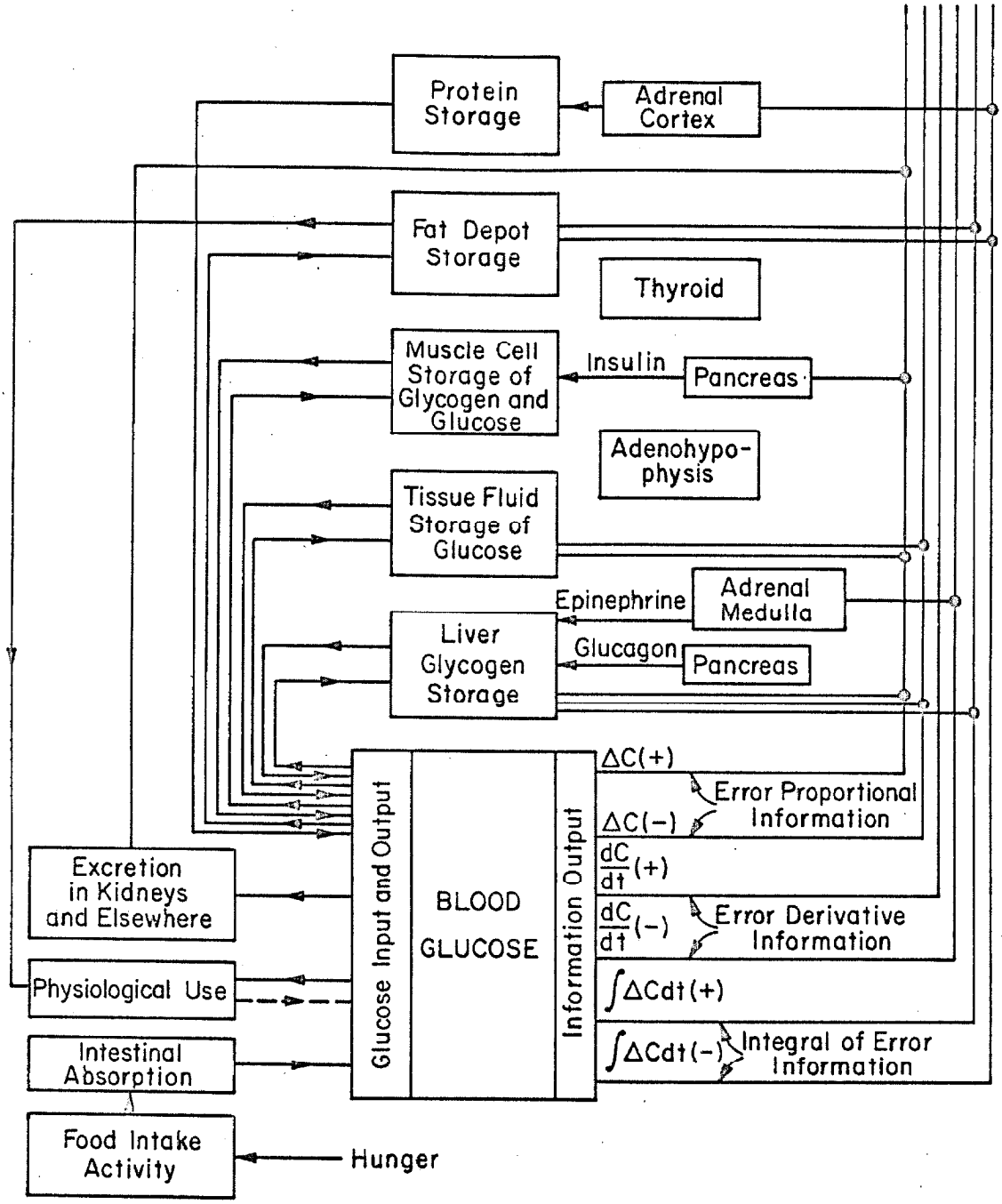

Figure 3. Goldman's Proposed Glucose Model.

in characterizing clinical abnormalities and in endocrine system research. Assuming that glucose regulation can be viewed as a classical regulating system, Goldman emphasized the need for new experiments to understand the physiological mechanism of set-point establishment and to identify which possible modes of control exist in this physiological system. Although this work does not enhance our physiological knowledge of glucose metabolism per se, it constitutes a logical first step in any detailed mathematical modeling of the system by identifying the major subsystems involved and their logical interconnection in a systematic manner consistent with standard control system terminology.

The next published work is that of Bolie[55,56] illustrating the use of analog computers in simulation of mathematical representation of glucose regulation. The first model treats the interaction of liver, kidney, pancreas, insulin, and glucose in two compartments, the vascular and extravascular. The model is a gross treatment of the glucose regulating system, involving only one controlling hormone and being strictly linear except for a renal threshold. It qualitatively reproduces insulin and glucose behavior after simulated 6 minute infusions of glucose and insulin of 50 g. and 2 units respectively. The model is represented by Equations (3-1) through (3-4):

$$V_B \dot{I}_v = I_i + (I_e - I_v)\, P_I + K_1 G_v - K_2 I_v \qquad (3\text{-}1)$$

i.e., the rate of accumulation of insulin in the blood stream equals the rate of injection plus the rate of transfer from the extravascular

compartment plus the rate at which it is released from the pancreas minus the rate at which it is degraded in the vascular compartment.

$$V_I \dot{I}_e = (I_v - I_e)\, P_I - K_3 I_e \qquad (3\text{-}2)$$

i.e., the rate of accumulation of insulin in the extravascular insulin space equals the rate of transfer from the vascular space minus the rate at which it is degraded in the extravascular space.

$$V_B \dot{G}_v = G_i + (G_e - G_v)\, P_G - f(G_v) - K_4 I_v - K_5 G_v \qquad (3\text{-}3)$$

i.e., the rate of accumulation of blood glucose equals the rate of injection plus the rate of transfer from the extravascular compartment minus renal excretion and storage in liver.

$$V_G \dot{G}_e = (G_v - G_e)\, P_G - K_6 I_e - K_7 G_e \qquad (3\text{-}4)$$

i.e., the rate of accumulation of extravascular glucose equals the rate of transfer from the vascular space minus tissue utilization.

Known nonlinear effects have been linearized and represented by the constants K_1 through K_7. The renal nonlinearity $f(G_v)$ consists of a threshold and constant gain. This work illustrates on a limited scale the use of simulation in verifying the consistency of a proposed model.

Bolie's second paper[56] neglects renal excretion and lumps the vascular system and extravascular system into one compartment. The

model then reduces to two first-order linear differential equations:

$$\dot{I} = \frac{I_i}{V} - \alpha I + \beta G \qquad (3\text{-}5)$$

$$\dot{G} = \frac{G_i}{V} - \gamma I - \delta G \qquad (3\text{-}6)$$

where (α) represents the sensitivity of insulinase activity to insulin concentration, (β) represents the sensitivity of pancreatic insulin output to glucose concentration, (γ) represents the combined sensitivity of liver glycogen storage and tissue glucose utilization to elevated glucose concentration, and (δ) represents the combined sensitivity of liver glycogen storage and tissue glucose utilization to elevated glucose concentration.

The parameters of this model were derived from data obtained from various sources, in some cases values were "averaged" across species! No attempt was made to verify the behavior of the model by predictability of experiments. It is evident that at best the model parameters are chosen optimally with respect to one experiment.

The next published effort in modeling of glucose regulation is that of Seed, Acton, and Stunkard.[57] The model relates liver, kidney, brain, pancreas, vascular and extravascular compartments, and a substance Z, presumably related to hormone action, in terms of three dependent variables connected by piecewise linear ordinary differential equations. The equations represent respectively, the rate of change of glucose in the "fast" compartment, the rate of change of glucose in the "slow" compartment, and the rate of change of substance Z in the

liver. The expressions in square brackets are zero unless the condition noted below each bracket is satisfied.

$$\dot{G}_f = - D_f G_f + D_s G_s - L_z G_f - M_a G_f - B - [M_f G_f - m_f] - [R G_f - r]$$
$$\{G_f > L_f\} \qquad \{G_f \geq L_v\}$$
$$+ [p_g - P_g Z] + [I] \tag{3-7}$$
$$\{Z < L_p\} \quad \{t < L_T\}$$

$$\dot{G}_s = D_f G_f - D_s G_s - [M_s G_s - m_s] \tag{3-8}$$
$$\{G_s > L_s\}$$

$$\dot{Z} = - c_z - C_z Z + F_z G_f \tag{3-9}$$

These equations were simulated, and by trial and error parameter adjustment showed qualitative agreement over a limited interval with some kind of an "average" of plasma glucose after a 25 g. infusion taken over 70 normal subjects. These data were obtained by Amatuzio.[58] However, this method of model verification was found to yield physiologically unrealistic parameters.

These investigators then expanded the model to include two new compartments, red blood cells and plasma. The equations represent, respectively, the rate of change of plasma glucose, fast compartment glucose, slow compartment glucose, red blood cell glucose, and substance Z in liver.

$$\dot{G}_p = -(D_{pf}G_p - D_{fp}G_f) - (D_{ps}G_p - D_{sp}G_s) - KV_{G_c}\left[\frac{G_p}{G_p + G_{\phi_p}} - \frac{G_c}{G_c + G_{\phi_c}}\right]$$

$$- [P_g Z - p_g] - L_z G_f - [RG_p - r] - B + [I] \quad (3\text{-}10)$$
$$\{Z < L_p\} \qquad \{G_p > L_r\} \; \{t < L_T\}$$

$$\dot{G}_f = (D_{pf}G_p - D_{fp}G_f) - M_a G_f - [M_f G_f - m_f] \quad (3\text{-}11)$$
$$\{G_f > L_f\}$$

$$\dot{G}_s = (D_{ps}G_p - D_{sp}G_s) - M_b G_s - [M_s G_s - m_s] \quad (3\text{-}12)$$
$$\{G_s > L_s\}$$

$$\dot{G}_c = KV_{G_c}\left[\frac{G_p}{G_p + G_{\phi_p}} - \frac{G_c}{G_c + G_{\phi_c}}\right] \quad (3\text{-}13)$$

$$\dot{Z} = F_z G_f - [C_z Z + c_z] \quad (3\text{-}14)$$
$$\{Z > 0\}$$

The authors attempted to substantiate all parameter values from published experimental results before computer simulations were undertaken. Again, roughly qualitative reproduction of experimental results was obtained. In view of the more recent results obtained in hormone effects and the fact that these are not explicitly included in this work, the deficiencies of the model are substantial. As in the previous two efforts, the model essentially amounts to a more sophisticated attempt at curve-fitting one specific stimulus-response characteristic, that resulting from a glucose input.

In 1962 Belilles[59] evaluated by experiments on dogs the coefficients in the Bolie model. In addition he proposed a five-compartment model in terms of linear ordinary differential equations and discussed preliminary estimates of the parameters. The compartments consist of arterial blood, pancreas, liver, splanchnic area minus pancreas and liver, and peripheral tissue.

A schematic illustrating the model is shown in Figure 4. The detailed equations of the model are given by (3-16) through (3-34), but they can be represented by the vector equation:

$$\dot{x} = Ax + f \tag{3-15}$$

where x and f are eight-dimensional vectors, and A is an 8×8 constant coefficient matrix.

Insulin and glucose concentrations in the extracellular fluid of peripheral tissue are represented by:

$$\dot{I}_b = -\frac{F_b}{V_b}[I_b - I_a] \tag{3-16}$$

$$\dot{G}_b = -\frac{F_b}{V_b}[G_b - G_a] - \frac{M_b}{V_b} \tag{3-17}$$

The concentrations of insulin and glucose in pancreas efferent blood are represented by:

$$\dot{I}_p = -\frac{F_p}{V_p}[I_p - I_a] + \frac{R}{V_p} \tag{3-18}$$

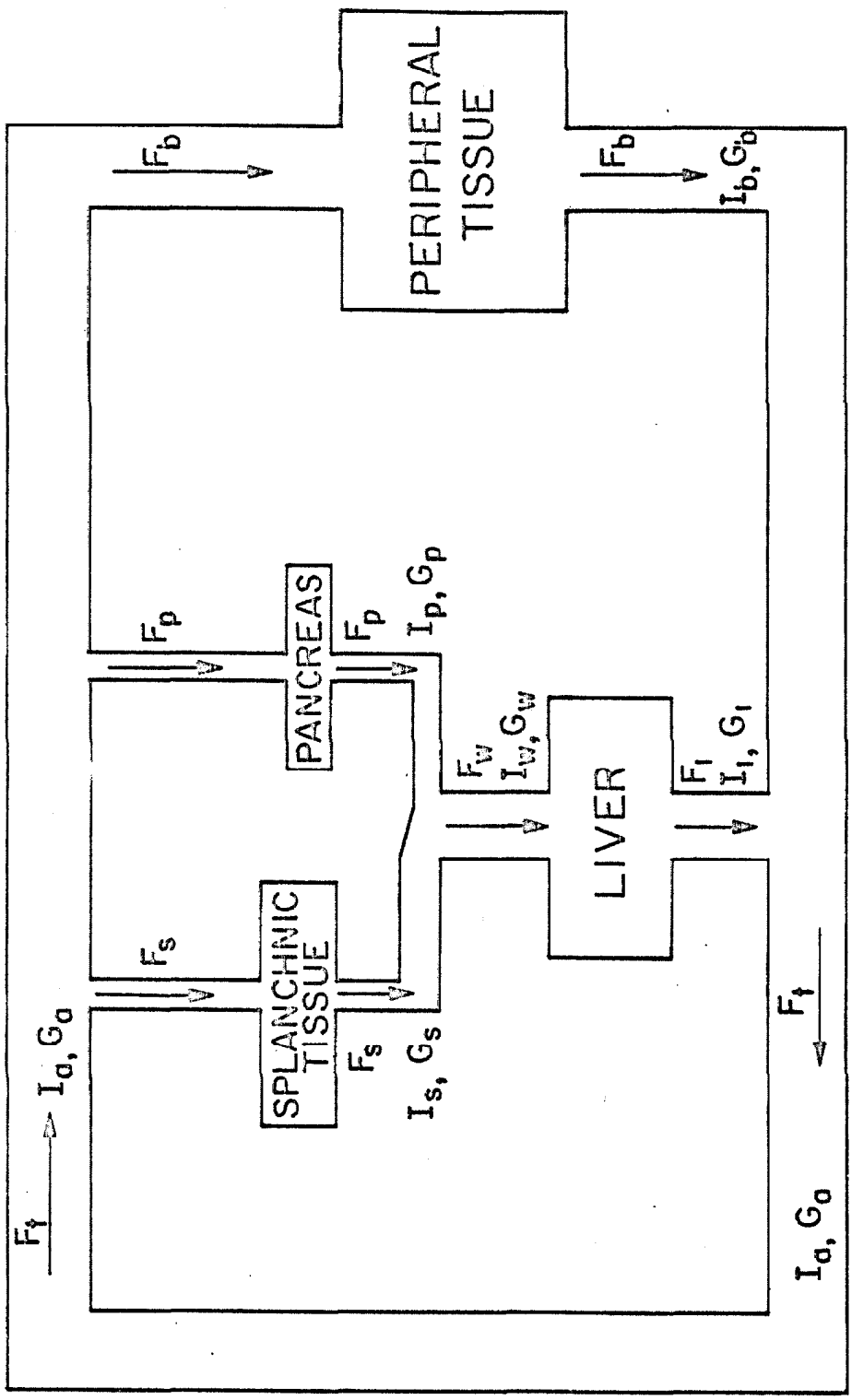

Figure 4. Bellies' Proposed Glucose Model.

$$\dot{G}_p = - \frac{F_p}{V_p} [G_p - G_a] - \frac{M_p}{V_p} \tag{3-19}$$

The concentrations of insulin and glucose in splanchnic tissues efferent blood are represented by:

$$\dot{I}_s = - \frac{F_s}{V_s} [I_s - I_a] \tag{3-20}$$

$$\dot{G}_s = - \frac{F_s}{V_s} [G_s - G_a] - \frac{M_s}{F_s} \tag{3-21}$$

And the concentrations of insulin and glucose in the liver efferent blood are represented by:

$$\dot{I}_\ell = - \frac{F}{V_\ell} [- I_\ell + I_\omega] - \frac{D}{V_\ell} \tag{3-22}$$

$$\dot{G}_\ell = - \frac{F_\ell}{V_\ell} [- G_\ell + G_\omega] - \frac{H}{V_\ell} \tag{3-23}$$

It can be seen that blood flow rates are related by:

$$\left.\begin{aligned} F_p + F_s &= F_\ell \\ F_\ell + F_b &= F_t \end{aligned}\right\} \tag{3-24}$$

Continuity of transport rates requires that:

$$F_p I_p + F_s I_s = F_\ell I_\omega \tag{3-25}$$

$$F_p G_p + F_s G_s = F_\ell G_\omega \tag{3-26}$$

$$F_\ell G_\ell + F_b G_b = F_t G_a \tag{3-27}$$

$$F_\ell I_\ell + F_b I_b = F_t I_a \tag{3-28}$$

Insulin production is linearly related to circulating glucose:

$$R = K_r G_p \tag{3-29}$$

Destruction of insulin by the liver is made proportional to the concentration of insulin leaving the liver:

$$D = K_b I_\ell \tag{3-30}$$

Storage of glucose by the liver is made linearly proportional to glucose and insulin levels above some minimal levels:

$$H = H_o + K_{\ell_1}(G_1+G_o) + K_{\ell_2}(I_1-I_o) \tag{3-31}$$

The rates of metabolism of glucose in peripheral tissue, splanchnic area and pancreas are represented by:

$$M_b = M_{b_o} + K_{b_1}(G_b-G_1) + K_{b_2}(I_b-I_1) \tag{3-32}$$

$$M_s = M_{s_o} + K_{s_1}(G_s - G_2) + K_{s_2}(I_s - I_2) \tag{3-33}$$

$$M_p = M_{p_o} + K_{p_1}(G_p - G_3) + K_{p_2}(I_p - I_3) \tag{3-34}$$

Values for the parameters of this model were obtained mostly from in vitro data taken on various animals. No attempt was made to compare the performance of this linear time-invariant model with actual experimental data on an intact animal. Because of the linear approximations made and the inclusion of only insulin as a controlling hormone, at best the model could only represent the system under small hyperglycemic perturbations about the nominal state, i.e. for small glucose inputs only.

As we have seen, Bolie's work resulted in a model which can be represented by the vector equation:

$$\dot{x} = Ax + f + g \tag{3-35}$$

where x, f and g are 4-vectors and A is a 4×4 constant coefficient matrix. The 4 components of x represent glucose and insulin concentrations in the vascular and extravascular compartments, f includes a nonlinearity for renal excretion and g represents glucose and insulin infusions. Bolie then reduced the order of the system by two to emphasize intravascular glucose and insulin coefficients, obtaining a system of the form:

$$\dot{x} = Ax + g \tag{3-36}$$

where x and g are 2-vectors and A is a 2×2 constant coefficient matrix. The g vector again represents glucose and insulin infusion.

In 1963 Wrede[60] extended these results to a linear model representing glucose metabolism as a function of the hormones insulin, glucagon, epinephrine, cortisol, thyroxin and growth hormone. His model can be represented:

$$\dot{x} = Ax + f \tag{3-37}$$

where x is a 7-vector representing plasma concentration of glucose and the six hormones under consideration; A is a 7×7 constant coefficient matrix; and f is a 7-vector representing infusion rates of glucose and six hormones.

Wrede attempted to derive the parameters of the model, i.e., the coefficients of the A matrix in (3-37), from the available experimental data. The author recognized that a desired goal in modeling is a physiologically meaningful representation in contrast to "curve-fitting". Because of the linearity of the model, all of the substantial body of control systems analysis techniques could be brought to bear on the problem. By striving for equation consistency and analyzing how equilibrium constraints dictate model behavior, he was able to establish theoretical values for unobservable parameters.

Analysis of the model yielded numerical values for certain parameters which were remarkably close to the experimentally determined values. However, of more interest is the fact that this model for the first time

predicted physiological consequences that had not been experimentally corroborated at that time. It is, of course, also possible that these conclusions were anomalous artifacts resulting from inadequacies of the model. However, this work does demonstrate on a limited scale how model building and simulation can be useful in studying metabolic processes. The author also simulated glucose and insulin tolerance tests on the model, obtaining qualitatively correct behavior for some of the components of x.

Although the limitations in Wrede's model are clearly evident, his is the first attempt at constructing a model that includes all of the known hormonal controls (except sex hormones) believed to affect adult glucose metabolism. All such efforts prior to Wrede considered only the effects of insulin, whereas he considered the effects of six hormones, albeit in a linear manner only.

In 1964 McLean[61] published a brief summary of glucose homeostasis focusing primarily on Goldman's work. He attempted to incorporate nervous system effects explicitly in a modified system block diagram. However, owing to our very rudimentary understanding of mathematical representations for neural processes, successful modeling of such processes await the results of more basic research.

Keeping in mind the complexity of the overall metabolic control system as depicted in Figure 1 we see that the above reported results are representative attempts at achieving some kind of a mathematical representation for certain portions of the complete system. Common to these efforts is a restricted emphasis on glucose metabolism, lipid and protein metabolism being neglected.

In 1965 Shames[62] reported on a mathematical model for the dynamic response of glucose in extracellular fluid and intracellular hepatic fluid, insulin in plasma and interstitial fluid, and free fatty acids (FFA) in extracellular fluid to a glucose input (Equations (3-38) to (3-42)).

$$V_e\dot{G}_e = s_1 + k_1(G_\ell - G_e) - k_2(G_e - G_{tm}) - B - [k_3 + k_4 I_i + k_5(F_b - F_e)](G_e - G_t) \tag{3-38}$$

$$V_\ell\dot{G}_\ell = b_1 - k_6 I_p\left(\frac{G_\ell}{G_\ell + M_{p\ell}}\right) - k_1(G_\ell - G_e) \tag{3-39}$$

$$V_p\dot{I}_p = b_2 + k_7 G_e^{\,2} + k_7 G_e^{\,2} - k_8(I_p - I_i) - k_9 I_p \tag{3-40}$$

$$V_i\dot{I}_i = k_8(I_p - I_i) - k_{10} I_i \tag{3-41}$$

$$V_e\dot{F}_e = b_3 - k_{11}\{[k_3 + k_4 I_i + k_5(F_b - F_e)](G_e - G_t) - P_b\} - k_{12} F_e \tag{3-42}$$

Pancreatic insulin production is made proportional to the square of extracellular glucose and exchange between the plasma and the interstitial space is by simple diffusion (see Equations (3-40) and (3-41)). Equation (3-39) reflects the fact that simple diffusion relates extracellular fluid glucose and hepatic intracellular fluid glucose and the assumption that the Michaelis-Menten kinetics of the hexokinose-glucose-6-phosphatase system are rapidly changed to produce net phosphorylation by plasma insulin through a constant. Both removal of FFA through oxi-

dation and recycling through adipose tissue stores are represented by a linear process and lumped into the constant k_{12}. The rate of decrease of FFA is proportional through k_{11} to the increase in the rate of peripheral utilization of glucose above the basal rate. These effects are represented by Equation (3-42). Equation (3-38), representing sources and sinks for glucose, contains the hepatic term as in Equation (3-39), a sink linearly related to glucose concentration above a threshold for renal excretion, a constant for CNS utilization, and a term linearly related to the extracellular fluid to the peripheral tissue intracellular fluid gradient weighted by insulin and FFA concentrations.

It was the intent of the author to study some aspects of glucose regulation from a theoretical systems viewpoint using experimental data in the reported literature. The model treats only one aspect of the glucose regulatory system, that pertaining to an elevated glucose condition. Combined into the model are data from both in vitro and in vivo experiments in animals and man. This is the first reported attempt to include in a model of glucose control the effects of free fatty acids. It constitutes a correct step toward the eventual mathematical representation of the full metabolic control system depicted in Figure 1, of which the glucose control system per se forms only a part.

Early in 1967 Cerasi published the results of some work on analog simulation of glucose regulation.[63] The model represents insulin and glucose in one compartment and includes renal excretion, peripheral glucose uptake, and insulin secretion. The release of insulin in response to glucose concentration is represented in two phases, the release of stored insulin and the release of newly formed insulin. The

model is not strictly linear, since the uptake rate of glucose by peripheral tissue, for example, is represented as proportional to the product of insulin and glucose concentrations, and a renal excretion threshold is included. The author claims successful simulation of many experimental tests performed on humans in the hospital laboratories. However, it is apparent that the model is an insufficient representation of the glucose regulatory system, considering what is known about the metabolic processes and the hormonal controls involved. The basic purpose of the author was to represent in a mathematical fashion the behavior of glucose and insulin concentration after a glucose input by means of a lumped model.

Some more recent work on glucose modeling is due to Wolaver.[64] His model consists of four first-order nonlinear differential equations depicting the behavior of glucose and insulin in two compartments, the vascular and the extravascular, i.e. functionally:

$$V_B \frac{d}{dt}(BG) = f_L(BG,BI) - f_R(BG) + P_G(CG-BG) \tag{3-43}$$

$$V_G \frac{d}{dt}(CG) = P_G(BG-CG) - f_U(BG,BI) \tag{3-44}$$

$$V_B \frac{d}{dt}(BI) = f_P(BG) - (K)(BI) + P_I(CI-BI) \tag{3-45}$$

$$V_I \frac{d}{dt}(CI) = P_I(BI-CI) - (KD)(CI) \tag{3-46}$$

Taking the by now familiar approach, Wolaver attempts to obtain reasonable numbers for as many parameters as possible from published experi-

mental data, and determines the remainder by fitting the model response to experimental results. The author recognizes some weaknesses of the model such as the questionable practice of extrapolating animal data to humans and the gross lumping of hormonal effects into one control signal called "insulin".

A model is not very useful unless it can predict in a consistent manner the responses to stimuli different from those used to determine the parameters of the model. It is evident that very little substantiation of the proposed models has been carried out in the literature by proper predictions.

Most of the proposed models of glucose regulation are concerned only with the hyperglycemic response. This approach ignores the all important effects of the hyperglycemic hormones which play an essential role in over-all glucose homeostasis.

3.4. A New Approach to Modeling Metabolic Control Systems.

A somewhat different approach to the modeling problem has been taken by the author in contrast to the methods surveyed in Section 3.3. Basically, the method is motivated by the kinetic theory of enzyme-catalyzed chemical reactions and corroborated by in vitro and in vivo experimental animal data. These considerations lead to a specific mathematical functional form for the input-output relation representing a process or group of related processes. Reliance is then placed on mathematical algorithms to estimate the values of the parameters of the process representations from in vivo human experimental data.

Since many of the processes under consideration involving different state variables have similar functional forms relating input to output, the model can be constructed from a relatively small number of functional forms representing subsystems. The most critical part of the procedure is the design of suitable experiments which are feasible on humans to solve the inverse problem, i.e. experiments must be designed which excite only portions of the overall system at any one time in order to uncouple subsystems from one another and reduce the dimensionality of the parameter estimation problem to manageable proportions.

A comprehensive mathematical model of the metabolic control system will involve thousands of coupled nonlinear differential equations representing enzyme-catalyzed chemical reactions. However, our knowledge of the extremely complex and manifold series of reactions involved in the processes of metabolism is still rudimentary. In addition, the popular method of viewing this subject is through the so-called "steady-state" approximations of Michaelis-Menten or Briggs-Haldane (see Appendix A) which has become an entrenched tool, of limited utility in systems studies, to the biological scientist.

A great amount of work has been done in recent years on computer simulation of the differential equations representing series of enzyme-catalyzed reactions. For example, Chance[65,66] and Macnichol[67] simulated the equations for the reaction:

$$E + S \underset{k_2}{\overset{k_1}{\rightleftarrows}} C \xrightarrow{k_3} E + P \qquad (3\text{-}47)$$

yielding a solution of all the variables as a function of time. It is

obvious from an inspection of the curve $C(t)$, that the approximation upon which the validity of the algebraic Michaelis-Menten equation depends, i.e. $dC/dt = 0$, is valid at only one point. Since the object of the Michaelis-Menten representation of biochemical kinetics is to allow a determination of the rate constants of the reaction from experimental measurements to characterize the behavior of a reaction such as (3-47), it is clear that such an approach is inferior to determining the complete time course of all the variables in the reaction by solving the differential equations.

Other investigators[68] have simulated the equations for a series of such reactions involving intermediates such as:

$$E + S \underset{k_2}{\overset{k_1}{\rightleftarrows}} C_1 \underset{k_4}{\overset{k_3}{\rightleftarrows}} C_2 \underset{k_6}{\overset{k_5}{\rightleftarrows}} E + P \qquad (3\text{-}48)$$

And yet more sophisticated simulations of multi-enzyme systems have been performed. For example, Garfinkel[69] has simulated a model of the mammalian muscle phosphofructokinase system which includes 22 differential equations representing 22 chemical species involved in 42 chemical reactions. This series of reactions constitutes only part of the overall process of glycolysis, but the author expresses the opinion that it may be the point of control for the process since it is the only known enzyme in this pathway the activity of which can be turned on and off.

Coincident with efforts at simulating complex sequences of biochemical reactions other investigators have turned to completely analytical investigations of biochemical kinetics. For example, Miller and Alberty[70] derived the complete analytic solution for the differential

equations governing the following reaction:

$$E + S \underset{k_2}{\overset{k_1}{\rightleftarrows}} C \underset{k_4}{\overset{k_3}{\rightleftarrows}} E + P \qquad (3\text{-}49)$$

for the case $k_1 = k_4$. In the general case, $k_1 \neq k_4$, they derived a perturbation approximation. The implications of the so-called "steady-state" view of enzyme kinetics as opposed to an analysis based on the underlying differential equations have been very clearly stated by Heineken, Tsuchiya, and Aris.[71] These authors show that the equation of Michaelis-Menten is the degenerate case in a singular perturbation of the full kinetic equations under the assumption that the enzyme is present in a relatively small concentration. Results such as these do not seem to be widely known among biological scientists who continue to view the pseudo steady-state models as the sine qua non of enzyme kinetics investigations.

For the purposes of the present investigation we seek a suitable mathematical representation for a coupled sequence of enzyme-catalyzed reactions. Many of the processes involved in glucose metabolism, e.g. glycogenesis, glycogenolysis, gluconeogenesis, etc., will be represented as in Figure 5. For example, if the subsystem referred to represents hepatic glycogen formation then the input represents plasma glucose concentration [mg/100 mℓ] and the output represents the rate of formation of glycogen [mg/min]. The control in this case refers to the possible hormonal effects on certain enzymes in the glucose-glycogen pathway. In general, a plot of the rate of product formation as a function of substrate concentration with enzyme activity as a parameter

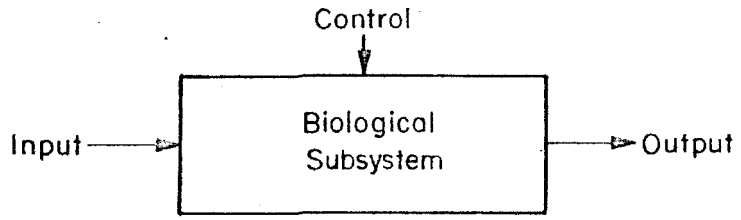

Figure 5. Parametrically Controlled Subsystem.

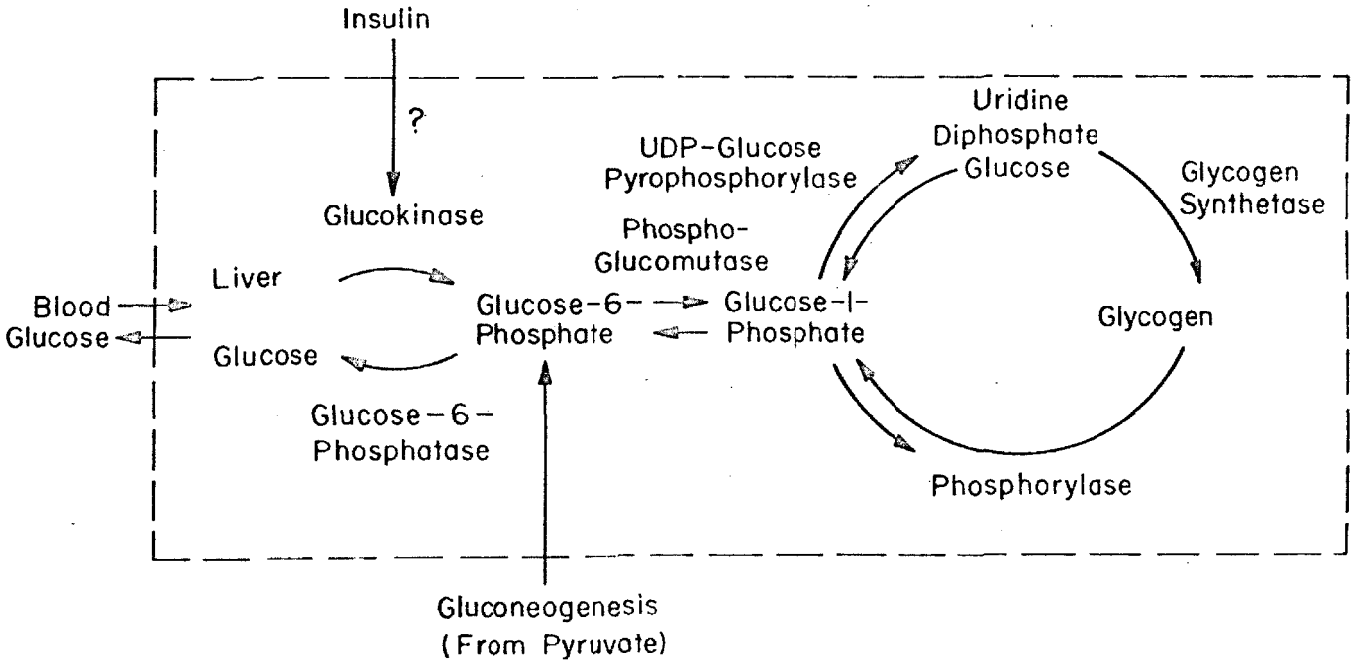

Figure 6. The Reactions of Hepatic Glycogen Metabolism.

for a multi-enzyme sequence of reactions is "sigmoid" in shape, i.e. the process is rate-limited at some saturation value. In addition, for the specific subsystem mentioned above, gross experimental animal data reveals the same general saturation characteristic.[72] A suitable analytic form for such a subsystem should be characterized by as few parameters as possible (to facilitate the solution of the inverse problem -- see Chapter IV), but it should be flexible enough to reproduce the main features of coupled sequences of enzyme-catalyzed reactions and gross experimental data for such sequences, and it should be consistent with the detailed dynamic description of such a subsystem involving all known intermediate state variables as these are eventually established.

In addition a model for such a subsystem must admit the incorporation of control effects by hormones. It is now commonly accepted that feedback control is exerted at the site of enzyme action in such a sequence of reactions, somehow affecting the enzyme's affinity for its substrates either in a positive (positive effector) or negative (negative effector) manner. As Atkinson[75] has shown, if we view enzyme activity as a parameter in a generalized sigmoid response curve for a regulatory enzyme then in some cases a change in the enzyme's activity shifts the entire sigmoid in the v-S plane. However, there is also evidence that in addition to control effects that lead to a different affinity of the enzyme for its substrate the maximum rate of the reaction, its saturation value, can also be changed.[74,75] Almost nothing is known concerning the actual molecular basis for modulation of an enzyme's kinetic behavior. However, it is thought that feedback

control is usually exerted on only one enzyme in a metabolic pathway.

Returning to the specific subsystem discussed above, hepatic glycogenesis, it is believed by some that control is effected by the hormone insulin although there is no general agreement on this point. Insulin is believed to have an effect on the rate of phosphorylation resulting in an increased rate of uptake of glucose for glycogen formation. At this point it is conjectural exactly how such a control effect should be modeled, however following Shames[62] and extrapolating from the investigations of Atkinson quoted above, we will represent such a hormone effect as a change in the saturation value of a reaction sequence. This kind of control action is characteristic of the endocrine control of carbohydrate, protein, and fat metabolism. Henceforth we will refer to such control effects as "parametric feedback".

Since the so-called sigmoid behavior seems to be characteristic of multistep bimolecular processes and bimolecular processes are general enough a framework for chemical kinetics, because any multimolecular reaction may be thought of as a multistep bimolecular process, an analytic form that reproduces the double saturation of the "sigmoid" may serve as a model for one or a coupled series of such reactions. It has been shown that the "steady-state" behavior of a linear system of complexes has some similarities to the "steady-state" behavior of a simple bimolecular system.[76] Many different kinds of such multistep processes exist with many different forms of feedback but for some such processes such as sequences of serially coupled linear systems of complexes the <u>functional form</u> of the input-output relation is identical in any part of the sequence.[77] For these reasons we have selected the

following functional form to represent many of the subsystems involved in metabolic control which are composed of sequences of enzyme-catalyzed reactions with hormonal control entering parametrically.

$$y = y_0 + \alpha \tanh[\beta(x-x_0)] \tag{3-50}$$

where

$$y_0 = (y_h + y_\ell)/2 \tag{3-51}$$

$$\alpha = (y_h - y_\ell)/2 \tag{3-52}$$

In the cases where the lower saturation value, y_ℓ, can be taken as zero, the expression reduces to:

$$y = \frac{y_h}{2} \{1 + \tanh[\beta(x-x_0)]\} \tag{3-53}$$

In Equation (3-50), x represents substrate concentration (or input), and y represents the rate of product formation (or output). An experimentally obtained "sigmoid" can be represented by an expression such as (3-53) with a choice of three parameters, y_h, β, and x_0.

It remains to suitably incorporate parametric control effects in an expression such as (3.53). From one point of view catalytic reactions in a biological system can be regarded as biologically effective amplifiers. Often a small amount of a substance such as a hormone can greatly influence the production of another substance; the hormone may act as an activator or an inhibitor of the enzyme.[78] As a consequence, and consistent with the previous remarks concerning possible control

action, we will incorporate these effects as a change in the saturation value of a sequence of reactions; if u represents plasma hormone concentration then (3-53) is modified to the following to account for control effects, i.e. functionally:

$$y = \frac{f(u)}{2} \{1 + \tanh[\beta(x-x_0)]\} \qquad (3\text{-}54)$$

An expression such as (3-54) for a subsystem comprised of the series of reactions relating plasma glucose concentration to the rate of formation of liver glycogen for example, is a grossly lumped representation, but one which is unavoidable at this point in time to elucidate the system characteristics of the hormonal control of carbohydrate, fat, and protein metabolism. Nevertheless, the model is believed to be well enough motivated that detailed investigations of the intermediate reactions of such subsystems will substantiate the functional form chosen for the overall input-output relation.

Detailed modeling of all the intermediate steps is hindered by problems of observability since all of these processes are taking place within the living cell. However, some work has been done along these lines.[79,80] For example, London[80] has attempted a detailed kinetic simulation of the major intermediate steps in the plasma glucose-hepatic glycogen subsystem. His model, which includes a constant rate of gluconeogenesis, contains 32 parameters for this subsystem, and is based on enzymatic reaction mechanisms and kinetic data in vitro pertaining to 6 reactions which convert plasma glucose to liver glycogen (see Figure 6). The entire model is constructed under the

assumption of "steady-state" kinetics and interpreted in terms of individual reaction mechanisms using the Briggs-Haldane kinetic theory. The behavior of London's model confirms the fact that a specific glucose concentration determines the net rate of glycogen synthesis or glucose production, the steady-state concentration of the three intermediates, and the rates of the six enzymatic reactions. The rate of glycogen formation is extremely sensitive to the glucokinase-glucose-6-phosphatase enzyme step. Some authors[62] have modeled the control effect of insulin in this overall reaction as occurring at this point. For our purposes in this investigation, the precise point of action of such a control will not be delineated since the enzyme upon which the control acts is not a state variable in evidence at this level of modeling of the system.

The function form, (3-53) will also be used to model the complex processes of hormone generation and release (see Section 3.5). Other processes such as distribution dynamics, accumulation, and degradation are represented analytically in a straightforward manner.

3.5. Modeling the Endocrine Controller.

All of the hormones included in the subsequent models of this investigation represent the physiological sequence, generation and secretion, distribution, accumulation, and degradation as depicted in Figure 7, for example for one-compartment distribution dynamics. The symbols in this figure are defined as follows.

$e \triangleq$ [mass/unit volume], plasma glucose concentration error.

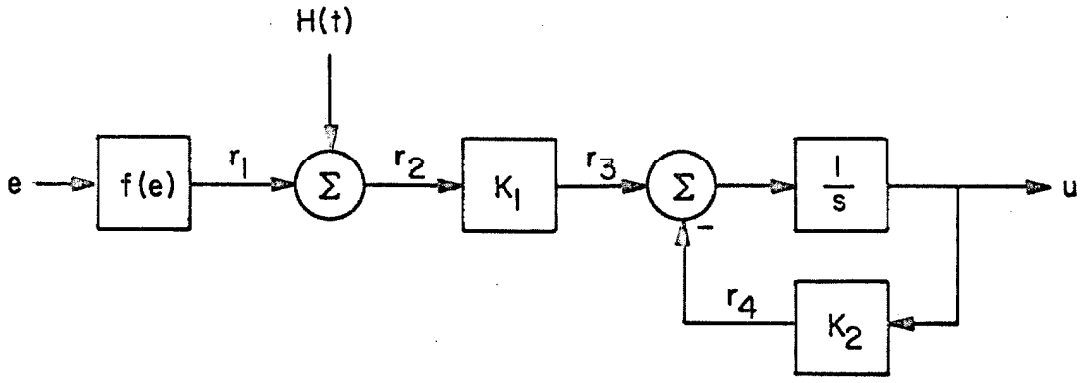

Figure 7. Single Space Hormone Model.

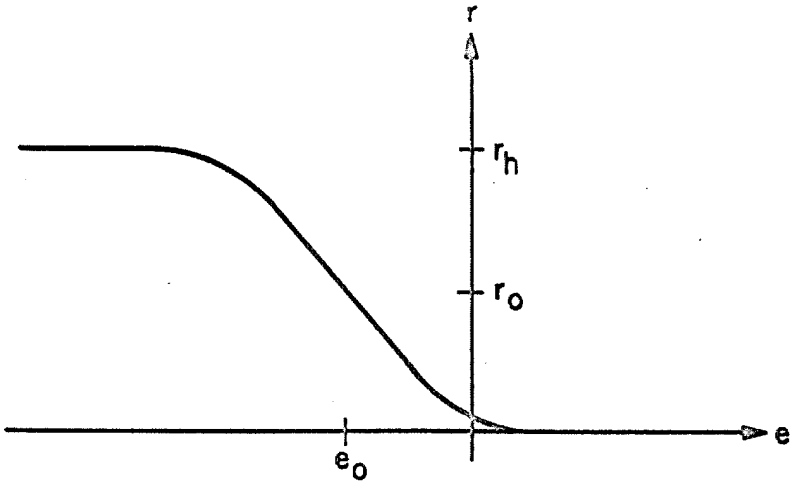

Figure 8. Typical Saturating Nonlinearity.

$r_1 \triangleq$ [mass/unit time], rate of hormone secretion.

$H(t) \triangleq$ [mass/unit time], rate of exogenous hormone intravenous input.

$r_2 \triangleq$ [mass/unit time], rate of hormone input to distribution space.

$r_3 \triangleq$ [mass/unit time/unit volume], rate of hormone input to unit distribution space.

$r_4 \triangleq$ [mass/unit time/unit volume], rate of disappearance of hormone from unit distribution space.

$u \triangleq$ [mass/unit volume], plasma hormone concentration.

$f(e) \triangleq$ [mass hormone/unit time: mass glucose/unit volume], hormone generation and release function.

$K_1 \triangleq$ [1/unit volume], distribution space.

$K_2 \triangleq$ [1/unit time], disappearance coefficient.

In terms of differential equations this basic model is written:

$$\dot{u} = - K_2 u + K_1[f(e) + H(t)] \tag{3-55}$$

In the cases where a specific hormone secretion mechanism is believed to be rate dependent, (3-55) is modified to the following:

$$\dot{u} = - K_2 u + K_1[f_1(e) + f_2(\dot{e}) + H(t)] \tag{3-56}$$

In this model, K_1 represents the extracellular fluid distribution space (plasma and interstitial fluid) and since simple first-order disappearance kinetics are assumed, K_2 represents the combined disappearance rate coefficient.

Physiologically, hormone secretion rates are expected to increase monotonically from some nominal value until saturation occurs under the appropriate stimulus. This action is represented by the symmetric nonlinearity:

$$r = r_0 + \alpha \tanh[\beta(e-e_0)] \tag{3-57}$$

i.e. $f(e) = r$, where r is hormone secretion rate [mass/unit time], e is the stimulus [mg glucose/100 mℓ plasma], and

$$r_0 = (r_h + r_\ell)/2 \tag{3-58}$$

$$\alpha = (r_h - r_\ell)/2 \tag{3-59}$$

These symbols are depicted in Figure 8 for a typical nonlinearity representing insulin secretion as a function of plasma glucose error. The parameter β is defined in terms of the slope at (e_0, r_0),

$$f(e) = r_0 + \alpha \tanh[\beta(e-e_0)] \tag{3-60}$$

$$\frac{df}{de} = \alpha \beta \, \mathrm{sech}^2[\beta(e-e_0)] \tag{3-61}$$

$$\left.\frac{df}{de}\right|_{e=e_0} = \alpha \beta \tag{3-62}$$

The typical situation encountered, as depicted in the diagram, is one for which $r_\ell = 0$. Then (3-60) reduces to,

$$f(e) = \frac{r_h}{2} \{1 + \tanh[\beta(e-e_0)]\} \tag{3-63}$$

Three parameter values completely specify this nonlinearity: r_h, β, and e_0. However, the value of $f(e)$ when e is zero represents the nominal secretion rate of the hormone under equilibrium conditions, i.e. when the plasma glucose concentration is nominal.

$$f(0) \triangleq r_{nom} \tag{3-64}$$

If we specify r_h and e_0 and require r to pass through r_{nom} when $e = 0$ then β is dictated, i.e.

$$r_{nom} = r_0 - \alpha \tanh[\beta e_0] \tag{3-65}$$

$$\beta = \frac{1}{e_0} \tanh^{-1}\left(\frac{r_0 - r_{nom}}{\alpha}\right)$$

$$\beta = \frac{1}{2e_0} \ln\left(\frac{r_h - r_{nom}}{r_{nom}}\right) \tag{3-66}$$

And in this specific case $\beta < 0$ since $e_0 < 0$.

The parameters r_h, r_{nom}, and e_0 are the most convenient characterization of the secretion nonlinearity from the viewpoint of what the physiologist can measure. However, these parameters will be obtained, not by direct physiologic measurement, which in most cases is impossible in vivo, but by using the systems techniques of Chapter IV. Nevertheless, it is helpful to try to get reasonable approximations for these parameters from direct physiological measurements. In terms of the estimation of parameters problem, such considerations can lead to reasonably valid "first guesses". It isn't particularly difficult to conceive of an experiment which will yield the parameter r_h, the maximal secretion rate. But r_h and r_{nom} are most easily obtained from the u which they dictate. For example, in equilibrium conditions a nominal plasma hormone concentration u, can be measured. Assuming known values for K_1 and K_2, then r_{nom} can be obtained as follows. From (3-55) and (3-57),

$$\dot{u} = - K_2 u + K_1\{r_0 + \alpha \tanh[\beta(e-e_0)] + H(t)\} \qquad (3\text{-}67)$$

Since no exogenous input exists in this case, and $r = r_{nom}$ by definition:

$$\dot{u} = - K_2 u + K_1 r_{nom} \qquad (3\text{-}68)$$

Taking the Laplace transform of (3-68), setting $u(0) = 0$, and letting the measured value of u be u_{nom}:

$$u(s) = \frac{K_1}{s + K_2} \frac{r_{nom}}{s} \tag{3-69}$$

then

$$u_{nom} = \lim_{s \to 0} s \left(\frac{K_1}{s + K_2} \frac{r_{nom}}{s} \right)$$

$$u_{nom} = \frac{K_1}{K_2} r_{nom} \tag{3-70}$$

Hence r_{nom} can be obtained from measurements on u and r_h can be obtained in a similar manner under an appropriate stimulus e. The parameter e_0 is more difficult to motivate physiologically, but it should be possible to approximate it fairly closely from data on the resulting u from steady stimuli e, at various levels.

All of the modeling discussed in Section 3.7 uses the above type of secretion nonlinearity as a function of glucose error or the derivative of glucose error and one or two-compartment distribution kinetics. In Chapter IV, the inverse problem for two-compartment hormone distribution kinetics is discussed hence the appropriate equations will be introduced here. The two compartments in this case correspond to the plasma space and the interstitial fluid space; simple diffusion kinetics connect the two spaces.

Let: $u_p \triangleq$ plasma hormone concentration

$u_i \triangleq$ interstitial fluid hormone concentration

$V_p \triangleq$ plasma volume

$V_i \triangleq$ interstitial fluid volume

$H(t) \triangleq$ exogenous hormone rate input

$f(e) \triangleq$ endogenous hormone secretion rate

$\alpha_p \triangleq$ plasma space disappearance coefficient

$\alpha_d \triangleq$ diffusion coefficient

$\alpha_i \triangleq$ interstitial fluid space disappearance coefficient

Then the model analogous to that of (3-55) is:

$$\left.\begin{aligned} V_p \dot{u}_p &= \alpha_d(u_i - u_p) - \alpha_p u_p + f(e) + H(t) \\ V_i \dot{u}_i &= \alpha_d(u_p - u_i) - \alpha_i u_i \end{aligned}\right\} \qquad (3\text{-}71)$$

Whether this is a more appropriate model to use at the present time, instead of (3-55), is debatable. The variable u_i of course is not observable, i.e. it can not be measured directly, whereas u_p can be measured directly. The inverse problem for (3-71), i.e. identifying the requisite parameters from experimental data on intact systems, is presented in Chapter IV. It may be possible sometime in the near future to measure u_i directly by means of a technique known as lympatic cannulation.

3.6. Modeling the Metabolic Plant.

The glucose control system is viewed as a classical regulator with the desired circulating level of glucose determined by the central nervous system. The liver, the primary short-term reservoir of glucose, is sensitive to the glucose actuating error which is by definition the difference between the desired level of plasma glucose and the actual circulating level. For ease of simulation, and without loss of generality, all dynamics can be represented in terms of deviations from the nominal state.

The models discussed in Section 3.7 deal with glucose metabolism alone; the functions associated with protein and lipid metabolism are relegated to future efforts. However, the glucose control system has been modeled with a view to incorporating these functions and the loop coupling (primarily the processes of gluconeogenesis) with a minimum of modification to the glucose loop model. Accordingly, the present models incorporate the following processes associated with glucose metabolism: hepatic glycogenesis, hepatic glycogenolysis, renal excretion of glucose, hormone independent tissue utilization of glucose, hormone dependent adipose tissue utilization of glucose, hormone dependent muscle tissue utilization of glucose, storage mechanisms, and circulation dynamics.

These processes are altered dynamically by hormonal controls through parametric feedback, typically altering the saturation value of a series of rate limiting reactions, in such a way that the concentration of glucose in plasma is regulated to some nominal level. These processes are represented in the way indicated by (3-54). The explicit functional

dependence between process dynamics and a hormonal control signal is discussed in Section (3.7).

Reasonable numerical values for the model parameters were first obtained from published results in the biologic, physiologic and medical literature. However, the final values were obtained by simulating certain experiments on normal male subjects. The models represent a 70 kg. normal male adult under relatively benign laboratory conditions. Since all experimental inputs to the subject were administered intravenously with the subject in the post-absorptive state, no gastrointestinal tract dynamics are included in the models. Confidence in the models was obtained by simulating the response to a glucose infusion, insulin infusion, insulin followed by periodic glucose inputs, and insulin infusion followed by a glucagon input, all with the same set of model parameter values. The observed data consist of a continuous record of plasma glucose concentration and spaced samples of certain hormones over a time period of approximately 100 minutes, the usual duration of these tests. The experimental technique employed and the method by which the instrumentation yields a continuous record of plasma glucose are briefly described in Appendix D.

3.7. Models of the Glucose Control System.

We will present three models of the glucose control system in this Section. The first model is preliminary in the sense that modeling techniques were still being investigated during its derivation and the controller incorporates only two controlling hormones strictly in a proportional control mode. The second model is more refined, containing

all of the most important physiological functions involved in glucose regulation and the dominant short-term controlling hormones with more complicated distribution dynamics. The third model clears up some of the problems associated with the second model.

3.7.1. Two Hormone Model.

In terms of differential equations this model can be expressed:

$$\dot{c} = - K_{19}c + K_{18}[F(t) + f_{LO}(c,x_2) - f_{LU}(c,x_1,y_3) - f_R(c) - f_U(c,x_1) - GU] \quad (3\text{-}72)$$

$$\dot{x}_1 = - K_8 x_1 + K_7[I(t) + f_1(c)] \quad (3\text{-}73)$$

$$\dot{x}_2 = - K_{11}x_2 + K_{10}[G(t) + f_2(c)] \quad (3\text{-}74)$$

where:

c = plasma glucose concentration, [mg/100 mℓ]

x_1 = plasma insulin concentration, [μU/mℓ]

x_2 = plasma glucagon concentration, [mμg/mℓ]

y_3 = liver glycogen content, [g]

$F(t)$ = intravenous glucose input rate, [mg/min]

GU = central nervous system mean glucose utilization rate, [mg/min]

$I(t)$ = intravenous insulin input rate, [U/min]

$G(t)$ = intravenous glucagon input rate, [μg/min]

$f_{LO}(c,x_2)$ = liver glucose output rate, [mg/min]

$f_{LU}(c,x_1,y_3)$ = liver glucose uptake rate, [mg/min]

$f_R(c)$ = renal excretion rate, [mg/min]

$f_U(c,x_1)$ = peripheral tissue glucose utilization rate dependent on insulin, [mg/min]

K_{19} = hormone independent tissue utilization rate coefficient, [1/min]

This model is depicted in a control system format in Figure 9. The considerations that led to the initially chosen parameter values will be presented. The final values chosen, however, resulted from the simulation of several systems experiments.

It is commonly accepted that the rate of hepatic glucose uptake for glycogen formation is a direct function of the plasma glucose concentration.[47] A mean disappearance rate of glucose in normal subjects has been measured to be 3.71 ± 0.40 mg%/min.[81] Assuming a 14 liter extracellular space[82] and a 4 mg%/min disappearance rate this implies a total of 560 mg/min. If it is assumed that of this total 10% is the amount being taken up by liver[46] then 56 mg/min are being stored in hepatic tissues with the remainder going to peripheral utilization and fat storage. From Figure 9 and the previous comments we have:

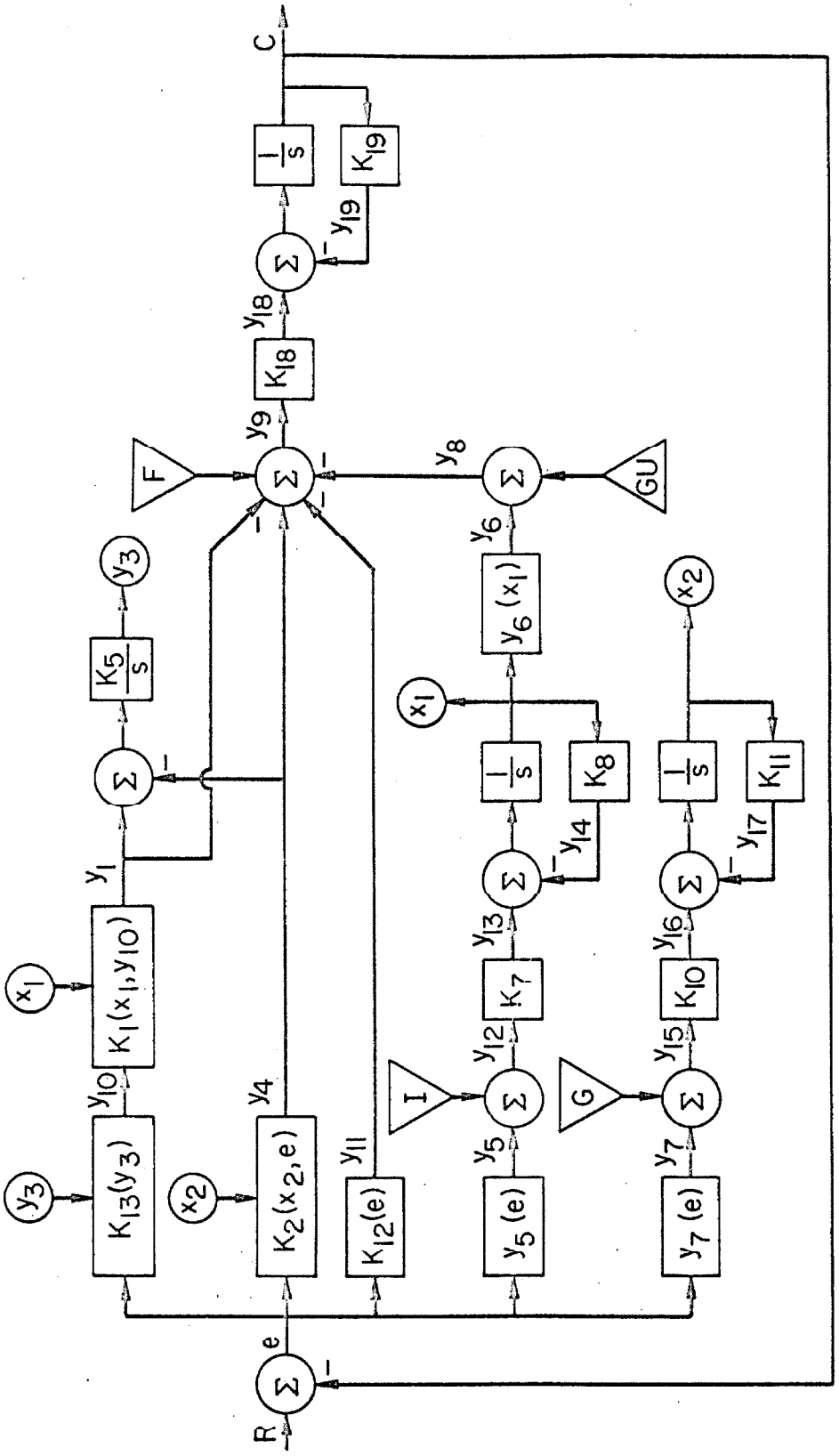

Figure 9. Glucose Metabolism Controlled by Two Hormones.

$$f_{LU}(c,x_1,y_3) = \frac{K_1(x_1)}{2}\{1 - \tanh[\beta_{y_1}(y_{10} - y_0^{10})]\} \tag{3-75}$$

where $y_{10} = K_{13}(y_3)\, e$

$$e = R - c$$

$$K_1(x_1) = K_{10} + \alpha_{K_1} \tanh[\beta_{K_1}(x_1 - x_0^1)] \tag{3-76}$$

$$K_{10} = \frac{K_{1H} + K_{1L}}{2}$$

$$\alpha_{K_1} = \frac{K_{1H} - K_{1L}}{2}$$

$$K_{13}(y_3) = \frac{1}{2}\{1 - \tanh[\beta_{K_{13}}(y_3 - y_0^3)]\} \tag{3-77}$$

A reasonable value for K_{1L} is then about 60 mg/min. The function $K_1(x_1)$, represents the dependence of the saturation value of the glucose uptake rate for storage as glycogen on the plasma concentration of insulin. At this time it is difficult to justify a value for K_{1H} directly from the physiological data. However, some studies have shown that insulin increases liver uptake rate by about three,[15] implying a value of 180 mg/min for K_{1H}. Other considerations indicate that this is too low a value. For example, Wolaver[64] indirectly derived a glucose uptake function from the data of Soskin and Levine[83] and Wierzuchowski[84] "extrapolated" to humans which yields uptake rates as high as 3000 mg/min when C is approximately 400 mg%. From the limited number of glucose tolerance tests which we have performed in this investigation such uptake rates for liver appear to be much too high.

The function $K_{13}(y_3)$ acts as a switch, attenuating the uptake of glucose for storage as glycogen when the hepatic glycogen stores are replenished. For a 70 kg man with a 1.8 kg[85] liver the maximum glycogen storage achievable is believed to be on the order of 125 g. In normal metabolic control it is thought that this store is never fully depleted under normal conditions, but is lowered only to about 75 g. before protein and lipids are substantially mobilized to provide the precursors for gluconeogenesis.[49,52,86,87] Under these conditions we would expect the hepatic glycogen stores under postabsorptive conditions to be on the order of 75 g. Under the assumption that such stores can be fully replenished over a three hour period after an oral glucose input, a maximum uptake rate by liver of 278 mg/min would be indicated. Accordingly, for the purposes of simulation, we have taken a guessed value for K_{1H} of 300 mg/min.

The only remaining function in the glycogen storage pathway is K_5/S, representing the accumulation process, i.e.

$$y_3(t) = \int_{t_0}^{t} K_5[y_1(\tau) - y_4(\tau)]\, d\tau \qquad (3\text{-}78)$$

Assuming that one gram of glucose results in the storage of one gram of glycogen, the dimensions of the variables in (3-78) require that $K_5 = .001$. In Equation (3-76), K_1 varies from K_{1L} to K_{1H} as the hormone insulin x_1, varies from 10 $\mu U/m\ell$ to 510 $\mu U/m\ell$. These values will be justified in the discussion of the insulin release and distribution pathway.

The body at rest utilizes approximately 200 mg glucose/kg/hr.[85]

Assuming a 70 kg. man and that all of this glucose is supplied by the liver, we obtain a fasting state release rate of about 230 mg/min. In the fasting state and under the influence of glucagon, rat liver can achieve a mean glucose release rate of 0.7 mg/min/g.[26] Assuming that human liver can achieve substantially the same output, and assuming a liver mass of 1.8 kg., we obtain about 1250 mg/min as the maximum liver glucose release rate under the influence of a stimulating hormone. Accordingly, in the following equations we take the preliminary parameter values $K_{2H} = 1250$ and $K_{2L} = 230$ mg/min.

$$f_{LO}(c,x_2) = \frac{K_2(x_2)}{2}\{1 + \tanh[\beta_{y_4}(e-e_0^1)]\} \qquad (3\text{-}79)$$

where: $e = R - c$

$$K_2(x_2) = K_{20} + \alpha_{K_2}\tanh[\beta_{K_2}(x_2-x_0^2)] \qquad (3\text{-}80)$$

$$K_{20} = \frac{K_{2H} + K_{2L}}{2}$$

$$\alpha_{K_2} = \frac{K_{2H} - K_{2L}}{2}$$

In Equation (3-80), K_2 varies from K_{1L} to K_{1H} as the hormone glucagon x_2, varies from 1 mμg/mℓ to 3 mμg/mℓ. These values will be justified in the discussion of the glucagon release and distribution pathway.

Normally the quantity of glucose in urine is negligible, but if the blood sugar concentration reaches a level of approximately 180 mg% (the renal threshold) the tubular reabsorption capacity of the kidney is

exceeded and glucose is excreted via urine. As a first-order approximation this process is represented as an excretion rate proportional to the absolute blood glucose concentration once the threshold has been exceeded, i.e.:

$$f_R(c) = K_{12}(e)\, e \tag{3-81}$$

where: $e = K - c$

$$K_{12}(e) = K_{120} + \alpha_{K12} \tanh[\beta_{K12}(e-e_0^2)] \tag{3-82}$$

$$K_{120} = \frac{K_{12H} + K_{12L}}{2}$$

$$\alpha_{K12} = \frac{K_{12H} - K_{12L}}{2}$$

Actually we have made $K_{12L} = 0$ and a preliminary value for $K_{12H} = -.375$ which results in an average renal excretion rate of 40 mg/min once threshold is exceeded in a 30 g intravenous glucose input test.

The normal glucose uptake rate by the brain has been determined by several independent studies to lie between 5.5 and 6.2 mg/min/100 g.[88] Since the normal weight of the brain is 1400 g., a total glucose uptake rate independent of plasma glucose concentration of about 80 mg/min is indicated. This is incorporated in the model as a constant sink for plasma glucose, i.e. GU = 80.

The data of Soskin and Levine [83] for total peripheral glucose utilization "extrapolated" to that of a 70 kg. man results in a doubly saturating nonlinearity varying from 260 mg/min at c = 90 mg% to

610 mg/min at $c = 470$ mg%. Since insulin has been demonstrated to increase glucose uptake up to three times[48,89,90] this variation may be accounted for completely by this effect. From a material balance viewpoint we must recall that the fasting level liver release rate of glucose was 230 mg/min of which 80 mg/min was directed to CNS oxidation. Hence to be consistent the insulin dependent peripheral utilization rate must vary from a minimal level of 150 mg/min at nominal insulin levels or $x_1 = 10$ μU/mℓ. Hence in the equation for peripheral utilization:

$$f_U(c_1,x_1) = y_{60} + \alpha_{y6} \tanh[\beta_{y6}(x_1-x_0^2)] \qquad (3\text{-}83)$$

where

$$y_{60} = \frac{y_{6H} + y_{6L}}{2}$$

$$\alpha_{y6} = \frac{y_{6H} - y_{6L}}{2}$$

We take $y_{6H} = 610$ mg/min and $y_{6L} = 150$ mg/min. The effects of exercise on peripheral utilization[91] have not been incorporated due to the extreme difficulty of quantifying such effects at the present time.

The remaining plant parameters, K_{18} and K_{19} represent the glucose distribution space and hormone independent peripheral utilization, respectively. Since it is impossible to determine the distribution of peripheral glucose utilization between the variables y_6 and y_{19} from current physiological data, we can only guess at K_{19} and rely on simulation of experiments for more carefully substantiated values. If we choose $K_{19} = .01$, for example, then at $c = 150$ mg%, hormone independent peripheral utilization is 70 mg/min, if $c_{nom} = 100$ mg% and

the glucose space is 14ℓ. Assuming a distribution volume of 14ℓ implies $K_{18} = .00715$. If the set point $R = 100$ mg% then the simulation represents absolute quantities, however a "deviations from nominal" simulation results if we set $R = 0$, $GU = 0$, and change the appropriate nonlinearities above to have minimum values of zero under equilibrium conditions. The function $F(t)$ represents an intravenous infusion of glucose. For all of the experiments simulated this input took the form of a finite duration step, i.e.

$$F(t) = \begin{cases} A_1 \ , & 0 \le t \le \tau_1 \\ 0 \ , & t > \tau_1 \end{cases} \tag{3-84}$$

For an infusion of 30 g. over a period of 5 minutes, for example, $A_1 = 6000$ and $\tau_1 = 5$.

Equation (3-73) represents the secretion, distribution, and degradation of insulin:

$$\dot{x}_1 = - K_8 x_1 + K_7[I(t) + f_1(c)]$$

where:

$$I(t) = \begin{cases} A_2 \ , & 0 \le t \le \tau_2 \\ 0 \ , & t > \tau_2 \end{cases} \tag{3-85}$$

$$f_1(c) = \frac{y_{50}}{2} \{1 - \tanh[\beta_{y5}(e - e_0^3)]\} \tag{3-86}$$

$$y_{50} = \frac{y_{5H} + y_{tL}}{2}$$

$$e = R - c$$

Here $I(t)$ represents an intravenous input of insulin and the function $f_1(c)$ represents the endogenous release of insulin as a function of plasma glucose concentration.[92] We expect plasma insulin concentration x_1, to vary from a fasting concentration of about 10 $\mu U/m\ell$[17] to a maximum level of about 510 $\mu U/m\ell$[18] under maximal stimulation of the pancreas. The values of y_{5H} and y_{5L} required for such results can be determined once K_7 and K_8 have been established. The half-life of endogenously secreted insulin has been determined to lie in the range 7-15 min.[18] and 7-1/2-11 min.[93], also a disappearance rate of 2%/min has been reported.[94] Since a half-life of 7 minutes corresponds to a time constant of about 10 minutes ($7/\ell n(2)$), and $\tau = 1/K_8$, then for such a value $K_8 = .01$. If a distribution volume of 14 ℓ. is assumed then the dimensions of the appropriate variables in (3-73) require that $K_7 = 71.5$. With K_7 and K_8 thus determined y_{5H} and y_{5L} are found by using (3-69) and (3-70).

Equation (3-74) represents the secretion, distribution and degradation of glucagon:

$$\dot{x}_2 = - K_{11}x_2 + K_{10}[G(t) + f_2(c)]$$

where:

$$G(t) = \begin{cases} A_3 \ , & 0 \le t \le \tau_3 \\ 0 \ , & t > \tau_3 \end{cases} \qquad (3\text{-}87)$$

$$f_2(c) = \frac{y_{7_0}}{2}\{1 + \tanh[\beta_{y_7}(e - e_0^4)]\} \qquad (3\text{-}88)$$

$$y_{7_0} = \frac{y_{7H} + y_{7L}}{2}$$

$$e = R - c$$

The function of glucagon is to stimulate hepatic production of glucose in order to maintain the plasma concentration of glucose.[26,50] If we assume a distribution volume of 14ℓ, then the dimensions of the variables in (3-74) require that $K_{10} = 7.15$. The disappearance rate of circulating glucagon in rat has been reported as 80% in 5 min.[95] This implies that $K_{11} = .321$ hence the time constant for this hormone, if first-order kinetics are applicable, is 3.12 minutes. With K_{10} and K_{11} thus determined y_{7H} and y_{7L} are found by using (3-69) and (3-70).

The remaining parameters in the argument of the hyperbolic tangent nonlinearity, i.e. β and e_0, were chosen in each specific case to yield a smooth variation over the dynamic range of the independent variable.

Some of the initial simulation results obtained using this model were reported by the author in August 1967.[96] For these simulations initial conditions were chosen to represent a normal human plasma glucose regulator in steady-state, i.e., in metabolic and endocrine equilibrium, hence parameter dependencies were represented in terms of deviations from the nominal state.

Confidence was obtained in the model, and the parameter values justified from the literature above were in some cases modified, to simulate the response of a subject to an intravenous glucose input $F(t)$, and an intravenous insulin input $I(t)$. At this stage of the investigation distribution spaces for glucose, insulin, and glucagon, K_{18}, K_7, and K_{10} respectively were viewed as adjustable parameters

in accordance with the accepted view among biological scientists that these spaces are different depending upon the substance in question and in some cases are capable of dynamic variation, such as the glucose space for example, which by many investigators is believed to increase under the influence of insulin. In retrospect the author believes that this is the wrong approach to be taken for modeling purposes. Whether we are dealing with a one compartment distribution space for glucose (plasma and interstitial fluid) or a two compartment model connected by a transport mechanism these spaces should be viewed as relatively fixed physical entities. However, biological scientists sometimes view this extracellular space as being enlarged to include some of the intracellular space under the demonstrated effect of insulin to allow entry of glucose inside the cells. In the opinion of the author this practice of viewing the demonstrated disappearance of glucose from the extracellular fluid space as due to the enlargement of the space is an artificial and not very informative way to look at disappearance dynamics. Rather, the distribution of glucose in circulation should be viewed as a strictly mechanical affair and a lowering of circulating glucose due to entry into the intracellular compartment should be viewed as part of the dynamics of peripheral utilization of glucose. Accordingly this view takes precedence in the discussion of the refined model to be presented later.

After some confidence was obtained in the model of Figure 9 an attempt was made to simulate the results of a rather complicated test that had been performed on a normal adult subject some months previously. The approach followed in this experiment has been described elsewhere,[97]

but a brief presentation of the experimental technique employed with the human subject and the equipment which yields continuous blood glucose concentration measurements are presented in Appendix D. The test was performed for the specific purpose of determining how much glucose would be required to be exogenously administered to maintain the subject's plasma glucose concentration at or near nominal after a potent hypoglycemic agent had been administered. Ten units of insulin were administered at the start, plasma glucose was continuously monitored, and depending upon the monitored plasma glucose concentration varying quantities of glucose were injected every two minutes in an attempt to manually maintain the subject's plasma glucose at or near nominal for a period of 100 minutes. The monitor has an inherent time delay of approximately eight minutes. The subject's glucose response is shown in Figure 10 and the actual administered glucose input is shown in Figure 11. The effect of the equipment time delay which limits the performance of the human in the control loop in such a control scheme is clearly evident in Figure 10 since relatively poor control was achieved. The initial rise in the plasma glucose response is believed due to trace amounts of glucagon in the initial intravenous injection of insulin.

It is a reasonable expectation that the performance obtained in this experiment can be improved through the application of feedback control techniques and automating the entire procedure to remove the human experimenter from the controller. The most important new facility required to be added to the control loop is a predictor to alleviate the problem of basing control

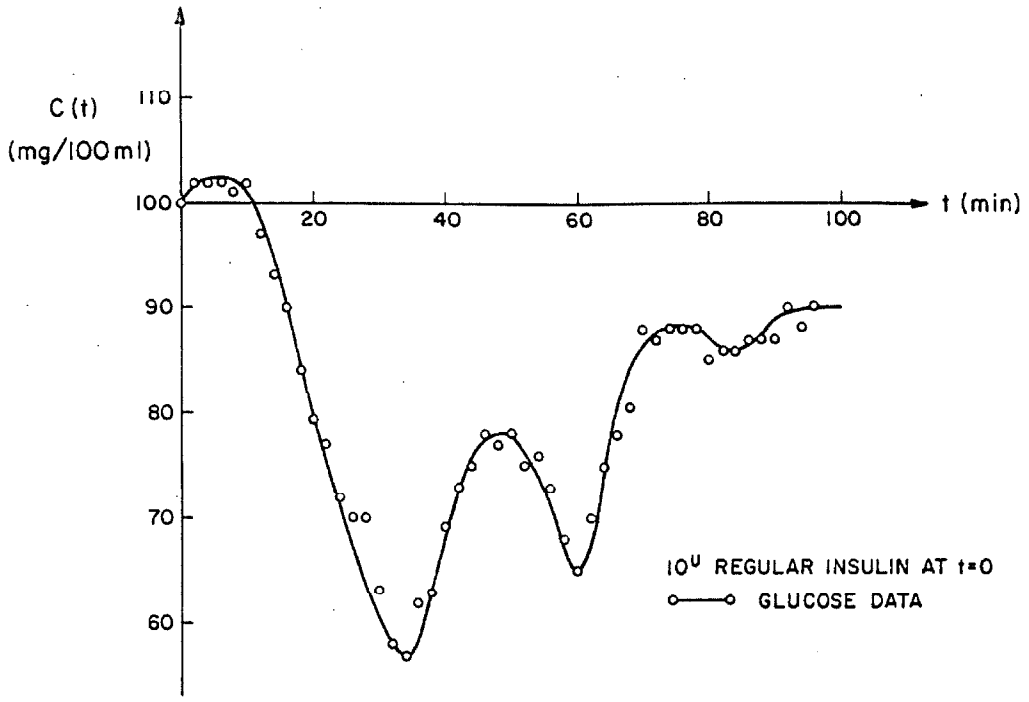

Figure 10. Plasma Glucose - Subject Z (9-10-66).

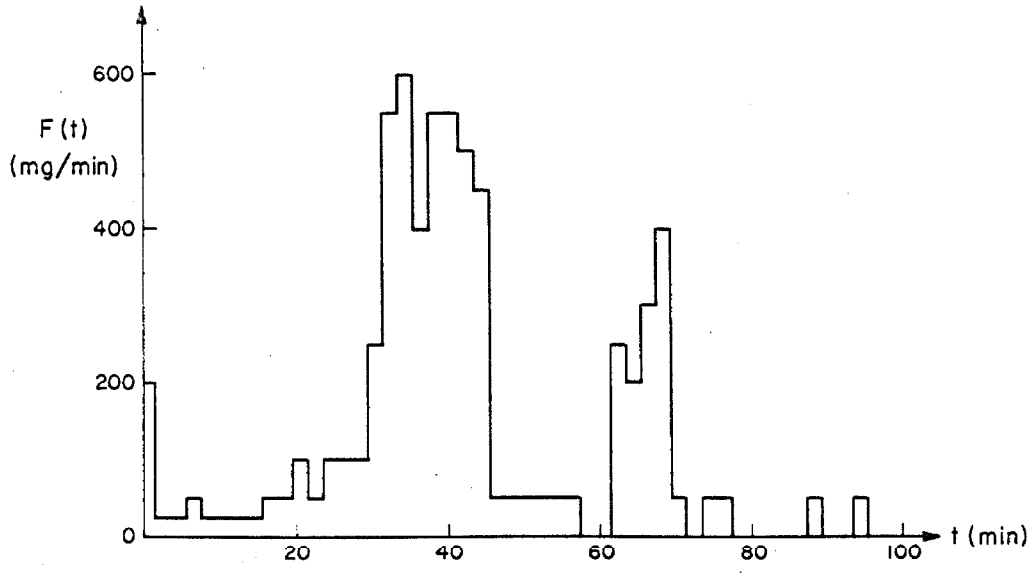

Figure 11. Glucose Input-Subject Z (9-10-66).

on delayed observations. These possibilities will be discussed further in Chapter IV.

This experiment was simulated with the model of Figure 9. In this case the insulin input $I(t)$, was simulated as an impulse function of magnitude 10 units at time zero, and the glucose input $F(t)$, was simulated as a variable step function exactly as depicted in Figure 11. Before this particular simulation was undertaken the parameters of the model were chosen to reproduce experimental results due to a glucose input alone and an insulin input alone. These parameters were then viewed as more or less constrained and a simulation of the data in Figure 10 was sought such that the model's simulation of a glucose or insulin input was not deteriorated from that obtained previously. The simulation results are shown in Figure 12. Other choices of parameters yielded a closer match to the actual response, but resulted in less than satisfactory glucose alone or insulin alone responses. The response shown was obtained with circulation volumes for glucose, insulin, and glucagon of 26, 7, and 14 liters respectively (k_{18}, k_7, and k_{10}), degradation factors of .07, .03, and .222 respectively (k_{19}, k_8, and k_{11}) corresponding to time constants of 14.43, 33.33, and 4.5 minutes respectively. Physiologic considerations dictate circulation volumes within a factor of about two and the same can be said of degradation factors based on tracer experiments.[98,99] The maximum freedom in choice of parameters was found to lie in the area of greatest physiologic variation, viz. parameter values for the nonlinearities $f_{LU}(c,x_1,y_3)$ the rate of uptake of glucose by liver as a function of glucose error and insulin concentration, and $f_U(c,x_1)$ the rate of

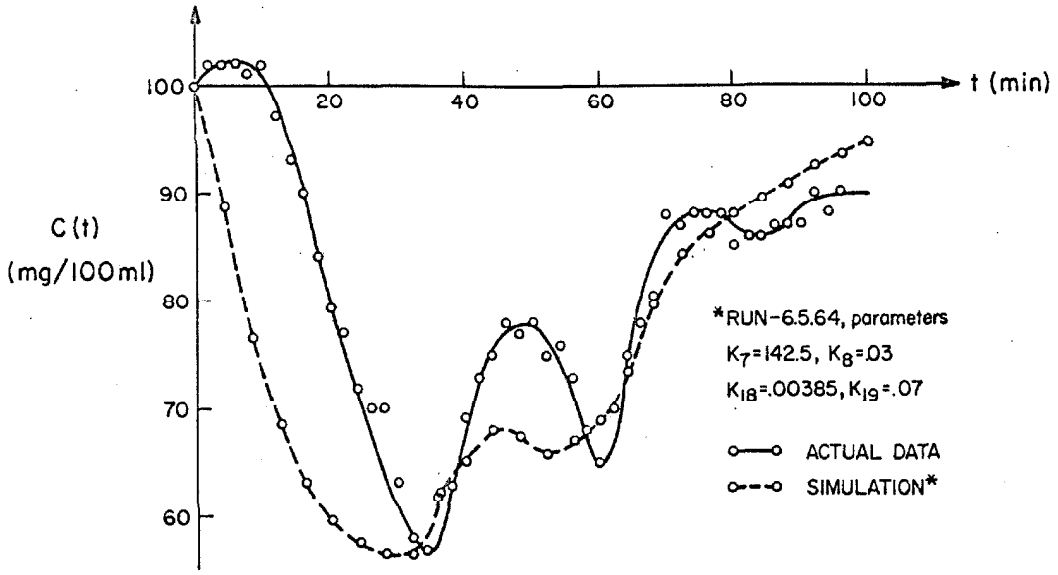

Figure 12. Simulation of Subject Z Exp. (9-10-66).

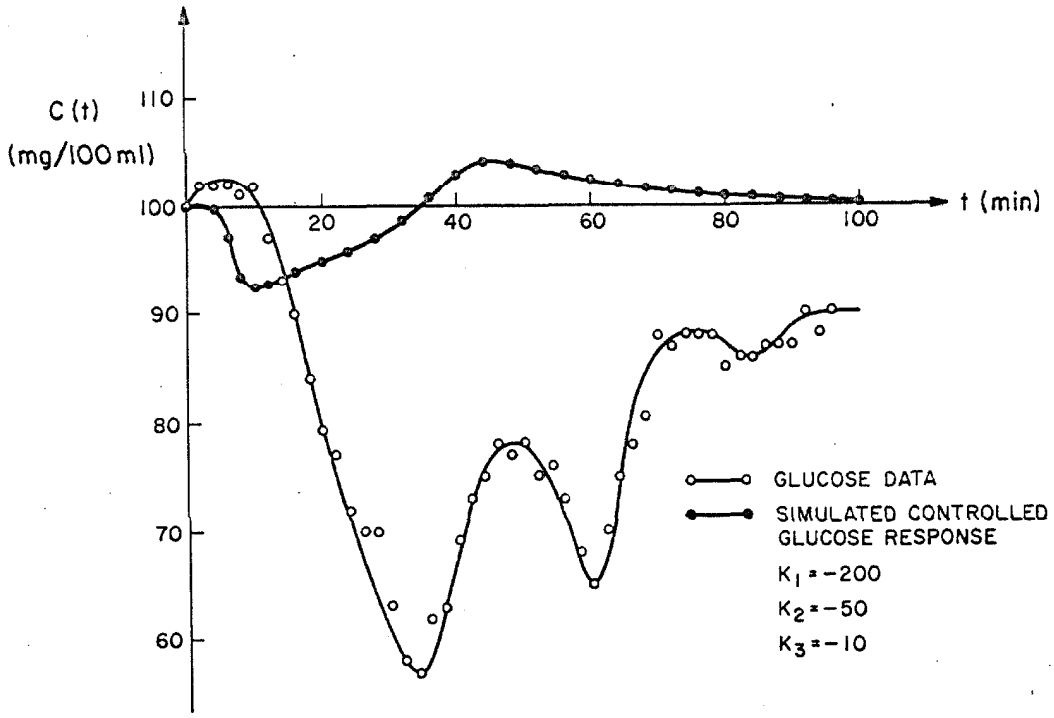

Figure 13. Simulated Closed Loop Control of Subject Z Exp. (9-10-66).

glucose utilization by tissue under the influence of insulin.

The rather large difference between data and simulation in the period $0 \leq t < 30$ minutes was later corrected by incorporating a first order lag with a time constant of 1.5 minutes to account for circulation dynamics.

Although this crude model did not adequately reproduce the finer details of the actual response this limited success supports the general approach to the problem and indicates that the inclusion of the remaining hormonal controls as well as more complex control laws should yield better results. It should be mentioned at this point for the benefit of those unfamiliar with biological systems problems, who might tend to be rather critical of the results depicted in Figure 12, that there are many factors mitigating against accurate results in such biological experiments. There are many important environmental and experimental factors which tend to corrupt the observed data in a manner extremely difficult to ascertain. For example, we estimate ex post facto that the measuring instrument in this case had an error standard deviation on the order of 5% at a glucose concentration of 100 mg%. In addition, we have other evidence that this error varies in a nonlinear manner as a function of glucose concentration. Such effects, have as yet not been quantitatively determined. Another error was certain to be introduced from the possible nonhomogeneous mixing of the glucose solution administered intravenously. In addition, the continuous glucose monitor, aside from the pure time lag of about eight minutes, also has an inherent first-order lag or time constant of about one to one and a half minutes. Unfortunately,

these parameters had not been determined at the time of the experiment hence the available data could not be corrected for these effects. Finally, from our knowledge of the reconstructed experimental scene, Figure 11 represents a mathematically idealized view of what may have happened during the course of the experiment. Biological systems studies present many unique challenges in experimental technique which must be resolved before any meaningful results can be expected to emerge from an analysis of the resulting data.

As an illustration of how control systems techniques can improve experimental methods, the above experiment, in which the human experimenter inserts himself in the control loop to administer glucose after observing the delayed subject's response to an insulin input, was simulated with the model described above and a simple control law of the following type was used to determine the control function, F(t).

$$F(t) = K_1\, c(t) + K_2 \frac{dc(t)}{dt} + K_3 \int_0^t c(t)\, dt \qquad (3\text{-}89)$$

No attempt was made to optimize some criterion function of glucose deviation from nominal, but the coefficients in (3-89) were selected by

simulation to obtain better control than that which was achieved manually. With $K_1 = -200$, $K_2 = -50$, and $K_3 = -10$, the simulated response shown in Figure 11 by the line connecting black dots was obtained. The resulting $F(t)$ yielding this system response is illustrated in Figure 14 and the simulated insulin response is illustrated in Figure 15. If the model used in this simulation is representative of the dynamics of the real system - Subject Z - then we would expect the experiment - 10^u regular insulin administered at $t = 0$ - repeated with the open loop glucose input policy illustrated in Figure 14 will yield better results than those obtained when the glucose input policy was manually determined, i.e. the experiment should now yield a response more similar to the black dots in Figure 13. How this entire experiment could be done automatically with a closed-loop control system incorporating a predictor will be discussed in Chapter IV.

3.7.2. Preliminary Four Hormone Model.

This work has been reported elsewhere[116] hence only a brief summary of the simulation results will be included here. The detailed justification of each process representation will be deferred to Section 3.7.3 in the presentation of the more refined four-hormone model. The first model was changed to incorporate muscle and adipose tissue glucose utilization affected by insulin and growth hormone. Glycogenolysis is made a function of both glucagon and epinephrine. A first-order lag is included for the peripheral effects of insulin to approximate distribution through the interstitial fluid space. Circulation dynamics for glucose are also incorporated as well as insulin and epinephrine secretion as a function of glucose error rate. The

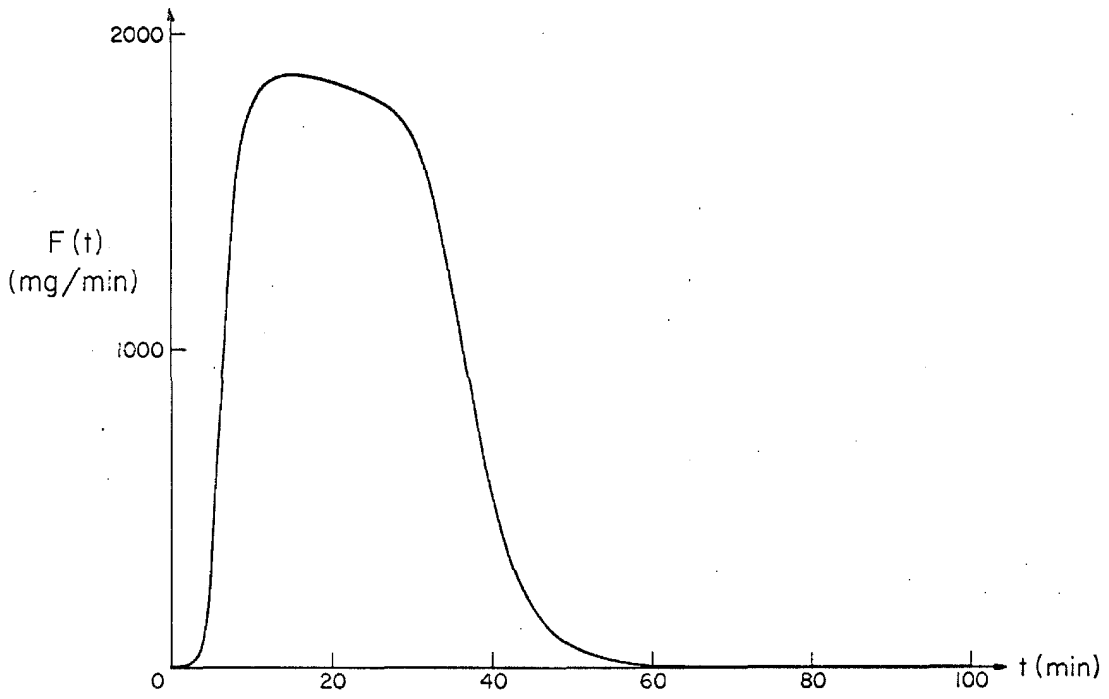

Figure 14. Simulated Glucose Input Policy.

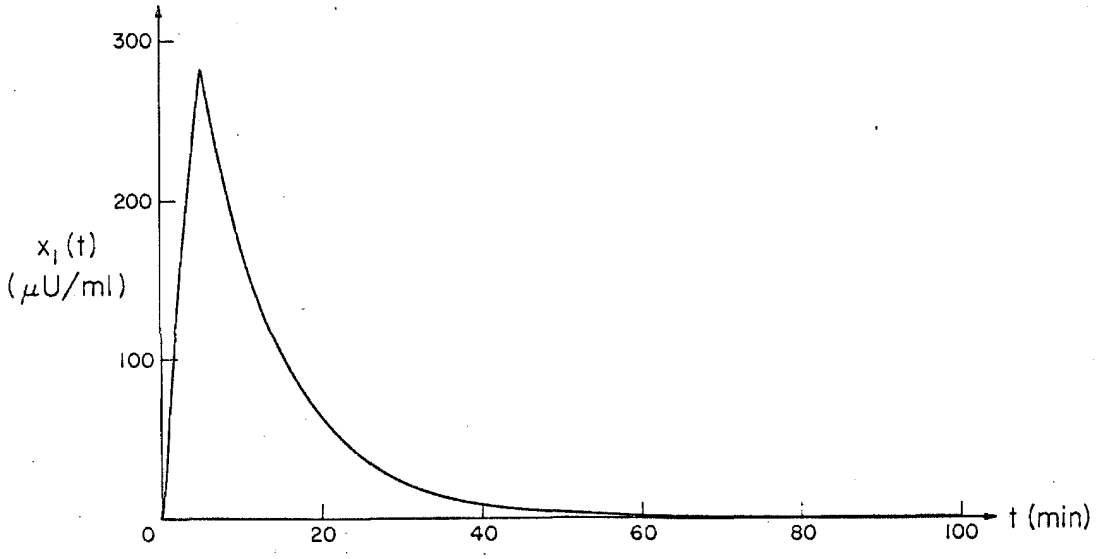

Figure 15. Simulated Insulin Response.

capability of epinephrine to inhibit insulin secretion is included. Pure time lags are placed after each input function to account for the different dynamic stimulus seen by the system depending upon whether a substance is exogenously or endogenously supplied.

The model for the metabolic plant is shown in Figure 16 depicting the control of liver function, renal function, and peripheral utilization of glucose by four hormonal controls through parametric feedback in a one-compartment configuration. The model used for the four component hormonal controller is shown in Figure 17 and includes both rate and proportional control modes as well as cross coupling between two of the controls.

The model can also be represented as follows:

$$\tau_{18}\ddot{c}_1 + \dot{c}_1 = G_{18}[F(t-\tau_1) + f_{LO}(c_1, h_2, h_3) - f_{LU}(c_1, x_4, h_1) - f_R(c_1) - G_9 c_1 - f_M(x_{11}) - f_L(x_{11}, h_4)] \quad (3\text{-}90)$$

$$\dot{h}_1 = - K_6 h_1 + K_5\{K_1(h_3)[f_1(c_1) + f_2(\dot{c}_1)] + I(t-\tau_2)\} \quad (3\text{-}91)$$

$$\dot{h}_2 = - K_{11} h_2 + K_{10}[f_3(c_1) + G(t-\tau_3)] \quad (3\text{-}92)$$

$$\dot{h}_3 = - K_{21} h_3 + K_{20}[f_4(c_1) + f_5(\dot{c}_1) + E(t-\tau_4)] \quad (3\text{-}93)$$

$$\dot{h}_4 = - K_{31} h_4 + K_{30}[f_6(c_1) + S(t-\tau_5)] \quad (3\text{-}94)$$

where:

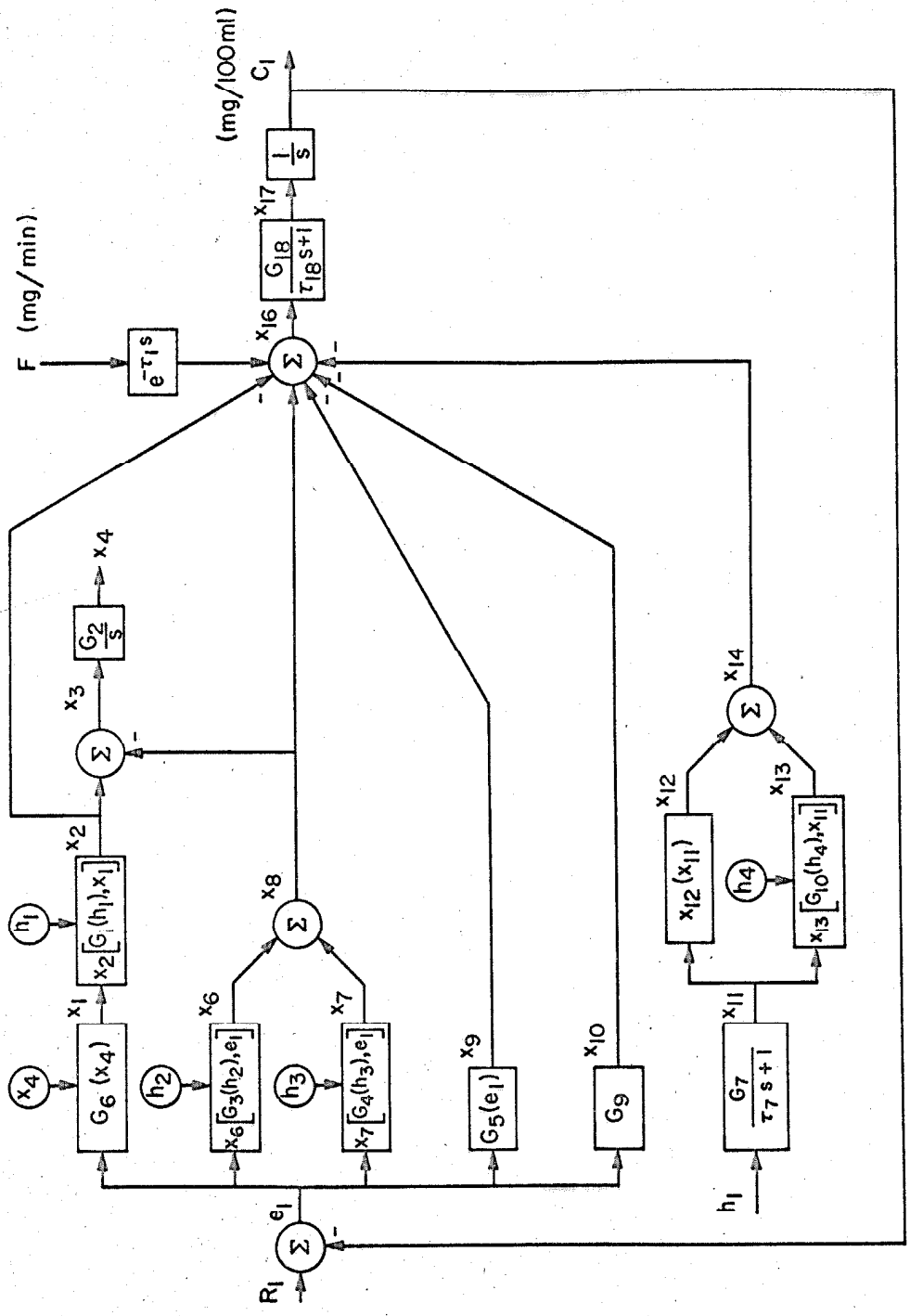

Figure 16. Preliminary Glucose Metabolic Plant Model.

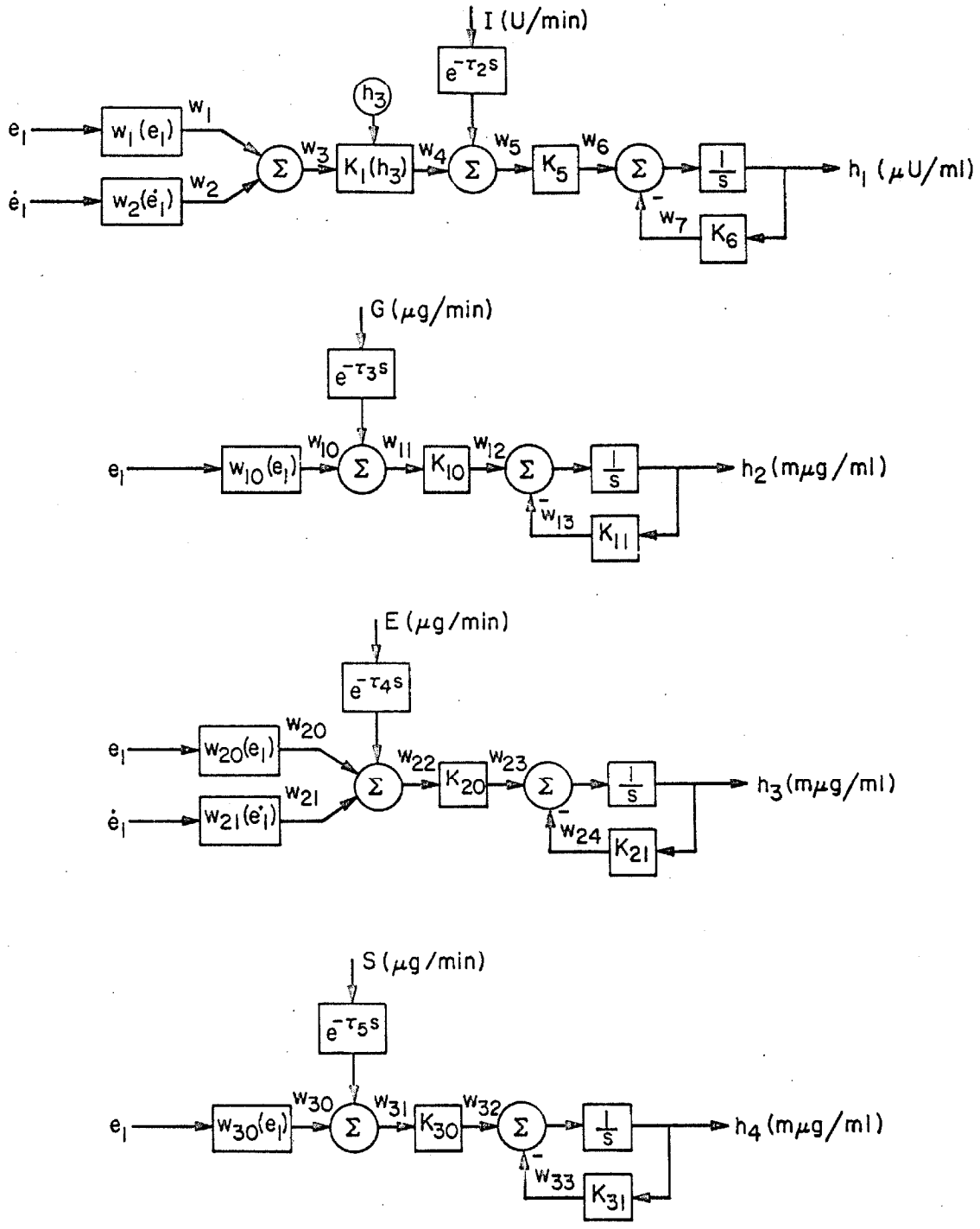

Figure 17. Preliminary Four Hormone Controller Model.

$$x_{11}(t) = \frac{G_7}{\tau_7} \int_0^t e^{-(t-\tau)/\tau_7} h_1(\tau)\, d\tau \qquad (3\text{-}95)$$

The parameters of this model were manually adjusted to simulate the results of two experiments. In the first, 15 g. of glucose was infused over three minutes in a normal male subject, and in the second, 5^u of regular insulin was injected at $t = 0$ followed by 1 mg. of glucagon at $t = 58$ minutes; the results of the simulations are shown in Figures 18 and 19 respectively.

Using the same parameter values resulting from the above in the model, a 30 g. infusion of glucose over three minutes was simulated. The comparison of the model predicted behavior with the subject's response to this new input is depicted in Figure 20.

Figures 18 and 20 illustrate one of the problems associated with obtaining data in intact biological systems, the solid lines in both cases showing discontinued recordings due to experimental difficulties.

3.7.3. Refined Four Hormone Model.

3.7.3.1. Plant.

The glucose metabolic plant model is shown in block diagram form in Figure 21. The following discussion can be followed most easily by referring to this diagram.

We take the size of the glucose space V_g, to be 25% of body weight, or for a 70 kg. man to be 17.5ℓ which breaks down as follows: interstitial fluid 10.5ℓ, plasma volume 3.5ℓ, red blood cells, liver, brain, and intestinal mucosa 3.5ℓ. Since the glucose molecule is so readily diffusible throughout these spaces we are considering the whole

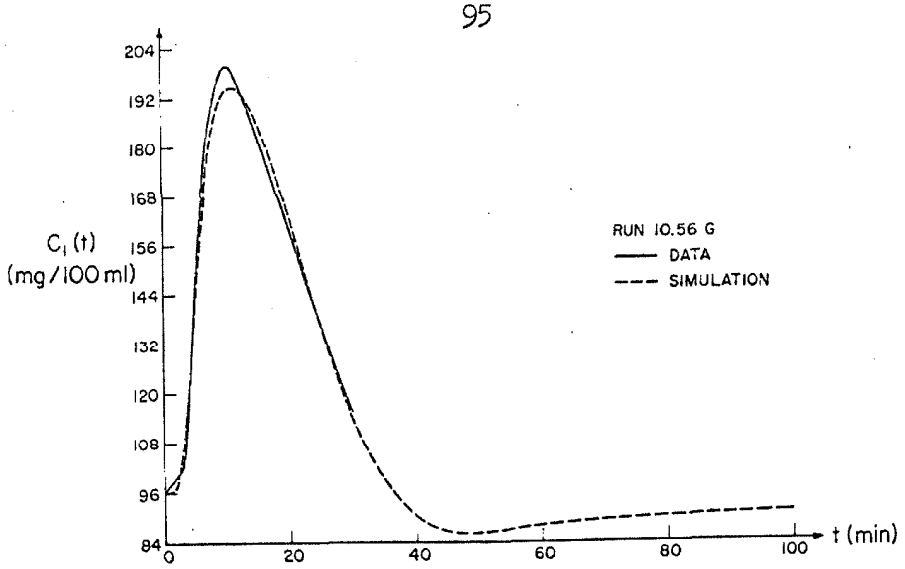

Figure 18. Subject K - 15 g. IV Glucose over 3 Minutes.

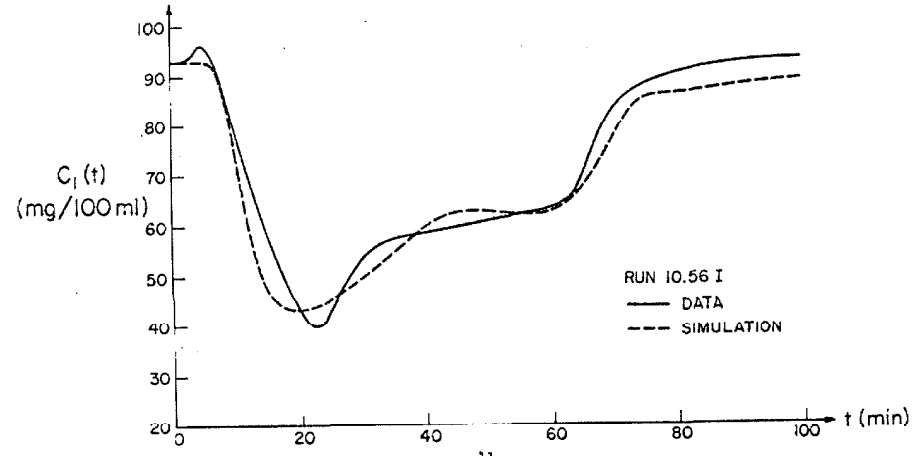

Figure 19. Subject K - 5^u Insulin at T = 0, 1 mg. Glucagon at T = 58.

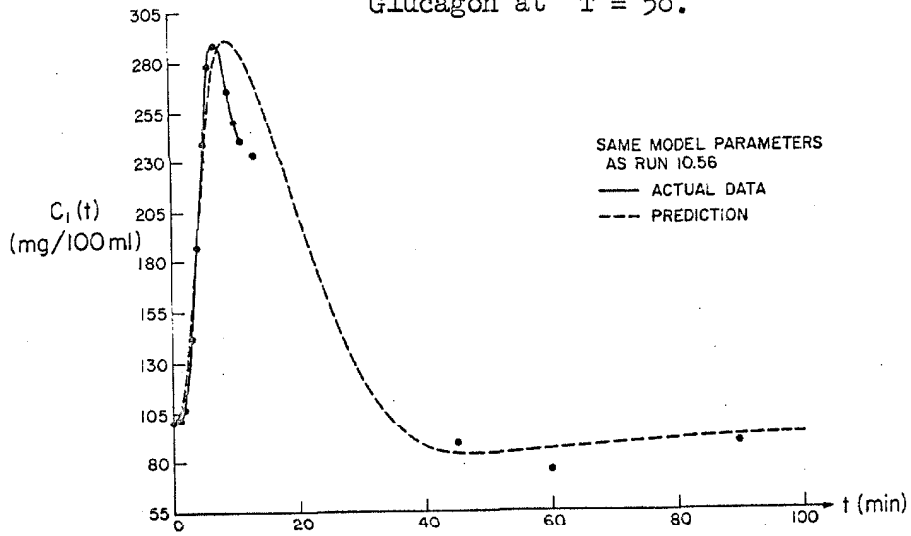

Figure 20. Subject K - 30 g. IV Glucose Predicted Response.

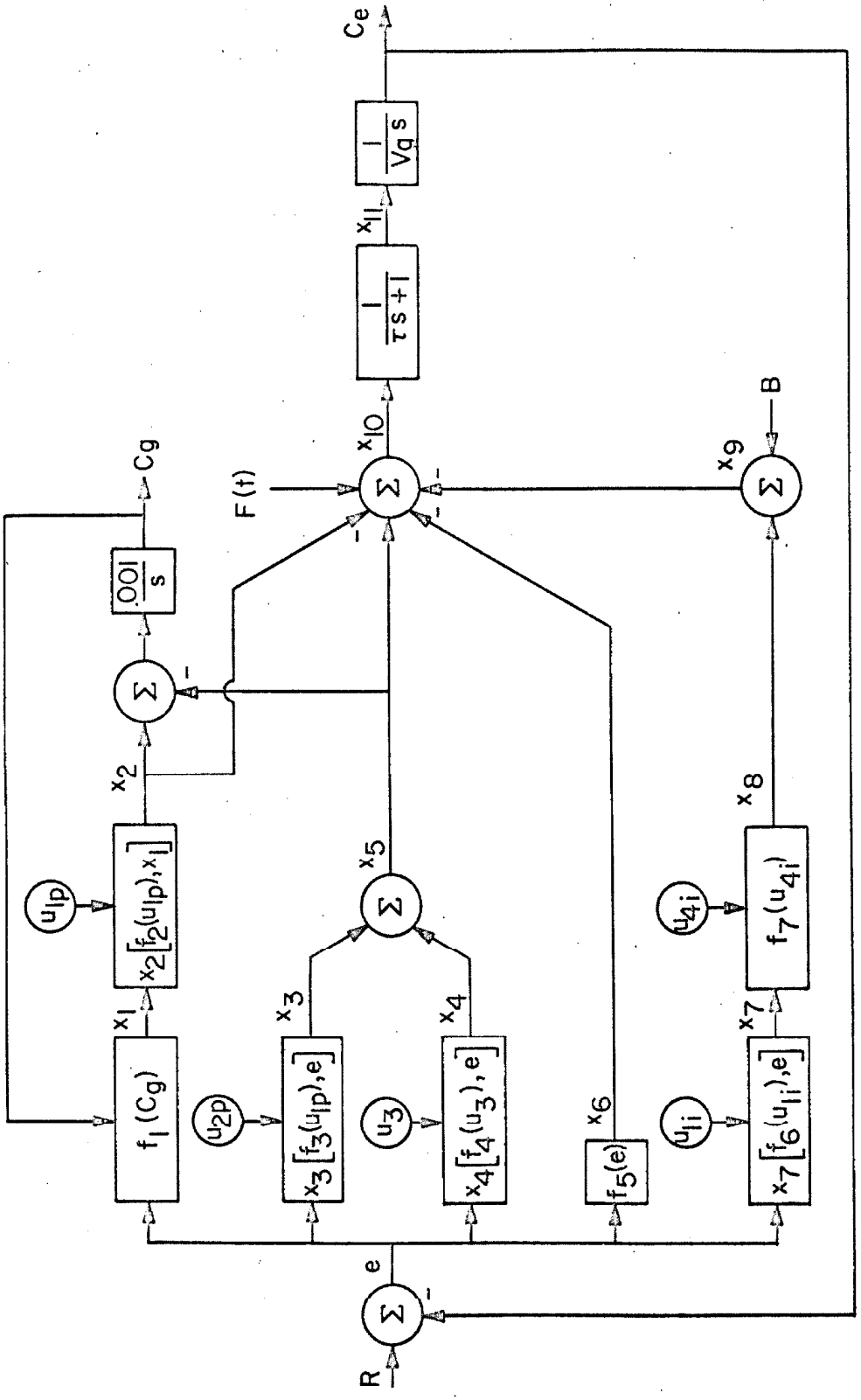

Figure 21. Glucose Metabolic Plant Model.

as one compartment. However, in a dynamic sense, any changes to the rate of input or exit of glucose from this space is accompanied by a time lag before the change is homogeneously distributed throughout the medium. Accordingly a first-order lag is inserted to account for distribution dynamics. The time constant τ is thought to be a fraction of a minute and is primarily accounted for by the time required for a few complete circuits of the systemic circulation.

The desired plasma concentration of glucose is believed to be determined by the central nervous system and is represented by a regulator set point, R. There is evidence that the brain reacts to a glucose antagonist by activating mechanisms to increase the blood glucose level.[117] In the post-absorptive state, for example, plasma glucose may fall to 75 mg%, but under normal conditions not much lower than this. For our purposes we initially take R = 100 mg%. The comparator action indicated is believed to be performed by the hypothalamus at the base of the brain.[45]

Since the brain appears to utilize glucose at a steady rate independent of plasma glucose concentration,[118] a constant sink B on plasma glucose is included. Several studies have determined that the normal glucose uptake rate by brain lies in the range 5.5 to 6.2 mg/min/100g.[88] For a 70 kg. man a 1400 g. brain is expected, indicating a reasonable value of 80 mg/min for B.

Hepatic intracellular glucose and extracellular fluid glucose seem to be connected by simple diffusion kinetics since when glucose - C^{14} is injected intravenously a rapid equilibrium results which seems to be independent of hepatic uptake or release of unlabled glucose.[119] At

any point in time hepatic glucose output equals the rate of breakdown of glycogen minus the rate of formation of glycogen from glucose or other precursors. Cahill's data on rat liver in the above quoted reference indicates that when extracellular glucose c_e = 80 mg%, liver is releasing glucose into the circulation the rate of which decreases to zero as c_e increases to about 145 mg%. At this point the gradient reverses, with liver performing a net uptake of glucose at a rate which reaches maximum when $c_e \simeq 400$ mg%. From these data and those of Madison[120] on dogs, Shames[62] computes figures for mean hepatic glucose output when c_e = 80 mg% and uptake when c_e = 400 mg%, which when transformed to that of 70 kg man are 163 mg/min and 709 mg/min, respectively. These figures correspond then to the fasting release rate of glucose when hormonal controls are at their nominal levels and the maximum uptake rate of glucose in the hyperglycemic state presumably stimulated by insulin.

Other investigators seem to have obtained similar results. For example, Seed, et.al.[57] using the data of Shreeve[121] use a hepatic glucose release rate of 100 mg/min at c_e = 110 mg%. They also assume that liver becomes a net sink for glucose when c_e = 143 mg% based on Myers[122] data that when blood glucose is elevated 30 mg% over fasting level there is no difference between the glucose concentration in arterial and hepatic venous blood. However, in view of the fact that in the resting postabsorptive state the plasma glucose concentration remains constant with no excretion of glucose into the urine, under these conditions glucose production and utilization are equal.[123] But the data of Soskin and Levine[83] in eviscerated normal dogs indicates a

peripheral utilization rate of about 225 mg/kg/hr at c_e = 100 mg% increasing in sigmoid fashion to a maximum of about 525 mg/kg/hr when c_e = 500 mg%. Converting this data to that of a 70 kg man yields fasting and maximum peripheral utilization rates of 260 mg/min and 610 mg/min respectively. Therefore, at nominal plasma glucose concentration we should expect the net hepatic release of glucose to be in the vicinity of 260 mg/min, of which we are allocating 80 mg/min to be utilized by brain and the remainder, 180 mg/min to be utilized by other tissues all of which we lump in the "peripheral utilization sink".

We represent the hepatic uptake of glucose for conversion to glycogen, using the symbols of Figure 21 as:

$$x_2 = \frac{d_9 + \alpha_1 u_{1p}}{2} \{1 - \tanh[b_9(x_1 - x_{10})]\} \qquad (3\text{-}96)$$

where α_1 is chosen such that when x_1 = - 300 mg%, x_2 = 700 mg/min. For example, if we expect that at x_1 = - 300 mg%, u_{1p} = 520 μU/mℓ, and at x_1 = 0 mg%, u_{1p} = 20 μU/mℓ, then

$$x_{10} = -150$$

$$b_9 = .02$$

$$d_9 = 128$$

$$\alpha_1 = 1.1$$

The parameters x_{10} and b_9 having been chosen to yield a smooth variation in the hyperbolic tangent as x_1 varies between 0 and

- 300. With the above parameters, insulin is seen to increase the rate of hepatic uptake of glucose by a factor of about three which has been reported.[15]

Although there is little doubt that insulin is important to the regulation of liver metabolism there is little agreement on the precise role played by insulin. Some view the effect as attenuation of glycogenolysis while others have it as the acceleration of glycogensis. It has been found that insulin added to rabbit liver slices in vitro increases the incorporation of C^{14} from labled glucose into hepatic glycogen.[124] Others also have found increased glycogen synthesis to be the process which is more directly stimulated by insulin action.[125] Following Shames[62] we take this view of hepatic insulin action and represent it as in Equation (3-96).

It is interesting that some investigators have interpreted the rapid synthesis of glycogen observed after a glucose input to be due to the possible error rate sensitivity of the liver,[47] whereas as we will see in the sequel, this effect is explainable in terms of the rate sensitivity of insulin release which in turn rapidly increases glycogenesis through parametric feedback as in (3-96).

An additional effect has been incorporated in the plasma glucose to hepatic glycogen pathway to account for the theory that under normal conditions glycogen stores have a definite maximum value of about 125 g. and are never fully depleted in the healthy animal. It is believed for example, that glycogen deposits normally will not fall below 75g. before the processes of gluconeogenesis become fully active supplying the required glucose for hepatic glucose release. Accordingly we include an

attenuation factor in the hepatic glycogenesis pathway which is a function of hepatic glycogen stores. Again referring to Figure 21:

$$x_1 = f_1(c_g)\, e \tag{3-97}$$

$$f_1(c_g) = \frac{1}{2}\{1 - \tanh[b_8(c_g - c_{g0})]\} \tag{3-98}$$

where:

$$b_8 = 0.6$$

$$c_{g0} = 125.$$

Hepatic glycogen storage is then a function of the difference between the rate of glycogenesis and glycogenolysis or:

$$c_g(t) = \int_0^t .001[x_2(\tau) - x_5(\tau)]\, d\tau + c_g(0) \tag{3-99}$$

where we take $c_g(0) = 75$ g. as the initial value for the size of the hepatic glycogen store in all experiment simulations undertaken.

The process of glycogenolysis is modeled as two functions in order to separately incorporate the reported effects of glucagon and epinephrine on accelerating glycogenolysis.[34] The remarks made above, however, allow us to obtain the parameters of the x_3 and x_4 nonlinearities under conditions of nominal hormonal control concentrations. We wish to establish $x_5(0) = 260$ mg/min and x_5 approaching zero as e approaches - 45 mg%, corresponding to a nominal hepatic glucose

release rate of 260 mg/min and the cessation of net glycogenesis as c_e approaches 145 mg%. It remains to choose an appropriate saturation value of x_5 at an appropriate value of e. There is no direct physiologic data in existence which would allow this, but since we would expect the glycogenolytic capacity of the liver to be stimulated to full production even in the absence of glucagon and epinephrine by a developing hypoglycemia, then a value of e = 75 mg%, i.e. c_e = 25 mg% seems reasonable. With this information the saturation value can be obtained from:

$$x_5 = \frac{x_{5H}}{2}\{1 + \tanh[\beta(e-e_0)]\} \qquad (3\text{-}100)$$

Choosing $e_L = -45$, $e_H = 75$, hence $e_0 = 15$ and $\beta = .0334$ for a smooth variation over the specified range of the independent variable then:

$$260 = \frac{x_{5H}}{2}\{1 + \tanh[.0334(-15)]\}$$

or $x_{5H} = 960$. These values will now be equally distributed between x_3 and x_4 under the condition of no hormone effect present because we have no data upon which to base any other arrangement at this time. Hence for the glucagon affected glycogenolytic process we have:

$$x_3 = \frac{d_{10} + \alpha_2 u_{2p}}{2}\{1 + \tanh[b_{10}(e-e_{05})]\} \qquad (3\text{-}101)$$

where $b_{10} = .0334$, $e_{05} = 15.$, and $d_{10} + \alpha_2 u_{2p}(0) = 480$. Here

$u_{2p}(0)$ refers to the fasting concentration of glucagon in plasma. Similarly, for the epinephrine affected glycogenolytic process we have:

$$x_{1_1} = \frac{d_{11} + \alpha_3 u_3}{2} \{1 + \tanh[b_{11}(e-e_{06})]\} \qquad (3\text{-}102)$$

where $b_{11} = .0334$, $e_{06} = 15$, and $d_{11} + \alpha_3 u_3(0) = 480$. Here $u_3(0)$ represents the fasting concentration of epinephrine in plasma.

The maximum rates of glycogen breakdown observed in vivo[126] are about three times as great as the maximum rates of glycogen deposition.[127] Since the evidence presented above is for a maximum rate of glycogenesis in the presence of insulin of about 700 mg/min, then a maximum rate of hepatic release of glucose of about 2100 mg/min in the presence of glucagon and epinephrine would be indicated.

The normal response to insulin hypoglycemia includes an abrupt and substantial increase of the hepatic glucose output, which begins to rise before the declining blood glucose level reaches 40 mg%.[128,129] It is generally stated that the glycogenolytic action of glucagon is mediated through activation of hepatic phosphorylase. There is a direct correlation between the activation of phosphorylase and glycogenolysis over the physiologic range of glucagon concentration.[26] Hepatic glucose output rates in excess of 1(mg/min)/g liver during peak glucagon action on the isolated rat liver have been observed.[130] This marked stimulation of glycogenolysis occurs at plasma glucagon concentrations of 4 mμg/mℓ. Assuming the same effect in man and an 1800 g liver implies a saturation value for x_3 of 1800 mg/min.

Values in the same range as that quoted above have been reported by Shoemaker.[131] Using a fasting plasma glucagon concentration of 0.5 mμg/mℓ, a maximum physiologic concentration of 3.5 mμg/mℓ, and a desired maximally glucagon stimulated glycogenolysis rate of 1500 mg/min implies that in Equation (3-101) we require approximately $d_{10} = 310$ and $\alpha_2 = 340$ if we assume an unstimulated maximal rate for x_3 of 480 mg/min.

The glycogenolytic effect of epinephrine on liver is also believed to be mediated through activation of liver phosphorylase.[132] Although a glycogenolytic action of epinephrine on the isolated liver could be demonstrated only at the near lethal concentration of 100 mμg/mℓ,[133] it is still believed by some that the concentrations of epinephrine observed during the reaction to insulin-induced hypoglycemia, i.e. 2 to 3 mμg/mℓ,[32] have a definite glycogenolytic effect. In fact, it has been reported that physiologic epinephrine can increase the rate of glycogenolysis by a factor of three.[30]

In order to obtain first guesses on parameters for Equation (3-102) we will assume that epinephrine enhanced glycogenolysis can increase the saturation value of x_4 to 1000 mg/min. Hence using a fasting plasma epinephrine concentration of 0.5 mμg/mℓ, a maximum physiologically induced concentration of 2.5 mμg/mℓ, an epinephrine independent maximum x_4 of 480 mg/min, and an epinephrine induced maximum x_4 of 1000 mg/min implies that $d_{11} = 350$ and $\alpha_3 = 260$ in Equation (3-102).

It will be noted that effects upon gluconeogenesis have not been incorporated per se in the model since the impact of such effects on

the behavior of the glucose control loop is not felt. To this loop, non-glucose precursors function simply as an alternate glucose source and need be specifically delineated only when coupling among fat, protein, and glucose regulation are implemented. The total glycogenolytic effect of the liver is represented:

$$x_5 = x_3[f_3(u_{1p}), e] + x_4[f_4(u_3), e] \tag{3-103}$$

Plasma normally contains anywhere between 70 and 140 mg% of glucose with only minute traces excreted in the urine. Under these conditions virtually all the filtered glucose is reabsorbed. As the concentration of glucose in plasma rises, the rate of passage of glucose through the renal glomerules rises proportionally until the reabsorption capacity is exceeded. Some glucose will begin to appear in the urine as soon as $c_e = 180$ mg%, but the rate of reabsorption will continue to rise somewhat until the excretion rate is a linear function of c_e. From the data of Woolf[134] (Figure 4B, Page 13), and assuming a constant glomerular filtration rate of 125 mℓ/min, we compute that this constant excretion rate is 1.25 mg/min and is reached approximately at $c_e = 320$ mg%. Since we represent renal excretion as follows:

$$x_6 = f_5(e)\, e \tag{3-104}$$

$$f_5(e) = \frac{d_{12}}{2}\{1 - \tanh[b_{12}(e - e_{07})]\} \tag{3-105}$$

From the above we have, $d_{12} = -1.25$, $b_{12} = .043$, and $e_{07} = -150$.

Other sinks for glucose not accounted for by B, $f_5(e)$, and $x_2[f_1(u_{1p}), x_1]$ are lumped together in the peripheral utilization sink. The major components of this sink for glucose are muscle and adipose tissue glucose utilization, but other smaller yet significant glucose users such as red blood cells are also included. Two functions will be used to represent the effects of insulin and growth hormone on peripheral glucose utilization rates.

It is now generally accepted that the chief peripheral effect of insulin is to facilitate the transport of glucose from the interstitial fluid space across the cell membrane to the interior of the cell.[135] Adipose tissue has been found to be extremely sensitive to insulin, responding by accelerated glucose uptake measured as a factor of six in the presence of 0.1 U/mℓ insulin in rat adipose tissue.[136] Other investigators have found insulin to accelerate adipose tissue take up of glucose up to a factor of three in dog and man.[89,90] It is also generally accepted that the action of insulin on muscle is extremely rapid and accelerates the transfer of glucose across the cell membrane.[137] In contrast to the peripheral effects of insulin, growth hormone has been found to decelerate the rate of transfer of glucose to intracellular spaces.[138]

We will represent the above effects by the functions $x_7[f_6(u_{1i}), e]$ and $f_7(u_{4i})$. Interstitial fluid insulin, u_{1i}, will increase the saturation value of the peripheral glucose take up nonlinearity and growth hormone will attenuate the net glucose utilization rate. We have:

$$x_7 = \frac{d_{13} + \alpha_4 u_{1i}}{2} \{1 - \tanh[b_{13}(e-e_{08})]\} \qquad (3\text{-}106)$$

From the previous remarks we desire fasting x_7 to be equal to 180 mg/min. It will be shown in the discussion on the controller model that as plasma insulin, u_{1p}, varies from 20 μU/mℓ to 520 μU/mℓ, interstitial fluid insulin, u_{1i}, varies from 14 μU/mℓ to 346 μU/mℓ. Hence we must have $x_7 = 180$ mg/min when $u_{1i} = 14$ μU/mℓ. Having chosen $e_{08} = -100$ and $b_{13} = .0067$ to yield a smooth variation over $e = [-300, 100]$, implies a nonhormonal dependent saturation value for x_7 of 870 mg/min. If we allow the insulin effect to increase this rate by a factor of three, or $x_7 = 2610$, then $d_{13} + \alpha_4\, 14 = 870$ and $d_{13} + \alpha_4\, 346 = 2610$ implies that in Equation (3-106) we must take $d_{13} = 797$, and $\alpha_4 = 5.24$. Growth hormone then attenuates this rate as follows:

$$x_8 = f_7(u_{4i})\, x_7 \qquad (3\text{-}107)$$

$$f_7(u_{4i}) = \frac{1}{2} \{1 - \tanh[b_{14}(u_{4i}-u_{4i0})]\} \qquad (3\text{-}108)$$

There is no quantitative data in existence which will precisely establish the parameters of (3-108), but for initial first guesses we will take $u_{4i0} = 50$ and $b_{14} = .04$ and establish more meaningful values by simulation of experiments.

Whereas hepatic glucose storage and release are probably affected by the concentration of insulin in the portal vein, the peripheral rate

of glucose utilization is more likely dependent upon the concentration of insulin in interstitial fluid. Similar considerations apply to the other hormones included in the controller and motivates the explicit inclusion of two variables for these hormonal distribution and degradation kinetics.

Plant Equations.

Referring to Figure 21 we have:

$$\tau\ddot{c}_e + \dot{c}_e = \frac{1}{V_g}\{F(t) + x_3[f_3(u_{1p}),e] + x_4[f_4(u_3),e] - x_2[f_1(u_{1p}),f_1(c_g)e] - f_5(e)\, e - f_7(u_{4i})\, x_7[f_6(u_{1i}),e] - B\} \quad (3\text{-}109)$$

$$\dot{c}_g = .001\,\{x_2[f_2(u_{1p}),f_1(c_g)e] - x_3[f_3(u_{2p}),e] - x_4[f_4(u_3),e]\} \quad (3\text{-}110)$$

Let:

$$z_1 \triangleq c_e$$

$$z_2 \triangleq \dot{z}_1$$

$$z_3 \triangleq c_g$$

then:

$$\dot{z}_1 = z_2 \quad (3\text{-}111)$$

$$\dot{z}_2 = -\frac{1}{\tau} z_2 + \frac{1}{V_g}\{F(t) + x_2(t) - x_5(t) - x_6(t) - x_9(t)\} \quad (3\text{-}112)$$

$$\dot{z}_3 = .001\,\{x_2(t) - x_5(t)\} \quad (3\text{-}113)$$

Simulation Equations.

$$
\begin{aligned}
e &= R - c_e \\
x_1 &= f_1(c_g)\, e \\
x_2 &= x_2[f_2(u_{1p}),\ x_1] \\
x_3 &= x_3[f_3(u_{2p}),\ e] \\
x_4 &= x_4[f_4(u_3),\ e] \\
x_5 &= x_3 + x_4 \\
\dot{c}_g &= .001\,[x_2 - x_5] \\
x_6 &= f_5(e)\, e \\
x_7 &= x_7[f_6(u_{1i}),\ e] \\
x_8 &= f_7(u_{4i})\, x_7 \\
x_9 &= x_8 + B \\
x_{10} &= F - x_2 + x_5 - x_6 - x_9 \\
\dot{x}_{11} &= -\frac{1}{\tau} x_{11} + \frac{1}{\tau} x_{10} \\
\dot{c}_e &= \frac{1}{V_g} x_{11}
\end{aligned}
\qquad (3\text{-}114)
$$

where:

$$f_1 = \frac{1}{2}\{1 - \tanh[b_8(c_g - c_{g0})]\}$$

$$x_2 = \frac{d_9 + \alpha_1 u_{1p}}{2}\{1 - \tanh[b_9(x_1 - x_{10})]\}$$

$$x_3 = \frac{d_{10} + \alpha_2 u_{2p}}{2}\{1 + \tanh[b_{10}(e - e_{05})]\}$$

$$x_4 = \frac{d_{11} + \alpha_3 u_3}{2}\{1 + \tanh[b_{11}(e - e_{06})]\} \qquad (3\text{-}115)$$

$$f_5 = \frac{d_{12}}{2}\{1 - \tanh[b_{12}(e - e_{07})]\}$$

$$x_7 = \frac{d_{13} + \alpha_4 u_{1i}}{2}\{1 - \tanh[b_{13}(e - e_{08})]\}$$

$$f_7 = \frac{1}{2}\{1 - \tanh[b_{14}(u_{4i} - u_{4i0})]\}$$

Definitions of Terms.

$R \triangleq$ [mg/100mℓ] plasma glucose concentration set point

$F \triangleq$ [mg/min] exogenous glucose intravenous input

$B \triangleq$ [mg/min] CNS glucose utilization

$c_e \triangleq$ [mg/100mℓ] plasma glucose concentration

$c_g \triangleq$ [g] hepatic glycogen store

$e \triangleq$ [mg/100mℓ] glucose actuating error

$x_1 \triangleq$ [mg/100mℓ] effective glucose actuating error for glycogenesis.

$x_2 \triangleq$ [mg/min] hepatic glucose uptake

$x_3 \triangleq$ [mg/min] glycogenolysis as a function of glucagon

$x_4 \triangleq$ [mg/min] glycogenolysis as a function of epinephrine

$x_5 \triangleq$ [mg/min] total hepatic glycogenolysis

$x_6 \triangleq$ [mg/min] renal glucose excretion

$x_7 \triangleq$ [mg/min] peripheral glucose uptake as a function of insulin

$x_8 \triangleq$ [mg/min] peripheral glucose uptake as a function of growth hormone

$x_9 \triangleq$ [mg/min] total peripheral glucose uptake

$x_{10} \triangleq$ [mg/min] glucose entering system circulation

$x_{11} \triangleq$ [mg/min] glucose entering glucose space

$V_g \triangleq$ [100mℓ] glucose space

$\tau \triangleq$ [min] systemic circulation time constant

$b_8 \triangleq$ [1/g Glycogen]

$c_{g0} \triangleq$ [g Glycogen]

$\alpha_1 \triangleq$ [mℓ-mg Glucose/min-μU Insulin]

$b_9 \triangleq$ [100mℓ/mg Glucose]

$x_{10} \triangleq$ [mg Glucose/100mℓ]

$d_9 \triangleq$ [mg Glucose/min]

$\alpha_2 \triangleq$ [mℓ-mg Glucose/min-mμg Glucagon]

$b_{10} \triangleq$ [100 mℓ/mg Glucose]

$e_{05} \triangleq$ [mg Glucose/100mℓ]

$d_{10} \triangleq$ [mg Glucose/min]

$\alpha_3 \triangleq$ [mℓ-mg Glucose/min-mμg Epinephrine]

$b_{11} \triangleq$ [100 mℓ/mg Glucose]

$e_{06} \triangleq$ [mg Glucose/100mℓ]

$d_{11} \triangleq$ [mg Glucose/min]

$d_{12} \triangleq$ [100 mℓ/min]

$b_{12} \triangleq$ [100 mℓ/mg Glucose]

$e_{07} \triangleq$ [mg Glucose/100 mℓ]

$\alpha_4 \triangleq$ [mℓ-mg Glucose/min-mμg Insulin]

$b_{13} \triangleq$ [100 mℓ/mg Glucose]

$e_{08} \triangleq$ [mg Glucose/100 mℓ]

$d_{13} \triangleq$ [mg Glucose/min]

$b_{14} \triangleq$ [mℓ/mμg Growth Hormose]

$u_{4io} \triangleq$ [mμg Growth Hormone/mℓ]

3.7.3.2. Controller.

Since insulin has a high molecular weight (about 6000), its diffusion across capillaries may contribute significantly to the dynamic behavior of the endogenously generated substance. Experimental evidence suggests a bi-exponential decay of I^{131} labled insulin in man.[94] Hence we would expect that at least a two-compartment model composed of plasma and interstitial fluid will be required to represent the dynamic behavior of insulin distribution and degradation. Unless simulation results indicate otherwise we will take $V_p = 3.5\ \ell$ and $V_i = 10.5\ \ell$ for the size of these spaces. Simple passive diffusion is assumed to connect the two compartments. Insulin degradation in the plasma space is represented by parameter a_1 and in the interstitial space by parameter a_3. We then have:

$$\left.\begin{aligned} V_p\,\dot{u}_{1p} &= -a_1\,u_{1p} + a_2(u_{1i} - u_{1p}) + w_5(t,e,\dot{e}) \\ V_i\,\dot{u}_{1i} &= -a_3\,u_{1i} + a_2(u_{1p} - u_{1i}) \end{aligned}\right\} \qquad (3\text{-}116)$$

where $w_5(t,e,\dot{e})$ represents the endogenous secretion of insulin as a function of glucose error and error rate and any exogenous input.

The mean, basal plasma insulin concentration in man has been measured to be 21 μU/mℓ.[139] From the data of Berson and Yalow,[94] the coefficients of (3-116) have been computed to be:

$$a_1 = 248 \text{ m}\ell/\text{min}$$

$$a_2 = 309 \text{ m}\ell/\text{min}$$

$$a_3 = 156 \text{ m}\ell/\text{min}$$

These numbers imply the following time constants for the plasma space and the interstitial space.

$$\tau_p = \frac{V_p}{a_1 + a_2} \tag{3-117}$$

$$= 6.29 \text{ min.}$$

$$\tau_i = \frac{V_i}{a_2 + a_3} \tag{3-118}$$

$$= 30.1$$

Since decay dynamics are usually characterized in terms of the "half-life" by biological scientists, for comparison purposes the above time constants imply from $T_{1/2} = \ln(2)\ \tau$ that $T_{1/2\ p} = 4.35$ min. and $T_{1/2\ i} = 20.8$ min.

Given the steady-state value of plasma insulin, $u_{1p}(ss) = 21\ \mu U/m\ell$, we compute $u_{1i}(ss)$ and the required rate of endogenous insulin secretion, $w_5(ss)$. From (3-116), in steady state:

$$\left.\begin{aligned} w_5(ss) &= 248\ (21) + 309[21 - u_{1i}(ss)] \\ 0 &= -\ 156\ u_{1i}(ss) + 309[21 - u_{1i}(ss)] \end{aligned}\right\} \tag{3-119}$$

$$\therefore \quad u_{1i}(ss) = \left(\frac{309}{465}\right) 21$$

$$= 14 \ \mu U/m\ell$$

$$\therefore \quad w_5(ss) = .0074 \ U/min$$

In other words, given the above degradation factors for insulin in the plasma and interstitial spaces and the diffusion coefficient, a steady-state insulin secretion rate from the pancreas of .0074 U/min results in a steady-state plasma insulin concentration of 21 $\mu U/m\ell$ and a steady-state interstitial fluid space insulin concentration of 14 $\mu U/m\ell$.

Although the variable u_{1i} is not directly observable at the present time it may be possible eventually to measure u_{1i} directly by means of lymphatic cannulation. The value chosen for the plasma space insulin degradation coefficient, a_1 yields a rate of insulin destruction (a_1/V_p = .071 1/min), close to Madison's observations on dog, i.e. 0.1 1/min,[140] and Mortimore's observations on rat, i.e. .08 1/min.[141] As we have seen above, the steady-state endogenous secretion rate of insulin required to maintain $u_{1p}(ss)$ = 21 $\mu U/m\ell$ and $u_{1i}(ss)$ = 14 $\mu U/m\ell$ is .0074 U/min. Taking Metz's measurements on dogs,[92] assuming an average weight of 16 kg., and a 50% destruction rate of insulin in first hepatic passage results in an endogenous secretion rate of .00875 U/min.

It is now generally accepted that insulin is released as some function of glucose error. Although explicit quantitative data are

lacking for a precise characterization of this relation, many of the remarks made in the biological literature point to the possible dependence of insulin secretion on both the glucose error and the derivative of glucose error. Insulin generation as a function of error rate has been suggested by Tepperman.[112] As shown in Figure 22 the model for insulin generation is as follows:

$$w_5 = 10^6\{IN(t) + f_8(u_3)[w_1(e) + w_2(\dot{e})]\} \qquad (3\text{-}120)$$

where $w_1(e)$ represents insulin secretion proportional to glucose error,

$$w_1(e) = \frac{d_1}{2}\{1 - \tanh[b_1(e-e_{01})]\} \qquad (3\text{-}121)$$

$w_2(\dot{e})$ represents insulin secretion proportional to glucose error rate,

$$w_2(\dot{e}) = \frac{d_2}{2}\{1 - \tanh[b_2(\dot{e}-\dot{e}_{01})]\} \qquad (3\text{-}122)$$

and $f_8(u_3)$ represents the inhibition of insulin secretion by epinephrine:

$$f_8(u_3) = \frac{1}{2}\{1 - \tanh[b_3(u_3-u_{30})]\} \qquad (3\text{-}123)$$

The parameter values for (3-121) are obtained by considering that $w_1 = 0$ when $e = 20$, $w_1 = .0074$ U/min when $e = 0$, and $w_1 =$ max secretion rate when $e = -180$. We obtain w_1 max from (3-119) with

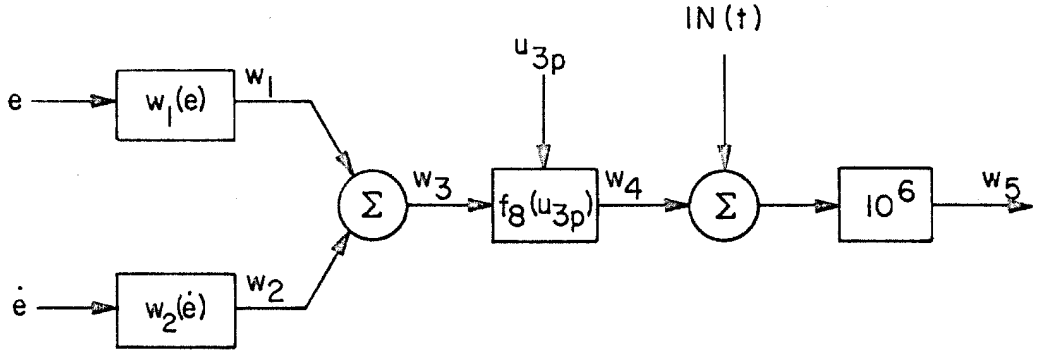

Figure 22. Insulin Secretion.

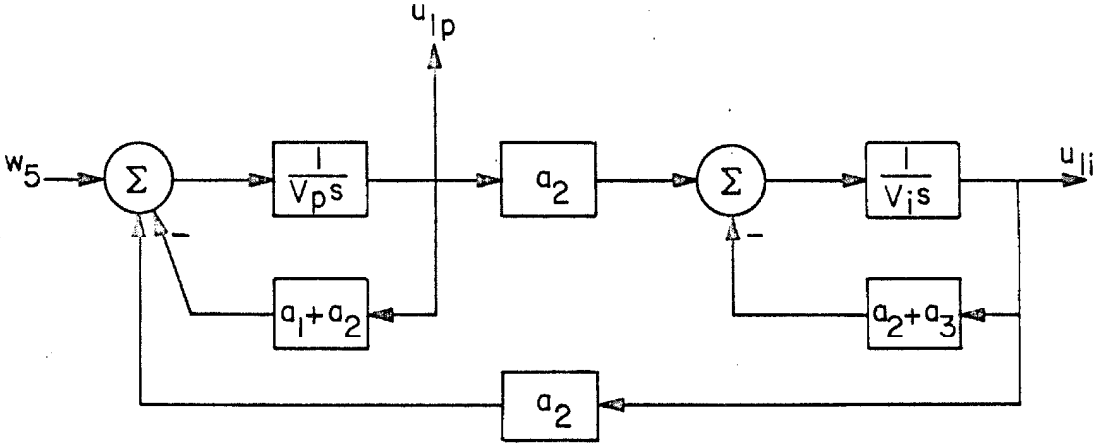

Figure 23. Insulin Distribution and Degradation.

$u_{1p} = 520\ \mu U/m\ell.$

$$w_1(ss) = 248(520) + 309[520 - u_{1i}(ss)]$$

$$0 = -156\, u_{1i}(ss) + 309[520 - u_{1i}(ss)]$$

$$\therefore \quad u_{1i}(ss) = \frac{309}{465}(520)$$

$$= 346\ \mu U/m\ell$$

Hence w_{1max} or $d_1 = .183$ U/min. From these values we now obtain b_1. Since $e_{01} = -80$ we have:

$$b_1 = \frac{1}{80} \tanh^{-1}\left(\frac{.0915 - .0074}{.0915}\right)$$

$$= .02$$

The function $w_1(e)$ is now completely specified. The weakest justification of parameter values here is d_1, but properly designed systems experiments can yield this information just as $w_1(0)$ was obtained. This will be further discussed in Chapter IV.

The basic idea underlying the error rate insulin secretion nonlinearity (3-122) is that a too rapidly rising plasma glucose concentration will cause more insulin to be generated at a particular glucose concentration than would otherwise be the case. We choose as first guesses on the parameter values of (3-122) to have $w_2(\dot{e})$ vary from minimum to maximum over the range $\dot{e} = -10$ mg%/min to $\dot{e} = -60$ mg%/min with $w_{2max} = d_2 = .09$ U/min. Consequently, $\dot{e}_{01} = -35$ mg%/

min, d_2 = .09 U/min, and for a smooth variation over this range, b_2 = .08.

The results of several experiments suggest that epinephrine somehow can inhibit the secretion of insulin, in fact, epinephrine is believed capable of this action directly at the site of the β-cell.[27] Porte's results show that even a relatively small amount of plasma epinephrine, probably a fraction of a mμg/mℓ can completely inhibit the secretion of insulin in spite of the resulting hyperglycemia. In the representation of this particular effect, Equation (3-123), we will vary the inhibition by epinephrine smoothly over the range u_3 = [0.5, 2.5] mμg/mℓ. Hence in (3-123) we take u_{30} = 1.5, b_3 = 2.0.

Since glucagon has a relatively high molecular weight, 3450, it is expected that at least a two-compartment model for distribution and degradation will be required to represent its dynamic behavior. Although measurements of labeled glucagon decay have been made,[142] clear and unequivocal data are lacking upon which to base computation of degradation factors and a diffusion coefficient. As previously mentioned, however, the disappearance rate of circulating glucagon in rat has been reported as 80% in 5 min,[95] which translates into a time constant of 3.12 minutes if first-order kinetics are assumed. Glucagon is rapidly inactivated by liver,[143, 144] and its concentration in fasting dogs has been measured to average 0.5 mμg/mℓ with peak values of 4 mμg/mℓ in hypoglycemic dogs.[145] Glucagon release is believed to be stimulated by neural pathways as a function of hypoglycemia.[26] In addition to the degradation rate mentioned above, plasma glucagon levels measured by immunoassay have indicated a half-life of about 10

minutes,[22] i.e. a time constant of about 14 minutes.

The model shown in Figures 24 and 25 for glucagon secretion, distribution and degradation is as follows:

$$\left.\begin{aligned} V_p \dot{u}_{2p} &= - a_4 u_{2p} + a_5(u_{2i}-u_{2p}) + w_{11}(t,e) \\ V_i \dot{u}_{2i} &= - a_6 u_{2i} + a_5(u_{2p}-u_{2i}) \end{aligned}\right\} \qquad (3\text{-}124)$$

where $w_{11}(t,e)$ represents the endogenous secretion of glucagon by the pancreas as a function of glucose error and any exogenous input.

We will assume a mean basal plasma glucagon concentration of 0.5 mμg/mℓ and initial guessed values for degradation and diffusion coefficients of:

$$a_4 = 350 \text{ mℓ/min}$$

$$a_5 = 425 \text{ mℓ/min}$$

$$a_6 = 250 \text{ mℓ/min}$$

These values imply:

$$\tau_p = \frac{V_p}{a_4 + a_5} \qquad (3\text{-}125)$$

$$= 4.52 \text{ min}$$

$$\therefore \quad T_{1/2\ p} = 3.13 \text{ min.}$$

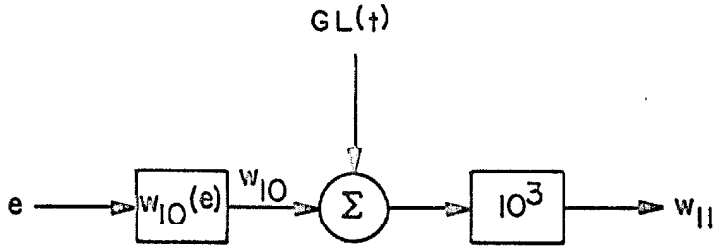

Figure 24. Glucagon Secretion.

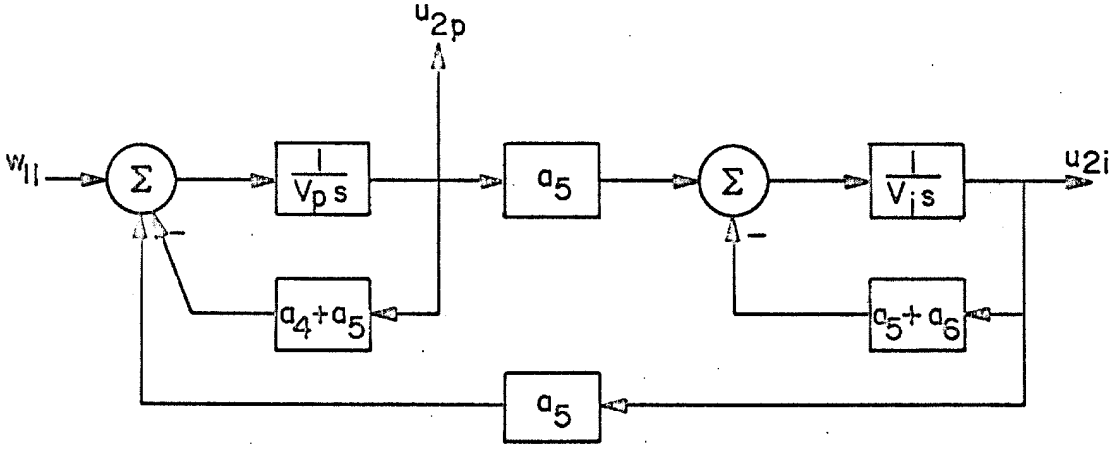

Figure 25. Glucagon Distribution and Degradation.

$$\tau_i = \frac{V_i}{a_5 + a_6} \qquad (3\text{-}126)$$

$$= 15.6 \text{ min.}$$

$$\therefore \quad T_{i/2\ i} = 10.8 \text{ min.}$$

Given the steady-state value of plasma glucagon, $u_{2p}(ss) = 0.5$ mμg/mℓ, we compute $u_{2i}(ss)$ and the required rate of endogenous glucagon secretion, $w_{10}(ss)$. From (3-124), in steady-state:

$$\left.\begin{aligned} w_{10}(ss) &= 350(0.5) + 425[0.5 - u_{2i}(ss)] \\ 0 &= -250\, u_{2i}(ss) + 425[0.5 - u_{2i}(ss)] \end{aligned}\right\} \qquad (3\text{-}127)$$

$$\therefore \quad u_{2i}(ss) = \left(\frac{425}{675}\right) 0.5$$

$$= 0.32 \text{ mμg/mℓ}$$

$$\therefore \quad w_{10}(ss) = 0.252 \text{ μg/min}$$

In other words, given the above values for degradation factors and the diffusion coefficient, a steady-state glucagon secretion rate of .252 μg/min from the pancreas results in a nominal plasma glucagon concentration of 0.5 mμg/mℓ and a nominal interstitial fluid space glucagon concentration of 0.32 mμg/mℓ.

As shown in Figure 24 the model for glucagon secretion is as

follows:

$$w_{11} = 10^3[GL(t) + w_{10}(e)] \tag{3-128}$$

where $w_{10}(e)$ represents glucagon secretion proportional to glucose error.

$$w_{10}(e) = \frac{d_4}{2}\{1 + \tanh[b_4(e-e_{02})]\} \tag{3-129}$$

The parameter values for (3-129) are obtained by considering $w_{10} = 0$ when $e = -20$, $w_{10} = 0.252$ μg/min when $e = 0$, and $w_{10\ max}$ occurs when $e = 60$. We obtain $w_{10\ max}$ from (3-127) with $u_{2p} = 3.5$ mμg/mℓ.

$$w_{10}(ss) = 350(3.5) + 425[3.5 - u_{2i}(ss)]$$

$$0 = -250\, u_{2i}(ss) + 425[3.5 - u_{2i}(ss)]$$

$$\therefore \quad u_{2i}(ss) = \left(\frac{425}{675}\right) 3.5$$

$$= 2.2 \text{ mμg/mℓ}$$

Hence $w_{10\ max}$ or $d_4 = 1.78$ μg/min. Since $e_{02} = 20$, we have:

$$b_4 = \frac{1}{20} \tanh^{-1}\left(\frac{.89 - .252}{.89}\right)$$

$$= .045$$

which completely specifies the function (3-129).

Because of the low molecular weight of epinephrine, 183.2, we would expect it to be freely diffusible across the capillary membrane, hence rapid dynamic equilibrium between plasma epinephrine and interstitial fluid epinephrine should be the rule. For this reason a one-compartment (extracellular fluid, $V_e = 14\ell.$) model for the distribution and degradation of epinephrine should be adequate for our purposes, see Figure 27.

As already mentioned in the discussion on insulin dynamics above, epinephrine will be secreted in response to a too rapidly falling plasma glucose concentration. Hence in the epinephrine secretion model shown in Figure 26, epinephrine is secreted as a function of glucose error and glucose error rate. Epinephrine has an extremely fast disappearance rate; a half-life of 10-30 seconds has been estimated.[29] We will take the fasting level of epinephrine to be 0.5 mμg/mℓ. The concentration observed during the reaction to insulin-induced hypoglycemia is 2-3 mμg/mℓ.[32] Consequently, the range of endogenously secreted epinephrine will be taken as [0.5, 2.5] mμg/mℓ.

We have for epinephrine secretion, distribution, and degradation:

$$V_e \dot{u}_3 = - a_7 u_3 + 10^3[EP(t) + w_{20}(e) + w_{21}(\dot{e})] \qquad (3\text{-}130)$$

where $w_{20}(e)$ represents glucose error epinephrine secretion and $w_{21}(\dot{e})$ represents glucose error rate epinephrine secretion.

We will assume a mean basal plasma epinephrine concentration of 0.5 mμg/mℓ, a distribution volume of fourteen liters, i.e. $V_e = 14\ell.$,

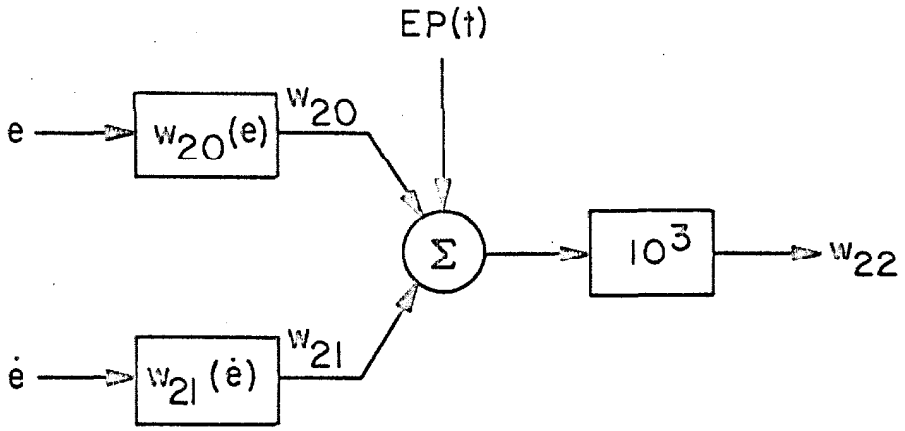

Figure 26. Epinephrine Secretion.

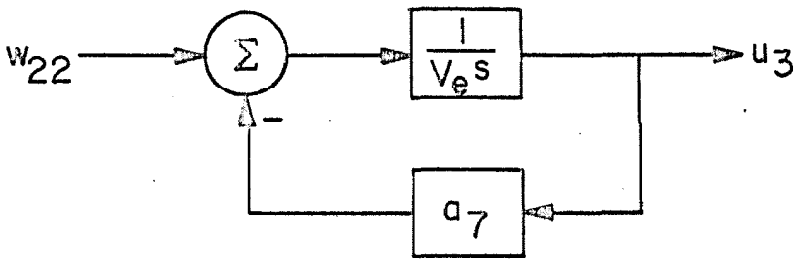

Figure 27. Epinephrine Distribution and Degradation.

and a decay time constant of 0.5 min., i.e. $a_7 = 2.8 \times 10^4$ mℓ/min.

Given the steady-state value of plasma epinephrine, $u_3(ss) =$ 0.5 mμg/mℓ, the required rate of endogenously secreted epinephrine is obtained from:

$$u_3(ss) = \lim_{s \to 0} \left\{ s \left(\frac{1}{V_e s + a_7} \right) \frac{w_{20}(0)}{s} \right\} \qquad (3\text{-}131)$$

hence the nominal rate of epinephrine secretion when the glucose error is zero is $w_{20}(0) = 14$ μg/min.

The secretion of epinephrine as a function of glucose error is expressed by:

$$w_{20}(e) = \frac{d_5}{2} \{1 + \tanh[b_5(e-e_{03})]\} \qquad (3\text{-}132)$$

Parameter values for (3-132) are obtained by considering $w_{20} = 0$ when $e = -10$, $w_{20} = 14$ μg/min when $e = 0$, and $w_{20\ max}$ occurs when $e = 40$. Hence $e_{03} = 15$ and since $w_{20\ max}$ is obtained from (3-131) with $u_3(ss) = 2.5$ mμg/mℓ, or $w_{20\ max} = d_5 = 70$ μg/min, then b_5 is obtained from:

$$b_5 = \frac{1}{15} \tanh^{-1} \left(\frac{35 - 14}{35} \right)$$

$$= .046$$

The error rate epinephrine secretion nonlinearity, $w_{21}(\dot{e})$ where:

$$w_{21}(\dot{e}) = \frac{d_6}{2} \{1 + \tanh[b_6(\dot{e}-\dot{e}_{02})]\} \qquad (3\text{-}133)$$

reflects the belief that a too rapidly falling plasma glucose concentration will cause epinephrine to be secreted even in a hyperglycemic state. However, there doesn't exist any quantitative data upon which a mathematical representation of this effect could be based. Consequently we will choose as a reasonable first guess to have $w_{21}(\dot{e})$ vary from minimum to maximum over the range $\dot{e}$ = 2 mg%/min to $\dot{e}$ = 10 mg%/min with $w_{21\ max} = d_6 = 35$ μg/min. Hence $\dot{e}_{02} = 6$ mg%/min, and for a smooth variation over the range $\dot{e} = [2,10]$, $b_6 = 0.5$.

Since growth hormone has a high molecular weight, 21,500, we should expect at least a two-compartment model to represent its dynamics of distribution and degradation will be required. Random plasma specimens from normal subjects usually exhibit a growth hormone concentration less than 5 mμg/mℓ;[39] we will assume a mean basal growth hormone concentration in plasma of 1 mμg/mℓ. Growth hormone is secreted when plasma glucose is below nominal; a drop of more than 10 mg% below nominal results in a noticeable secretion of growth hormone.[38] During insulin-induced hypoglycemia, with initial values of plasma growth hormone less than 5 mμg/mℓ, this concentration was observed to rise by a factor of five while plasma glucose fell to less than one-half of its initial value.[146] After an insulin input plasma growth hormone rises to its maximum usually in about one hour.[40] This maximum typically is in the vicinity of 50 mμg/mℓ. This response is obtained with an insulin input of 0.1 U/kg which causes an average drop in blood glucose to 34% of its original value. Measurements of plasma growth hormone by the radioimmunoassay method[147] indicate a plasma half-life in adults of twenty to thirty minutes. There is evidence

accumulating that the secretion of growth hormone is under hypothalamic control.[41] It is conjectured that a rapid fall in blood glucose even without hypoglycemia is also capable of stimulating growth hormone release.[44] In this investigation we will view growth hormone secretion strictly as a function of glucose error since the evidence for error rate dependence is somewhat contradictory to other documented evidence on the mode of secretion.

The model shown in Figures 28 and 29 for growth hormone secretion, distribution, and degradation is as follows:

$$\left.\begin{aligned} V_p \dot{u}_{4p} &= - a_8 u_{4p} + a_9(u_{4i}-u_{4p}) + 10^3[GH(t)+w_{30}(e)] \\ V_i \dot{u}_{4i} &= - a_{10} u_{4i} + a_9(u_{4p}-u_{4i}) \end{aligned}\right\} \quad (3\text{-}134)$$

where the endogenous secretion of growth hormone is represented as:

$$w_{30}(e) = \frac{d_7}{2}\{1 + \tanh[b_7(e-e_{04})]\} \quad (3\text{-}135)$$

We will assume a mean basal plasma growth hormone concentration of 1 mμg/mℓ. Based on the observed variation in growth hormone concentrations due to age and sex,[148] this choice of basal concentration applies to young adult males. We will also assume initial guessed values for degradation and diffusion coefficients of:

$$a_8 = 100 \text{ mℓ/min}$$

$$a_9 = 125 \text{ mℓ/min}$$

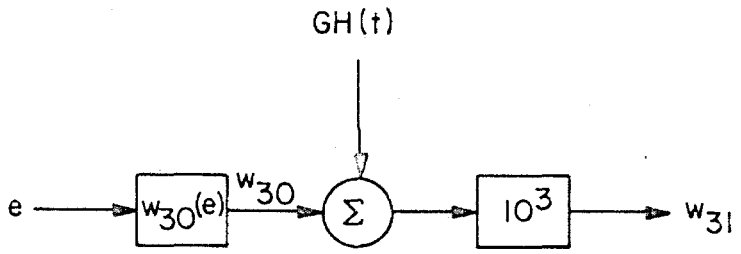

Figure 28. Growth Hormone Secretion.

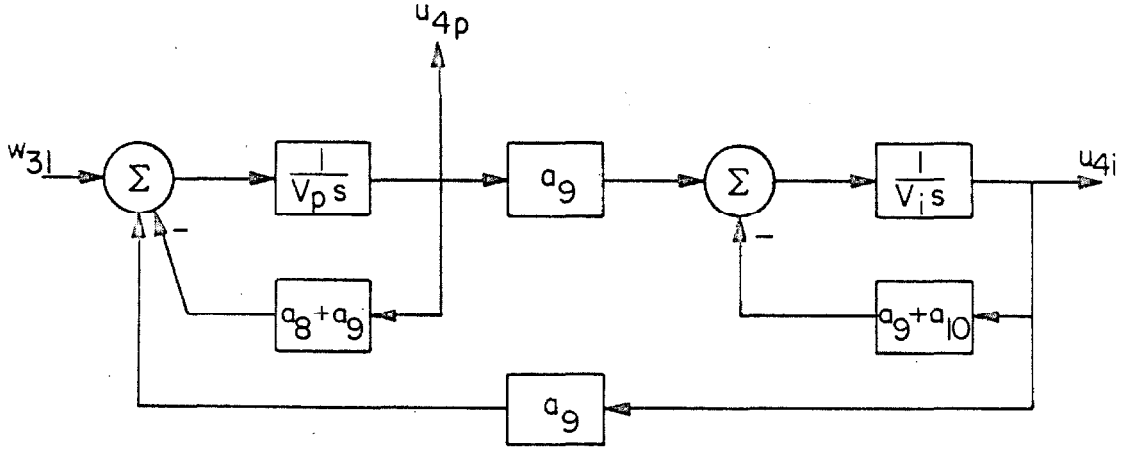

Figure 29. Growth Hormone Distribution and Degradation.

$$a_{10} = 80 \text{ m}\ell/\text{min}$$

These values imply:

$$\tau_p = \frac{V_p}{a_8 + a_9} \tag{3-136}$$

$$= 15.56 \text{ min.}$$

$$\therefore \quad T_{1/2\ p} = 10.78 \text{ min.}$$

$$\tau_i = \frac{V_i}{a_9 + a_{10}} \tag{3-137}$$

$$= 51.2 \text{ min.}$$

$$\therefore \quad T_{1/2\ i} = 35.5 \text{ min.}$$

Given the steady-state concentration of plasma growth hormone, $u_{4p}(ss) = 1$ mμg/mℓ, we compute $u_{4i}(ss)$ and the required rate of endogenous secretion, $w_{30}(ss)$, from (3-134):

$$\left.\begin{aligned} w_{30}(ss) &= 100(1) + 125[1-u_{4i}(ss)] \\ 0 &= -80\, u_{4i}(ss) + 125[1-u_{4i}(ss)] \end{aligned}\right\} \tag{3-138}$$

$$\therefore \quad u_{4i}(ss) = \left(\frac{125}{205}\right) 1$$

$$= 0.61 \text{ m}\mu\text{g/m}\ell$$

$$\therefore \qquad w_{30}(ss) = .149 \ \mu g/min$$

The parameter values for (3-135) are obtained by considering $w_{30} = 0$ when $e = -10$, $w_{30} = .149$ μg/min when $e = 0$, and $w_{30\ max}$ occurs when $e = 70$. We obtain $w_{30\ max}$ from (3-138) with $u_{4p} = 50$ mμg/mℓ.

$$w_{30}(ss) = 100(50) + 125[50 - u_{4i}(ss)]$$

$$0 = -80\ u_{4i}(ss) + 125[50 - u_{4i}(ss)]$$

$$\therefore \qquad u_{4i}(ss) = \left(\frac{125}{205}\right) 50$$

$$= 30.5 \ m\mu g/m\ell$$

Hence $w_{30\ max}$ or $d_7 = 7.5$ μg/min. Now since $e_{04} = 30$, we have:

$$b_7 = \frac{1}{30} \tanh^{-1}\left(\frac{3.75 - .149}{3.75}\right)$$

$$= .065$$

which completely specifies the function (3-135).

Controller Equations.

Referring to Figures 22 through 29 we have:

$$V_p \dot{u}_{1p} = -a_1 u_{1p} + a_2(u_{1i} - u_{1p}) + 10^6\{IN(t) + f_8(u_3)[w_1(e) + w_2(\dot{e})]\}$$

$$
\begin{aligned}
V_i\dot{u}_{1i} &= -a_3u_{1i} + a_2(u_{1p}-u_{1i}) \\
V_p\dot{u}_{2p} &= -a_4u_{2p} + a_5(u_{2i}-u_{2p}) + 10^3[GL(t)+w_{10}(e)] \\
V_i\dot{u}_{2i} &= -a_6u_{2i} + a_5(u_{2p}-u_{2i}) \\
V_e\dot{u}_3 &= -a_7u_3 + 10^3[EP(t)+w_{20}(e)+w_{21}(\dot{e})] \\
V_p\dot{u}_{4p} &= -a_8u_{4p} + a_9(u_{4i}-u_{4p}) + 10^3[GH(t)+w_{30}(e)] \\
V_i\dot{u}_{4i} &= -a_{10}u_{4i} + a_9(u_{4p}-u_{4i})
\end{aligned}
\tag{3-139}
$$

where:

$$
\begin{aligned}
w_1(e) &= \frac{d_1}{2}\{1 - \tanh[b_1(e-e_{01})]\} \\
w_2(\dot{e}) &= \frac{d_2}{2}\{1 - \tanh[b_2(\dot{e}-\dot{e}_{01})]\} \\
f_8(u_3) &= \frac{1}{2}\{1 - \tanh[b_3(u_3-u_{30})]\} \\
w_{10}(e) &= \frac{d_4}{2}\{1 + \tanh[b_4(e-e_{02})]\} \\
w_{20}(e) &= \frac{d_5}{2}\{1 + \tanh[b_5(e-e_{03})]\} \\
w_{21}(\dot{e}) &= \frac{d_6}{2}\{1 + \tanh[b_6(\dot{e}-\dot{e}_{02})]\} \\
w_{30}(e) &= \frac{d_7}{2}\{1 + \tanh[b_7(e-e_{04})]\}
\end{aligned}
\tag{3-140}
$$

Simulation Equations.

$$w_1 = w_1(e)$$

$$w_2 = w_2(\dot{e})$$

$$w_3 = w_1 + w_2$$

$$w_4 = f_8(u_3)\, w_3 \qquad (3\text{-}141)$$

$$w_5 = 10^6[w_4 + IN(t)]$$

$$\dot{u}_{1p} = \frac{1}{V_p}\{- a_1 u_{1p} + a_2(u_{1i}-u_{1p}) + w_5\}$$

$$\dot{u}_{1i} = \frac{1}{V_i}\{- a_3 u_{1i} + a_2(u_{1p}-u_{1i})\}$$

$$w_{10} = w_{10}(e)$$

$$w_{11} = 10^3[w_{10} + GL(t)] \qquad (3\text{-}142)$$

$$\dot{u}_{2p} = \frac{1}{V_p}\{- a_4 u_{2p} + a_5(u_{2i}-u_{2p}) + w_{11}\}$$

$$\dot{u}_{2i} = \frac{1}{V_i}\{- a_6 u_{2i} + a_5(u_{2p}-u_{2i})\}$$

$$w_{20} = w_{20}(e)$$

$$W_{21} = w_{21}(\dot{e})$$

$$w_{22} = 10^3[w_{20} + w_{21} + EP(t)] \qquad (3\text{-}143)$$

$$\dot{u}_3 = \frac{1}{V_e}[- a_7 u_3 + w_{22}]$$

$$w_{30} = w_{30}(e)$$

$$w_{31} = 10^3[w_{30} + GH(t)] \qquad (3\text{-}144)$$

$$\dot{u}_{4p} = \frac{1}{V_p}\{- a_8 u_{4p} + a_9(u_{4i}-u_{4p}) + w_{31}\}$$

$$\dot{u}_{4i} = \frac{1}{V_i}\{- a_{10} u_{4i} + a_9(u_{4p}-u_{4i})\}$$

Definitions of Terms.

$V_p \triangleq [m\ell]$ plasma volume

$V_i \triangleq [m\ell]$ interstitial fluid volume

$V_e \triangleq [m\ell]$ extracellular fluid volume $(V_p + V_i)$

$IN \triangleq [U/min]$ exogenous intravenous insulin input

$GL \triangleq [\mu g/min]$ exogenous intravenous glucagon input

$EP \triangleq [\mu g/min]$ exogenous intravenous epinephrine input

$GH \triangleq [\mu g/min]$ exogenous intravenous growth hormone input

$u_{1p} \triangleq [\mu U/m\ell]$ plasma insulin

$u_{2p} \triangleq [m\mu g/m\ell]$ plasma glucagon

$u_{4p} \triangleq [m\mu g/m\ell]$ plasma growth hormone

$u_{1i} \triangleq [\mu U/m\ell]$ interstitial fluid insulin

$u_{2i} \triangleq [m\mu g/m\ell]$ interstitial fluid glucagon

$u_{4i} \triangleq [m\mu g/m\ell]$ interstitial fluid growth hormone

$u_3 \triangleq [m\mu g/m\ell]$ extracellular fluid epinephrine

$w_1 \triangleq [U/min]$ pancreas insulin release

$w_2 \triangleq [U/min]$ pancreas insulin release

$w_3 \triangleq [U/min]$ total pancreas insulin release

$w_4 \triangleq [U/min]$ effective pancreas insulin release

$w_5 \triangleq [\mu U/min]$ total insulin into plasma space

$w_{10} \triangleq [\mu g/min]$ pancreas glucagon release

$w_{11} \triangleq [m\mu g/min]$ total glucagon into plasma space

$w_{20} \triangleq [\mu g/min]$ adrenal medulla epinephrine release

$w_{21} \triangleq$ [μg/min] adrenal medulla epinephrine release

$w_{22} \triangleq$ [mμg/min] total epinephrine into extracellular space

$w_{30} \triangleq$ [μg/min] anterior pituitary growth hormone release

$w_{31} \triangleq$ [mμg/min] total growth hormone into plasma space

$a_1 \triangleq$ [mℓ/min] plasma insulin degradation coefficient

$a_4 \triangleq$ [mℓ/min] plasma glucagon degradation coefficient

$a_8 \triangleq$ [mℓ/min] plasma growth hormone degradation coefficient

$a_7 \triangleq$ [mℓ/min] extracellular fluid epinephrine degradation coefficient

$a_2 \triangleq$ [mℓ/min] insulin diffusion coefficient

$a_5 \triangleq$ [mℓ/min] glucagon diffusion coefficient

$a_9 \triangleq$ [mℓ/min] growth hormone diffusion coefficient

$a_3 \triangleq$ [mℓ/min] interstitial fluid insulin degradation coefficient

$a_6 \triangleq$ [mℓ/min] interstitial fluid glucagon degradation coefficient

$a_{10} \triangleq$ [mℓ/min] interstitial fluid growth hormone degradation coefficient

$d_1 \triangleq$ [U Insulin/min]

$b_1 \triangleq$ [100 mℓ/mg Glucose]

$e_{01} \triangleq$ [mg Glucose/100 mℓ]

$d_2 \triangleq$ [U Insulin/min]

$b_2 \triangleq$ [100 mℓ/(mg/min) Glucose]

$\dot{e}_{01} \triangleq$ [(mg/min) Glucose/100 mℓ]

$b_3 \triangleq$ [mℓ/mμg Epinephrine]

$u_{30} \triangleq$ [mμg Epinephrine/mℓ]

$d_4 \triangleq$ [μg Glucagon/min]

$b_4 \triangleq$ [100 mℓ/mg Glucose]

$e_{02} \triangleq$ [mg Glucose/100 mℓ]

$d_5 \triangleq$ [μg Epinephrine/min]

$b_5 \triangleq$ [100 mℓ/mg Glucose]

$e_{03} \triangleq$ [mg Glucose/100 mℓ]

$d_6 \triangleq$ [μg Epinephrine/min]

$b_6 \triangleq$ [100 mℓ/(mg/min) Glucose]

$\dot{e}_{02} \triangleq$ [(mg/min) Glucose/100 mℓ]

$d_7 \triangleq$ [μg Growth Hormone/min]

$b_7 \triangleq$ [100 mℓ/mg Glucose]

$e_{04} \triangleq$ [mg Glucose/100 mℓ]

IV. SYSTEMS TECHNIQUES IN THE STUDY OF METABOLIC CONTROL

4.1. Introduction.

In this chapter we formulate and demonstrate the feasibility of an approach to estimate the parameters in the proposed model of Section 3.7.3. The system parameter estimation problem is formulated in terms of a sequence of subsystem parameter estimation problems. These in turn are converted to multi-point boundary value problems and algorithms based on the method of quasilinearization[149] are developed for their solution. Controlled experiments performed by digital computer demonstrate the feasibility of this approach. An algorithm is derived for the complete system identification which is based on the results of subsystem identification. A logical series of physiologic systems experiments is specified from the data requirements of the estimation algorithms. Further applications of systems techniques are considered including the modifications required of the above scheme in order to implement sophisticated closed loop control experiments on the metabolic system.

4.2. The Inverse Problem for Metabolic Control Systems.

Any mathematical representation of a physical system is by necessity an idealization of reality imposed for analytical tractability. To the extent that our basic physical understanding of metabolic processes is sufficient to permit a description in terms of ordinary nonlinear differential equations with certain free parameters, the derivation of an accurate quantitative model constitutes a problem in parameter estimation, the so-called inverse problem.

Using the symbols of Section 3.7.3, the complete system is represented as follows. Here let:

$$f_1(\alpha,x,\beta) \triangleq \frac{1}{2}\{1 + \tanh[\alpha(x-\beta)]\} \tag{4-1}$$

$$f_2(\alpha,x,\beta) \triangleq \frac{1}{2}\{1 - \tanh[\alpha(x-\beta)]\} \tag{4-2}$$

$$e = R - z_1 \tag{4-3}$$

Then the plant equations are:

$$\dot{z}_1 = z_2 \tag{4-4}$$

$$\begin{aligned}\dot{z}_2 = &- \frac{1}{\tau} z_2 + \frac{1}{v_g}\{(d_9+\alpha_1 u_{1p})\, f_2[b_9, f_1(b_8, z_3, c_{g0})e, x_{10}] \\ &- (d_{10}+\alpha_2 u_{2p})\, f_1(b_{10}, e, e_{05}) - (d_{11}+\alpha_3 u_3)\, f_1(b_{11}, e, e_{06}) \\ &- d_{12} f_2(b_{12}, e, e_{07})\, e - (d_{13}+\alpha_4 u_{1i})\, f_2(b_{13}, e, e_{08}) \\ &\quad f_2(b_{14}, u_{4i}, u_{40}) - B + F(t)\}\end{aligned} \tag{4-5}$$

$$\begin{aligned}\dot{z}_3 = (10^{-3})\{&(d_9+\alpha_1 u_{1p})\, f_2[b_9, f_1(b_8, z_3, c_{g0})\, e, x_{10}] \\ &- (d_{10}+\alpha_2 u_{2p}) f_1(b_{10}, e, e_{05}) - (d_{11}+\alpha_3 u_3) f_1(b_{11}, e, e_{06})\}\end{aligned} \tag{4-6}$$

And the controller equations are:

$$\dot{u}_{1p} = \frac{1}{v_p}\{-a_1u_{1p}+a_2(u_{1i}-u_{1p}) + (10^6)\{f_2(b_3,u_3,u_{30})[d_1f_2(b_1,e,e_{01}) + d_2f_2(b_2,\dot{e},\dot{e}_{01})] + IN(t)\} \quad (4\text{-}7)$$

$$\dot{u}_{1i} = \frac{1}{v_i}\{-a_3u_{1i} + a_2(u_{1p}-u_{1i})\} \quad (4\text{-}8)$$

$$\dot{u}_{2p} = \frac{1}{v_p}\{-a_4u_{2p} + a_5(u_{2i}-u_{2p}) + (10^3)[d_4f_1(b_4,e,e_{02}) + GL(t)]\} \quad (4\text{-}9)$$

$$\dot{u}_{2i} = \frac{1}{v_i}\{-a_6u_{2i} + a_5(u_{2p}-u_{2i})\} \quad (4\text{-}10)$$

$$\dot{u}_3 = \frac{1}{v_e}\{-a_7u_3 + (10^3)[d_5f_1(b_5,e,e_{03}) + d_6f_1(b_6,\dot{e},\dot{e}_{02}) + EP(t)]\} \quad (4\text{-}11)$$

$$\dot{u}_{4p} = \frac{1}{v_p}\{-a_8u_{4p} + a_9(u_{4i}-u_{4p}) + (10^3)[d_7f_1(b_7,e,e_{04}) + GH(t)]\} \quad (4\text{-}12)$$

$$\dot{u}_{4i} = \frac{1}{v_i}\{-a_{10}u_{4i} + a_9(u_{4p}-u_{4i})\} \quad (4\text{-}13)$$

Hence the plant model contains twenty-seven free parameters and the controller model contains thirty-three free parameters. The inverse problem then becomes, given a knowledge of the inputs $F(t)$, $IN(t)$, $GL(t)$, $EP(t)$, and $GH(t)$, $0 \le t \le T$, and possibly noisy measurement of $z_1(t)$, $0 \le t \le T$, and samples $u_{1p}(t_i)$, $u_{2p}(t_i)$, $u_3(t_i)$, and $u_{4p}(t_i)$, $0 \le t_i \le T$, obtaining numerical values for the free parameters which results in model behavior which is in some sense a valid representation of the behavior of the actual system.

Estimation techniques have a long history with the ubiquitous method of least-squares for example, dating back to Legendre[150] and Gauss.[151] Common to all such techniques applied to the identification

of unknown systems is the use of input-output data to infer something about the characteristics of the system. Of the many different methods that exist certain broad categorizations are suggested such as sequential and nonsequential schemes, time domain and frequency domain methods, and those applicable only to linear or to both linear and nonlinear systems. Classical frequency domain methods such as impulse response and random response involve the intermediate construction of transfer functions. On the other hand, classical statistical schemes such as least-squares regression, maximum likelihood estimation, and Bayesian estimation require valid statistical representations of measurement errors. Modern computer oriented methods treat the underlying differential equations directly obviating the introduction of restrictive constructions such as transfer functions. But in addition, computer methods are adaptable to other than least-squares criteria such as min-max optimization, and more varied solution approaches such as gradient techniques[152], random search methods,[153,154] and dynamic programming.[155]

The approach we will use is nonsequential, allowing computations to be done off-line, it is applicable to systems of ordinary nonlinear differential equations, it does not require a statistical model of measurement errors, and it uses a least-squares criterion with solutions obtained by a modified quasilinearization method.[156,157]

Let the system be described by:

$$\dot{x} = g(t,x,\alpha,u) \quad ; \quad x(0) = x_0 \tag{4-14}$$

where:

x is an $n \times 1$ state vector

g is an $n \times 1$ vector function differentiable with respect to x and α

α is an $r \times 1$ parameter vector

u is an $m \times 1$ input vector

Let the observations upon the system be described by:

$$y(t) = H(t)\, x(t) + \eta \tag{4-15}$$

where:

y is a $q \times 1$ output vector

H is a $q \times n$ known matrix

η is a $q \times 1$ random vector representing measurement error about which no specific statistical form will be assumed

Suppose a least-squares criterion is used to fit the model output to the observed data. Define the residual error:

$$\epsilon(t) = y(t) - H(t)\, \hat{x}(t) \tag{4-16}$$

where $\hat{x}(t)$ represents the solution of (4-14) with an estimated parameter vector $\hat{\alpha}$ and initial conditions $\hat{x}(0)$. If N observations are available at discrete instants of time then:

$$\sum_{i=1}^{N} \|\epsilon(t_i)\|_{Q_i}^2 = \sum_{i=1}^{N} \|y(t_i) - H(t_i)\, \hat{x}(t_i)\|_{Q_i}^2 \tag{4-17}$$

$$= \sum_{i=1}^{N} \langle y(t_i)-H(t_i)\hat{x}(t_i), Q_i[y(t_i)-H(t_i)\hat{x}(t_i)]\rangle$$

The weighting matrix Q_i is positive semi-definite. In the controlled experiments of 4.3 this matrix is taken as the identity matrix.

The problem of finding a least-squares estimate of the parameter vector α, given:

$$\dot{x} = g(t,x,\alpha,u) \quad , \quad x(0) = x_0$$

$$u(t) \quad ; \quad 0 \leq t \leq T$$

$$y(t_i) = H(t_i)\, x(t_i) + \eta$$

is then equivalent to minimizing (4-17) with respect to α.

The problem of simultaneously determining all the free parameters in Eqs.(4-4) through (4-13) is a formidable task. However a method is suggested which takes advantage of the structure and function of the system. It is possible by suitable choices of inputs and observations to isolate independent subsystems within the overall system. By designing several experiments and using the data in a specific order a hierarchy of subsystem parameter estimation will be established which will result in full identification of all the system parameters. For each subsystem parameter estimation problem the input is specified as a continuous function of time over the duration of the experiment. For observations we assume continuous measurement of plasma glucose concentration and discrete samples of the plasma concentration of the four hormones included in the controller. Since in all cases, observations

will be made on only a subset of the states in any particular subsystem, the parameter estimation problem constitutes a multi-point boundary value problem.

Suppose, for example, that $N > n + r$ noisy measurements are made on x_1, the first component of x, i.e. we have $y(t_i)$, $i = 1, 2, \cdots, N$.

$$y(t_i) = x_1(t_i) + \eta$$

The remaining n-1 initial conditions on x, $x_2(0), \cdots, x_n(0)$ and the constant parameter vector α, must be determined such that the trajectory resulting from the solution of (4-14) with these values satisfies the remaining N-1 measured values of $x_1(t)$. This is precisely formulated as a multi-point boundary value problem by adjoining the constant parameter vector α, to the Eq.(4-14). Let:

$$\dot{\alpha} \triangleq 0 \tag{4-18}$$

$$z \triangleq \begin{Bmatrix} x \\ \alpha \end{Bmatrix} \tag{4-19}$$

$$f \triangleq \begin{Bmatrix} g \\ 0 \end{Bmatrix} \tag{4-20}$$

then the MPBVP is, given $N > n + r$ noisy measurements on $z_1(t) = x_1(t)$, determine the remaining $n + r - 1$ initial conditions on $z(0)$ such that the solution of

$$\dot{z} = f(t, z, u) \tag{4-21}$$

approximates the remaining N-1 measured values of $z_1(t)$ in a least-squares sense.

This problem will be solved by a generalized root finding technique, the Newton-Raphson-Kantarovich method. An analysis of the existence, uniqueness, and convergence properties of the method is given by Kalaba[158] who shows for example, that when the method converges it does so quadratically. For computer applications this is the chief advantage of the method compared with other schemes such as Picard successive approximation which exhibits first order convergence. The Newton-Raphson-Kantarovich method converts the nonlinear multipoint boundary value problem:

$$\left.\begin{aligned} \dot{z} &= f(t, z, u) \\ z(t_i) &= y(t_i) \quad , \quad i = 1, 2, \cdots, N \end{aligned}\right\} \tag{4-22}$$

to a sequence of linear multi-point boundary value problems which are solved recursively.

Let iterations be denoted by k, then expanding (4-21) in the space of functions $z(t)$, $0 \le t \le T$ and retaining terms to first order:

$$\dot{z}^{k+1} = f(t, z^k, u) + \left(\frac{\partial f}{\partial z}\right)\Big|_{z=z^k} (z^{k+1} - z^k) \tag{4-23}$$

where the Jacobian matrix has the ij term $(\partial f_i/\partial z_j)$. The solution of (4-23) must satisfy the boundary conditions $z_1^{k+1}(t_i) = x_1(t_i)$, $i = 1, 2, \cdots, N$ in a least-squares sense. Since (4-23) is a linear differential equation in the variable z^{k+1} we have the general solution by superposition:

$$z^{k+1}(t) = \Phi^{k+1}(t)\,\beta^{k+1} + p^{k+1}(t) \tag{4-24}$$

where $\Phi^{k+1}(t)$ satisfies the matrix differential equation:

$$\dot{\Phi}^{k+1}(t) = \left(\frac{\partial f}{\partial z}\right)\Big|_{z=z^k} \Phi^{k+1}(t) \tag{4-25}$$

made unique by the initial condition, for example:

$$\Phi^{k+1}(0) = I \tag{4-26}$$

and $p^{k+1}(t)$ is the solution of the nonhomogeneous equation:

$$\dot{p}^{k+1}(t) = f(t, z^k, u) + \left(\frac{\partial f}{\partial z}\right)\Big|_{z=z^k}(p^{k+1}(t) - z^k(t)) \tag{4-27}$$

made unique by,

$$p^{k+1}(0) = 0 \tag{4-28}$$

In Eq.(4-24), β^{k+1} is an $(n+r) \times 1$ constant vector selected in such a way that the solution of (4-23) satisfies the appropriate boundary

conditions. In the case of $N = n + r$ exact observations, β^{k+1} is obtained by solving a system of $n + r$ linear algebraic equations. With $N > n + r$ noisy observations, $y(t_i)$, $i = 1, 2, \cdots, N$, $z^{k+1}(t)$ is made to approximate the data in a least squares sense by minimizing

$$\sum_{i=1}^{N} \|G(t_i)\, z^{k+1}(t_i) - y(t_i)\|_I^2 = \sum_{i=1}^{N} \|G(t_i)[\Phi^{k+1}(t_i)\, \beta^{k+1} + p^{k+1}(t_i)] - y(t_i)\|_I^2 \qquad (4\text{-}29)$$

with respect to β^{k+1}. Here $G(t_i)$ is a $q \times (n+r)$ matrix with the first n columns identical to $H(t_i)$ and the remaining r columns identically zero. Differentiating (4-29) with respect to the $n+r$ components of β^{k+1} results in an $n+r$ linear algebraic system to be solved for β^{k+1}.

$$A^{k+1}\, \beta^{k+1} = b^{k+1} \qquad (4\text{-}30)$$

where:

$$A^{k+1} = \sum_{i=1}^{N} \Phi'^{k+1}(t_i)\, G'(t_i)\, G(t_i)\, \Phi^{k+1}(t_i) \qquad (4\text{-}31)$$

$$b^{k+1} = \sum_{i=1}^{N} \Phi'^{k+1}(t_i)\, G'(t_i)[y(t_i) - G(t_i) p^{k+1}(t_i)] \qquad (4\text{-}32)$$

where primes denote the matrix transpose.

The computational algorithm proceeds as follows:

1. Select a zeroth iteration $z^{o}(t)$, either by specifying a complete vector function over the time interval of interest, $0 \le t \le T$, or by specifying a vector initial condition $z^{o}(0)$ and integrating (4-21) to obtain $z^{o}(t)$, $0 \le t \le T$.
2. Using $z^{o}(t)$, $0 \le t \le T$, solve (4-25) for $\Phi^{1}(t)$, $0 \le t \le T$ and (4-27) for $p^{1}(t)$, $0 \le t \le T$.
3. With these results and the appropriate data, $y(t_i)$, $i = 1, 2, \cdots, N$, solve (4-30) for β^{1}.
4. Obtain $z^{1}(t)$, $0 \le t \le T$ from (4-24).
5. Repeat steps 2. through 4. for as many iterations as desired or until an appropriate convergence criterion is satisfied.

The above procedure requires the storage of the matrix $\Phi^{k+1}(t)$ and the vector $p^{k+1}(t)$ over the time interval of interest at points determined by the size of the integration interval. For large problems or where a very small step size is required for numerical stability, this approach can easily exhaust the core storage capability of even the most modern large digital computers. In such cases an alternate approach which requires more computation time can be used. After β^{k+1}, the new estimate for the initial conditions, has been obtained the following systems of equations are solved simultaneously:

$$\dot{\Phi}^{k+1}(t) = \left(\frac{\partial f}{\partial z}\right)\Big|_{z=z^{k}} \Phi^{k+1}(t) \quad ; \quad \Phi^{k+1}(0) = I \qquad (4\text{-}33)$$

$$\dot{p}^{k+1}(t) = f(t, z^{k}, u) + \left(\frac{\partial f}{\partial z}\right)\Big|_{z=z^{k}} (p^{k+1}(t) - z^{k}(t)) \quad ;$$

$$p^{k+1}(0) = 0 \qquad (4\text{-}34)$$

$$\dot{z}^{k+1} = f(t, z^{k+1}, u) \quad ; \quad z^{k+1}(0) = \beta^{k+1} \tag{4-35}$$

Hence the fundamental matrix and particular solution need be stored only at the points of observation, t_i, for Eq.(4-30) and in addition a variable step size integration algorithm can be used to solve (4-33), (4-34), and (4-35) ensuring numerical stability. In the sequel, results obtained by both methods will be reported.

It would appear from the above that in general $(n+r)^2 + 2(n+r)$ differential equations must be solved simultaneously along with an $n+r$ algebraic system at each iteration. However, with an r-dimensional constant parameter vector, the last r rows of the fundamental matrix and particular solution vector have the trivial solutions 0 or 1. Introducing the consequent simplifications in the remaining nontrivial equations results in a system of $2n + n(n+r)$ differential equations to be solved for each iteration, a reduction of $2r + r(n+r)$ equations.

Section 4.3 contains the results of "controlled experiments" in parameter estimation performed upon the proposed glucose regulation system model. For this purpose reasonable numerical values are substituted in the Eqs.(4-4) through (4-13) to generate "ideal" system behavior. Observations are then deliberately corrupted to simulate laboratory measurement errors and the resultant "data" along with "guessed" values of the parameters of interest are introduced in the parameter estimation algorithms. The object is to demonstrate the feasibility of the approach for this class of problems and to specify the data which will be required to use the scheme to obtain numerical

values for the proposed model which represents the specific normal subject upon whom the experiments have been performed.

Equation (4-15) represents system observations. The noise model used in the controlled experiments is as follows:

$$\eta(t_i) = P_1 R_1(t_i)|z_1(t_i)| + P_2 R_2(t_i) \qquad (4\text{-}36)$$

where, for example, z_1 is the state variable measured, R_1 and R_2 are statistically independent uniformly distributed random variables in the range $[-0.5, 0.5]$, and P_1 and P_2 are constant coefficients, $0 \leq P_1, P_2 \leq 1$. For example if $P_1 = 0.2$, when $z_1 = 100$ the maximum possible error is $\pm$ 10%; for small values of the measured variable the second term in (4-36) dominates. In the results to be reported, the phrase "10% noise" implies that $P_1 = P_2 = 0.2$ in Eq.(4-36).

The numerical algorithm used to solve the required differential equations consists of an Adams-Moulton predictor-corrector formula with the method of Runge-Kutta-Gill used to start the integration. Variable step-size capability is an integral part of the method to automatically control truncation error, and double precision computation is incorporated where appropriate to control round-off error. The numerical algorithm used to solve the algebraic system, (4-30), consists of Gaussian elimination with iterative improvement and accuracy controlled by a tolerance setting and a limitation on the maximum number of forward and backward passes.

4.3. Algorithms for Subsystem Parameters Estimation.

Five core algorithms have been developed to identify parameters in five representative subsystems of the overall model of Section 3.7.3. The underlying idea of the subsystem approach to the identification problem is that experiments can be performed which excite only portions of the overall system thereby uncoupling loops and allowing specific portions of the system to be treated independently. For example, referring to Figures 22 and 23, which depict the model for insulin generation and subsequent distribution and degradation, an intravenous infusion of insulin $IN(t)$, causes a hypoglycemic response which results in an uncoupling of insulin secretion dynamics from insulin distribution and degradation dynamics. Therefore given an input $IN(t)$, $0 \leq t \leq T$ and sampled measurements on u_{1p}, i.e. $u_{1p}(t_i)$, $i = 1, 2, \cdots, N$, the estimation algorithm can focus exclusively on the parameters v_p, v_i, a_1, a_2, a_3. Then fixing these parameters and specifying $e(t)$, $0 \leq t \leq T$ which would result from an infusion of glucose $F(t)$, $0 \leq t \leq T$, allows us to identify the parameters of the secretion dynamics. Although some details may differ from subsystem to subsystem the above constitute the essential ingredients of the approach.

It was found that five basic subsystem parameter estimation algorithms will suffice to identify all of the parameters of the proposed model from systems experiments which are feasible on human subjects and data which are obtainable. The manner in which the subsystem algorithms must be used is indicated in Section 4.5. The required systems experiments are presented in Section 4.4.

Algorithms A through D are applicable to estimating the parameters of the controller while algorithm E applies to plant subsystem identification. In all cases the total simulated system time was $T = 100$ min. In each case the detailed estimator algorithm equations are given in Appendix E.

A. One Compartment Distribution Dynamics.

$$\text{Model:} \qquad \dot{x} = -k_2 x + k_1 h(t) \quad ; \quad x(0) = x_0 \tag{4-37}$$

$$\text{Input:} \qquad h(t) \quad ; \quad 0 \le t \le T \tag{4-38}$$

$$\text{Observations:} \qquad y(t_i) = x(t_i) + \eta \tag{4-39}$$

$$\text{Estimate:} \qquad k_1,\ k_2$$

If this model represented one compartment dynamics for insulin, for example, then representative values for the parameters might be $k_1 = 70$ representing approximately a 14 ℓ. distribution space, and $k_2 = .07$ representing a disappearance time constant of approximately 14 minutes. The initial condition used was $x(0) = 10\ \mu U/m\ell + \eta$. The input used in this instance was:

$$h(t) = \begin{cases} 1 \ \text{U/min} & , \quad 0 \le t \le 5 \ \text{min} \\ 0 & , \quad t > 5 \ \text{min} \end{cases} \tag{4-40}$$

These numerical values were used to generate the true trajectory of (4-37) which was then corrupted as in (4-36) to represent the "observations".

The behavior of the estimator is depicted in Figure 30. In all cases the estimated value of the parameter is given as a function of

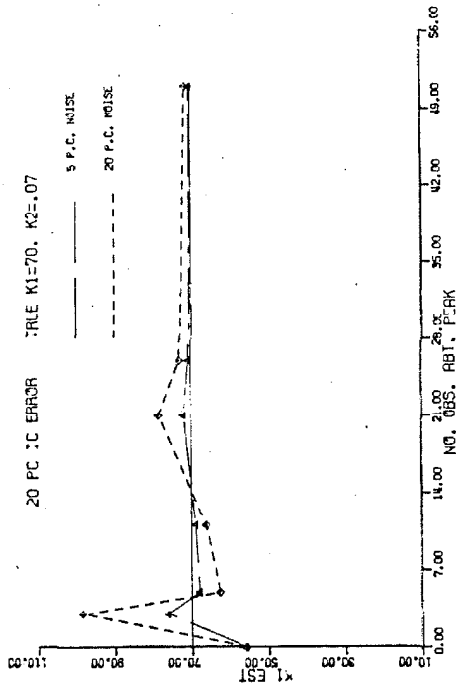

Figure 30-2.

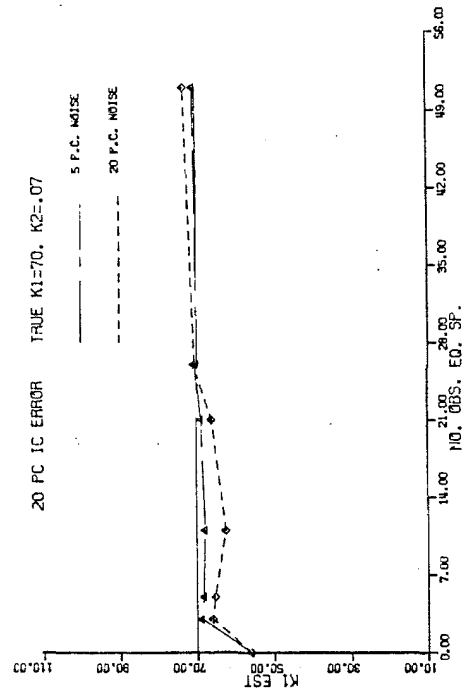

Figure 30-1.

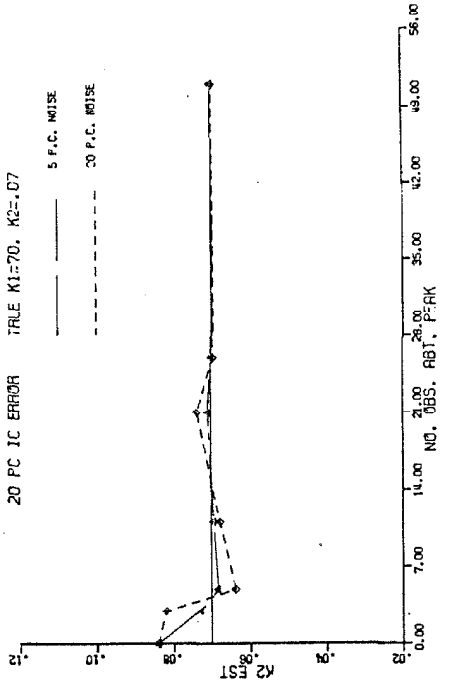

Figure 30-4.

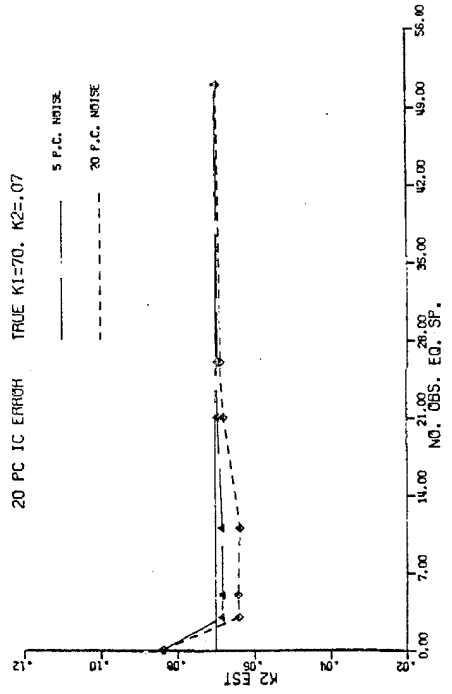

Figure 30-3.

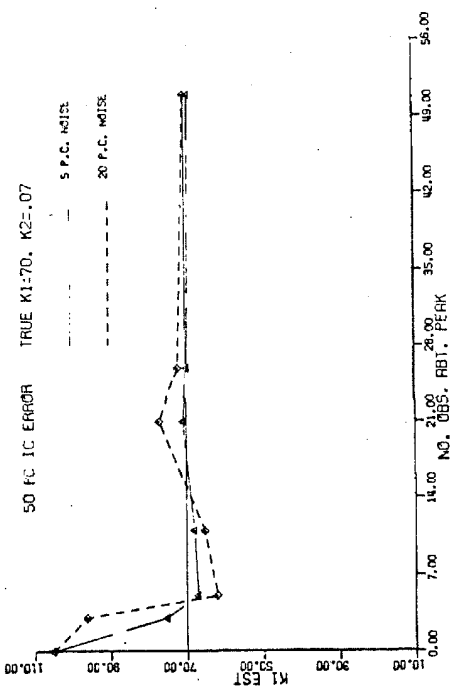

Figure 30-6.

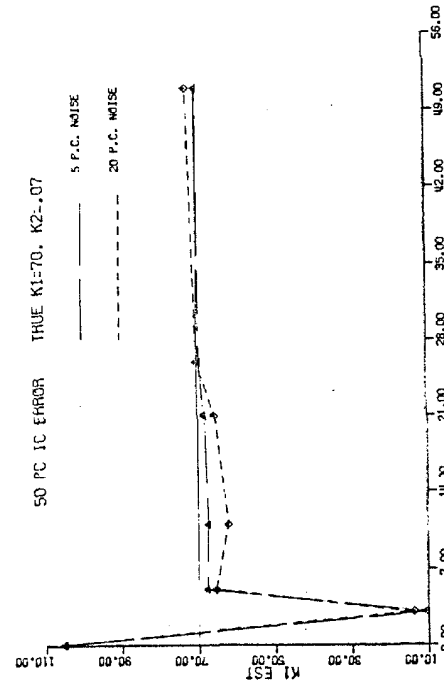

Figure 30-5.

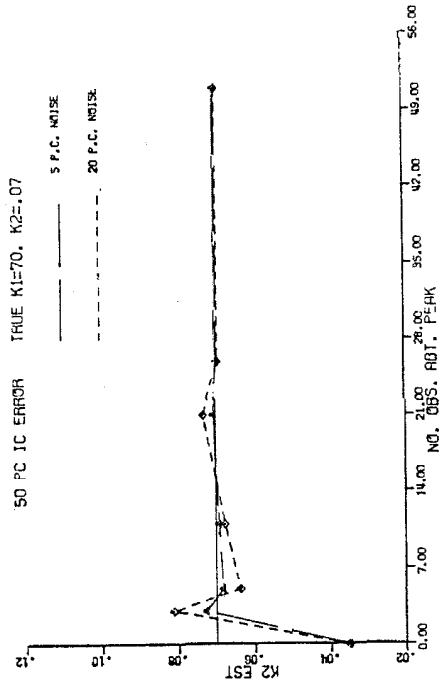

Figure 30-8.

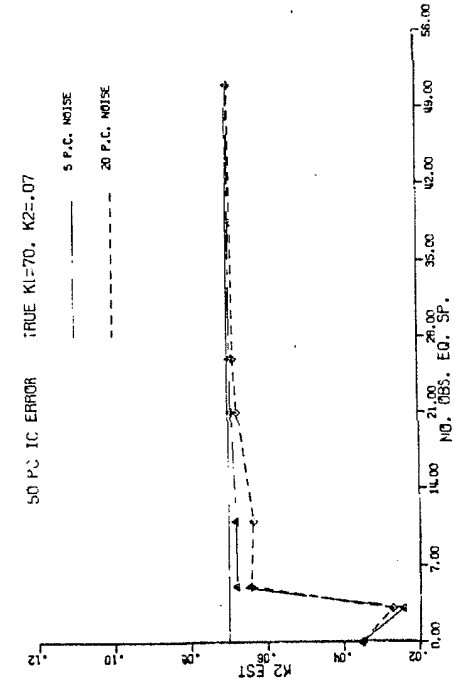

Figure 30-7.

the number of observations. Results are shown for initial guesses of parameters deviating 20% and 50% from the true values, with 5% and 20% observational noise. In addition observations were either equally spaced, Figure 30-1,3,5, and 7 or clustered about the peak in the response, Figures 30-2,4,6, and 8. The results show that only five sample points result in a reasonable estimate of the parameters even with 20% noise on the observations and an initial guess which is 50% in error! The important characteristic of all these results is the pattern of improved estimates as more observations are included. Other combinations of initial guesses and other random noise samples led to substantially the same pattern of results. For each observation set, the estimated parameter value is that resulting from three iterations of the algorithm.

Although the feasibility of the algorithm was demonstrated with numerical values representative of insulin dynamics, the method is applicable to any other hormone of interest with numerical values and dimensions modified accordingly.

Much effort has been expended in biological laboratories to develop techniques for estimating parameters such as biological decay constants by means of radioactive tracer injection. These methods are much more time consuming and demanding of investigative expertise than the experiment required to implement the above scheme. In this case an intravenous infusion of insulin is administered over five minutes and five or more plasma insulin samples are taken over a period of 100 minutes. This total time period is not a fixed quantity, but could be reduced to something more convenient experimentally with no substantial

change to the estimator algorithm. The indications are that present knowledge of the required parameters for "initial guesses" and hormone assay techniques are well within the level of accuracy demonstrated to be sufficient for convergence of the algorithm in Figure 30.

B. Two Compartment Distribution Dynamics.

Model:
$$\dot{x}_1 = (1/v_1)[-a_1x_1+a_2(x_2-x_1) + h(t)]$$
$$\dot{x}_2 = (1/v_2)[-a_3x_2+a_2(x_1-x_2)] \qquad (4\text{-}41)$$

Input:
$$h(t) \quad , \quad 0 \le t \le T \qquad (4\text{-}42)$$

Observations:
$$y(t_i) = x_1(t_i) + \eta \qquad (4\text{-}43)$$

or:

$$\left.\begin{aligned} y_1(t_i) &= x_1(t_i) + \eta_1 \\ y_2(t_i) &= x_2(t_i) + \eta_2 \end{aligned}\right\} \qquad (4\text{-}44)$$

Estimate:
$$a_1, \ a_2, \ a_3$$

If this model represented two-compartment dynamics for insulin, for example, then true parameter values (as derived in Section 3.7.3.2) might be $v_1 = 3.5$ ℓ. the plasma space, $v_2 = 10.5$ ℓ. the interstitial fluid space, $a_1 = 248$ mℓ/min the plasma space disappearance coefficient, $a_2 = 309$ mℓ/min the diffusion coefficient, and $a_3 = 156$ the interstitial fluid disappearance coefficient. Typical initial conditions are $x_1(0) = 21$ μU/mℓ + η , $x_2(0) = 14$ μU/mℓ + η. The input used in this case was:

$$h(t) = \begin{cases} 1 \text{ U/min} & , \quad 0 \le t \le 5 \text{ min} \\ 0 & , \quad t > 5 \text{ min} \end{cases} \tag{4-45}$$

These numerical values were used to generate the true trajectories of (4-41).

The operation of the estimator for observations assumed only on x_1, the plasma concentration of the hormone, is illustrated in Figures 31-1, 3, 5, 7, 9, and 11. Results are shown for initial parameter guesses deviating 20% and 50% from the true values, with 2% and 5% measurement error on x_1. The indications are that approximately 25 samples suffice to obtain reasonable parameter estimates under the experimental conditions simulated.

It should be emphasized here that although this algorithm is no more difficult to use than the one-compartment algorithm the advantage over classical methods of estimating these parameters is more dramatic. The variable x_2 is not directly observable and values for the parameters a_2 and a_3 can only be conjectured from indirect evidence.

However, in the event that techniques such as lymphatic cannulation are perfected to allow a measurement of x_2, interstitial fluid hormone concentration, the operation of the estimator can be markedly improved. Figures 31-2, 4, 6, 8, 10, and 12 display the results obtained assuming observations on both x_1 and x_2. Although the same initial guess errors have been assumed, the algorithm displays much better properties even with 20% measurement noise on both x_1 and x_2! Here about five measurements of both x_1 and x_2 are sufficient to obtain close estimates when 5% measurement error is assumed compared with about 25

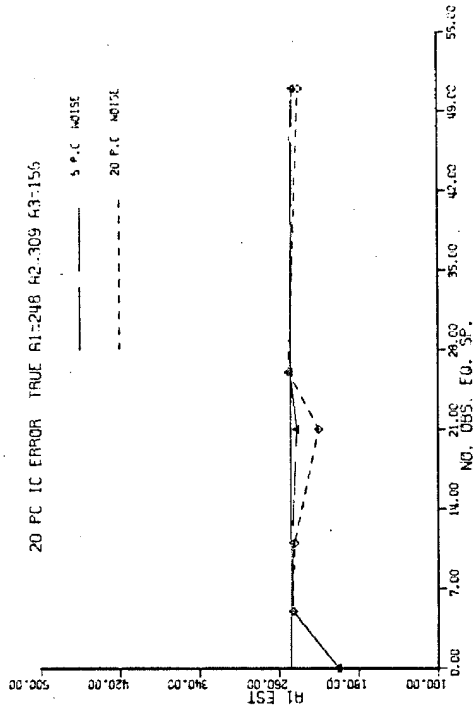

Figure 31-2.

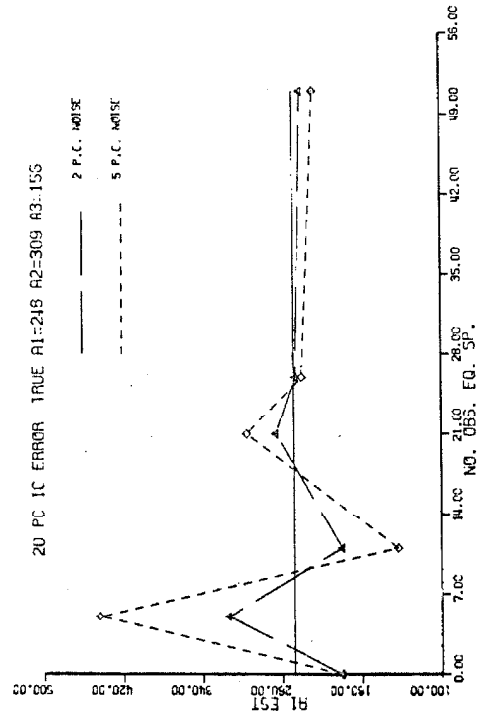

Figure 31-1.

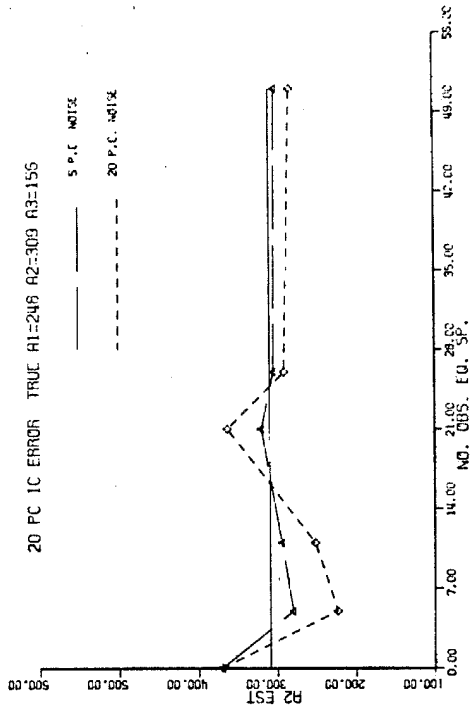

Figure 31-4.

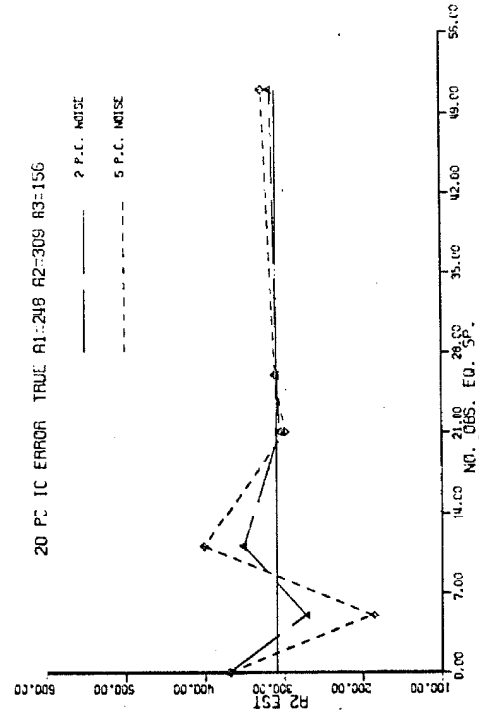

Figure 31-3.

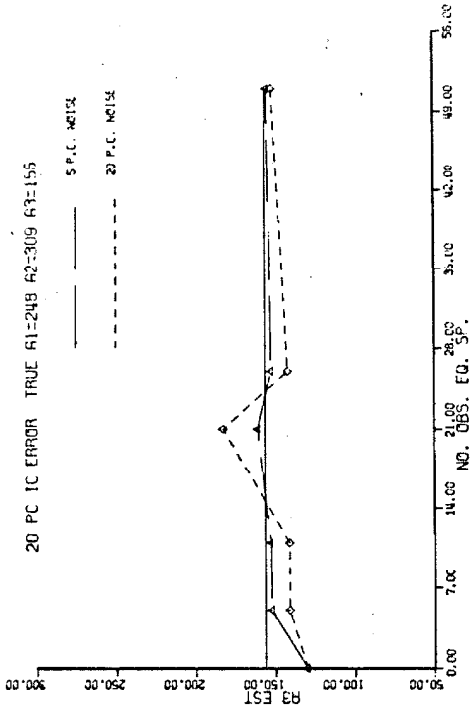

Figure 31-6.

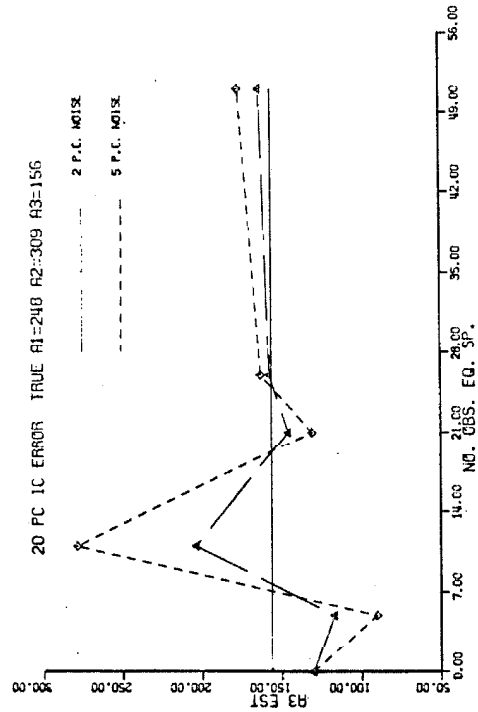

Figure 31-5.

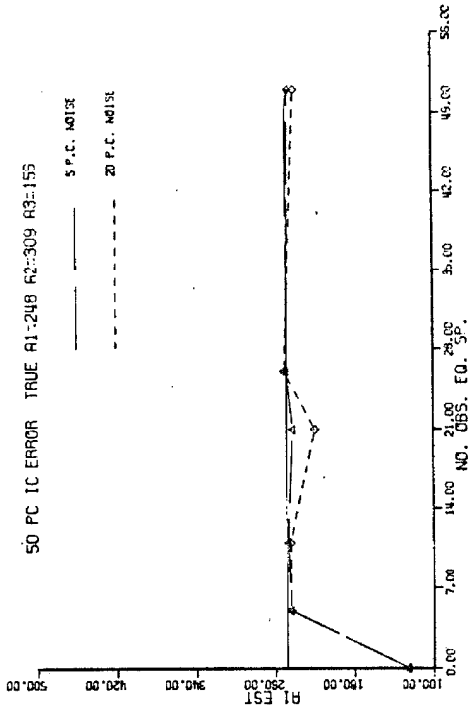

Figure 31-8.

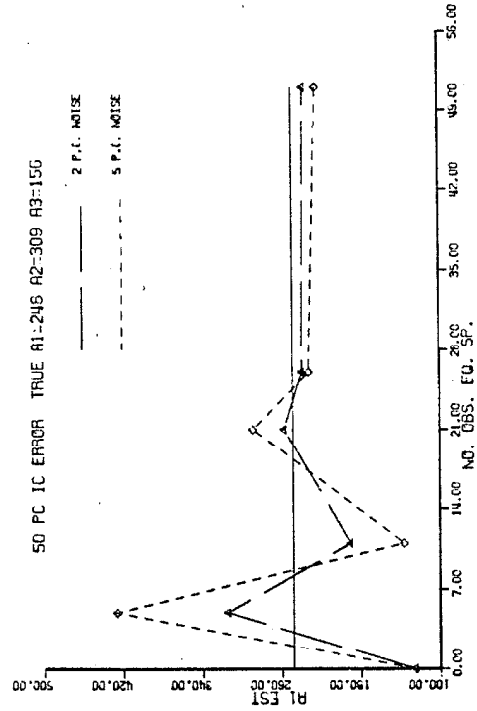

Figure 31-7.

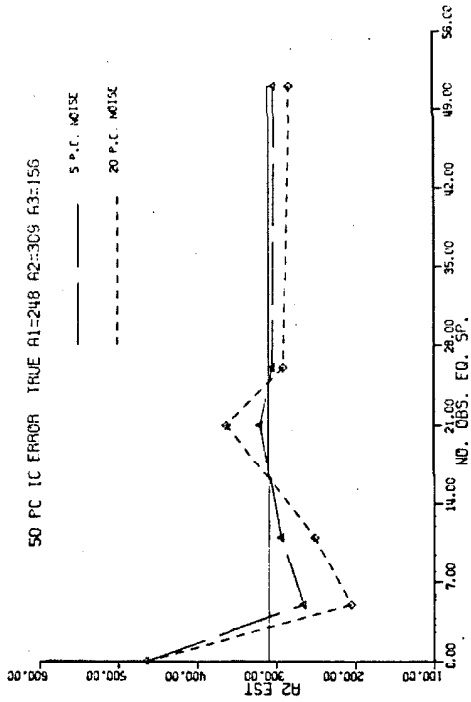

Figure 31-9.

Figure 31-10.

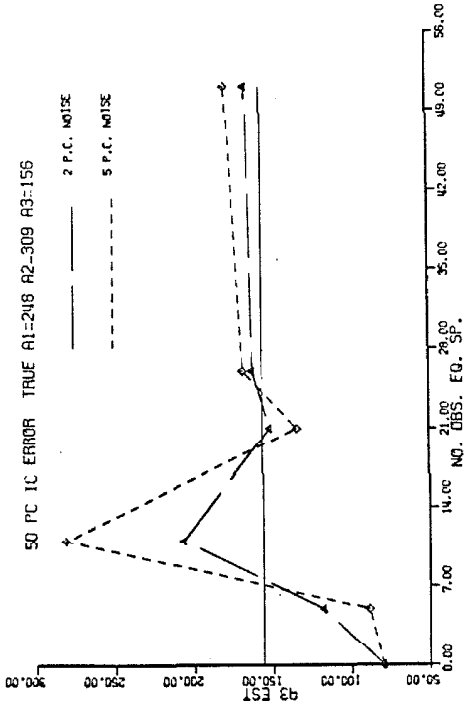

Figure 31-11.

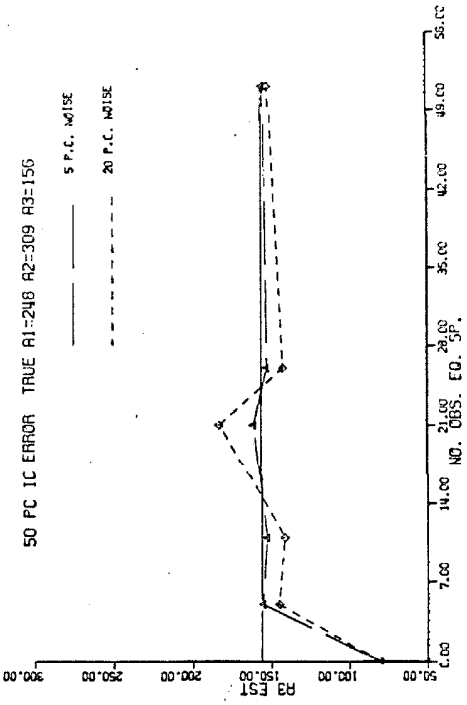

Figure 31-12.

samples required when only x_1 is observable.

It might be asked at this point why the parameters v_1, the plasma compartment volume and v_2, the interstitial fluid compartment volume were assumed known? Reiterating the modeling point of view carefully developed in Chapter 3, these distribution volumes are viewed as mechanical properties of the system and such phenomena as the entry of glucose into intracellular spaces is considered not as an enlargement of the distribution space, but as an active biochemical removal mechansim from the viewpoint of the interstitial fluid volume. The results of numerous biological investigations have fixed these parameter values with far more accuracy than any other parameter in the system under study. For example, for a 70 kg. young adult male the plasma volume is 3.5 ℓ. exclusive of red blood cell volume, and the interstitial fluid volume is 10.5 ℓ. These values vary with age and sex but those variations are well documented statistically. Accordingly, in this investigation the above numerical values are assumed as well as v_g = 17.5 ℓ. for the mechanical distribution volume of glucose which includes plasma, interstitial fluid, and red blood cell volumes. On the other hand, when a one-compartment distribution model is assumed, as is the case for epinephrine in Section 3.7.3.2, the distribution volume cannot be assumed known since it is an artificially which has to represent in a lumped fashion plasma volume, interstitial fluid volume, and the diffusion process connecting these two compartments. Accordingly, in Algorithm A both the distribution space parameter and the disappearance coefficient parameter are required to be estimated from experimental data.

C. Error Proportional Saturating Nonlinearity.

Model: $$\dot{x} = - k_2 x + k_1 \frac{\alpha}{2} \{1 + \tanh[\beta(c-\gamma)]\} \quad (4\text{-}46)$$

Input: $$c(t) \quad ; \quad 0 \leq t \leq T \quad (4\text{-}47)$$

Observations: $$y(t_i) = x(t_i) + \eta \quad (4\text{-}48)$$

Estimate: α, β, γ

Equation (4-46), for example, might represent the secretion of insulin as a function of plasma glucose concentration, $c(t)$, into a one-compartment distribution volume. The choice of one or two-compartment distribution dynamics is irrelevant to the operation of the estimator for secretion dynamics since in either case the parameters are assumed known, having been determined through the use of either Algorithm A or B.

To simulate the hyperglycemic response which would be expected from an intravenous infusion of glucose of approximately 15 grams over 5 minutes, the following function was used for $c(t)$:

$$c(t) = 400 \, (e^{-t/10} - e^{-t/5}) \quad (4\text{-}49)$$

Fixed parameter values assumed were $k_1 = 70$, $k_2 = .07$, and the true trajectory was generated with variable parameter values $\alpha = 0.5$, $\beta = .078$, and $\gamma = 25$. The initial condition on (4-46) was taken to be $x(0) = 10 \ \mu U/m\ell + \eta$.

The estimator algorithm results are displayed in Figures 32-1, 3, 5, 7, 9, and 11 for equally spaced observations over [0,100] minutes

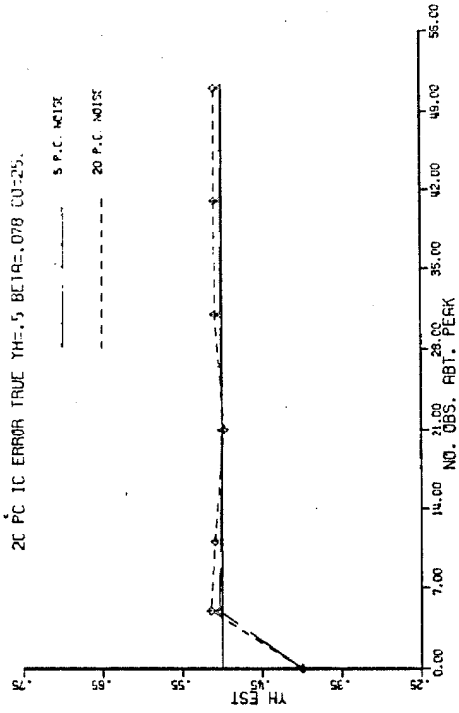

Figure 32-2.

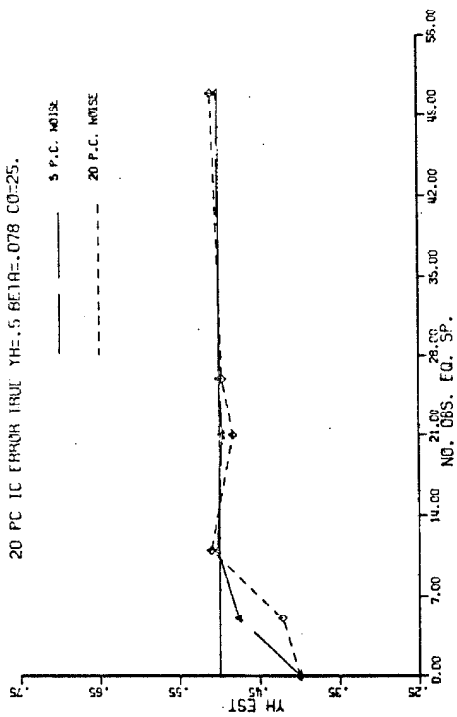

Figure 32-1.

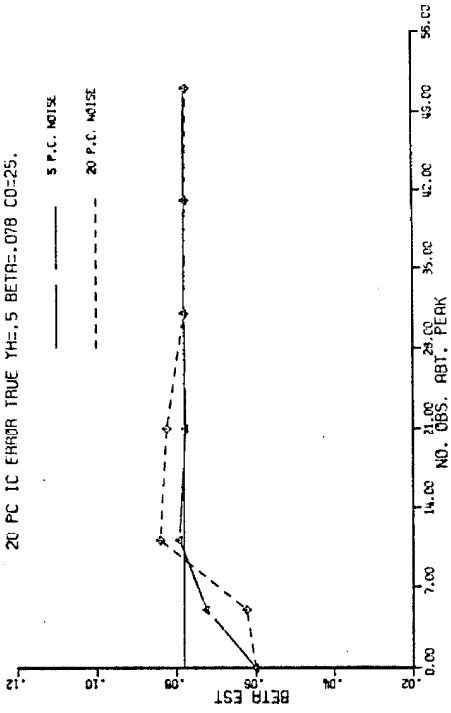

Figure 32-4.

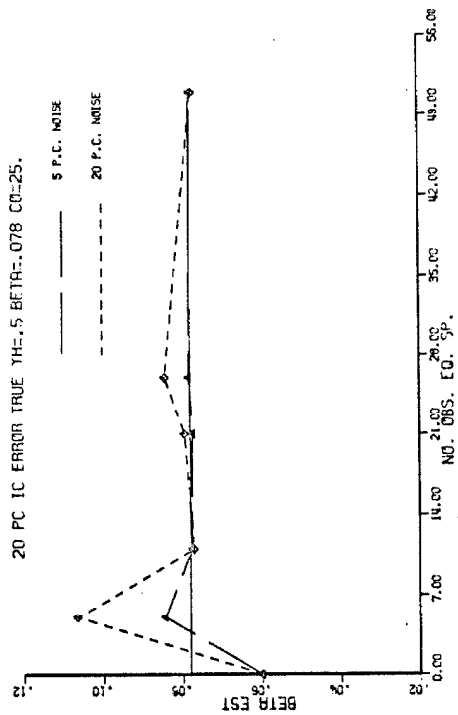

Figure 32-3.

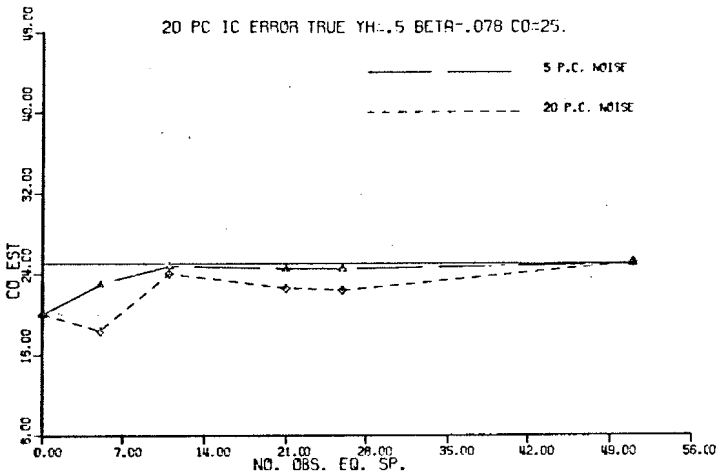

Figure 32-5.

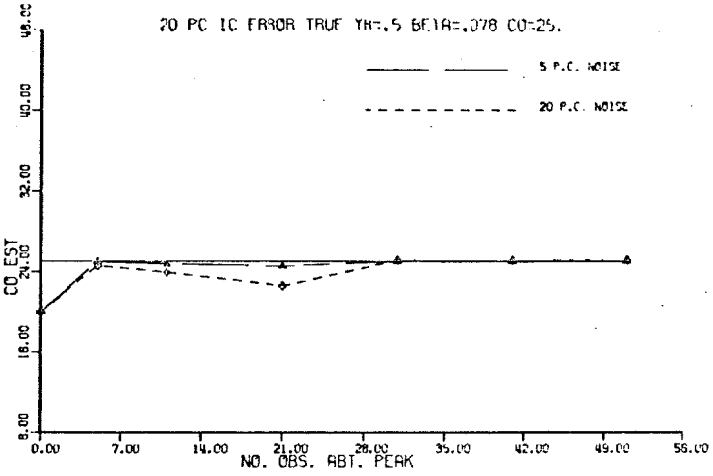

Figure 32-6.

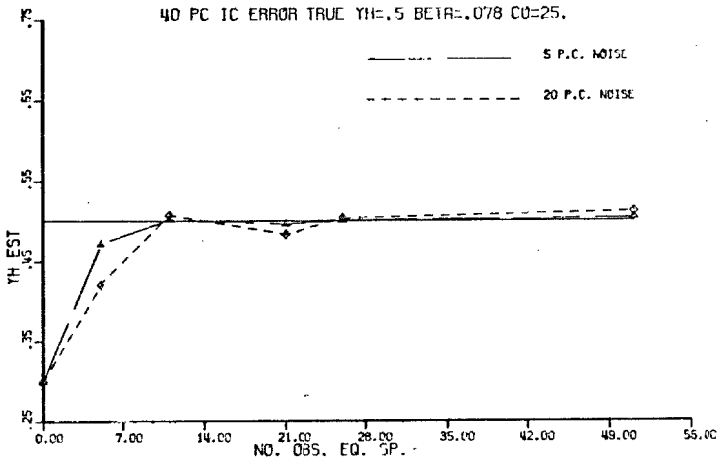

Figure 32-7.

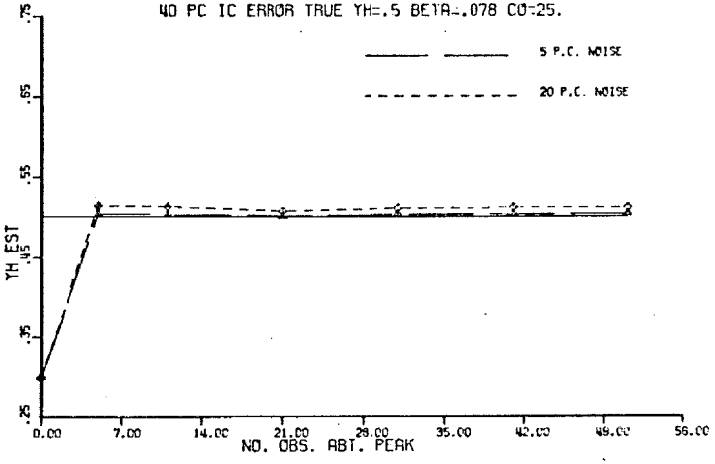

Figure 32-8.

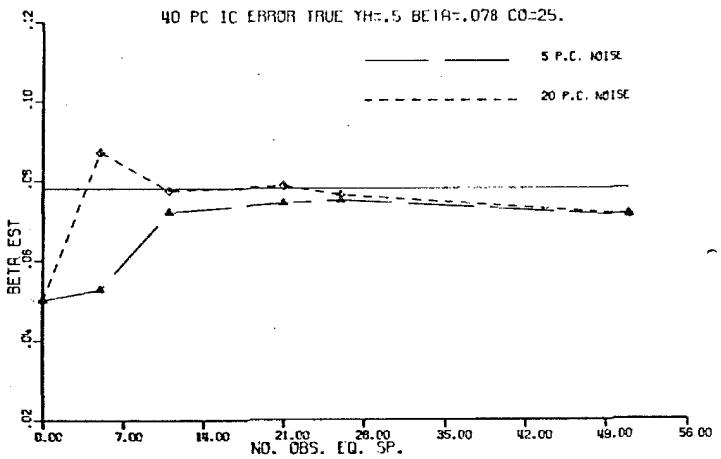

Figure 32-9.

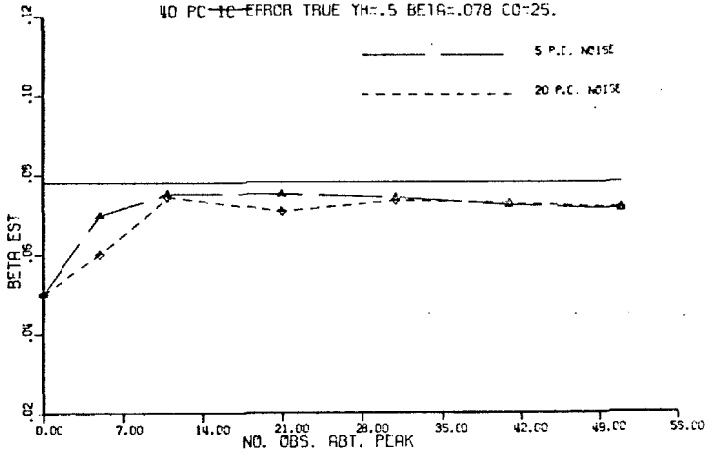

Figure 32-10.

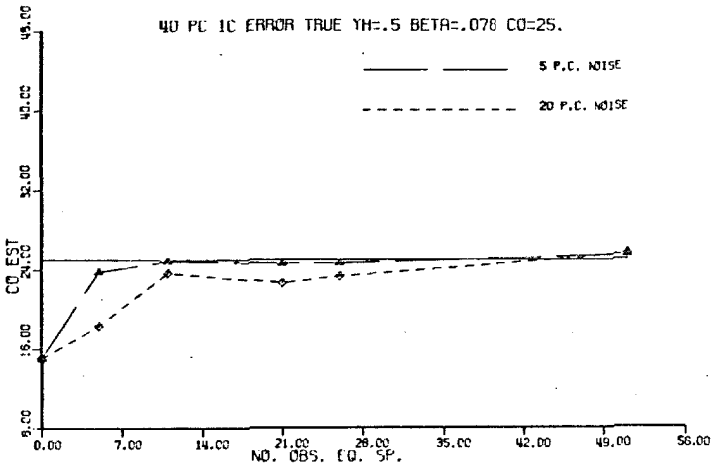

Figure 32-11.

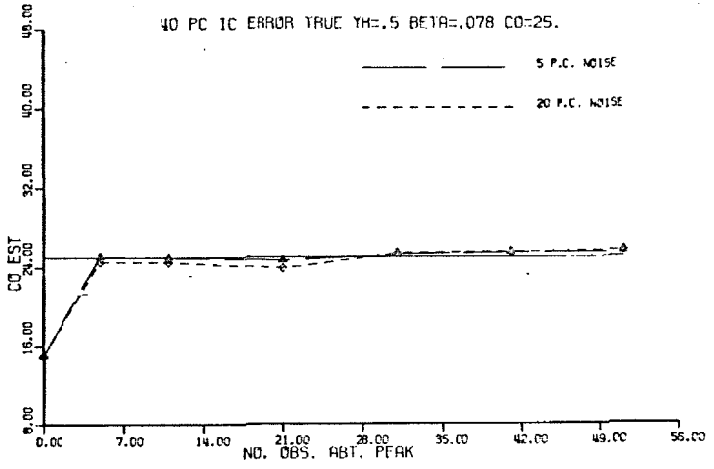

Figure 32-12.

and in Figures 32-2, 4, 6, 8, 10, and 12 for observations clustered about the peak in the response, which occurs in this case at approximately $t = 20$ minutes. These results indicate that eleven sample points seem to be sufficient for reasonable estimates of the parameters even with initial guesses deviating 40% from true values and 20% measurement error.

It can be seen from these results that the parameter β is the most difficult to estimate properly in this particular case which would indicate that the trajectory, $x(t)$, $0 \leq t \leq T$ is least sensitive to variations in β. Such a result can also be obtained by performing a standard sensitivity analysis.[160] Proceeding formally,

$$x(t,\alpha,\beta,\gamma) = x(t,\alpha_0,\beta_0,\gamma_0) + \left(\frac{\partial x}{\partial \alpha}\right)_{\alpha_0} \Delta\alpha + \left(\frac{\partial x}{\partial \beta}\right)_{\beta_0} \Delta\beta + \left(\frac{\partial x}{\partial \gamma}\right)_{\gamma_0} \Delta\gamma \tag{4-50}$$

where higher order terms have been truncated. Expressions for the gradient terms of (4-50) are obtained from (4-46):

$$\left.\begin{aligned}
&\frac{\partial}{\partial t}\left(\frac{\partial x}{\partial \alpha}\right) + k_2 \frac{\partial x}{\partial \alpha} = \frac{k_1}{2}\{1 + \tanh[\beta(c-\gamma)]\} \quad ; \quad \left(\frac{\partial x}{\partial \alpha}\right)_{t=0} = 0 \\
&\frac{\partial}{\partial t}\left(\frac{\partial x}{\partial \beta}\right) + k_2 \frac{\partial x}{\partial \beta} = k_1 \frac{\alpha}{2}(c-\gamma)\,\mathrm{sech}^2[\beta(c-\gamma)] \quad ; \quad \left(\frac{\partial x}{\partial \beta}\right)_{t=0} = 0 \\
&\frac{\partial}{\partial t}\left(\frac{\partial x}{\partial \gamma}\right) + k_2 \frac{\partial x}{\partial \gamma} = -k_1 \frac{\alpha}{2}\beta\,\mathrm{sech}^2[\beta(c-\gamma)] \quad ; \quad \left(\frac{\partial x}{\partial \gamma}\right)_{t=0} = 0
\end{aligned}\right\} \tag{4-51}$$

Let:

$$\left.\begin{aligned} u_1 &\triangleq \frac{\partial x}{\partial \alpha} \\ u_2 &\triangleq \frac{\partial x}{\partial \beta} \\ u_3 &\triangleq \frac{\partial x}{\partial \gamma} \end{aligned}\right\} \qquad (4\text{-}52)$$

Then the dynamic sensitivity equations for α, β, and γ are:

$$\left.\begin{aligned} \frac{\partial u_1}{\partial t} + k_2 u_1 &= \frac{k_1}{2}\{1 + \tanh[\beta(c-\gamma)]\} \quad ; \quad u_1(0) = 0 \\ \frac{\partial u_2}{\partial t} + k_2 u_2 &= \frac{k_1}{2}\alpha(c-\gamma)\,\operatorname{sech}^2[\beta(c-\gamma)] \quad ; \quad u_2(0) = 0 \\ \frac{\partial u_3}{\partial t} + k_2 u_3 &= -k_1 \frac{\alpha}{2}\beta\,\operatorname{sech}^2[\beta(c-\gamma)] \quad ; \quad u_3(0) = 0 \end{aligned}\right\} \qquad (4\text{-}53)$$

Trajectory variations can now be determined from (4-46), (4-50) and (4-53) for any small perturbation in α, β, and γ. Although the result is already known in this case and has been obtained by an entirely different means, some situations might require such analysis beforehand in order to motivate a weighting matrix (see Eq.(4-29)) for improved performance of the estimator algorithm.

D. Error Proportional and Error Rate Saturating Nonlinearity.

Model:
$$\dot{x} = -k_2 x + k_1 \frac{\alpha_1}{2}\{1 + \tanh[\beta_1(c-\gamma_1)]\} + k_1 \frac{\alpha_2}{2}\{1 + \tanh[\beta_2(\dot{c}-\gamma_2)]\} \qquad (4\text{-}54)$$

Input: $c(t)$; $0 \leq t \leq T$ (4-55)

Observations: $y(t_i) = x(t_i) + \eta$ (4-56)

Estimate: $\alpha_1, \beta_1, \gamma_1, \alpha_2, \beta_2, \gamma_2$

Equation (4-54) might represent the secretion of insulin as a function of plasma glucose concentration, and the derivative of plasma glucose concentration when glucose is increasing. Again, the choice of a one-compartment model for distribution is irrelevant to the operation of the estimator for secretion dynamics.

The response of plasma glucose to a finite duration step input of glucose is simulated by Eq.(4-49), from which we also obtain dc/dt, $0 \leq t \leq T$.

An attempt to estimate all six parameters of (4-54) simultaneously by means of the quasilinearization algorithm was unsuccessful. However, an alternative approach is suggested by the fact that the rate secretion term of (4-54) is operative only when $dc/dt > 0$. With a forcing function, $c(t)$, that rises exponentially to a peak at $t \simeq 7$ min and decays exponentially thereafter, the rate secretion term will be excited only in the interval $[0,7]$. In the interval $[0,7]$ both rate and proportional modes are excited, while in the interval $[7,T]$ only the proportional mode is excited. It should be possible then to segment the identification algorithm to exploit this fact.

The identification problem is segmented into two passes. In the first, only the proportional mode terms are obtained which are then fixed and used in the second pass which obtains the rate mode terms.

For the first pass:

$$\text{Model:} \qquad \dot{x} = - k_2 x + k_1 \frac{\alpha_1}{2} \{1 + \tanh[\beta_1(c-\gamma_1)]\} \quad ;$$

$$x(10) = x_0 \qquad (4\text{-}57)$$

$$\text{Input:} \qquad c(t) \quad ; \quad 10 \le t \le T \qquad (4\text{-}58)$$

$$\text{Observations:} \qquad y(t_i) = x(t_i) + \eta \quad ; \quad 10 \le t_i \le T \qquad (4\text{-}59)$$

$$\text{Estimate:} \qquad \alpha_1, \beta_1, \gamma_1$$

where observations are confined to the interval $[10, T]$ and the initial condition for (4-57) is $y(10)$. For the second pass let α_1, β_1, and γ_1 be fixed at the estimated values obtained from the first pass, then:

$$\text{Model:} \qquad \dot{x} = - k_2 x + k_1 \frac{\alpha_1}{2} \{1 + \tanh[\beta_1(c-\gamma_1)]\} + k_1 \frac{\alpha_2}{2}$$

$$\{1 + \tanh[\beta_2(\dot{c}-\gamma_2)]\} \qquad (4\text{-}60)$$

$$\text{Input:} \qquad c(t) \quad ; \quad 0 \le t \le T \qquad (4\text{-}61)$$

$$\dot{c}(t) \quad ; \quad 0 \le t \le T$$

$$\text{Observations:} \qquad y(t_i) = x(t_i) + \eta \quad ; \quad 0 \le t_i \le T \qquad (4\text{-}62)$$

$$\text{Estimate:} \qquad \alpha_2, \beta_2, \gamma_2$$

The true trajectory was obtained with the following parameter values: $k_1 = 70$, $k_2 = .07$, $\alpha_1 = 0.5$, $\beta_1 = .078$, $\gamma_1 = 25$, $\alpha_2 = 0.5$, $\beta_2 = 0.25$, and $\gamma_2 = 20$. The estimator algorithm results are displayed

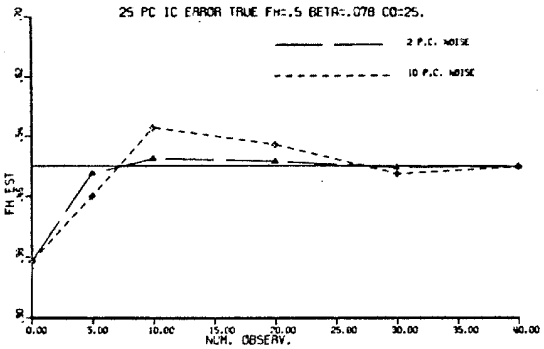

Figure 33-1.

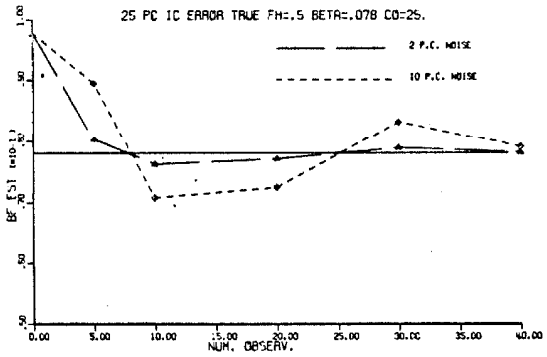

Figure 33-2.

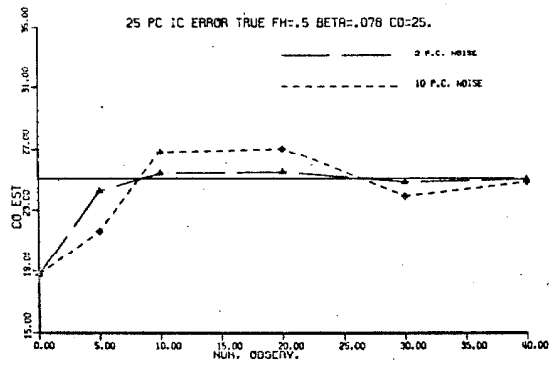

Figure 33-3.

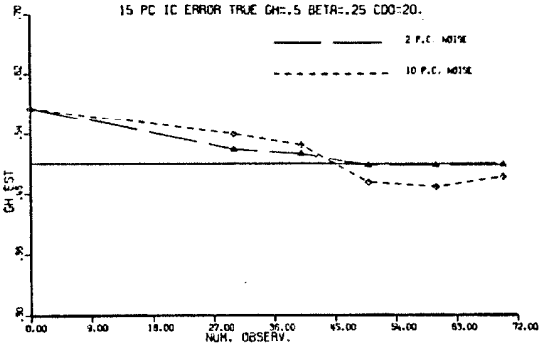

Figure 33-4.

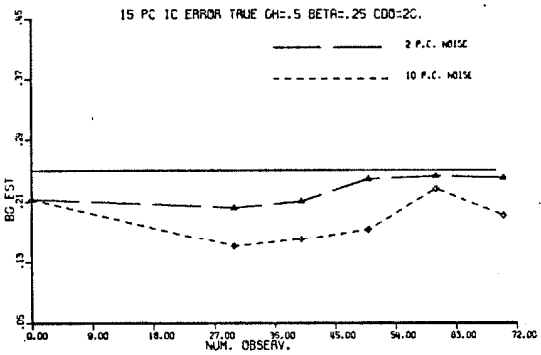

Figure 33-5.

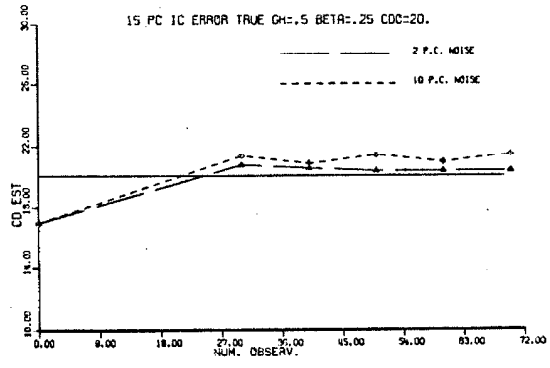

Figure 33-6.

in Figure 33. Here $\alpha_1 = FH$, $\beta_1 = BF$, $\gamma_1 = CO$, $\alpha_2 = GH$, $\beta_2 = BG$, and $\gamma_2 = CD$. Figures 33-1, 2, 3 depict estimation of the proportional mode terms, while Figures 33-4, 5, 6 depict estimation of the rate mode terms. Results are displayed for 2% and 10% measurement error, 25% error in the proportional mode parameter initial guesses, and 15% error in the rate mode parameter initial guesses.

It is evident that more studies could be performed in this particular case to select an input which enhances the operation of the estimator algorithm. While the proportional mode is excited by any hyperglycemic input, the rate mode can only be properly excited by a rapidly rising input. Even with a fixed glucose input to be simulated, eg. 15 grams, some choice of input magnitude and duration will be more suitable to the estimation problem than others. Further comments will be directed to this topic in Section 4.6.

E. Error Proportional Compound Saturating Nonlinearity.

Model:

$$\dot{x}_1 = (1/\tau)\left\{- x_1 - \left(\frac{d_9+a_9x_3}{2}\right)\{1-\tanh[b_9(e-e_0)]\} + F(t)\right\}$$

$$\dot{x}_2 = (1/v_g)\, x_1$$

$$\dot{x}_3 = (1/v_p)\left\{- a_1x_3 + a_2(x_4-x_3) + \frac{10^6}{2} d_1 \{1 - \tanh[b_1(e-e_1)]\}\right\} \qquad (4\text{-}63)$$

$$\dot{x}_4 = (1/v_i)\{- a_3x_4 + a_2(x_3-x_4)\}$$

$$e = R - x_2$$

Input: $F(t) \quad ; \quad 0 \leq t \leq T$ (4-64)

Observations:
$$\left.\begin{aligned} y_1(t_i) &= x_2(t_i) + \eta_1 \\ y_2(t_i) &= x_3(t_i) + \eta_2 \end{aligned}\right\} \quad (4\text{-}65)$$

Estimate: d_9, a_9, b_9, and e_0

The system, (4-63), represents the model dynamics pertinent to the process of glycogenesis. Accordingly, it includes the compound nonlinearity for hepatic uptake of glucose as a function of plasma glucose error and plasma insulin, distribution dynamics for glucose, and the secretion and two-compartment distribution dynamics of insulin. We assume that numerical values for all parameters other than those of the compound nonlinearity have been previously obtained by application of previous algorithms. All other plant processes involving the glucose error as input and a hormonal control as a variable parameter can be identified in an analogous fashion.

The fixed parameters used were $v_g = 175$, $\tau = 0.8$, $v_p = 3500$, $v_i = 10500$, $a_1 = 248$, $a_2 = 309$, $a_3 = 156$, $d_1 = .07$, $b_1 = .0535$, $e_1 = -20$, and $R = 100$. Initial conditions assumed were $x_1(0) = 0$, $x_2(0) = 100$, $x_3(0) = 21 + \eta_1$ and $x_4(0) = 14 + \eta$. The numerical values taken for the parameters to be estimated in order to generate the true trajectories were $d_9 = 90$, $a_9 = 3$, $b_9 = 0.1$, and $e_0 = -30$. The input taken was a finite duration step, corresponding to an intravenous infusion of glucose of 6 g/min for 5 minutes.

The results obtained on this problem are displayed in Figures 34-1, 2, 3, and 4. Under the conditions assumed, i.e. 20% error in

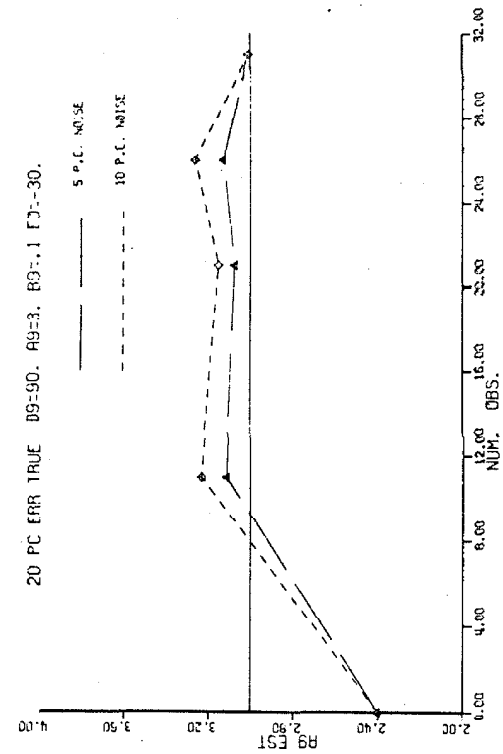

Figure 34-1.

Figure 34-2.

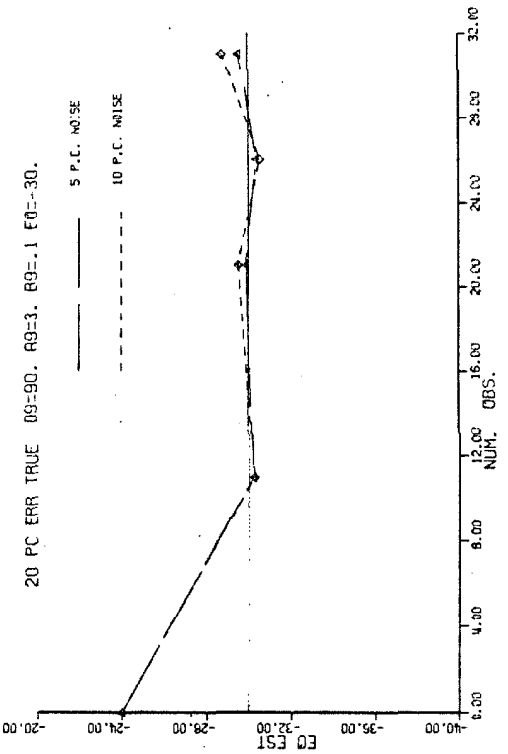

Figure 34-4.

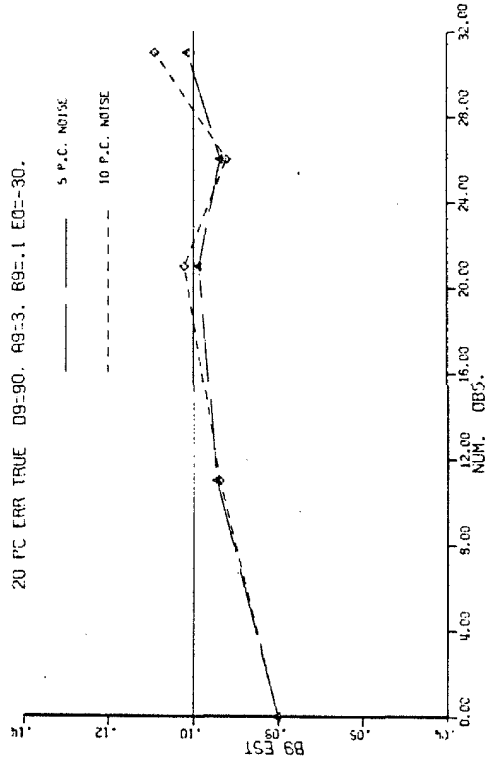

Figure 34-3.

initial parameter guesses and 5% or 10% measurement error, the results indicate that 11 sample points result in reasonable parameter estimates with significant improvement on parameters d_9, b_9 and a_9 only after 31 samples have been assumed.

4.4. Physiologic Systems Experiments for the Inverse Problem.

The system identification algorithm of section 4.5 requires that data be obtained from five basic physiologic experiments. These experiments must be performed on the same experimental subject under conditions which are controlled and reproduced to the greatest extent possible.

The required experiments are as follows:

I. Insulin infusion

$$IN(t) = \begin{cases} a_1 \text{ U/min} & , \ 0 \le t \le \tau_1 \\ 0 & , \ \tau_1 \le t \le T \end{cases} \tag{4-66}$$

II. Glucagon infusion

$$GL(t) = \begin{cases} a_2 \ \mu\text{g/min} & , \ 0 \le t \le \tau_2 \\ 0 & , \ \tau_2 < t \le T \end{cases} \tag{4-67}$$

III. Epinephrine infusion

$$EP(t) = \begin{cases} a_3 \ \mu\text{g/min} & , \ 0 \le t \le \tau_3 \\ 0 & , \ \tau_3 < t \le T \end{cases} \tag{4-68}$$

IV. Growth Hormone infusion

$$GH(t) = \begin{cases} a_4 \ \mu g/min & , \ 0 \le t \le \tau_4 \\ 0 & , \ \tau_4 < t \le T \end{cases} \tag{4-69}$$

V. Glucose infusion

$$F(t) = \begin{cases} a_5 \ g/min & , \ 0 \le t \le \tau_5 \\ 0 & , \ \tau_5 < t \le T \end{cases} \tag{4-70}$$

During each experiment samples must be obtained on the variables u_{1p}, u_{2p}, u_3, and u_{4p}. In addition plasma glucose $c(t)$, must be continuously measured over the course of the experiment, $[0,T]$.

The magnitudes a_i, and the durations of the infusions τ_i, for these experiments have not been specified and can be chosen for experimental or physiologic convenience. However, in the controlled experiments of Section 4.3 the following numerical values were taken: $a_1 = 1$ U/min, $\tau_1 = 5$ min, $a_5 = 6$ g/min, $\tau_5 = 5$ min, and $T = 100$ min.

Although many other experiments which could be performed suggest themselves, it seems that the above constitutes the simplest experimental requirements for the application of the methods under investigation. Once the experimental techniques for the above have been perfected then more ambitious experiments and identification algorithms can be explored.

To the best of our knowledge, the above series of experiments have never been performed on the same subject, or at least have not been reported in the literature. But even with these minimal experimental requirements many problems of technique are encountered. For our purposes careful consideration must be given to insuring reproducible pre-experimental subject regime, to minimizing catheterization trauma,

and to obtaining a more precise characterization of measurement errors associated with the assays of insulin u_{1p}, glucagon u_{2p}, epinephrine u_3, and growth hormone u_{4p}. Some studies have been performed on the effect of catheterization on serum levels of growth hormone and glucose.[161] Such studies for all the variables under consideration must be performed before we can have any confidence that the data reflect system dynamics and not unwanted experimental disturbances. Since hormone assays are extremely complicated procedures and vary from laboratory to laboratory more careful consideration must be given to measurement variance. With these expected errors more accurately specified, the model which we have used for the controlled experiments of section 4.3, i.e. Eq.(4-36), can be adapted to the experimental situation for the measurement of each specific hormone. Since the measurement error model used in the controlled experiments was extremely conservative, these new error models may result in better estimator performance with less required sampled data.

4.5. An Algorithm for the Identification of the Complete Model.

The model of Eqs.(4-4) through (4-13) is to represent a 70 kg. young adult male. Accordingly, on the basis of physiology we obtain several distribution volumes, viz. v_p, v_i and v_g. The glucose regulation set point R, and the rate of glucose utilization by the brain B are assumed known. The parameters associated with hepatic glucose uptake attenuation are also assumed known since measures of glycogen deposit would be required for their determination. In the normal subject, however, these dynamics are not excited. The time con-

stant associated with systemic circulation is also assumed known. In the controlled experiments of Section 4.3 these parameter values were taken: $v_p = 3.5\ \ell$, $v_i = 10.5\ \ell$, $v_g = 17.5\ \ell$, $R = 100$ mg%, $B = 80$ mg/min, and $\tau = 0.8$ min. Initial conditions on the differential equations are determined from measured values of the variables under observation. Hence the following parameters remain to be identified on the basis of experimental data.

Controller (31 parameters)

Insulin

Distribution: a_1, a_2, a_3

Attenuation: b_3, u_{30}

Secretion:

Proportional: d_1, b_1, e_{01}

Rate: $d_2, b_2, \dot{e}_{01}$

Glucagon

Distribution: a_4, a_5, a_6

Secretion: d_4, b_4, e_{02}

Epinephrine

Distribution: v_e, a_7

Secretion:

Proportional: d_5, b_5, e_{03}

Rate: $d_6, b_6, \dot{e}_{02}$

Growth Hormone

Distribution: a_8, a_9, a_{10}

Secretion: d_7, b_7, e_{04}

Plant (21 parameters)

Glycogenesis d_9, a_{11}, b_9, x_{10}

Glycogenolysis d_{10}, a_{12}, b_{10}, e_{05}
d_{11}, a_{13}, b_{11}, e_{06}

Peripheral Utilization d_{13}, a_{14}, b_{13}, e_{08}
b_{14}, u_{4i0}

Renal Excretion d_{12}, b_{12}, e_{07}

Using the data of experiments I through V of Section (4.4) and algorithms A through E of Section (4.3), the above parameters are obtained by performing subsystem estimation in the following order. Estimated parameter values obtained are fixed and assumed known in the subsequent steps.

Step	Algorithm	Experiment	Observations	Estimate
1	B	I	$u_{1p}(t_i)$	a_1, a_2, a_3
2	B	II	$u_{2p}(t_i)$	a_4, a_5, a_6
3	A	III	$u_3(t_i)$	v_e, a_7
4	B	IV	$u_{4p}(t_i)$	a_8, a_9, a_{10}

5	D	V	$u_{1p}(t_i), c(t)$	$d_1, b_1, e_{01}, d_2, b_2, \dot{e}_{01}$
6	C	I	$u_{2p}(t_i), c(t)$	d_4, b_4, e_{02}
7	D	I	$u_3(t_i), c(t)$	$d_5, b_5, e_{03}, d_6, b_6, \dot{e}_{02}$
8	C	I	$u_{4p}(t_i), c(t)$	d_7, b_7, e_{04}
9	E	III	$u_{1p}(t_i), u_3(t_i), c(t)$	b_3, u_{30}
10	C	V	Renal Excretion	d_{12}, b_{12}, e_{07}
11	E	V	$u_{1p}(t_i), c(t)$	d_9, a_{11}, b_9, x_{10}
				$d_{13}, a_{14}, b_{13}, e_{08}$
12	E	I	$u_{2p}(t_i), c(t)$	$d_{10}, a_{12}, b_{10}, e_{05}$
			$u_3(t_i), c(t)$	$d_{11}, a_{13}, b_{11}, e_{06}$
			$u_{4p}(t_i), c(t)$	b_{14}, u_{4i0}

4.6. Control of Metabolic Systems Experiments.

Recent laboratory efforts have been directed to the implementation of feedback control techniques in various metabolic systems investigations. For example, Andres and co-workers[162] have attempted to maintain an elevated blood glucose by means of an initial open-loop glucose input policy followed by corrections made at ten minute intervals based on batch determinations of blood glucose level. The approach taken is highly intuitive and very laborious to implement depending as it does on a high level of investigator-experiment interaction. Another approach, representative of a true closed-loop feedback control system, has been implemented by Kadish.[163] Here a continuous glucose monitor with an inherent time delay of approximately seven minutes generates a voltage

proportional to blood glucose level. A control law of the bang-bang type with dead-zone then determines whether insulin or glucose will be infused for control. To the best of our knowledge this is the most ambitious attempt at implementing closed-loop feedback control of a metabolic system experiment. However, the scheme suffers from two serious deficiencies which may be amenable to analysis. First the effects of the inherent time delay in the measurement apparatus must be overcome. Second, the dead-zone in the control law is much too great to allow a fine control of blood glucose. While the latter problem is easily overcome, the complications arising from an inherent time delay of seven minutes are more serious. Clearly some kind of prediction must be included in the feedback control loop.

We will examine the feasibility of polynomial prediction in this application. We assume the presence of a continuous glucose monitor with an inherent time delay of p minutes $(6 < p < 8)$ and the computational capability of a small digital computer such as the PDP-8S. The computer will operate in the data collection mode to obtain blood glucose samples at intervals of one minute and will perform any necessary calculations between analog-to-digital conversions.

In the general least-squares polynomial approximation[164] to discrete data $g(t_i)$, we seek an approximation of the form:

$$g(t) \approx \sum_{k=0}^{n} a_k \varphi_k(t) \qquad (4\text{-}71)$$

which holds over a set of $N+1$ points, $t_0, t_1, \cdots, t_N$, where $N \geq n$, in the sense that the aggregate weighted squared error is

minimized, i.e.

$$\underset{a_k}{\text{Min}} \sum_{i=0}^{N} \omega(t_i)\left[g(t_i) - \sum_{k=0}^{n} a_k\varphi_k(t_i)\right]^2 \tag{4-72}$$

This imposes the conditions:

$$\frac{\partial}{\partial a_j}\left\{\sum_{i=0}^{N} \omega(t_i)\left[g(t_i) - \sum_{k=0}^{n} a_k\varphi_k(t_i)\right]^2\right\} = 0 \tag{4-73}$$

$$j = 0, 1, \cdots, n$$

Performing the indicated operations results in the n+1 "normal" equations:

$$\sum_{i=0}^{N} \omega(t_i)\varphi_j(t_i) \sum_{k=0}^{n} a_k\varphi_k(t_i) = \sum_{i=0}^{N} \omega(t_i)\varphi_j(t_i)g(t_i)$$

$$j = 0, 1, \cdots, n \tag{4-74}$$

When $N = n$, the system (4-74) is equivalent to requiring that (4-71) be an equality at the n+1 points, i.e. we obtain n+1 equations in the n+1 unknowns a_k.

Denote the sampled data $x(t_i) = b_i$, with sampling interval $\Delta = 1$ min. and make a prediction over p intervals. Let:

b_i = discrete observations

t_n = current time (glucose monitor time)

t_{n+p} = predictor time (experimental subject time)

Δ = sampling interval

Then:

$$x(t_{n+p}) = x[(n+p)\Delta] \tag{4-75}$$

Denote the approximating polynomial:

$$x(t) = \sum_{k=0}^{n} a_k t^k \quad ; \quad t_i = i\Delta \tag{4-76}$$

Assuming n+1 observations with N = n and a unity weighting yields:

$$\begin{aligned} &a_0 + a_1\Delta + a_2\Delta^2 + \cdots + a_n\Delta^n = b_0 \\ &a_0 + a_1(2\Delta) + a_2(2\Delta)^2 + \cdots + a_n(2\Delta)^n = b_1 \\ &\qquad\qquad \cdots \\ &a_0 + a_1(n\Delta) + a_2(n\Delta)^2 + \cdots + a_n(n\Delta)^n = b_n \end{aligned} \tag{4-77}$$

This algebraic system yields $a_0, a_1, \cdots, a_n$. The prediction is then obtained from:

$$x(t_{n+p}) = \sum_{k=0}^{n} a_n[(n+p)\Delta]^k \tag{4-78}$$

To obtain $\dot{x}(t_{n+p})$, evaluate:

$$\dot{x}(t_{n+p}) = \sum_{k=0}^{n} k\, a_k[(n+p)\Delta]^{k-1} \tag{4-79}$$

To obtain $\int_0^{t_{n+p}} x(t)\,dt$, evaluate:

$$\int_0^{t_{n+p}} x(t)\,dt = \int_0^{t_n} x(t)\,dt + \int_{t_n}^{t_{n+p}} x(t)\,dt$$

$$= c_n + \sum_{k=0}^{n} \frac{a_k}{k+1} [p\Delta]^{k+1} \qquad (4\text{-}80)$$

where c_n may be obtained directly from the data.

To be specific we will assume $n = 2$, i.e. three observations will be used to fit a parabola. Let:

t_{n+p} = predictor point

t_n = current data point

t_{n-1} = previous data point

t_{n-2} = first data point

We must fit:

$$x(t) = a_0 + a_1 t + a_2 t^2 \qquad (4\text{-}81)$$

Let the observations be designated:

$$x(t_{n-2}) = b_{n-2}$$

$$x(t_{n-1}) = b_{n-1} \qquad (4\text{-}82)$$

$$x(t_n) = b_n$$

Hence we obtain:

$$\begin{aligned} a_0 + a_1\Delta + a_2\Delta^2 &= b_0 \\ a_0 + a_1(2\Delta) + a_2(2\Delta)^2 &= b_1 \\ a_0 + a_1(3\Delta) + a_2(3\Delta)^2 &= b_2 \end{aligned} \tag{4.83}$$

which must be solved for a_0, a_1, and a_2. Since $\Delta = 1$ we obtain:

$$\begin{Bmatrix} a_0 \\ a_1 \\ a_2 \end{Bmatrix} = \begin{bmatrix} 3 & -3 & 1 \\ -2.5 & 4 & -1.5 \\ 0.5 & -1 & 0.5 \end{bmatrix} \begin{Bmatrix} b_0 \\ b_1 \\ b_2 \end{Bmatrix} \tag{4-84}$$

Hence by using a three-point observation window the matrix of (4-84) can be precomputed and stored. The alternative of using a higher order polynomial with each observation is impractical because of the huge demands upon computer capability made by the matrix inversion problem.

The three point predictor algorithm is then as follows:

1. Read at least three data points:

$$x(0) = b_0$$

$$x(1) = b_1$$

$$x(2) = b_2$$

2. Compute c_n.
3. Obtain a_0, a_1, a_2 from (4-84).
4. Obtain $x(t_{n+p})$, $\dot{x}(t_{n+p})$, and $\int_{t_n}^{t_{n+p}} x(t)\,dt$ from (4-78, (4-79), and (4-80) respectively.
5. Transfer $b_2 \rightarrow b_1$, $b_1 \rightarrow b_0$.
6. Read the next data point $x(t_n) \triangleq b_2$.
7. Repeat from step 2.

Preliminary trials with this algorithm on the types of problems encountered in this investigation have not been satisfactory. The typical situation in which the above would find application is as follows: inject intravenously an insulin dose sufficient to induce a significant hypoglycemic response and mechanize a control law for glucose infusion based on predicted glucose concentration to maintain the subject's blood glucose at or near nominal. The control law could be of the following type:

$$f(t_{n+p}) = k_1\, x(t_{n+p}) + k_2\, \dot{x}(t_{n+p}) + k_3 \int_0^{t_{n+p}} x(t)\,dt \qquad (4\text{-}85)$$

where $f(t)$ = mg Glucose/min. The predictor algorithm will work satisfactorily only for small and slowly varying excursions of blood glucose about the nominal value. It is incapable of predicting a major change in response that occurs over a short time interval. These are precisely the events of greatest importance for effective control. The problem cannot be circumvented by the use of higher order polynomials since these run the risk of having the data window overlap the time at which an important event is expected. This is clear from an examination

of Figure 13 which is a typical response to be expected from an insulin input.

Even supposing that suitable predictions are available, however, it remains to select a criterion and determine a method by which k_1, k_2, and k_3 of Eq.(4-85) are to be obtained. Without entering into a discussion of the possible applications of optimal control theory to this problem, which at this stage of these investigations present serious questions of formulation, a feasible approach would be to use the method of Section 4.5 to obtain a subject model, apply (4-85) to the simulated experiment on the model to determine k_1, k_2, and k_3 in a least-squares sense, and finally use these coefficients with the predicted states in the actual experiment. A less ambitious goal would be to use the simulated glucose input function, determined from the use of k_1, k_2, and k_3 on the simulated experiment with the model, as an open-loop glucose input policy in the actual experiment. Such an approach was discussed in Chapter 3 using the preliminary two-hormone glucose model.

Returning to the problem of deriving adequate predictions of the states to be controlled, it would appear that the only feasible solution meeting the experimental and physiologic constraints must involve some kind of model simulation in real time. That is, the controller must contain a subject representative system model to simulate system response at least p sampling intervals in the future of actual data upon which closed loop control is to be based. Again two alternatives present themselves. The model can be obtained off line by the methods of Section 4.5 or the model can be obtained on-line by means of

sequential estimation techniques.[165,166,167,168] Both approaches require computation facilities which exceed the capabilities of most biological or medical laboratory installations. But in addition, the mechanization of an approximate vector nonlinear sequential filter may require such excessive computation time that the types of closed loop control possibilities which we have discussed would be severely constrained.

V. CONCLUSIONS

5.1. A Unified View of Metabolic Control.

The major organs and processes comprising the metabolic function of the intact organism can be considered as the "plant" to be controlled, and the endocrine system can be considered as the "controller" which produces control signals, i.e. hormones, in response to external or internal disturbances in such a way that the organism's homeostasis is maintained. Within the framework of differential equations the system may be represented:

$$\dot{x} = f(x, u, v) \tag{5-1}$$

$$\dot{u} = g(x, \dot{x}, u) \tag{5-2}$$

where:

x is an (nx1) metabolic state vector

u is an (mx1) internal hormonal control vector

v is a (px1) external input vector

or equivalently:

$$\dot{z} = h(z, v) \tag{5-3}$$

where:

$$z \triangleq \begin{bmatrix} x \\ n \end{bmatrix}$$

$$h \triangleq \begin{bmatrix} f \\ g \end{bmatrix}$$

The metabolic control system consists of several major intercoupled control loops related to carbohydrate, protein, and lipid metabolism. Models for the individual loops can be constructed independent of one another and coupling dynamics can be introduced at the final stage of metabolic control system model development.

5.2. Techniques for Developing Mathematical Models.

Developing mathematical models for metabolic control systems is a necessary prerequisite before advanced analyses can be undertaken. The modeling procedure is an iterative one starting with a proposed model, simulating experiments, and correcting deficiencies in the model.

Heretofore, modeling efforts have relied primarily on physiologic ensemble information to justify numerical values for parameters. This investigation has yielded a feasible technique for obtaining model parameters from experimental data on the intact living organism. Such information should be more representative of the processes which are being modeled than data obtained from surgical animal preparations. Since our primary interest is a comprehensive model for humans, the technique allows the experiments to concentrate on human experimental subjects.

As a vehicle for demonstrating the method this investigation has yielded a more comprehensive dynamic mathematical model of glucose regulation than any now extant. Although we do not have the required data of Section 4.4 performed on one experimental subject, which would allow a subject model to be derived, enough simulations have been performed with the "refined four-hormone model" to be convinced that the model contains all of the necessary dynamics to reproduce such systems experiments as those performed by Porte[27] and Madison.[72]

5.3. The Design of Metabolic Systems Experiments.

Mathematical models are, in addition to being a necessary prerequisite for advanced analyses, an invaluable aid in the design of systems experiments. Even a cursory review of the literature related to metabolism reveals the fact that most experiments in metabolism are component oriented rather than systems oriented. In such situations the effects of inter-process coupling and feedback upon the variable or variables under observation are often ignored. Naturally the results obtained from such experiments must be viewed with suspicion when used in a systems context.

Mathematical models of metabolic control can help to ameliorate this situation in two ways. First, the very process of deriving such models forces us to express in much more precise terms the relationships among components and processes comprising the system. Second, the digital computer can be profitably applied through model simulation to check the consequences of conflicting hypotheses and in fact to simulate experiments. In the early stages of model development any conflict

between model behavior and system behavior is interpreted as a deficiency of the model which should be modified appropriately. But precise models, by answering questions of state variable observability and parameter sensitivity for example, can improve the design of experiments by precisely specifying precautions to be considered and the results to be expected from particular measurements.

5.4. Future Efforts.

The ways in which models of metabolic control must be improved are clear from the previous remarks. Additional hormonal controls, eg. corticosteroids, thyroid hormone, and sex hormones must be included. Models for the protein and lipid loop must be developed and coupled together. Finally gastrointestinal dynamics must be included to allow simulation of oral inputs to the system. Eventually, it may be possible to consider neural control effects in addition to hormonal controls.

Applications of control systems techniques in this area have hardly begun. Efforts directed at the inverse problem such as those of Chapter 4 can be improved. Here the identification problem was formulated with no theoretical justification for the type of input used. However, in biological systems, system or subsystem inputs can usually be characterized at least qualitatively as a single or rather small set of functions. It would seem reasonable to seek an identification scheme which could make use of such knowledge of the input to improve the identification algorithm. It would be of more general interest to see whether the identification scheme itself could prescribe the input in order to "optimize" the identification process.

As we have seen, implementation of sophisticated closed loop experiments will require the development of sequential state and parameter estimation schemes. In addition attention must be directed to the criterion to be used for control. Although a least-squares criterion has been suggested the possibility of whether other criteria such as min-max might be more meaningful in such applications requires investigation. Finally it would be interesting to seek answers to what, if anything, the hormonal controller optimizes in the functioning of metabolic processes. It would seem that this is the most fruitful area of study for applications of optimal control theory.

The present investigation has considered only models of glucose regulation for a "normal" subject. The development of automatic methods for diagnosing metabolic abnormalities will require numerous investigations of models representing abnormal responses. We believe that the investigative framework established in these studies will be conducive to these developments.

APPENDIX A

ENZYME KINETICS[7,100,101]

Enzymes are proteins with catalytic properties and are produced by all living organisms. By catalysis they increase the rates of nearly all intracellular chemical reactions. Without catalysis by enzymes, these reactions would occur so slowly that life as we know it would not be possible. For almost every organic compound that occurs in nature there is an enzyme capable of reacting with it and bringing about some chemical change.

Enzymes are made reaction specific by the primary structure of the enzyme protein, i.e. the sequence of amino acids in its polypeptide chains. The enzyme content of an individual cell is under strict genetic control through DNA. The most significant property of enzymes is their high degree of specificity for their substrates.

All chemical reactions, including enzyme-catalyzed reactions, are to some extent reversible. Within the living cell, however, reversibility may not in fact occur because reaction products are promptly removed by a further series of reactions catalyzed by other enzymes. The living cell may be envisioned as a steady-state system maintained by a unidirectional flow of metabolites.

Many enzymes catalyze reactions of their substrates only in the presence of a particular nonprotein organic compound called the coenzyme. Unless both enzyme and coenzyme are present, no catalysis takes place.

Certain proteolytic enzymes concerned either with digestion or with

the clotting of the blood are originally produced and secreted as inactive enzyme precursors which are called zymogens or pre-enzymes. In some instances the formation of pre-enzymes may be regarded as a way of protecting the tissues that secrete proteolytic enzymes from autodigestion.

Certain highly purified enzymes consist of several molecular species. The term isozyme is used to describe enzymes which, although they catalyze the same reaction, are chemically or physically distinct.

Although over 1000 different enzymatic activities have been detected in animal and plant tissues and in microorganisms, as yet only about 75 of these have been isolated as purified crystalline proteins.

The fundamental theory underlying all chemical reactions is the collision theory. Anything that increases the frequency of collisions between molecules will increase the rate of their reaction. At high concentrations of reactants, collision frequency and hence the reaction velocity will be high. For reactions involving two different molecules, A and B, with molar concentrations [A] and [B],

$$A + B \xrightarrow{k_1} AB \qquad (A\text{-}1)$$

then,

$$\text{Rate}_1 = k_1[A]\,[B]$$

And for the situation,

$$A + 2B \xrightarrow{k_1} AB_2 \qquad \text{(A-2)}$$

$$\text{Rate}_1 = k_1[A]\,[B]^2$$

In general for,

$$nA + mB \underset{k_2}{\overset{k_1}{\rightleftharpoons}} A_n B_m \qquad \text{(A-3)}$$

$$\text{Rate}_1 = k_1[A]^n\,[B]^m$$

and for the reverse reaction,

$$\text{Rate}_2 = k_2[A_nB_m]$$

In equilibrium,

$$\text{Rate}_1 = \text{Rate}_2$$

$$k_1[A]^n[B]^m = k_2[A_nB_m]$$

$$\frac{k_1}{k_2} = \frac{[A_nB_m]}{[A]^n\,[B]^m} \triangleq K_{eq} \qquad \text{(A-4)}$$

where K_{eq} denotes the equilibrium constant. Notice that although the equilibrium constant for a reaction indicates the direction in which a reaction would be expected to proceed, it does not indicate whether it will take place spontaneously.

Most factors affecting the velocity of enzyme-catalyzed reactions do so by changing reactant concentration. These include:

(1) Enzyme Concentration: The initial velocity v, of an enzyme-catalyzed reaction is directly proportional to the enzyme concentration [E]. The enzyme is a reactant that combines with substrate forming an enzyme-substrate complex ES, which decomposes to form a product P, and free enzyme:

$$E + S \underset{k_2}{\overset{k_1}{\rightleftarrows}} ES \underset{k_4}{\overset{k_3}{\rightleftarrows}} E + P \qquad \text{(A-5)}$$

Note that [E] cancels out of the final equilibrium constant expression:

$$E + S \underset{k_4}{\overset{k_1}{\rightleftarrows}} E + P$$

$$\text{Rate}_1 = k_1[E]\,[S]$$

$$\text{Rate}_2 = k_4[E]\,[P]$$

$$K_{eq} = \frac{k_1}{k_4} = \frac{[P]}{[S]} \qquad \text{(A-6)}$$

Thus the enzyme concentration has no effect on the equilibrium constant, i.e. enzymes affect rates not rate constants hence the K_{eq} of a reaction is invariant with respect to catalysis by enzyme.

(2) Substrate Concentration: If the concentration of the substrate [S] is increased and all other conditions are kept constant, the

initial velocity v, measured when very little substrate has reacted, increases to a maximum value V, and no further. Velocity reaches a maximum value which is unaffected by further increases in substrate concentration because even at very low concentrations the substrate is still present in excess of the enzyme by a large molar ratio. If an enzyme with a molecular weight of 100,000 acts on a substrate with a molecular weight of 100 and both are present at a concentration of 1 mg/mℓ, there are 1000 mols of substrate per mol of enzyme. Some realistic figures are:

$$[E] = .01\ \mu g/m\ell = 10^{-8}\ \text{mols}$$

$$[S] = .1\ \ mg/m\ell = 10^{-3}\ \text{mols}$$

giving a 10^5 molar excess of substrate. The net effect is that the enzyme limits the attainable maximum velocity. The substrate concentration that produces half the maximum velocity is called the K_m value or Michaelis constant. It is determined experimentally by plotting v as a function of [S] (see Figure A-1). The Michaelis-Menten equation describes this dependence of the initial velocity of an enzyme-catalyzed reaction on [S] and on K_m:

$$v = \frac{V[S]}{K_m + [S]} \qquad \text{(A-7)}$$

Manipulating (A-7) we obtain:

$$\frac{1}{v} = \left(\frac{K_m}{V}\right)\frac{1}{[S]} + \frac{1}{V} \qquad \text{(A-8)}$$

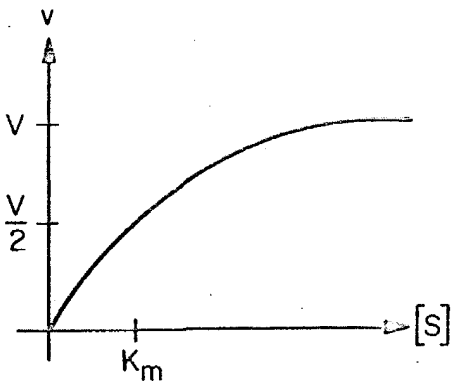

Figure A-1. Rate vs Substrate.

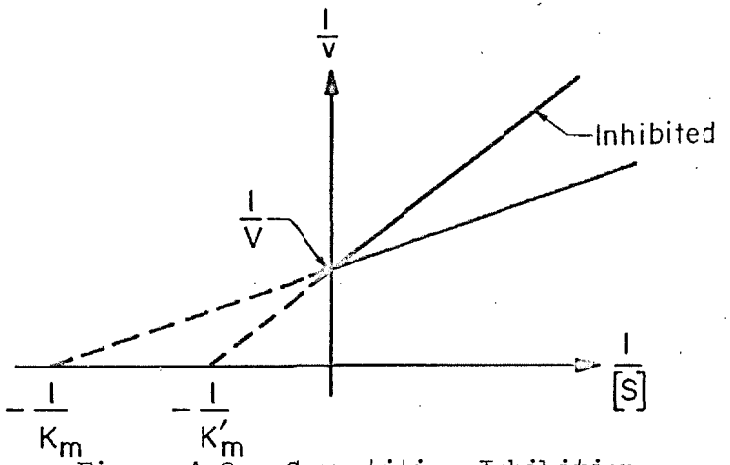

Figure A-2. Competitive Inhibition.

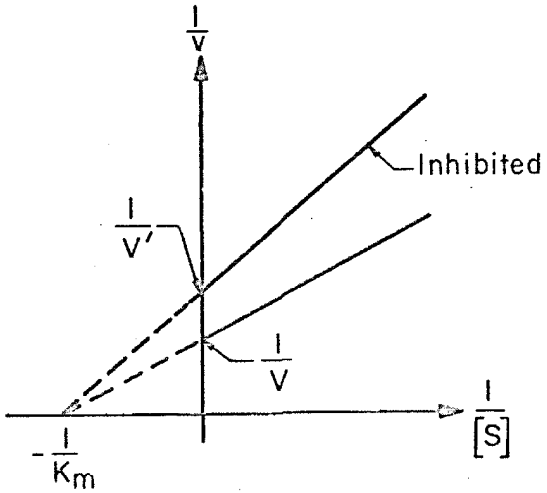

Figure A-3. Noncompetitive Inhibition.

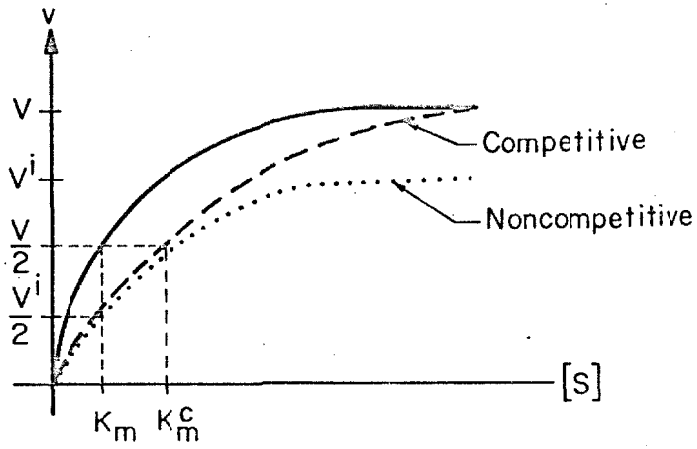

Figure A-4. Enzyme Inhibition.

i.e., the equation for a straight line relating $1/v$ and $1/[S]$ which represents a more convenient means for estimating K_m.

Equation (A-7) can be derived as follows for the reaction where the enzyme combines reversibly with its substrate to form an intermediate complex which reacts irreversibly with a second substrate to yield free enzyme and product.

$$E + S \underset{k_2}{\overset{k_1}{\rightleftarrows}} C \xrightarrow{k_3} E + P \qquad \text{(A-9)}$$

Applying the law of mass-action for the concentration of enzyme-substrate complex,

$$\dot{C} = k_1(E-C)\ S - (k_2 + k_3)\ C \qquad \text{(A-10)}$$

Assuming that the concentration of the enzyme-substrate complex doesn't change, at least over the period of time required to take a velocity measurement, i.e. $\dot{C} = 0$, then,

$$C = \frac{ES}{\frac{k_2 + k_3}{k_1} + S} \qquad \text{(A-11)}$$

The rate of breakdown of enzyme-substrate complex is given by,

$$\dot{P} = k_3 C \qquad \text{(A-12)}$$

$$\dot{P} = \frac{k_3\ ES}{\frac{k_2 + k_3}{k_1} + S} \qquad \text{(A-13)}$$

Defining,

$$V_m \triangleq k_3 E \tag{A-14}$$

$$v \triangleq \dot{P} \tag{A-15}$$

$$K_m \triangleq \frac{k_2 + k_3}{k_1} \quad \text{(Briggs-Haldane form of } K_m\text{)} \tag{A-16}$$

We obtain the rate equation (A-7) with the Briggs-Haldane form of the Michaelis constant. However, when $k_3 \ll k_2$, i.e. when the breakdown of complex is slow compared to the rate of achievement of equilibrium between enzyme and substrate, then

$$K_m \triangleq \frac{k_2}{k_1} \tag{A-17}$$

and (A-7) assumes the form originally specified by Michaelis and Menten.

(3) Temperature: Over a limited range of values the velocity of an enzyme-catalyzed reaction increases as temperature increases. The velocity of many biologic reactions roughly doubles with a 10°C rise in temperature, and is halved by a decrease of 10°C. For animal enzymes, optimal temperatures are close to that of the body.

(4) pH: Optimal enzyme activity is generally observed between pH values of 5.0 and 9.0.

(5) Oxidation: The sulfhydryl SH, groups of many enzymes, notably the dehydrogenases, are essential for enzymatic activity.

Oxidation (dehydrogenation) of these SH groups, forming disulfide linkages (S-S), brought about by many oxidizing agents including the O_2 of air, results in loss of activity.

(6) Radiation: Enzymes are highly sensitive to short wavelength radiation. This is in part due to oxidation of the enzyme by peroxides formed by such radiation.

To measure the amount of an enzyme in a sample of tissue extract or other biologic fluid, the rate of reaction catalyzed by the enzyme in the sample is measured.

Much of our knowledge about the pathways of metabolism has come from in vitro studies of purified enzymes.

An inhibitor (metabolic antagonist) is a compound (other than a substrate) that combines with an enzyme and results in decreased catalytic activity. Inhibitors are of two general types: competitive and noncompetitive. Competitive inhibition of enzyme activity is gradually reversed by an increase in the concentration of substrate. They have structures closely resembling that of the substrate and are inhibitors for only a single enzyme. Noncompetitive inhibitors, e.g. heavy metal ions A_g^+, H_g^{++} or iodoacetic acid (reacts with -SH groups) will inhibit many enzymes. Since these inhibitors bear no structural resemblance to the substrate, an increase in the substrate concentration is generally ineffective in relieving noncompetitive inhibition. Competitive and noncompetitive inhibitors may be distinguished by kinetic analysis. When $1/v$ is plotted against $1/[S]$ at various concentrations of inhibitor we obtain the curves of Figures A-2 and A-3. Noncompetitive inhibitors lower the maximal velocity V, by lowering the effective concentration of active enzyme; but they leave K_m unchanged

since it is independent of enzyme concentration. Competitive inhibitors do not affect V, but raise K_m because at the concentration of substrate that half-saturates the enzyme in the absence of inhibitor, the concentration of free enzyme is decreased by the amount combined with inhibitor.

In terms of the initial velocity diagram, these effects may be represented as in Figure A-4.

APPENDIX B

TRANSPORT PROCESSES

The intracellular-extracellular concentration differences of many substances reflect the characteristics of the cell wall rather than those of the cytoplasm. That region of the cell wall which sustains concentration and electrical gradients and manifests the transport mechanisms peculiar to living systems is called the cell membrane.

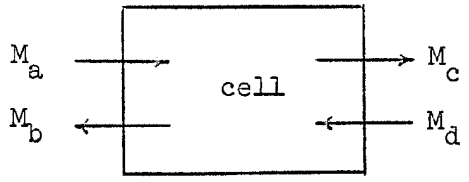

$$M_{cell} = M_a + M_d - (M_c + M_b) \qquad \text{(B-1)}$$

$$M_{trans} = M_a - M_b = M_c - M_d \qquad \text{(B-2)}$$

M_{cell} is the net flux entering the cell while M_{trans} is the net transport through the tissue layer. The intracellular concentration can remain constant $(M_{cell} = 0)$ even if transcellular net flux is present $(M_{trans} \neq 0)$.

A substance transported through a membrane is in equilibrium if its net flux across the membrane is zero and all movement through the membrane is due to passive forces, e.g. electric potentials or concentration gradients.

Passive forces are those that develop spontaneously and don't depend on an energy supply linked to metabolism, e.g. diffusion, migration of

ions in an electric field, osmosis.

Active forces are those that use the energy created by biologic metabolism at the site of transfer.

Two factors control the rate with which a substance passes through a membrane: the magnitude of forces responsible for the movement such as concentration and potential gradients, and the ease of movement of the particle through the membrane; the latter is denoted permeability or conductance. The ease of particle movement within a membrane depends in turn upon the mode of transport.

Diffusion through a membrane which is aided by combination with carriers is called facilitated diffusion. In general small particles are found to pass through membranes more rapidly than larger ones. For many biological membranes, the major mode of transport for small lipid-insoluble particles is through membrane pores.

Passive Mechanisms.

Diffusion. The unidirectional flux M_{12}, of a solute at concentration C_1, is proportional to the concentration with the constant known as the diffusion permeability P.

$$M_{12} = PC_1$$

Similarly,

$$M_{21} = PC_2$$

$$\therefore \quad M_{net} = P(C_1 - C_2) \qquad \text{(B-3)}$$

Permeability is related to the average diffusion coefficient $\bar{D}$, and the membrane thickness x_0.

$$P = \frac{\bar{D}}{x_0} \tag{B-4}$$

Incorporating area, A, we obtain the total transport:

$$MA = \frac{\bar{D}A}{x_0} (C_1 - C_2) \tag{B-5}$$

In differential form:

$$M = - D\left(\frac{\partial C}{\partial x}\right) \tag{B-6}$$

Or more generally,

$$M = - D \nabla C \tag{B-7}$$

In practice these equations are written in terms of activities rather than concentrations:

$$A = \gamma C \tag{B-8}$$

where: $\gamma \leq 1$

The activity may be viewed as an effective concentration. As concentration increases activity decreases. Concentrations in biological fluids

usually are less than 0.01 molar. At these relatively low levels, little error is made by assuming that concentration and activity are approximately equal unless the particles in solution are ions or there are sites of attraction which immobilize certain solute molecules. The ionic strength of blood plasma is about 244 mEq/ℓ., resulting in an activity coefficient of approximately 0.7 for all univalent ions; activity of polyvalent ions is even smaller.

In summary, the diffusion equations should be modified: (1) if the particles are charged, by multiplying the concentration by the activity coefficient to account for the electrical interaction between particles, (2) if some of the solute molecules are bound, by substituting the "free concentration" for the total concentration, and (3) if the solute molecules are dissolved gas, by substituting partial pressure for concentration.

Electrical Forces: The electrical flux through the membrane depends on the potential difference, $(V_1 - V_2)$, the concentration of particles C, the electrical permeability m, and the charge on an individual ion z.

$$M_{net} = z\ m\ C(V_1 - V_2) \qquad \text{(B-9)}$$

We can express the permeability:

$$m = \frac{\eta}{\Delta x} \qquad \text{(B-10)}$$

where η is the membrane property for electrical migration analogous to

D in the case of diffusion. At constant temperature, the ratio between η and D is constant.

$$\frac{\eta}{D} = \frac{F}{RT} \tag{B-11}$$

where F is Faraday's constant, the net charge per mol of univalent ions (96,496 coulombs), T is the absolute temperature in ^{o}K, and R is the gas constant, the thermal energy per degree temperature (8.31 joules per mol per degree centigrade).

Writing (B-9) in differential form,

$$M = - \eta z C \frac{\partial V}{\partial x}$$

or,

$$M = - \eta z C E \tag{B-12}$$

Membrane current density is,

$$J = z F M \tag{B-13}$$

$$= z^2 F m C(V_1 - V_2)$$

where $g = z^2 F m C$ is the specific membrane conductance for a particular ionic species, so

$$J = g(V_1 - V_2) \tag{B-14}$$

is the Ohm's law analog for biologic membrances.

Water Movement and Osmosis: If the pressures on each side of a membrane are not equal, water flows from the side of higher pressure to the side of lower pressure.

$$Q = P_h(P_1 - P_2) \tag{B-15}$$

where P_h is the hydrostatic permeability of the membrane. Water can also move by a mechanism similar to that responsible for solute diffusion, this is called osmosis. If $C_2 > C_1$, water will move from side 1 to side 2:

$$Q = P_{os}\{a(H_2O)_1 - a(H_2O)_2\} \tag{B-16}$$

where the terms in the brackets are the thermodynamic activities of water on the two sides of the membrane.

Water activity is not determined by water concentration but rather by the total concentration of all particles dissolved in the water,

$$a(H_2O) = 1 - k\sum_i C_i \tag{B-17}$$

where k is a constant with approximate value 0.018.

Active Transport.

Two mechanisms are used by living cells to hold materials out of equilibrium across membrances. One is the transport at O_2 into the cell and CO_2 out of the cell. The combination of O_2 with metabolic

substrates makes free energy available at the expense of substrate energy. Part of this energy is used to provide the gradients for O_2 and CO_2 diffusion. The second mechanism is the coupling of metabolic energy to transport within the membrane, i.e. active membrane transport. So an active force may be viewed as a means of transferring energy released by biochemical reactions to particle movement through the membrane.

Most sustained active transport is aerobic; thus oxygen is consumed so that the withdrawal of either the substrate (e.g. glucose) or oxygen eventually stops active transport.

For simple passive diffusion, the unidirectional flux increases linearly in direct proportion to the concentration. In contrast, an active transporting system would be expected to be limited by the rate at which it can supply energy to the transported particles. In other words the flux rate is concentration limited at low concentrations, but transport mechanism limited at high concentrations. So a plot of flux vs. concentration levels off as the active transport mechanism becomes saturated! Saturation can also be evidenced by those passive diffusion processes facilitated by intramembrane carriers; there are limitations on the number of carriers and the rate at which they can shuttle across the membrane.

Quantitative Aspects.

The net flux for simple passive movement within a membrane from the combined effects of diffusion and electric migration, where $\beta = F/RT$ is given by,

$$M = - D \left(\frac{dC}{dx} + z\beta C \frac{dV}{dx} \right) \tag{B-18}$$

or,

$$M = - D\, e^{-z\beta V} \frac{d}{dx} \left(Ce^{z\beta V} \right) \tag{B-19}$$

where $Ce^{z\beta V}$ is called the electrochemical activity. Its natural log multiplied by RT is the electrochemical potential μ, which represents the work necessary to accumulate a concentration C, at potential V, starting from an initial state,

$$\mu = RT \ln(Ce^{z\beta V}) + \mu_0$$

$$\mu = RT \ln C + z F V + \mu_0 \tag{B-20}$$

Further development depends on specific circumstances.

No net flux; Nernst equation.

For an ionic species in equilibrium, i.e. no net flux,

$$0 = - D\, e^{-z\beta V} \frac{d}{dx} \left(Ce^{z\beta V} \right)$$

$$\rightarrow \quad \frac{d}{dx} \left(Ce^{z\beta V} \right) = 0$$

$$\Rightarrow \quad Ce^{z\beta V} \equiv \text{constant}$$

$$\therefore \quad C_1 e^{z\beta V_1} = C_2 e^{z\beta V_2} \tag{B-21}$$

Rearranging we obtain the Nernst equation:

$$V_2 - V_1 = \frac{1}{z\beta} \ln \left(\frac{C_1}{C_2} \right) \qquad \text{(B-22)}$$

This equation has three major applications: (1) development of a criterion for passive equilibrium, (2) prediction of the membrane potential, and (3) derivation of the Gibbs-Donnan relation. The Nernst equation can also be used to determine the necessity for and the direction of membrane forces other than simple passive diffusion and electrical migration.

A membrane potential can be maintained by purely passive means. If the permeating particles are influenced only by simple passive forces, the resulting concentration distribution is called a Gibbs-Donnan equilibrium.

Net flux; Ussing equation.

Integrating (B-18),

$$M \int_1^2 - \frac{e^{z\beta V}}{D} dx = C_2 e^{z\beta V_2} \cdot C_1 e^{z\beta V_1} \qquad \text{(B-23)}$$

however V and D can only be approximated within the membrane so the integration is impossible to perform from physical data. However, if we consider unidirectional fluxes for M_{21}, $C_1 = 0$ and for M_{12}, $C_2 = 0$, so,

$$M_{21} \int_1^2 - \frac{e^{z\beta V}}{D} dx = C_2 e^{z\beta V_2}$$

and

$$M_{12}\int_{1}^{2} -\frac{e^{z\beta V}}{D}\,dx = -C_1 e^{z\beta V_1}$$

Taking the ratio yields Ussing's equation:

$$\left|\frac{M_{21}}{M_{12}}\right| = \frac{C_2}{C_1}\, e^{z\beta(V_2-V_1)} \qquad \text{(B-24)}$$

Summary.

If the net flux through a membrane occurs against an electrochemical gradient, active transport is indicated. If the net flux is in the direction of the electrochemical gradient and the unidirectional flux ratio fits Ussing's equation, no forces other than simple passive diffusion in an electric field need be postulated. If the previous is true but the equation doesn't apply then the simple passive mechanisms which led to (B-24) are insufficient explanation to account for the observed fluxes.[102]

An example of the above considerations occurs in the glucose control model proposed by Seed, Acton, and Stunkard[57] for the passive carrier transfer process between glucose in plasma and glucose in red blood cells. They obtain:

$$\dot{G}_c = K\, V_{G_c}\left\{\frac{G_p}{G_p + G_{\phi_p}} - \frac{G_c}{G_c + G_{\phi_c}}\right\} \qquad \text{(B-25)}$$

where:

$G_c \triangleq$ Glucose (grams) contained in all the circulating red blood cells.

$K \triangleq$ [mass/unit time] into a unit volume of intracellular water.

If [g/min] into 1 liter, then $K = 0.75\ (58.86)$.

$V_{G_c} \triangleq$ Volume (liters) of water contained in all red blood cells.

$G_p \triangleq$ Glucose (grams) in plasma.

$G_{\phi_p} \triangleq$ Mass action equilibrium constant for the combination of glucose with glucose carrier in the red blood cell wall. Here it would be expressed as grams of glucose in plasma corresponding to the concentration represented by the equilibrium constant.

$G_{\phi_c} \triangleq$ Same but expressed as grams of glucose contained in the red blood cells.

APPENDIX C

CARBOHYDRATE TOLERANCE TESTS

At the present time there is no widely accepted standard clinical procedure for diagnosing a failure of the glucose control system, diabetes mellitus. The criteria in use for diagnosing diabetes by means of the "standard" oral glucose tolerance test or the "standard" intravenous glucose tolerance test vary from clinic to clinic.[103,104, 105,106]

The tolerance test consists of administering a given quantity of glucose either orally or intravenously and measuring the body's response by sampling the concentration of blood glucose at some chosen times over an appropriate time interval. The intravenous tolerance test avoids the variable absorption from the gastrointestinal tract making it more reproducible and of shorter duration.[107,108]

Most uses of this test involve rapidly elevating the concentration of blood glucose and determining a single constant of the subsequent decay. The inherent assumption here is that glucose disappearance from plasma follows simple first order kinetics, i.e. that it is a passive process with the rate of disappearance proportional to the concentration. Obviously, the whole host of active processes that come into play under these conditions cannot be accurately represented by such a grossly lumped model. Nevertheless, much effort has been expended in an attempt to diagnose diabetes by the evaluation of an exponential decay constant.

If: $C_o \triangleq$ The blood glucose concentration when suitably elevated

$k \triangleq$ The disappearance rate of glucose from the blood

then: $$C(t) = C_0 e^{-kt} \qquad (C\text{-}1)$$

By evaluating k in this way it has been found by Amatuzio[81] that the mean disappearance rate of glucose in normal subjects was 3.71 ± .4 per cent per minute with a range of 3.01 to 4.85 %/min. In subjects with mild diabetes mellitus not requiring insulin it was 1.81 ± .51 %/min with a range of 0.93 to 2.46 %/min. It has also been demonstrated that the disappearance rate of glucose is reproducible in the same individual and independent of the glucose load.

Even if the glucose tolerance test was an infallible test for diagnosing diabetes, it gives no indication of where in the complex glucose control system the abnormality might lie. It isn't unrealistic to expect that the derivation of a comprehensive mathematical model for the metabolic control system will eventually motivate a procedure that not only can diagnose an abnormality but also pinpoint its source.

APPENDIX D

EXPERIMENTAL PROCEDURES AND THE CONTINUOUS MONITORING OF BLOOD GLUCOSE

The experimental procedure used with the subject is as follows. One end of a double-lumen catheter is introduced into an antecubital or forearm vein and the other is connected to the glucose monitor. A sterile heparin solution is pumped at 0.2 c.c. per minute through the inner lumen to approximately one quarter of an inch at the distal end of the catheter inside the vein. At this point the heparin mixes with the in-flowing blood from the subject and the heparin-blood mixture is withdrawn through the outer lumen of the catheter at 0.4 c.c. per minute for passage through the instrument. The amount of blood withdrawn is 0.2 c.c. per minute, or 12 c.c. per hour.

The operation of the continuous glucose monitor is based on the following considerations. The enzyme glucose oxidase (G.OD.) catalyzes the oxidation of glucose by oxygen whereby gluconolactone and hydrogen peroxide are formed:

$$\underset{\text{Glucose}}{C_6H_{12}O_6} + O_2 \xrightarrow{\text{G.OD.}} \underset{\text{Gluconolactone}}{C_6H_{10}O_6} + H_2O_2 \qquad \text{(D-1)}$$

A number of colorimetric methods have been devised for following this reaction, based on the fact that H_2O_2 in the presence of a peroxidase enzyme will oxidize certain colorless substances to highly colored ones. These may be summarized as:

$$H_2O_2 + \text{"Chromogen"} \xrightarrow{\text{Peroxidase}} \text{"Color"} \qquad \text{(D-2)}$$

The intensity of the color is proportional to the amount of H_2O_2 present and this in turn is proportional to the amount of glucose oxidized in (D-1). These methods are subject to interference by substances which will react with H_2O_2 or with the colored species.

An alternative method of measuring the extent of reaction (D-1) is to monitor the amount of O_2 consumed. The problem here is the instability of H_2O_2 with respect to decomposition into water and oxygen. To the extent that this occurs, some of the oxygen consumed in (D-1) will be liberated again and the ratio of O_2 consumed to glucose oxidized will be affected. One way around this problem is to ensure that all the H_2O_2 decomposes. This reaction is catalyzed by an enzyme catalase which is usually a contaminant of G.OD. preparations anyway. Thus we have:

$$H_2O_2 \xrightarrow{\text{Catalase}} H_2O + \tfrac{1}{2}O_2 \qquad \text{(D-3)}$$

and the net reaction (D-1) + (D-3) is:

$$C_6H_{12}O_6 + \tfrac{1}{2}O_2 \xrightarrow[\text{Catalase}]{\text{G.OD.}} C_6H_{10}O_6 + H_2O \qquad \text{(D-4)}$$

This insures a constant glucose to O_2 uptake ratio, but unfortunately lowers the sensitivity of the method since only one-half mole of O_2 is consumed per mole of glucose.

A solution to the sensitivity problem is to provide for the destruction of peroxide by routes not leading to O_2 formation. In the method of "coupled oxidation," alcohol is added to the reaction mixture. The reaction of peroxide in the presence of catalase then becomes:

$$C_2H_6O + H_2O_2 \xrightarrow{\text{Catalase}} \underset{\text{Acetaldehyde}}{C_2H_4O} + 2H_2O \qquad \text{(D-5)}$$

Another way of removing peroxide uses the non-enzymatic reaction with I^- catalyzed by ammonium molybdate:

$$H_2O_2 + 2H^+ + 2I^- \xrightarrow[\text{Molybdate}]{\text{Ammonium}} I_2 + 2H_2O \qquad \text{(D-6)}$$

We use both approaches by providing for reactions (D-5) and (D-6). This is because the enzyme solution contains catalase and in the absence of alcohol reaction (D-3) is competitive with (D-6). However, catalase is not particularly stable, and is gradually depleted from the solution so that I^- and molybdate are required also. The formation of I_2 in (D-6) is also advantageous in retarding bacterial growth in the reagent.

The rate of (D-1) is pH dependent so that the reagent must be buffered. To summarize this rather complex affair:

$$\begin{array}{l}\text{G.OD.}\\ \text{catalase,}\\ I^-\text{, ethanol,}\\ \text{molybdate}\\ \text{buffered}\\ \text{at pH 6.0}\end{array} + \text{glucose} + O_2 \longrightarrow \begin{array}{l}\text{gluconolactone}\\ + \text{ acetaldehyde}\\ \text{and/or } I_2\end{array} \qquad \text{(D-7)}$$

G.OD. reagent

The net result of this reaction is that one mole of O_2 is consumed per mole of glucose present.

Under the conditions we use the reaction can be shown to be kinetically 1st order in glucose and independent of oxygen. Thus we have in the delay line the situation of Figure D-1. Where:

$$G_f = G_i \, e^{-bT} \tag{D-8}$$

and G_i and G_f are the initial and final glucose concentrations. The oxygen consumption, ΔO_2 is equal to the change in glucose concentrations as seen above, hence:

$$\Delta O_2 = G_i - G_f = G_i(1 - e^{-kT}) \tag{D-9}$$

and the O_2 consumption is proportional to the initial glucose concentration. T is chosen to give a substantial fraction of the reaction (4-5 half-lives). Note that k is a function of G.OD. concentration, pH and temperature, all of which should be constant.

The oxygen sensors are polarographic, i.e. they produce a current proportional to the oxygen level at an essentially fixed voltage. Very roughly, we have the configuration of Figure D-2, where:

$$V = iR$$

$$i = K[O_2]$$

$$V \propto [O_2]$$

The teflon membrane protects the cathode from deposits of protein and

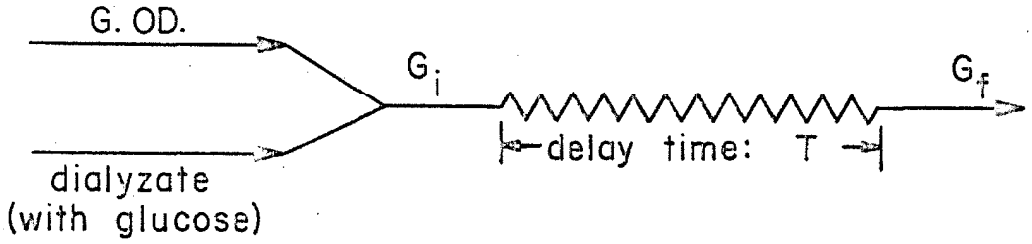

Figure D-1. Monitor Delay Line.

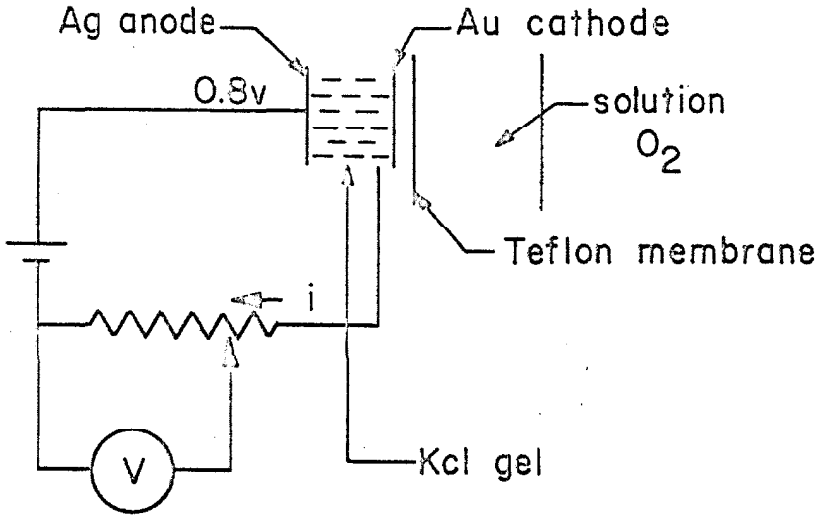

Figure D-2. Sensor Configuration.

other substances. It is permeable to O_2 but not to H_2O.

Cathode: $$O_2 + 2\ H_2O + 4e \longrightarrow 4OH^- \qquad \text{(D-10)}$$

Anode: $$4Ag + 4e + 4Cl^- \longrightarrow 4AgCl \qquad \text{(D-11)}$$

In a flowing solution the current is limited by the diffusion rate of O_2 to the cathode. This is highly temperature dependent and as a result the sensor output increases with temperature (~2%/°C).

As a check on the operation of the continuous glucose monitor and for calibration of the instrument as well as corrections for drift due to the laboratory environment, batch samples of blood glucose are determined by the method described in reference [115].

APPENDIX E

ESTIMATOR ALGORITHM EQUATIONS

Algorithm A.

Let the system be represented:

$$\dot{x} = - k_2 x + k_1 h(t) \tag{E-1}$$

with parameters k_1 and k_2 to be estimated. Let:

$$\begin{aligned} z_1 &\triangleq x \\ z_2 &\triangleq k_2 \\ z_3 &\triangleq k_1 \end{aligned} \tag{E-2}$$

Then:

$$\begin{aligned} \dot{z}_1 &= - z_2 z_1 + z_3 h(t) \\ \dot{z}_2 &= 0 \\ \dot{z}_3 &= 0 \end{aligned} \tag{E-3}$$

Omitting iteration superscripts for convenience, nontrivial terms, of the fundamental matrix and particular solution are:

$$\dot{\varphi}_{11} = - z_2 \varphi_{11} \qquad ; \quad \varphi_{11}(0) = 1$$

$$\dot{\varphi}_{12} = - z_2 \varphi_{12} - z_1 \quad ; \quad \varphi_{12}(0) = 0$$

$$\dot{\varphi}_{13} = - z_2 \varphi_{13} + h(t) \quad ; \quad \varphi_{13}(0) = 0 \qquad \text{(E-4)}$$

$$\dot{p}_1 = - z_2 p_1 + z_1 z_2 \quad ; \quad p_1(0) = 0$$

The algebraic system to be solved for the updated initial condition is:

$$\sum_{i=1}^{N} \varphi_{1j}(t_i)[\varphi_{11}(t_i)\beta_1 + \varphi_{12}(t_i)\beta_2 + \varphi_{13}(t_i)\beta_3 + p_1(t_i) - y(t_i)] = 0 \qquad \text{(E-5)}$$

$$j = 1, 2, 3$$

Algorithm B.

Let the system be represented:

$$v_1\dot{x}_1 = - a_1x_1 + a_2(x_2-x_1) + h(t)$$

$$\text{(E-6)}$$

$$v_2\dot{x}_2 = - a_3x_2 + a_2(x_1-x_2)$$

with parameters a_1, a_2, a_3 to be estimated. Let:

$$z_1 \triangleq x_1$$

$$z_2 \triangleq x_2 \qquad \text{(E-7)}$$

$$z_3 \triangleq a_1$$

$$z_4 \triangleq a_2$$

$$z_5 \triangleq a_3$$

Then:

$$\dot{z}_1 = (1/v_1)[-z_3 z_1 + z_4(z_2 - z_1) + h(t)]$$

$$\dot{z}_2 = (1/v_2)[-z_5 z_2 + z_4(z_1 - z_2)]$$

$$\dot{z}_3 = 0 \qquad \text{(E-8)}$$

$$\dot{z}_4 = 0$$

$$\dot{z}_5 = 0$$

Omitting iteration symbols for convenience, nontrivial terms of the fundamental matrix and particular solution are:

$$\dot{\varphi}_{11} = (1/v_1)[-(z_3+z_4)\varphi_{11} + z_4\varphi_{21}] \quad ; \quad \varphi_{11}(0) = 1$$

$$\dot{\varphi}_{12} = (1/v_1)[-(z_3+z_4)\varphi_{12} + z_4\varphi_{22}] \quad ; \quad \varphi_{12}(0) = 0$$

$$\dot{\varphi}_{13} = (1/v_1)[-(z_3+z_4)\varphi_{13} + z_4\varphi_{23} - z_1] \quad ; \quad \varphi_{13}(0) = 0$$

$$\dot{\varphi}_{14} = (1/v_1)[-(z_3+z_4)\varphi_{14} + z_4\varphi_{24} - z_1 + z_2] \quad ; \quad \varphi_{14}(0) = 0$$

$$\dot{\varphi}_{15} = (1/v_1)[-(z_3+z_4)\varphi_{15} + z_4\varphi_{25}] \quad ; \quad \varphi_{15}(0) = 0 \qquad \text{(E-9)}$$

$$\dot{\varphi}_{21} = (1/v_2)[-(z_4+z_5)\varphi_{21} + z_4\varphi_{11}] \quad ; \quad \varphi_{21}(0) = 0$$

$$\dot{\varphi}_{22} = (1/v_2)[-(z_4+z_5)\varphi_{22} + z_4\varphi_{12}] \quad ; \quad \varphi_{22}(0) = 1$$

$$\dot{\varphi}_{23} = (1/v_2)[-(z_4+z_5)\varphi_{23} + z_4\varphi_{13}] \quad ; \quad \varphi_{23}(0) = 0$$

$$\dot{\varphi}_{24} = (1/v_2)[-(z_4+z_5)\varphi_{24} + z_4\varphi_{14} + z_1 - z_2] \quad ; \quad \varphi_{24}(0) = 0$$

$$\dot{\varphi}_{25} = (1/v_2)[-(z_4+z_5)\varphi_{25} + z_4 - z_2] \qquad ; \quad \varphi_{25}(0) = 0$$

$$\dot{p}_1 = (1/v_1)[(z_3+z_4)(z_1-p_1) + z_4(p_2-z_2) + h(t)] \quad ; \quad p_1(0) = 0$$

$$\dot{p}_2 = (1/v_2)[(z_4+z_5)(z_2-p_2) + z_4(p_1-z_1)] \qquad ; \quad p_2(0) = 0 \tag{E-10}$$

Assuming observations on x_1 only, the algebraic system to be solved for the updated initial condition is:

$$\sum_{i=1}^{N} \varphi_{1j}(t_i)[\varphi_{11}(t_i)\beta_1 + \varphi_{12}(t_i)\beta_2 + \varphi_{13}(t_i)\beta_3 + \varphi_{14}(t_i)\beta_4 + \varphi_{15}(t_i)\beta_5 + p_1(t_i) - y(t_i)] = 0 \; ; \quad j = 1, \cdots, 5 \tag{E-11}$$

In the event that observations on both x_1 and x_2 are possible the above system modifies to:

$$\sum_{i=1}^{N} (\varphi_{1j}\varphi_{11}+\varphi_{2j}\varphi_{21})\beta_1 + (\varphi_{1j}\varphi_{12}+\varphi_{2j}\varphi_{22})\beta_2 + (\varphi_{1j}\varphi_{13}+\varphi_{2j}\varphi_{23})\beta_3 + (\varphi_{1j}\varphi_{14}+\varphi_{2j}\varphi_{24})\beta_4 + (\varphi_{1j}\varphi_{15}+\varphi_{2j}\varphi_{25})\beta_5 = \sum_{i=1}^{N} \varphi_{1j}(y_1-p_1) + \varphi_{2j}(y_2-p_2) \; ; \quad j = 1, \cdots, 5 \tag{E-12}$$

where all variable terms are evaluated at times $t_1, t_2, \cdots, t_N$.

Algorithm C.

Let the system be represented:

$$\dot{x} = -k_2 x + k_1 \frac{\alpha}{2}\{1 + \tanh[\beta(c-\gamma)]\} \tag{E-13}$$

with parameters α, β, γ to be estimated. Let:

$$\begin{aligned} z_1 &\triangleq x \\ z_2 &\triangleq \alpha \\ z_3 &\triangleq \beta \\ z_4 &\triangleq \gamma \end{aligned} \tag{E-14}$$

then:

$$\begin{aligned} \dot{z}_1 &= - k_2 z_1 + k_1 \frac{z_2}{2} \{1 + \tanh[z_3(c(t)-z_4)]\} \\ \dot{z}_2 &= 0 \\ \dot{z}_3 &= 0 \\ \dot{z}_4 &= 0 \end{aligned} \tag{E-15}$$

Omitting iteration symbols for convenience, nontrivial terms of the fundamental matrix and particular solution are:

$$\begin{aligned} \dot{\varphi}_{11} &= - k_2 \varphi_{11} && ; \quad \varphi_{11}(0) = 1 \\ \dot{\varphi}_{12} &= - k_2 \varphi_{12} + \frac{k_1}{2} \{1 + \tanh[z_3(c-z_4)]\} && ; \quad \varphi_{12}(0) = 0 \\ \dot{\varphi}_{13} &= - k_2 \varphi_{13} + \frac{k_1}{2} z_2 (c-z_4) \operatorname{sech}^2[z_3(c-z_4)] && ; \quad \varphi_{13}(0) = 0 \\ \dot{\varphi}_{14} &= - k_2 \varphi_{14} - \frac{k_1}{2} z_2 z_3 \operatorname{sech}^2[z_3(c-z_4)] && ; \quad \varphi_{14}(0) = 0 \end{aligned} \tag{E-16}$$

$$\dot{p}_1 = - k_2 p_1 + k_1 z_2 z_3 (z_4 - \frac{c}{2}) \operatorname{sech}^2[z_3(c-z_4)] \quad ; \quad p_1(0) = 0 \qquad \text{(E-17)}$$

The algebraic system to be solved for the updated initial condition is:

$$\sum_{i=1}^{N} \varphi_{1j}(t_i)[\varphi_{11}(t_i)\beta_1 + \varphi_{12}(t_i)\beta_2 + \varphi_{13}(t_i)\beta_3$$

$$+ \varphi_{14}(t_i)\beta_4 + p_1(t_i) - y(t_i)] = 0 \quad ; \quad j = 1, 2, 3, 4, \qquad \text{(E-18)}$$

Algorithm D.

Let the system be represented:

$$\dot{x} = - k_2 x + \frac{k_1}{2} \{\alpha_1 + \alpha_1 \tanh[\beta_1(c-\gamma_1)] + \alpha_2 + \alpha_2 \tanh[\beta_2(c-\gamma_2)]\} \qquad \text{(E-19)}$$

with parameters α_1, β_1, γ_1 and α_2, β_2, γ_2 to be estimated.

Phase 1 - Error Proportional Terms.

$$\dot{x} = - k_2 x + k_1 \frac{\alpha_1}{2} \{1 + \tanh[\beta_1(c-\gamma_1)]\}$$

Let:

$$\begin{aligned} z_1 &\triangleq x \\ z_2 &\triangleq \alpha_1 \\ z_3 &\triangleq \beta_1 \\ z_4 &\triangleq \gamma_1 \end{aligned} \qquad \text{(E-20)}$$

Then:

$$\begin{aligned}
\dot{z}_1 &= - k_2 z_1 + k_1 \frac{z_2}{2} \{1 + \tanh[z_3(c-z_4)]\} \\
\dot{z}_2 &= 0 \\
\dot{z}_3 &= 0 \\
\dot{z}_4 &= 0
\end{aligned} \tag{E-21}$$

Omitting iteration symbols for convenience, nontrivial terms of the fundamental matrix and particular solution are:

$$\begin{aligned}
\dot{\varphi}_{11} &= - k_2 \varphi_{11} && ; \quad \varphi_{11}(0) = 1 \\
\dot{\varphi}_{12} &= - k_2 \varphi_{12} + \frac{k_1}{2} \{1 + \tanh[z_3(c-z_4)]\} && ; \quad \varphi_{12}(0) = 0 \\
\dot{\varphi}_{13} &= - k_2 \varphi_{13} + \frac{k_1}{2} z_2(c-z_4) \operatorname{sech}^2[z_3(c-z_4)] && ; \quad \varphi_{13}(0) = 0 \\
\dot{\varphi}_{14} &= - k_2 \varphi_{14} - \frac{k_1}{2} z_2 z_3 \operatorname{sech}^2[z_3(c-z_4)] && ; \quad \varphi_{14}(0) = 0
\end{aligned} \tag{E-22}$$

$$\dot{p}_1 = - k_2 p_1 + \frac{k_1}{2} z_2 z_3 (2z_4 - c) \operatorname{sech}^2[z_3(c-z_4)] \; ; \quad p_1(0) = 0 \tag{E-23}$$

The algebraic system to be solved for the updated initial condition is:

$$\sum_{i=1}^{N} \varphi_{1j}(t_i)[\varphi_{11}(t_i)\beta_1 + \varphi_{12}(t_i)\beta_2 + \varphi_{13}(t_i)\beta_3 + \varphi_{14}(t_i)\beta_4 + p_1(t_i) - y(t_i)] = 0 \, , \; j = 1, \cdots, 4 \tag{E-24}$$

At the final iteration, let:

$$\alpha_1 \triangleq z_2^{k+1}$$

$$\beta_1 \triangleq z_3^{k+1} \qquad \text{(E-25)}$$

$$\gamma_1 \triangleq z_4^{k+1}$$

Phase 2 - Error Rate Terms.

$$\dot{x} = - k_2 x + k_1 \frac{\alpha_1}{2} \{1 + \tanh[\beta_1(c-\gamma_1)]\} + k_1 \frac{\alpha_2}{2} \{1 + \tanh[\beta_2(\dot{c}-\gamma_2)]\} \qquad \text{(E-26)}$$

Let:

$$z_1 \triangleq x$$

$$z_2 \triangleq \alpha_2 \qquad \text{(E-27)}$$

$$z_3 \triangleq \beta_2$$

$$z_4 \triangleq \gamma_2$$

Then:

$$\dot{z}_1 = - k_2 z_1 + k_1 \frac{\alpha_1}{2} \{1 + \tanh[\beta_1(c-\gamma_1)]\} + k_1 \frac{z_2}{2} \{1 + \tanh[z_3(\dot{c}-z_4)]\} \qquad \text{(E-28)}$$

$$\dot{z}_2 = 0$$

$$\dot{z}_3 = 0$$

$$\dot{z}_4 = 0$$

Omitting iteration symbols for convenience, the nontrivial terms of the fundamental matrix and particular solution are:

$$\dot{\varphi}_{11} = - k_2\varphi_{11} \qquad ; \quad \varphi_{11}(0) = 1$$

$$\dot{\varphi}_{12} = - k_2\varphi_{12} + \frac{k_1}{2}\{1 + \tanh[z_3(\dot{c}-z_4)]\} \qquad ; \quad \varphi_{12}(0) = 0$$

$$\dot{\varphi}_{13} = - k_2\varphi_{13} + \frac{k_1}{2} z_2(\dot{c}-z_4)\operatorname{sech}^2[z_3(\dot{c}-z_4)] \qquad ; \quad \varphi_{13}(0) = 0 \qquad \text{(E-29)}$$

$$\dot{\varphi}_{14} = - k_2\varphi_{14} - \frac{k_1}{2} z_2 z_3 \operatorname{sech}^2[z_3(\dot{c}-z_4)] \qquad ; \quad \varphi_{14}(0) = 0$$

$$\dot{p}_1 = - k_2 p_1 + k_1 \frac{\alpha_1}{2}\{1 + \tanh[\beta_1(c-\gamma_1)]\}$$
$$+ \frac{k_1}{2} z_2 z_3 (2z_4-\dot{c})\operatorname{sech}^2[z_3(\dot{c}-z_4)] \quad ; \quad p_1(0) = 0 \qquad \text{(E-30)}$$

The algebraic system to be solved for the updated initial condition is:

$$\sum_{i=1}^{N} \varphi_{1j}(t_i)[\varphi_{11}(t_i)\beta_1 + \varphi_{12}(t_i)\beta_2 + \varphi_{13}(t_i)\beta_3$$
$$+ \varphi_{14}(t_i)\beta_4 + p_1(t_i) - y(t_i)] = 0 \quad ; \quad j = 1, \cdots, 4 \qquad \text{(E-31)}$$

where β_1 in (E-31) should not be confused with β_1 in (E-28) and (E-30).

Algorithm E.

Let the system be represented:

$$\dot{x}_1 = (1/\tau)\left\{- x_1 - \left(\frac{d_9+a_9u_{1p}}{2}\right)\{1 - \tanh[b_9(e-e_0)]\} + F(t)\right\}$$

$$\dot{x}_2 = (1/v_g)\, x_1 \tag{E-32}$$

$$\dot{x}_3 = (1/v_p)\left\{- a_1 x_3 + a_2(x_4-x_3) + 10^6 \frac{d_1}{2}\{1 - \tanh[b_1(e-e_1)]\}\right\}$$

$$\dot{x}_4 = (1/v_i)\{- a_3 x_4 + a_2(x_3-x_4)\}$$

$$e = R - x_2$$

with parameters d_9, a_9, b_9, and e_0 to be estimated. Let:

$$z_1 \triangleq x_1$$

$$z_2 \triangleq x_2$$

$$z_3 \triangleq x_3$$

$$z_4 \triangleq x_4 \tag{E-33}$$

$$z_5 \triangleq d_9$$

$$z_6 \triangleq a_9$$

$$z_7 \triangleq b_9$$

$$z_8 \triangleq e_0$$

Then:

$$\dot{z}_1 = (1/\tau)\left\{- z_1 - \left(\frac{z_5+z_3 z_6}{2}\right)\{1 - \tanh[z_7(R-z_2-z_8)]\} + F(t)\right\}$$

$$\dot{z}_2 = (1/v_g)\, z_1$$

$$\dot{z}_3 = (1/v_p)\left\{-a_1 z_3 + a_2(z_4-z_3) + 10^6 \frac{d_1}{2}\{1 - \tanh[b_1(R-z_2-e_1)]\}\right\}$$

$$\dot{z}_4 = (1/v_i)\{- a_3 z_4 + z_2(z_3-z_4)\} \qquad \text{(E-34)}$$

$$\dot{z}_5 = 0$$

$$\dot{z}_6 = 0$$

$$\dot{z}_7 = 0$$

$$\dot{z}_8 = 0$$

Omitting iteration symbols for convenience, nontrivial terms of the fundamental matrix and particular solution are:

$$\dot{\varphi}_{11} = (1/\tau)\left\{- \varphi_{11} - \left(\frac{z_5+z_3z_6}{2}\right) z_7 \operatorname{sech}^2[z_7(R-z_2-z_8)]\varphi_{21} - \frac{z_6}{2}\{1 - \tanh[z_7(R-z_2-z_8)]\}\varphi_{31}\right\} ; \quad \varphi_{11}(0) = 1$$

$$\dot{\varphi}_{12} = (1/\tau)\left\{- \varphi_{12} - \left(\frac{z_5+z_3z_6}{2}\right) z_7 \operatorname{sech}^2[z_7(R-z_2-z_8)]\varphi_{22} - \frac{z_6}{2}\{1 - \tanh[z_7(R-z_2-z_8)]\}\varphi_{32}\right\} ; \quad \varphi_{12}(0) = 0$$

$$\dot{\varphi}_{13} = (1/\tau)\left\{- \varphi_{13} - \left(\frac{z_5+z_3z_6}{2}\right) z_7 \operatorname{sech}^2[z_7(R-z_2-z_8)]\varphi_{23} - \frac{z_6}{2}\{1 - \tanh[z_7(R-z_2-z_8)]\}\varphi_{32}\right\} ; \quad \varphi_{13}(0) = 0$$

$$\dot{\varphi}_{14} = (1/\tau)\left\{- \varphi_{14} - \left(\frac{z_5+z_3z_6}{2}\right) z_7 \operatorname{sech}^2[z_7(R-z_2-z_8)]\varphi_{24} - \frac{z_6}{2}\{1 - \tanh[z_7(R-z_2-z_8)]\}\varphi_{34}\right\} ; \quad \varphi_{14}(0) = 0$$

$$\dot{\varphi}_{15} = (1/\tau)\left\{- \varphi_{15} - \left(\frac{z_5+z_3z_6}{2}\right) z_7 \operatorname{sech}^2[z_7(R-z_2-z_8)]\, \varphi_{25} - \frac{z_6}{2}\{1 - \tanh[z_7(R-z_2-z_8)]\}\, \varphi_{35} - \frac{1}{2}\{1 - \tanh[z_7(R-z_2-z_8)]\}\right\};$$

$$\varphi_{15}(0) = 0$$

$$\dot{\varphi}_{16} = (1/\tau)\left\{- \varphi_{16} - \left(\frac{z_5+z_3z_6}{2}\right) z_7 \operatorname{sech}^2[z_7(R-z_2-z_8)]\varphi_{26} - \frac{z_6}{2}\{1 - \tanh[z_7(R-z_2-z_8)]\}\varphi_{36} - \frac{z_3}{2}\{1 - \tanh[z_7(R-z_2-z_8)]\}\right\};\quad \varphi_{16}(0) = 0$$

$$\dot{\varphi}_{17} = (1/\tau)\left\{- \varphi_{17} - \left(\frac{z_5+z_3z_6}{2}\right) z_7 \operatorname{sech}^2[z_7(R-z_2-z_8)]\varphi_{27} - \frac{z_6}{2}\{1 - \tanh[z_7(R-z_2-z_8)]\}\, \varphi_{37} + \left(\frac{z_5+z_3z_6}{2}\right)(R-z_2-z_8)\operatorname{sech}^2[z_7(R-z_2-z_8)]\right\};\quad \varphi_{17}(0) = 0$$

$$\dot{\varphi}_{18} = (1/\tau)\left\{- \varphi_{18} - \left(\frac{z_5+z_3z_6}{2}\right) z_7 \operatorname{sech}^2[z_7(R-z_2-z_8)]\varphi_{28} - \frac{z_6}{2}\{1 - \tanh[z_7(R-z_2-z_8)]\}\, \varphi_{38} - \left(\frac{z_5+z_3z_6}{2}\right) z_7 \operatorname{sech}^2[z_7(R-z_2-z_8)]\right\};\quad \varphi_{18}(0) = 0$$

$$\dot{\varphi}_{21} = (1/v_g)\, \varphi_{11} \quad ; \quad \varphi_{21}(0) = 0$$

$$\dot{\varphi}_{22} = (1/v_g)\, \varphi_{12} \quad ; \quad \varphi_{22}(0) = 1$$

$$\dot{\varphi}_{23} = (1/v_g)\, \varphi_{13} \quad ; \quad \varphi_{23}(0) = 0$$

$$\dot{\varphi}_{24} = (1/v_g)\, \varphi_{14} \quad ; \quad \varphi_{24}(0) = 0$$

$$\dot{\varphi}_{25} = (1/v_g)\, \varphi_{15} \quad ; \quad \varphi_{25}(0) = 0$$

$$\dot{\varphi}_{26} = (1/v_g)\,\varphi_{16} \qquad ; \qquad \varphi_{26}(0) = 0$$

$$\dot{\varphi}_{27} = (1/v_g)\,\varphi_{17} \qquad ; \qquad \varphi_{27}(0) = 0$$

$$\dot{\varphi}_{28} = (1/v_g)\,\varphi_{18} \qquad ; \qquad \varphi_{28}(0) = 0$$

$$\dot{\varphi}_{31} = (1/v_p)\left\{ -(a_1+a_2)\varphi_{31} + \frac{10^6 d_1}{2} b_1 \operatorname{sech}^2[b_1(R-z_2-e_1)]\varphi_{21} + a_2\varphi_{41} \right\} \qquad ; \qquad \varphi_{31}(0) = 0$$

$$\dot{\varphi}_{32} = (1/v_p)\left\{ -(a_1+a_2)\varphi_{32} + 10^6 \frac{d_1}{2} b_1 \operatorname{sech}^2[b_1(R-z_2-e_1)]\varphi_{22} + a_2\varphi_{42} \right\} \qquad ; \qquad \varphi_{32}(0) = 0$$

$$\dot{\varphi}_{33} = (1/v_p)\left\{ -(a_1+a_2)\varphi_{33} + 10^6 \frac{d_1}{2} b_1 \operatorname{sech}^2[b_1(R-z_2-e_1)]\varphi_{23} + a_2\varphi_{43} \right\} \qquad ; \qquad \varphi_{33}(0) = 1$$

$$\dot{\varphi}_{34} = (1/v_p)\left\{ -(a_1+a_2)\varphi_{34} + 10^6 \frac{d_1}{2} b_1 \operatorname{sech}^2[b_1(R-z_2-e_1)]\varphi_{24} + a_2\varphi_{44} \right\} \qquad ; \qquad \varphi_{34}(0) = 0$$

$$\dot{\varphi}_{35} = (1/v_p)\left\{ -(a_1+a_2)\varphi_{35} + 10^6 \frac{d_1}{2} b_1 \operatorname{sech}^2[b_1(R-z_2-e_1)]\varphi_{25} + a_2\varphi_{45} \right\} \qquad ; \qquad \varphi_{35}(0) = 0$$

$$\dot{\varphi}_{36} = (1/v_p)\left\{ -(a_1+a_2)\varphi_{36} + 10^6 \frac{d_1}{2} b_1 \operatorname{sech}^2[b_1(R-z_2-z_8)]\varphi_{26} + a_2\varphi_{46} \right\} \qquad ; \qquad \varphi_{36}(0) = 0$$

(E-35)

$$\dot{\varphi}_{37} = (1/v_p)\left\{ - (a_1+a_2)\varphi_{37} + 10^6 \frac{d_1}{2} b_1 \operatorname{sech}^2[b_1(R-z_2-z_8)]\varphi_{27} + a_2\varphi_{47} \right\} \quad ; \quad \varphi_{37}(0) = 0$$

$$\dot{\varphi}_{38} = (1/v_p)\left\{ - (a_1+a_2)\varphi_{38} + 10^6 \frac{d_1}{2} b_1 \operatorname{sech}^2[b_1(R-z_2-z_8)]\varphi_{28} + a_2\varphi_{48} \right\} \quad ; \quad \varphi_{38}(0) = 0$$

$$\dot{\varphi}_{41} = (1/v_i)\{ - (a_2+a_3)\varphi_{41} + a_2\varphi_{31}\} \quad ; \quad \varphi_{41}(0) = 0$$

$$\dot{\varphi}_{42} = (1/v_i)\{ - (a_2+a_3)\varphi_{42} + a_2\varphi_{32}\} \quad ; \quad \varphi_{42}(0) = 0$$

$$\dot{\varphi}_{43} = (1/v_i)\{ - (a_2+a_3)\varphi_{43} + a_2\varphi_{33}\} \quad ; \quad \varphi_{43}(0) = 0$$

$$\dot{\varphi}_{44} = (1/v_i)\{ - (a_2+a_3)\varphi_{44} + a_2\varphi_{34}\} \quad ; \quad \varphi_{44}(0) = 1$$

$$\dot{\varphi}_{45} = (1/v_i)\{ - (a_2+a_3)\varphi_{45} + a_2\varphi_{35}\} \quad ; \quad \varphi_{45}(0) = 0$$

$$\dot{\varphi}_{46} = (1/v_i)\{ - (a_2+a_3)\varphi_{46} + a_2\varphi_{36}\} \quad ; \quad \varphi_{46}(0) = 0$$

$$\dot{\varphi}_{47} = (1/v_i)\{ - (a_2+a_3)\varphi_{47} + a_2\varphi_{37}\} \quad ; \quad \varphi_{47}(0) = 0$$

$$\dot{\varphi}_{48} = (1/v_i)\{ - (a_2+a_3)\varphi_{48} + a_2\varphi_{38}\} \quad ; \quad \varphi_{48}(0) = 0$$

$$\dot{p}_1 = (1/\tau)\Bigg\{- p_1 - \left(\frac{z_5+z_3z_6}{2}\right) z_7 \operatorname{sech}^2[z_7(R-z_2-z_8)]\, p_2 - \frac{z_6}{2}\{1 - \tanh[z_7(R-z_2-z_8)]\}\, p_3 + \frac{z_3z_6}{2}\{1 - \tanh[z_7(R-z_2-z_8)]\} + \left(\frac{z_5+z_3z_6}{2}\right) z_7[2(z_2+z_8)-R]\operatorname{sech}^2[z_7(R-z_2-z_8)] + F(t)\Bigg\};\ p_1(0) = 0$$

$$\dot{p}_2 = (1/v_g)\, p_1 \qquad ;\ p_2(0) = 0$$

$$\dot{p}_3 = (1/v_p)\Bigg\{10^6 \frac{d_1}{2} b_1 \operatorname{sech}^2[b_1(R-z_2-e_1)]p_2 - (a_1+a_2)p_3 + a_2p_4 + 10^6 \frac{d_1}{2}\Big[\{1 - \tanh[b_1(R-z_2-e_1)]\} - b_1\operatorname{sech}^2[b_1(R-z_2-e_1)]\, z_2\Big]\Bigg\} \qquad (E\text{-}36)$$

$$;\ p_3(0) = 0$$

$$\dot{p}_4 = (1/v_i)\{- (a_2+a_3)p_4 + a_2p_3\} \qquad ;\ p_4(0) = 0$$

Assuming observations on c and u_{1p}, the algebraic system to be solved for the updated initial condition is:

$$\left\{\sum_{i=1}^{N} \Phi'(t_i)\, K'\, K\, \Phi(t_i)\right\}\beta = \sum_{i=1}^{N} \Phi'(t_i)\, K'\{y(t_i)-K\, p(t_i)\} \qquad (E\text{-}37)$$

where:

$$K = \begin{bmatrix} 0 & 1 & 0 & 0 & 0 & 0 & 0 & 0 \\ 0 & 0 & 1 & 0 & 0 & 0 & 0 & 0 \end{bmatrix}$$

and:

$$(\Phi'(t_i)K'K\Phi(t_i))_{jk} = \varphi_{2j}(t_i)\varphi_{2k}(t_i) + \varphi_{3j}(t_i)\varphi_{3k}(t_i)$$

$$(\Phi'(t_i)K'\{y(t_i) - Kp(t_i)\})_j = \varphi_{2j}(t_i)[y_1(t_i)-p_2(t_i)]$$

$$+ \varphi_{3j}(t_i)[y_2(t_i)-p_3(t_i)]$$

$$j,k = 1, \cdots, 8$$

LIST OF REFERENCES

[1] T. C. Ruch and H. D. Patton, (eds.), Physiology and Biophysics, W. B. Saunders Co., Phila., 1965.

[2] S. S. Kety, "General Metabolism of the Brain in Vivo", Metabolism of the Nervous System, D. Richter, (ed.), pp. 221-37, Pergamon Press, N.Y., 1957.

[3] A. Cantarow and B. Schepartz, Biochemistry, W. B. Saunders Co., Phila., 1962.

[4] W. F. Ganong, Medical Physiology, Lange Medical Publications, Los Altos, Calif., 1963.

[5] G. G. Duncan, (ed.), Diseases of Metabolism, W. B. Saunders Co., Phila., 1964.

[6] C. H. Best and N. B. Taylor, (eds.), The Physiological Basis of Medical Practice, The Williams and Wilkins Co., Baltimore, 1966.

[7] H. A. Harper, Physiological Chemistry, Lange Medical Publications, Los Altos, Calif., 1963.

[8] C. D. Turner, General Endocrinology, W. B. Saunders Co., Phila., 1966.

[9] W. B. Cannon, The Wisdom of the Body, W. W. Norton, N.Y., 1939.

[10] H. N. Antoniades, (ed.), Hormones in Human Plasma, Little, Brown and Co., New York, 1960.

[11] S. A. Berson and R. S. Yalow, "Radioimmunoassays of Peptide Hormones in Plasma", New England J. of Med., Vol. 227, pp. 640-7, 1967.

[12] R. J. Henry, Clinical Chemistry Principles and Techniques, Harper and Row, 1964.

[13] R. S. Yalow and S. Berson, "Dynamics of Insulin Secretion in Hypoglycemia", Diabetes, Vol. 14, pp. 341-9, 1965.

[14] R. Levine and M. S. Goldstein, "On the Mechanism of Action of Insulin", Recent Progress in Hormone Research, Vol. 11, p. 343, 1955.

[15] G. L. Searle, et.al., "Plasma Glucose Turnover in Humans as Studied with C^{14} Glucose", Diabetes, Vol. 8, p. 167, 1959.

[16] W. W. Shreeve, "Effects of Insulin on the Turnover of Plasma Carbohydrates and Lipids", Am. J. of Med., Vol. 40, pp. 724-34, 1966.

[17] S. A. Berson and R. S. Yalow, "Some Current Controversies in Diabetes Research", Diabetes, Vol. 14, pp. 549-72, 1965.

[18] E. Samols and V. Marks, "Disappearance-Rate of Endogenous Insulin in Man", The Lancet, p. 700, 1966.

[19] E. Samols, et.al., "Promotion of Insulin Secretion by Glucagon", The Lancet, Vol. 2, p. 415, 1965.

[20] R. G. Simpson, et.al., "Stimulation of Insulin Release by Glucagon in Noninsulin-Dependent Diabetics", Metabolism, Vol. 15, pp. 1046-9, 1966.

[21] G. M. Grodsky, et.al., "Effect of Pulse Administration of Glucose or Glucagon on Insulin Secretion in Vitro", Metabolism, Vol. 16, pp. 222-33, 1967.

[22] E. Samols, et.al., "Interrelationship of Glucagon, Insulin, and Glucose", Diabetes, Vol. 15, pp. 855-66, 1966.

[23] R. Levine, "Insulin-The Biography of a Small Protein", New England J. of Med., Vol. 277, pp. 1059-64, 1967.

[24] M. J. Perley and D. M. Kipnis, "Plasma Insulin Responses to Oral and I. V. Glucose - Studies in Normal and Diabetic Subjects", J. Clin. Invest., Vol. 46, pp. 1954-62, 1967.

[25] R. J. Jarrett and N. M. Cohen, "Intestinal Hormones and Plasma-Insulin", The Lancet, pp. 861-3, 1967.

[26] J. E. Sokal, "Glucagon - An Essential Hormone", Am. J. of Med., Vol. 41, pp. 331-341, 1966.

[27] D. Porte, et.al., "The Effect of Epinephrine on Immunoreactive Insulin Levels in Man", J. of Clin. Invest., Vol. 45, pp. 228-236, 1966.

[28] D. Porte and R. H. Williams, "Inhibition of Insulin Release by Norepinephrine in Man", Science, Vol. 152, pp. 1248-50, 1966.

[29] R. J. Wurtman, "Catecholamines", New England J. Med., Vol. 273, Nos. 12, 13, 14, September 1965.

[30] J. H. Exton, et.al., "Gluconeogenesis in the Perfused Liver", Am. J. of Med., Vol. 40, pp. 709-15, 1966.

[31] R. Levine, "Diabetes Mellitus", Clinical Symposia CIBA, Vol. 15, p. 118, 1963.

[32] A. Goldfien, "Plasma Epinephrine and Norepinephrine Levels During Insulin Induced Hypoglycemia in Man", J. Clin. Endocrinol., Vol. 21, p. 296, 1961.

[33] F. E. Yates and J. Urquhart, "Control of Plasma Concentrations of Adrenocortical Hormones", Physiological Reviews, Vol. 42, pp. 359-443, 1962.

[34] R. H. Williams and J. W. Ensinck, "Secretion, Fates, and Actions of Insulin and Related Products", Diabetes, Vol. 15, pp. 623-54, 1966.

[35] H. DeWulf and H. G. Hers, "The Stimulation of Glycogen Synthesis and of Glycogen Synthetase in the Liver by Glucocorticoids", European J. Biochem., Vol. 2, pp. 57-60, 1967.

[36] R. E. Peterson, "Miscible Pool and Turnover Rate of Adrenal Cortical Steroids in Man", Recent Prog. in Hor. Res., Vol. 15, p. 231, 1959.

[37] H. Friesen and E. B. Astwood, "Hormones of the Anterior Pituitary Body", New England J. of Med., Vol. 272, No. 23, 24, 25, June 1965.

[38] R. Luft, et.al., "Effect of a Small Decrease in Blood Glucose on Plasma GH and Urinary Excretion of Catecholamines in Man", The Lancet, pp. 254-6, 1966.

[39] J. Roth, S. M. Glick, R. S. Yalow, and S. A. Berson, "The Influence of Blood Glucose on the Plasma Concentration of Growth Hormone", Diabetes, Vol. 13, pp. 355-61, 1964.

[40] A. G. Frantz and M. T. Rabkin, "Human Growth Hormone", New England J. of Med., Vol. 271, pp. 1375-81, 1964.

[41] W. H. Daughaday and M. L. Parker, "Human Pituitary Growth Hormone", Annual Rev. of Med., Vol. 16, pp. 47-66, 1965.

[42] D. Rabinowitz, et.al., "Patterns of Hormonal Release After Glucose, Protein, and Glucose Plus Protein", The Lancet, pp. 454-6, 1966.

[43] J. Geller and A. Lok, "Identification and Measurement of Growth Hormone in Extracts of Human Urine", J. Clin. Endocrinol. and Metab., Vol. 23, pp. 1107-14, 1963.

[44] J. Roth, et.al., "Secretion of Human Growth Hormone: Physiologic and Experimental Modification", Metabolism, Vol. 12, p. 578, 1963.

[45] B. A. Cross, "The Hypothalamus in Mammalian Homeostasis", Homeostatic Mechanims, Report of Symposium at Brookhaven National Laboratory, N.Y., pp. 157-193, 1967.

[46] L. Madison, "Symposium on Effects of Insulin on Liver", Diabetes, 1963.

[47] H. DeWulf and H. G. Hers, "The Stimulation of Glycogen Synthesis and of Glycogen Synthetase in the Liver by the Administration of Glucose", European J. Biochem., Vol. 2, pp. 50-56, 1967.

[48] P. J. Randle, et.al., "The Glucose Fatty Acid Cycle in Obesity and Maturity Onset Diabetes Mellitus", Annals N.Y. Acad. of Sci., Vol. 131, pp. 324-33, 1965.

[49] P. J. Randle, "Fuel and Power in the Control of Carbohydrate Metabolism in Mammalian Muscle", Homeostatic Mechanisms, Report of Symposium at Brookhaven National Laboratory, N.Y., pp. 129-55, 1967.

[50] L. H. Miller, "Direct Actions of Insulin, Glucagon, and Epinephrine on the Isolated Perfused Rat Liver", Federation Proc., Vol. 24, pp. 737-44, 1965.

[51] A. B. Eisenstein, "Current Concepts of Gluconeogenesis", Amer. J. of Clin. Nutrition, Vol. 20, pp. 282-89, 1967.

[52] G. F. Cahill, et.al., "Hormone-Fuel Interrelationships during Fasting", J. of Clin. Invest., Vol. 45, pp. 1751-69, 1966.

[53] W. A. Seyffert and L. L. Madison, "Physiologic Effect of Metabolic Fuels on Carbohydrate Metabolism", Diabetes, Vol. 16, pp. 765-76, 1967.

[54] S. Goldman, "Cybernetic Aspects of Homeostasis", Mineral Metabolism, Academic Press, Vol. I, Part A, Chapter 3, 1960.

[55] V. W. Bolie, "Glucose-Insulin Feedback Theory", Third Int. Conf. on Med. Elec., 1960.

[56] V. W. Bolie, "Coefficients of Normal Blood Glucose Regulation", J. of Clin. Invest., Vol. 39, Part 2, pp. 783-788, 1960.

[57] J. C. Seed, F. S. Acton, A. J. Stunkard, "A Model for the Appraisal of Glucose Metabolism", Clin. Pharm. and Therapeutics, Vol. 3, pp. 191-215, 1962.

[58] D. S. Amatuzio, et.al., "Interpretation of the Rapid Intravenous Glucose Tolerance Test in Normal Individuals and in Mild Diabetes Mellitus", J. Clin. Invest., Vol. 32, pp. 428-435, 1953.

[59] R. P. Beliles, "Theoretical and Experimental Studies of Factors Affecting Blood Glucose Regulation", Ph.D. Thesis, Pharmacology, Iowa State University, 1962.

[60] D. E. Wrede, "Development of a Mathematical Model for a Biological Feedback System with Particular Application to Glucose Metabolism", Ph.D. Thesis, Biological Chemistry, University of Cincinnati, 1963.

[61] F. C. McLean, "The Homeostasis of Blood Sugar", Diabetes, Vol. 13, pp. 198-202, 1964.

[62] D. M. Shames, "A Theoretical Study of the Blood Glucose Regulatory System", M.D. Thesis, Yale University School of Medicine, 1965.

[63] E. Cerasi, "An Analog Computer Model for the Insulin Response to Glucose Infusion", Acta Endocrinologica, Vol. 55, pp. 163-183, 1967.

[64] L. E. Wolaver, "Mathematical Model for Blood Sugar Regulation of the Human Body and its Control in Diabetes Mellitus", AICA Congress, Lausanne, Switzerland, 1967.

[65] B. Chance, "Analogue and Digital Representations of Enzyme Kinetics", J. of Bio. Chem., Vol. 235, pp. 2440-43, 1960.

[66] B. Chance, J. Higgins, and D. Garfinkel, "Analogue and Digital Computer Representations of Biochemical Processes", Federation Proceedings, Vol. 21, pp. 75-86, 1962.

[67] E. F. MacNichol, "An Analog Computer to Simulate Systems of Coupled Bimolecular Reactions", Proc. of the IRE, Vol. 47, pp. 1816-20, 1959.

[68] C. F. Walter and M. F. Morales, "An Analogue Computer Investigation of Certain Issues in Enzyme Kinetics", J. of Bio. Chem., Vol. 239, pp. 1277-83, 1964.

[69] D. Garfinkel, "A Simulation Study of Mammalian Phosphofructokinase", J. of Bio. Chem., Vol. 241, pp. 286-94, 1966.

[70] W. G. Miller and R. A. Alberty, "Kinetics of the Reversible Michaelis-Menten Mechanism and the Applicability of the Steady-State Approximation", J. Am. Chem. Soc., Vol. 80, pp. 5146-51, 1958.

[71] F. G. Heineken, H. M. Tsuchiya, and R. Aris, "On the Mathematical Status of the Pseudo-steady State Hypothesis of Biochemical Kinetics," Mathematical Biosciences, Vol. 1, pp. 95-113, 1967.

[72] L. L. Madison, et.al., "Physiological Significance of the Secretion of Endogenous Insulin Into the Portal Circulation. The Quantitative Importance of the Liver in the Disposition of Glucose Loads", Diabetes, Vol. 12, pp. 8-15, 1963.

[73] D. E. Atkinson, "Biological Feedback Control at the Molecular Level", Science, Vol. 150, pp. 851-57, 1965.

[74] D. E. Atkinson and G. M. Walton, "Kinetics of Regulatory Enzymes", J. of Bio. Chem., Vol. 240, pp. 757-63, 1965.

[75] D. E. Atkinson, J. A. Hathaway, and E. C. Smith, "Kinetics of Regulatory Enzymes", J. of Bio. Chem., Vol. 240, pp. 2682-90, 1965.

[76] V. Licko, "Bimolecular Systems: I. Linear Systems of Complexes", Bull. of Math. Biophysics, Vol. 29, pp. 1-16, 1967.

[77] V. Licko, "Bimolecular Systems: II. Nonlinear Systems of Complexes", Bull. of Math. Biophysics, Vol. 29, pp. 605-13, 1967.

[78] V. Licko, "Bimolecular Systems: III. Catalytic Systems", Bull. of Math. Biophysics, Vol. 29, pp. 615-23, 1967.

[79] B. Chance, K. Pye, and J. Higgins, "Waveform Generation by Enzymatic Oscillators", IEEE Spectrum, pp. 79-86, 1967.

[80] W. P. London, "A Theoretical Study of Hepatic Glycogen Metabolism", J. of Bio. Chem., Vol. 241, pp. 3008-22, 1966.

[81] D. S. Amatuzio, Diagnosis: Intravenous Glucose Tolerance Tests, Diabetes Mellitus: Diagnosis and Treatment, T. S. Danowski, (ed.), Am. Diabetes Assoc. Inc., pp. 35-40, 1964.

[82] E. Goldberger, A Primer of Water, Electrolyte, and Acid-Base Syndromes, Lee & Feibeger, 1965.

[83] S. Soskin and R. Levine, "A Relationship Between the Blood Sugar Level and Rate of Sugar Utilization, Affecting the Theories of Diabetes", Amer. J. of Physiol., Vol. 120, p. 761, 1937.

[84] M. Wierzuchowski, "The Limiting Rate of Assimilation of Glucose Introduced Intravenously at Constant Speed in the Resting Dog", Amer. J. of Physiol., Vol. 87, p. 311, 1936.

[85] R. Levine, "Carbohydrate Metabolism", Diseases of Metabolism, G. G. Duncan, (ed.), Ch. 2, W. B. Saunders Co., Phila., 1964.

[86] D. Steinberg, "Fatty Acid Mobilization - Mechanisms of Regulation and Metabolic Consequences", The Control of Lipid Metabolism, J. K. Grant, (ed.), N.Y. Univ. Press, pp. 111-43, 1963.

[87] A. E. Renold, et.al., "Hormonal Control of Adipose Tissue Metabolism with Special Reference to the Effect of Insulin", Diabetologia, Vol. 1, pp. 4-12, 1965.

[88] N. A. Lassen, "Cerebral Blood Flow and Oxygen Consumption in Man", Physiological Reviews, Vol. 39, pp. 183-238, 1959.

[89] G. Hetenyi, G. A. Wrenshall, and C. H. Best, "Rates of Production, Utilization, Accumulation and Apparent Distribution Space of Glucose", Diabetes, Vol. 10, pp. 304-311, 1961.

[90] N. Forbath and G. Hetenyi, "Glucose Dynamics in Normal Subjects and Diabetic Patients Before and After a Glucose Load", Diabetes, Vol. 15, pp. 778-89, 1966.

[91] C. A. Sanders, et.al., "Effect of Exercise on the Peripheral Utilization of Glucose in Man", New England J. Med., Vol. 271, pp. 220-25, 1964.

[92] R. Metz, "The Effect of Blood Glucose Concentration on Insulin Output", Diabetes, Vol. 9, p. 89, 1960.

[93] H. Orsky and N. J. Christensen, "Disappearance Rate of Exogenous Human Insulin", The Lancet, p. 701, 1966.

[94] S. A. Berson, et.al., "Insulin - I^{131} Metabolism in Human Subjects", J. Clin. Invest., Vol. 35, pp. 170-90, 1965.

[95] H. T. Narahara, "Glucagon Degradation" Diabetes, R. H. Williams (ed.), Hoeber Inc., pp. 292-6, 1960.

[96] W. P. Charette, A. H. Kadish, R. Sridhar, "A Nonlinear Dynamic Model of Endocrine Control of Metabolic Processes", 7th Int. Conf. on Med. and Biol. Eng., Stockholm, 1967.

[97] A. H. Kadish, "Cybernetics of Blood Sugar Regulation and Servo System Disease Research", Instrumentation Methods for Predictive Medicine, Instrument Society of America, Ch. 8, pp. 87-106, 1966.

[98] H. E. Hart, "Analysis of Tracer Experiments in Nonconservative Steady-state Systems", Bull. Math. Biophysics, Vol. 17, pp. 87-94, 1955.

[99] S. A. Berson and R. S. Yalow, "Isotopic Tracers in the Study of Diabetes", Adv. in Biol. and Med. Physics, Vol. 6, Academic Press, 1958.

[100] C. Walter, Enzyme Kinetics, The Ronald Press Co., N.Y., 1966.

[101] E. A. Dawes, Quantitative Problems in Biochemistry, E.&S. Livingstone Ltd., London, 1967.

[102] A. C. Brown, "Passive and Active Transport", Chapter 43 in Physiology and Biophysics, T. C. Ruch and H. D. Patton, (eds.), W. B. Saunders Co., Phila., 1965.

[103] S. O. Waife, (ed.), Diabetes Mellitus, Eli Lilly and Co., Indianapolis, 1967.

[104] J. R. M. Franchson, et.al., "Physiologic Significance of the I.V. Glucose Tolerance Test", Metabolism, Vol. 11, p. 482, 1962.

[105] C. J. Hlad, H. Elrich, and T. A. Witten, "Studies on the Kinetics of Glucose Utilization", J. Clin. Invest., Vol. 35, pp. 1139-49, 1956.

[106] C. J. Hlad and H. Elrich, "Further Studies of the Kinetics of Glucose Utilization", J. Clin. Endocrin. and Metab., Vol. 19, pp. 1258-73, 1959.

[107] J. D. Acland, et.al., "Reproducibility of a Glucose Tolerance Test", J. of App. Physiology, Vol. 17, pp. 119-122, 1962.

[108] N. J. H. Butterfield, et.al., "The Intravenous Glucose Tolerance Test: Peripheral Disposal of the Glucose Load in Controls and Diabetics", Metabolism, Vol. 16, pp. 19-34, 1967.

[109] R. Levine, "Analysis of the Actions of the Hormonal Antagonists of Insulin", Diabetes, Vol. 13, pp. 362-5, 1964.

[110] S. A. Berson and R. S. Yalow, "Insulin in Blood and Insulin Antibodies", Amer. J. Med., Vol. 40, pp. 676-90, 1966.

[111] D. S. Goodman, "Cholesterol Ester Metabolism", Physiological Reviews, Vol. 45, pp. 747-839, 1965.

[112] J. Tepperman, Metabolic and Endocrine Physiology, Year Book Medical Publishers, Chicago, 1962.

[113] W. S. Yamamoto and J. R. Brobeck, (eds.), Physiological Controls and Regulations, W. B. Saunders Co., Phila., 1965.

[114] G. M. Hughes, (ed.), Homeostasis and Feedback Mechanisms, Symposium of the Soc. for Exp. Biol., Cambridge University Press, 1964.

[115] A. H. Kadish, R. L. Litle, and J. C. Sternberg, "A New and Rapid Method for the Determination of Glucose by Measurement of Rate of Oxygen Consumption", Clin. Chem., Vol. 14, pp. 116-131, 1968.

[116] W. P. Charette, A. H. Kadish, and R. Sridhar, "Modeling and Control Aspects of Glucose Homeostasis", Mathematical Biosciences, (Forthcoming Issue 1968).

[117] K. Sakata, S. Hayano, and H. A. Sloviter, "Effect of Blood Glucose Concentration of Changes in Availability of Glucose to the Brain", Amer. J. Physiol., Vol. 204, p. 1127, 1963.

[118] H. Shenkin, et.al., "The Acute Effects of On the Cerebral Circulation of the Reduction of Increased Intracronial Pressure by Means of Intravenous Glucose or Ventricular Drainage", J. Neurosurg., Vol. 5, pp. 466-77, 1948.

[119] G. F. Cahill Jr., et.al., "Glucose Penetration into Liver", Amer. J. Physiol., Vol. 192, p. 491, 1958.

[120] L. L. Madison, B. Combes, and R. Adams, "Insulin's Control of the Role of the Liver in the Disposition of a Glucose Load in Diabetic and Non-Diabetic Dogs", J. Clin. Invest., Vol. 39, p. 1009, 1960.

[121] W. W. Shreeve, et.al., "C^{14} Studies in Carbohydrate Metabolism. The Oxidation of Glucose in Diabetic Human Subjects", Metabolism, Vol. 5, pp. 22-34, 1956.

[122] J. D. Myers, "Net Splanchnic Glucose Production in Normal Man and In Various Disease States", J. Clin. Invest., Vol. 29, pp. 1421-9, 1950.

[123] R. C. deBodo, et.al., "Effects of Exogenous and Endogenous Insulin on Glucose Utilization and Production", Ann. N.Y. Acad. Sci., Vol. 82, pp. 431-51, 1959.

[124] J. P. Berthat, et.al., "Influences Hormonales Sur la Synthesis de Glycogen Hepatique in vitro", Arch. Intern. Physiol., Vol. 62, p. 282, 1954.

[125] J. R. Leonards and B. R. Landau, "A Study on the Equivalence of Metabolic Patterns in Rat Adipose Tissue: Insulin versus Glucose Concentration", Arch. Biochem. Biophys., Vol. 91, pp. 194-200, 1960.

[126] G. F. Cahill Jr., S. Zottu, and A. S. Earle, "In Vivo Effects of Glucagon on Hepatic Glycogen, Phosphorylase, and Glucose - 6 - Phosphatase", Endocrinology, Vol. 60, p. 265, 1967.

[127] J. E. Sokal, "The Duration of Glucagon Effect", Endocrinology, Vol. 67, p. 774, 1960.

[128] A. G. Bearn, B. H. Billing, and S. Sherlock, "The Response of the Liver to Insulin in Normal Subjects and in Diabetes Mellitus: Hepatic Vein Catheterization Studies", Clin. Sci., Vol. 11, p. 151, 1952.

[129] J. S. Wall, et.al., "Effect of Insulin on Utilization and Production of Circulating Glucose", Amer. J. Physiol., Vol. 189, p. 43, 1957.

[130] J. E. Sokal and B. Weintraub, "Failure of the Isolated Liver to React to Hypoglycemia", Amer. J. Physiol., Vol. 210, p. 63, 1966.

[131] W. C. Shoemaker, et.al., "Measurement of Hepatic Glucose Output and Hepatic Blood Flow in Response to Glucagon", Amer. J. Physiol., Vol. 196, p. 315, 1959.

[132] L. L. Miller, "Direct Actions of Insulin, Glucagon, and Epinephrine on the Isolated Perfused Rat Liver", Fed. Proc., Vol. 24, pp. 737-43, 1965.

[133] E. Z. Ezdinli and J. E. Sokal, "Comparison of Glucagon and Epinephrine Effects in the Dog", Endocrinology, Vol. 78, p. 47, 1966.

[134] L. I. Woolf, Renal Tubular Dysfunction, C. C. Thomas, Springfield, Illinois, p. 13, 1964.

[135] M. S. Goldstein, "Glucose Transport Theory of Insulin Action", Ann. N.Y. Acad. Sci., Vol. 82, pp. 378-86, 1959.

[136] G. F. Cahill, Jr., et.al., "Effects of Insulin on Adipose Tissue", Ann. N.Y. Acad. Sci., Vol. 82, pp. 403-11, 1959.

[137] R. Levine, et.al., "Action of Insulin on the Permeability of Cells to Free Hexoses As Studied by its Effect on the Distribution of Galactose", Amer. J. Physiol., Vol. 163, p. 70, 1950.

[138] N. Altszuler, et.al., "Diminution of Insulin Effect by Growth Hormone in Hypophysectonized Dogs; Studies with C^{14} Glucose", Amer. J. Physiol., Vol. 196, pp. 231-4, 1959.

[139] R. S. Yalow and S. A. Berson, "Immunoassay of Endogenous Plasma Insulin in Man", J. Clin. Invest., Vol. 39, pp. 1157-75, 1960.

[140] L. L. Madison, et.al., "Relationship Between the Mechanism of Action of the Sulfonylureas and the Secretions of Insulin Into the Portal Circulation", Ann. N.Y. Acad. Sci., Vol. 74, p. 548, 1959.

[141] G. E. Mortimore and F. Tietze, "Studies on the Mechanism of Capture and Degradation of Insulin - I^{131} by the Cyclically Perfused Rat Liver", Ann. N.Y. Acad. Sci., Vol. 82, p. 329, 1959.

[142] R. Unger, et.al., "Glucagon Antibodies and an Immunoassay for Glucagon", J. Clin. Invest., Vol. 40, p. 1280, 1961.

[143] M. G. Goldner, R. H. Jauregui, and S. Weisenfeld, "Disappearance of HGF From Insulin After Liver Perfusion", Amer. J. Physiol., Vol. 179, p. 25, 1954.

[144] S. A. Berson, R. S. Yalow, and B. W. Volk, "In Vivo and In Vitro Metabolism of Insulin - I^{131} and Glucagon - I^{131} in Normal and Cortisone-Treated Rabbits", J. Lab. and Clin. Med., Vol. 49, p. 331, 1957.

[145] R. H. Unger, et.al., "Measurements of Endogenous Glucagon in Plasma and the Influence of Blood Glucose on its Secretion", J. Clin. Invest., Vol. 41, p. 682, 1962.

[146] J. Roth, et.al., "Hypoglycemia: A Potent Stimulus to Secretion of Growth Hormone", Science, Vol. 140, pp. 987-8, 1963.

[147] S. M. Glick, R. S. Yalow, and S. A. Berson, "Immunoassay of Human Growth Hormone in Plasma", Nature, Vol. 199, pp. 784-7, 1963.

[148] G. Boden, J. S. Soeldner, J. Steinke, and G. W. Thorn, "Serum Human Growth Hormone (HGH) Response to IV Glucose: Diagnosis of Acromegaly in Females and Males", Metabolism, Vol. 27, pp. 1-9, 1968.

[149] R. Bellman and R. Kalaba, Quasilinearization and Nonlinear Boundary-Value Problems, American Elsevier, N.Y., 1965.

[150] A. M. Legendre, Nouvelles Methodes Pour la Determination des Orbits des Cometes, Paris, 1806.

[151] K. F. Gauss, Theoria Motus Corporum Coelestium in Sectimibus Conicis Solem Aurbientium, Perthes and Besser, Hamburg, 1809.

[152] H. J. Kelley, "Method of Gradients", Optimization Techniques, G. Leitmann (ed.), Academic Press, pp. 205-54, 1962.

[153] R. Hooke and T. A. Jeeves, "Direct Search Solution of Numerical and Statistical Problems", J. ACM, pp. 212-29, 1961.

[154] G. A. Bekey, et.al., "Parameter Optimization by Random Search Using Hybrid Computer Techniques", Proc.-Fall J.C.C., pp. 191-200, 1966.

[155] R. Bellman, Dynamic Programming, Princeton Univ. Press, N.J., 1957.

[156] D. M. Detchmendy and R. Sridhar, "On the Experimental Determination of the Dynamic Characteristics of Physical Systems", Proc. Nat. Electronics Conf., Chicago, 1965.

[157] R. Bellman, Adaptive Control Processes, Princeton Univ. Press, N.J., 1961.

[158] R. Kalaba, "On Nonlinear Differential Equations, the Maximum Operation, and Monotone Convergence", J. Math. and Mech., vol. 8, pp. 519-74, 1959.

[159] R. Bellman and S. E. Dreyfus, Applied Dynamic Programming, Princeton Univ. Press, N. J., 1962.

[160] R. Tomovic, Sensitivity Analysis of Dynamic Systems, McGraw-Hill, N. Y., 1963.

[161] G. Copinschi, et. al., "Effect of Various Blood Sampling Procedures on Serum Levels of Immunoreactive Human Growth Hormone", Metabolism, Vol. 16, pp. 402-9, 1967.

[162] R. Andres, et. al., "Manual Feedback Technique for the Control of Blood Glucose Concentration", Technicon Symposium, N. Y., pp. 486-91, 1966.

[163] A. H. Kadish, "Automation Control of Blood Sugar", Amer. J. Med. Electronics, pp. 82-6, 1964.

[164] F. B. Hildebrand, Introduction to Numerical Analysis, McGraw-Hill, N. Y., 1956.

[165] D. M. Detchmendy and R. Sridhar, "Sequential Estimation of States and Parameters in Noisy Nonlinear Dynamical Systems", Trans. ASME, Vol. 88, pp. 362-8, 1966.

[166] R. Sridhar and J. B. Pearson, "Digital Estimation of Nonlinear Processes", IEEE Region Six Conf. Record, 1966.

[167] R. Bellman, H. Kagiwada, R. Kalaba, and R. Sridhar, "Invariant Imbedding and Nonlinear Filtering Theory", RAND Research Memorandum, RM-4374-PR, 1964.

[168] H. Cox, "On the Estimation of State Variables and Parameters for Noisy Dynamic Systems," IEEE Trans. on Automatic Control, Vol. 9, pp. 5-12, 1964.